THE MODIFICATION OF ACTIVATED CARBON CLOTH BY ALUMINA DEPOSITION

A Thesis submitted for the degree of Doctor of Philosophy

by

Robert Andrew Hayes

Department of Chemistry, Brunel University

October 1988

ABSTRACT

The impregnation of mesoporous carbon cloth with alumina has been studied. The most successful method of impregnation resulted from preparation of the alumina phase by a sol/gel route. This method involves a boehmite intermediate, and the heating environment for the thermal transition of boehmite to the final alumina was investigated. Heat treatment of the boehmite intermediate under flowing N_2, flowing air and vacuum was found to give a different pore size distribution for the final alumina than did still air heat treatment. For the former environments the transition from boehmite to alumina was not accompanied by the usual increase in pore size. Alumina/carbon composites were made by dipping pieces of mesoporous carbon cloth in a boehmite sol. The distribution of boehmite about the carbon cloth was found to be improved by pre-wetting the carbon cloth and by the use of ultrasonic dispersion during boehmite impregnation. Dried boehmite/carbon composites, with loading levels of up to 180wt.%, were heated under vacuum to 500°C. In this manner alumina/carbon composites of up to 60wt.% alumina were fabricated. The distribution of the alumina phase about the carbon cloth was investigated by electron microscopy and by gas adsorption techniques. Nitrogen isotherm data indicated that the mesopores of the carbon cloth were not blocked by the deposited alumina, rather the pore volume of the carbon cloth was increased by the clustering of porous alumina about the pore entrances of the carbon cloth. Water isotherms were determined for the composite materials. The water activity of the composite, particularly at low relative pressures, was found to be significantly greater than that of the carbon cloth as a result of the presence of alumina. CO_2 activity of the composites was investigated by a gas chromatographic technique. The CO_2 activity of the composite material was found to be up to 500 times greater than that of virgin carbon cloth.

ACKNOWLEDGEMENTS

I would like to express my gratitude to my academic supervisor Ken Sing for giving me the opportunity to work upon this research project. I am also very grateful to John Ralston at the South Australian Institute of Technology (SAIT) for providing the initial impetus "to get things rolling".

The provision of a research grant by ALCOA is gratefully acknowledged.

One cannot obviously do research without the help and advice of others. I was particularly fortunate to have the benefit of many helpful discussions with Peter Carrott, John Freeman and Adrian Roberts, and the technical assistance of many others in the Chemistry Department at Brunel. The staff of the Experimental Techniques Center (ETC) at Brunel were very helpful with the SEM work.

Finally, thanks firstly Chit for typing this thesis, and secondly, and probably more importantly, for putting up with life as this chemist's wife.

CONTENTS

LIST OF TABLES

LIST OF FIGURES

LIST OF ABBREVIATIONS

Abbreviation	Meaning	Page First Used
AA	Atomic absorption	42
AIP	Aluminium isopropoxide	44
ASB	Aluminium sec-butoxide	31
BET	Brunauer-Emmett-Teller	11
cbd	Critical bed depth	143
CVD	Chemical vapour deposition	44
EGA	Evolved gas analysis	17
IP	Isopropanol	44
ppm	Parts per million	105
p/p^{o}	Relative pressure	22
PSD	Pore size distribution	56
RT	Room temperature	57
RVR	Regenerated viscose rayon	18
SB	Sec-butanol	44
SEM	Scanning electron microscopy	33
SGA	Sol/gel alumina	8
STP	Standard temperature and pressure	28
TG	Thermogravimetry	17

CHAPTER 1 : INTRODUCTION

1.1 Activated Carbon Cloth

The element carbon in its pure form has three major allotropic forms, diamond, hexagonal graphite and rhombohedral graphite. As well as these highly crystalline forms many other types of lesser order and of lower purity exist, which often exhibit distinctive and useful chemical and physical properties. Chars and cokes are examples of the latter group of solid carbons, which are produced by the pyrolysis of solid organic materials of mineral, animal, vegetable or synthetic origin. A char may be distinguished from a coke in that the former does not pass through a molten or liquid-crystalline stage during pyrolysis. As a result the shape of the char precursor is conserved during pyrolysis, the resulting char being "pseudomorphous" with respect to the starting material (Kochling et al,1983). Activated carbon cloth is an example of a char. Its preparation and properties are described in Section 2.2 of this thesis.

The great industrial and technological importance of activated carbon is primarily due to its highly developed internal pore structure which renders it extremely useful as an adsorbent in gas-phase and liquid-phase applications (Cheriminisoff and Morresi,1978; Carrubba et al,1984). Activated carbon cloth has been shown to offer certain advantages over most powdered and granular forms of activated carbon, with potentially a higher adsorption capacity and rate of adsorption (Maggs et al,1977) and also a higher adsorption affinity (Atkinson et al,1982).

1.2 Sol/Gel Processing and Coatings

The surface properties of many materials can be dramatically altered by the application of a ceramic coating. Conventional ceramic processing, involving densification of powders (Alford et al,1986), is energy intensive in that high temperatures (>1100^{o}C) are required, and

the process cannot be readily adapted to coating. However other methods of producing ceramics that can be readily adapted to coating are also in use. One such technique that will be described in Section 2.1 utilizes the organo sol/gel route (Segal,1985). Metal organic compounds, such as alkoxides, are used as the starting material. The metal organic compound may be converted to the oxide by hydrolysis and/or thermal degradation. Another feature of this method is that because metal linkages are forged at a molecular level the subsequent oxide formation occurs at a significantly lower temperature (500^{o}C) than for conventional powder mixing. However, the main advantage of the sol/gel route in the present context arises from the nature of liquid intermediate, in that it can readily be applied as a coating. The applications of sol/gel processing to coating phenomena have been many and varied, and include anti-reflectance (Mukherjee and Lowdermilk,1982), fibre (Guglielmi and Maddalena, 1985), and electronic component (Kordas et al,1985), coatings. The sol/gel technique is not restricted to a limited number of oxides. Indeed Yoldas (1977) concluded that , "high purity submicron-sized oxides of almost any element e.g. Hf, Y, Ce, Th, Ti, Sn, Ge, V, Nb, Ta, Fe, (as well as Zr and Al) can also be obtained from their alkoxides". The resultant oxides have an unusually small particle size, often less than 5 nm.

Sol/gel alumina (SGA) is the focus of the present work. The preparation of alumina by this route is described in detail in Sections 2.1 and 3.1.1. SGA has been used as an antireflective coating (Yoldas, 1980) for glass surfaces, a desiccant in semiconductor packages (Bonis, 1974) and for the mechanical and thermomechanical protection of dense alumina substrates (Gruninger et al,1986). Of more direct relevance to the present project was the work of Lannutti and Clark (1984) which described the coating of SiC and silicate fibres with SGA. Although their investigation was preliminary in nature they concluded that the

method showed promise for the fabrication of ceramic-ceramic composites.

SGA has also made an impact on the field of membrane technology (Leenaars et al,1986). In this application supported membranes were prepared by dipping one side of a porous ceramic support into an "alumina" sol. The sol was sucked into the support by capillary forces exerted by the pores. The resulting alumina membranes have been shown to be useful in liquid/liquid separations (Leenaars and Burgraaf,1985). The small pore size of the resultant alumina (<3nm) should also allow **gas** separations at low temperatures (20-400^{o}C). Indeed it was reported that specific interactions between the alumina membranes and CO_2 and H_2O were observed after the inclusion of ions in the alumina network. The identity of these ions was not reported, but they were presumably highly charged cations.

1.3 Objectives of the Present Study

The prime aim of the present work was to modify the surface chemistry of activated carbon cloth in order to broaden its range of application. For this purpose the impregnation, or deposition, of alumina on activated carbon cloth was investigated. A number of methods of depositing alumina were employed. Preliminary work involving impregnation of carbon cloth with aluminium salt solutions and also chemical vapour deposition is reported in Chapter 4. The deposition of alumina on carbon cloth via a sol/gel route is reported separately.

Despite the many uses of sol/gel alumina its application to carbon substrates has not been reported in the literature. The electroadsorption of alumina particles on fibrous carbon has recently been described (Cohen et al,1987), however this work involved the deposition of relatively large (ca. 1 micron) particles on the outer surface of the fibres (8-10 micron diameter). In the present work the distribution of alumina about an activated, and therefore porous, carbon

cloth was investigated. The preparation and characterisation of the sol/gel alumina and carbon phases is reported in Chapters 5 and 6, respectively. This is followed by a description of the preparation and characterisation of sol/gel alumina/carbon composites in Chapter 7, the adsorption properties of the composite materials being discussed with reference to the adsorption of the individual components. Finally, the application of the composite material to CO_2 removal was investigated. The nature of the interaction between the sol/gel alumina/carbon composites and gaseous CO_2 is reported in Chapter 8.

CHAPTER 2 : REVIEW

2.1 Sol/Gel Alumina

The aim of the present project was to modify the surface chemistry of activated carbon cloth by the deposition of alumina. In order to satisfy this aim the alumina phase, or a suitable precursor, must at some stage "wet" the carbon cloth. A major section of this project involved the impregnation of activated carbon cloth with an aluminium hydroxide sol (AlO(OH)). An oxide sol may be prepared by dispersion of a suitable powder in an aqueous medium (Ramsay et al,1978; Avery and Ramsay,1985). Alternatively oxide sols may be prepared via the hydrolysis of an alkoxide precursor (Segal,1985). The preparation of alumina using this latter method, known as organo sol/gel processing, is employed in the present work.

The production of alumina using the organo sol/gel route involves four basic steps (Yoldas,1975,a):

(i) Hydrolysis of an aluminium alkoxide.

(ii) Peptization of the resultant hydroxide to a clear sol.

(iii) Gel formation.

(iv) Heat treatment of gel to yield alumina.

2.1.1 Hydrolysis of Aluminium Alkoxide

Aluminium alkoxides, $Al(OR)_3$, hydrolyse vigorously with water to form hydroxides. Several important forms of the hydroxides exist corresponding to the stoichiometries AlO(OH) and $Al(OH)_3$. The hydrolysis of an aluminium alkoxide initially yields the monohydroxide. The stability of the monohydroxide has been found (Yoldas,1973) to be dependent upon the temperature at which hydrolysis is carried out.

The initial hydrolysis of an aluminium hydroxide may be described by:

$$Al(OR)_3 + H_2O \rightarrow Al(OR)_2(OH) + ROH$$

This exothermic reaction proceeds rapidly and further hydrolysis is accompanied by polymerisation:

$$2\ Al(OR)_2(OH) + H_2O \rightarrow OR\text{-}Al(OH)\text{-}O\text{-}Al(OH)\text{-}OR + 2ROH, \text{ etc}$$

The expressions above are not presented as exact formulae, but as a guide only, as aluminium alkoxides are known to be tetrameric in structure (Robinson and Peck,1935).

Hydrolysis of the aluminium alkoxide in hot water (>75^{o}C) results in the formation of the crystalline monohydroxide, boehmite, which is relatively unaffected by aging. X-ray diffraction and electron microscopic analysis (Yoldas,1973) have shown that hot water hydrolysis results in the production of fibrils of boehmite approximately 0.1 micron in length. However hydrolysis at room temperature results in the formation of an amorphous monohydroxide which converts to the trihydroxide (bayerite) in its mother liquor. In the present context this distinction is very important in that only the crystalline monohydroxide, boehmite, can be subsequently peptised to form a sol. Therefore high temperature hydrolysis is employed to prevent bayerite formation. The alkoxides normally used for the preparatiion of boehmite sols are aluminium isopropoxide ($Al(OC_3H_7)_3$) and aluminium sec-butoxide ($Al(OC_4H_9)_3$). The former is a white solid (d. 250^{o}C) and the latter a viscous liquid. In practice the hydrolysis of the alkoxide is normally carried out with a water:alkoxide mole ratio of 100:1, the large excess of water helping to contain the exothermic nature of the reaction (Yoldas et al,1979). An opaque slurry is formed.

2.1.2 Peptisation of Boehmite

To peptise the slurry of boehmite a critical amount of acid must be introduced, and the slurry must be maintained at a temperature in excess of 80^{o}C for a considerable period of time. Yoldas (1975,a) has

systematically investigated the peptisation of the boehmite slurry with a range of sixteen acids, both mineral and organic. Only five acids were found to be capable of successfully peptising the boehmite slurry : nitric, hydrochloric, perchloric, acetic and trichloroacetic. It was concluded (Yoldas,1975,a) that for successful peptisation two general requirements must be satisfied:

(i) The anion of the acid must at most be only weakly complexing with respect to aluminium.

(ii) The acid must be sufficiently strong to produce the necessary charge effect in relatively small quantities.

For the five successful peptising acids an acid/hydroxide mole ratio in excess of 0.03 was required for complete peptisation. Although excess acid does not inhibit the peptisation stage, for the resultant gel to maintain its integrity during subsequent drying and heat treatment a mole ratio in the range 0.03-0.10 is required. The acid addition alone is not sufficient to cause peptisation of the boehmite slurry, and heating (>80^{o}C) is required until a clear boehmite sol is formed. The rate of peptisation increases dramatically with temperature, with temperatures approaching 100^{o}C allowing complete peptisation in hours, while at 80^{o}C peptisation may take weeks.

Complete peptisation results in the production of a clear boehmite sol which scatters blue light. The optical transparency of the sol is due to the extremely small particle size of the boehmite units. The sol particle sizes have been estimated (Yoldas et al,1979) by Scanning Transmission Electron Microscopy to be in the range 2.5 to 10nm.

2.1.3 Gel Formation

The formation of a gel from a sol requires that the transitory motion of the colloidal particles be arrested. A traditional method of gelation (Kruyt,1952) requires the addition of electrolyte so that the interparticle repulsion can be overcome. Alternatively the sol may be gelled by reducing its volume (by evaporation) until the electrolyte already present (after acid addition) is sufficient to cause gelation. The latter method is preferred because it results in a lower gel volume giving the gel its best chance of maintaining its integrity during subsequent drying and heat treatment. The minumum gel volume corresponds to an acid/hydroxide mole ratio of 0.07 (Yoldas,1975,b).

The boehmite gel is best dried at room temperature in a desiccator to minimise cracking. Drying occurs in two stages. Initially the gel shrinks to its final size of about 65% of its original dimensions (for the minimum gel volume). The rigidity of the gel at this stage prevents further shrinkage and water is then lost internally with the consequent formation of porosity.

2.1.4 Heat Treatment of Dried Boehmite Gel

The thermally induced transition of boehmite (γ-AlO(OH)) to alumina has been investigated by several workers. Wilson et al (1980, 1981) concluded after a study utilising electron microscopic and X-ray techniques that, "the dehydration of crystalline boehmite is topotactic and produces γ-Al_2O_3 with a well-defined pore structure". The initial boehmite crystal size used was approximately 5 micron. However the primary crystallite size of boehmite resulting from Yoldas' sol/gel route is significantly less (<10nm) than this value, so that the conclusion of Wilson et al may not be strictly applicable. Leenaars et al (1984) and Yoldas (1975,a) have also used electron microscopic and

X-ray techniques to study the transition of sol/gel boehmite to alumina. Leenaars, in particular, found that due to the broadness of X-ray diffraction peaks, no distinction could be made as to whether γ-Al_2O_3 or δ-Al_2O_3 was formed from γ-AlO(OH).

A thermogravimetry (TG) curve for the dried gel is reproduced in Figure 2.1 (courtesy Yoldas,1975,b). Temperatures in excess of 200°C are required to initiate dehydration while transition to γ/δ-alumina is complete at 500°C. Yoldas (1975,b) found that the TG and evolved gas analysis (EGA) curves were unaffected by the heating environment (whether N_2, air or vacuum) although it was observed that the transition to γ/δ-alumina occurred at slightly lower temperatures under vacuum. The effect of heating environment on the porosity of the resultant alumina is discussed in some detail in the present work (Chapter 5). Extreme care must be taken during heat treatment in order to maintain the monolithicity of the dried gel. However coatings and films show much less tendency to crack.

FIGURE 2.1 - Weight Loss During Heat Treatment with Heating Rate 10°C/min. (courtesy Yoldas,1975,b)

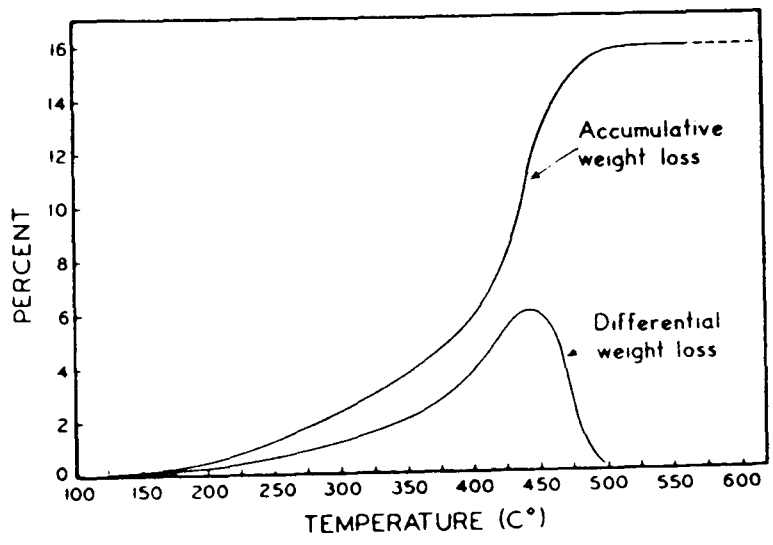

2.2 Activated Carbon Cloth

It is not intended in this thesis to present an exhaustive review of carbon chemistry and of gas/carbon reactions which form the cornerstone of activated carbon production. These subjects have been reviewed by Freeman (1986) and Roberts (1988). In this section the factors affecting the porosity of activated carbon cloth in the form utilized in the present work are discussed.

The production of activated carbon cloth from regenerated viscose rayon (RVR) involves several stages:

(i) impregnation,

(ii) carbonisation,

and (iii) activation.

While all three stages have a bearing on the porosity of the final material, it is the first and third that are of prime relevance.

2.2.1 Impregnation

The carbonisation and activation of an unimpregnated sample of RVR results in the production of an exclusively microporous (pores <2nm diameter) material (Hayes,a). However RVR is usually impregnated with inorganic halides (Capon and Maggs,1976) so as more control can be exercised on the subsequent carbonisation and activation stages. The fire-retardant properties of these impregnants increase the char yield after the carbonisation stage thus enhancing the mechanical properties of the final material. The impregnation of RVR with a solution of zinc, aluminium and ammonium chlorides (3% w/v of each - "3/3/3 mix") also results in the production of a predominantly microporous product after carbonisation and activation (Freeman,1986). This microporosity is generally thought to be dependent on the nature of the precursor itself. More recently it has been discovered that the impregnation of the

precursor with borate and phosphate salts (Freeman,1986; Freeman and Gimblett,1988) can lead to the production of mesoporosity. This mesoporosity does not replace the more typical microporosity of the product, rather the wider pore system is superimposed upon the microporous network. The porosity of activated carbon cloth may then be markedly affected by the nature of the precursor impregnants.

2.2.2 Carbonisation

Carbonisation has been described (Kochling et al,1982) as "a process of formation of material with increasing carbon content from organic material, usually by pyrolysis, ending with an almost pure carbon residue at temperatures up to about 1600 K". In other words the carbonisation stage involves the removal from the precursor of a large proportion of the non-carbon elements.

The carbonisation (and activation) of RVR is generally performed in a furnace that is flushed with gas (typically N_2, CO_2 or steam). The temperature of the furnace is ramped to an elevated temperature (typically 850^{o}C) during carbonisation (and maintained at this temperature during subsequent activation). Both batch (Simpson,1980) and continuous (Bailey et al,1973) processes have been developed. If the carbonisation stage is to be separated from that of activation, then N_2 is used during carbonisation and activation commences with the changeover to an oxidising gas such as CO_2. If CO_2 is to be used throughout the carbonisation and activation stages then activation would commence as soon as the temperature of the carbonised material is sufficiently high (>700^{o}C). Carbonisation of RVR is essentially complete at temperatures lower than 700^{o}C. The carbonisation of RVR, involving the removal of a considerable proportion of the non-carbon elements, results in a fairly drastic weight loss. Carbonisation

yields (Freeman,1986) of unimpregnated RVR are approximately 16%, and for RVR impregnated with metal chlorides (3/3/3 mix), 32% (heating rate 10^{o}C/min. to 850^{o}C). The carbonised material produced from RVR is non-porous. While most precursors yield non-porous products after carbonisation certain precursors do yield products having molecular sieve characteristics.

2.2.3 Activation

Activation has been described (Lewis and Metzner,1954) as, "any process which selectively removes the hydrogen or hydrogen-rich fractions from a carbonaceous raw material." The effect of activation on carbonised RVR is to produce a vast porous network within the volume of the solid. The amount of porosity can be controlled by altering the period of activation. In general the pore volume increases with the activation period. The **type** of porosity is affected by the nature of the precursor impregnants as described in Section 2.2.1.

Mesoporous carbon cloth, as used in the present work (resulting from phosphate impregnation of RVR), is typically activated to 70%. As a result the final activated carbon weighs less than 10% of the weight of the rayon precursor. The mechanical strength of such a material is therefore quite remarkable.

2.3 Characterisation of Pore Structure by Physical Adsorption

2.3.1 General

If a solid material contains within its bulk a network of cavities and channels then it may be said to possess pore structure. **Porosity** may be defined (Gregg and Sing,1982) as the "ratio of the volume of open pores to the total volume of the solid," and is generally expressed as a percentage. The nature of porosity with respect to both

pore size and pore shape has in practice been found to be extremely variable, both within and between materials. Pores may be conveniently classified (Sing et al,1985) according to their pore width:

micropores < 2nm

mesopores 2-50nm

macropores > 50nm

The precise boundary between the pore types is necessarily arbitrary, however the distinction between the three types of pore arises from the difference in the process of physical adsorption in each case. Indeed, one of the most important tools for the characterisation of porous solids is the measurement of the physical adsorption isotherm.

2.3.2 The Adsorption Isotherm

Physical adsorption has been defined (Gregg and Sing,1982,p.2) as, "the enrichment (ie. positive adsorption or simply adsorption) or depletion (ie. negative adsorption) of one or more components in an interfacial layer". When molecules of a gas or vapour (the **adsorptive**), are brought into contact with a solid surface (the **adsorbent**), the solid removes adsorptive molecules from the gas phase as a result of the attractive forces between the adsorptive and adsorbent, until an equilibrium state is reached. Adsorbed molecules are collectively termed **adsorbate.**

The quantity of gas taken up by the adsorbent is proportional to the mass (m) of the sample, and also depends on the temperature (T), the pressure (p) of the vapour and the nature of both the adsorbent and adsorptive. The quantity of gas adsorbed (n) expressed in moles per gram of solid is,

$$n = f(p, T, \text{adsorptive}, \text{adsorbent})$$

For a given adsorptive/adsorbent combination at a fixed temperature the

equation above simplifies to

$$n = f(p)_T$$

For convenience, when the temperature is below the critical temperature of the adsorptive, the expression

$$n = f(p/p^o)_T$$

is used, p^o being the saturated vapour pressure of the adsorptive.

This last expression is known as the adsorption isotherm. Many thousands of adsorption isotherms have been experimentally determined and reported in the literature. The vast majority of these isotherms may be classified into 6 types, as shown in Figure 2.2 below. Types I to V follow the original "BDDT" classification of Brunauer et al (1940), Type VI being added subsequently. Each of the isotherms corresponds to a particular adsorption process or combination of processes. Each isotherm type will be discussed in Section 2.3.5.

FIGURE 2.2

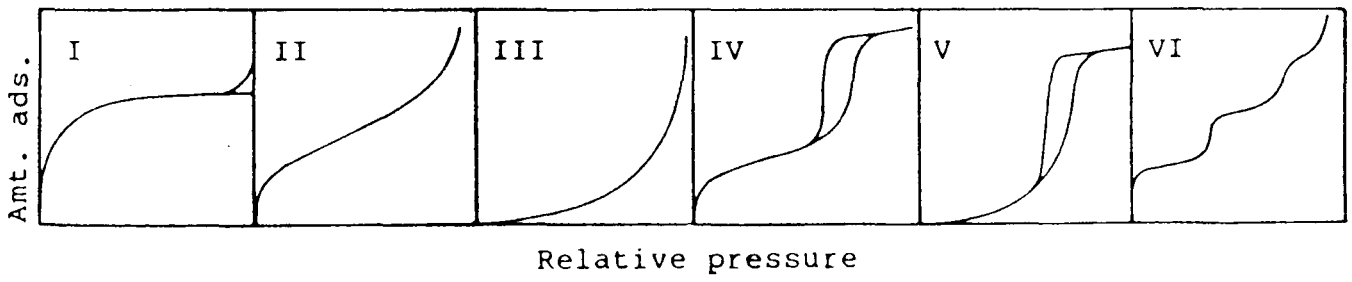

2.3.3 Adsorption Forces

The adsorption isotherm arises from interaction at a molecular level between the adsorbent and adsorptive and also from adsorbate/adsorbate interactions. Let us first consider a pair of atoms. The forces responsible for adsorption processes include attractive **dispersion** forces and also short-range repulsive forces. The former arise from the rapid fluctuations in electron density within

an atom which are then capable of inducing an electrical moment in another atom. Short-range repulsive forces result from the interpenetration of electron clouds of neighbouring atoms. This combination of forces has been described mathematically (Lennard-Jones,1937) for a pair of atoms as follows:

$$\varepsilon(r) = -Cr^{-6} + Br^{-12}$$

where $\varepsilon(r)$ is the total potential energy at separation r, and C and B are constants associated with the dispersion and the repulsive interactions, respectively. The general form of $\varepsilon(r)$ as a function of r is shown in Figure 2.3.

FIGURE 2.3

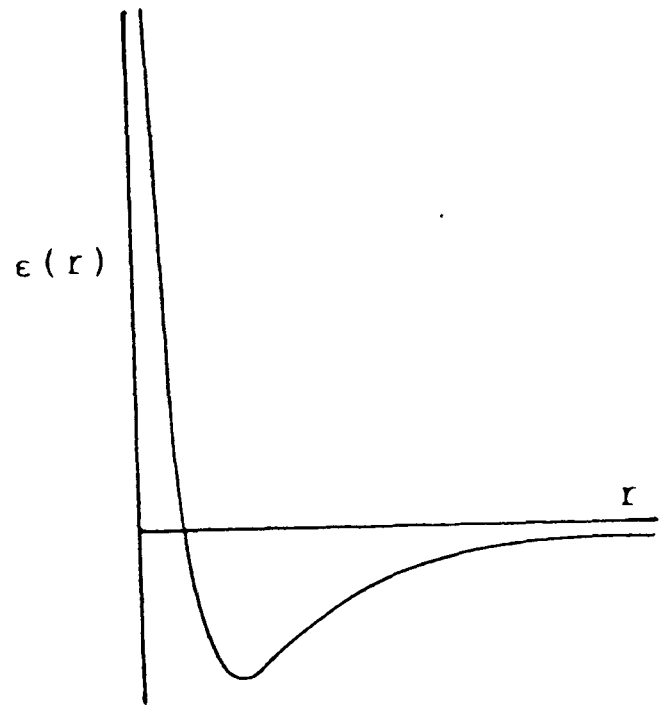

Let us now consider the interaction between a gas molecule and a solid surface. Firstly the gas molecule will interact with more than one atom of the solid. The situation is further complicated if either the gas or solid is polar in nature. If the solid consists of ions, or contains polar groups or π-electrons, it will give rise to an electric field capable of inducing a dipole in the gas molecule. If the gas

molecule possesses a permanent dipole or quadrupole moment a further contribution to the overall interaction energy will be made. The following general expression has been derived (Barrer,1966) to take account of these factors:

$$\Phi(z) = \Phi_D + \Phi_p + \Phi_{F\mu} + \Phi_{FQ} + \Phi_R$$

where $\Phi(z)$ is the overall interaction energy of a molecule a distance z from the surface, Φ_D and Φ_R correspond to the attractive and repulsive terms in the Lennard-Jones equation, Φ_P to the interaction energy resulting from an induced dipole in the molecule, $\Phi_{F\mu}$ to the interaction energy resulting from a permanent dipole and Φ_{FQ} to the interaction energy resulting from a quadrupole moment of the molecule.

Although the above equation can only be applied in practice as a rough appproximation, the general form of $\Phi(z)$ as a function of z resembles that for two isolated atoms (see Figure 2.3). The contributions from dispersion and repulsion forces are always present while the effect of the other terms depends upon the nature of both the adsorbent and adsorbate involved.

2.3.4 BET Method

In characterising the nature of a porous solid it has been found useful to determine its monolayer capacity, and subsequently its surface area. The monolayer capacity is defined as the amount of adsorbate required to completely cover the surface of a solid with a single layer. The specific area of the solid may then be calculated with the aid of an appropriate value for the molecular cross-sectional area occupied by an adsorbate molecule.

However, to obtain the monolayer capacity the isotherm must be interpreted in quantitative terms. The best known and most useful method for doing so is that of Brunauer, Emmett and Teller (BET,1938).

The BET treatment is based on a kinetic model of the adsorption process first put forward by Langmuir (1916), with the surface of the solid being regarded as an array of adsorption sites. The Langmuir equation described the adsorption of a single layer of adsorptive:

$$\frac{n}{n_m} = \frac{Bp}{1+Bp}$$

where n is the amount adsorbed (in moles) per g of adsorbent, n_m the monolayer capacity, p the pressure and B an empirical constant. Langmuir considered the adsorption of second and higher molecular layers but the equation he derived was of such complexity that it has been little used.

The BET method was based on the multilayer model of Langmuir, but introduced several simplifying assumptions:

(i) that the heat of adsorption is equal to the molar heat of condensation in all layers except the first

(ii) that the evaporation - condensation conditons are identical in all layers except the first

(iii) that when $p = p^o$ the adsorptive condenses to a bulk liquid on the surface of the solid, the number of layers becoming infinite.

The BET equation may be written

$$\frac{p}{n(p^o-p)} = \frac{1}{n_m c} + \frac{(c-1)}{n_m c}\frac{p}{p^o}$$

where c is the BET constant which is related exponentially to the heat of adsorption for the first layer, and the other terms are as defined previously. The equation is usually applied by plotting $p/(v(p^o-p))$ against p/p^o where v is the volume of gas adsorbed (at a given relative pressure), expressed in cm^3/g at STP. The resulting plot has been found to have a linear region for a limited range of

relative pressures for which the slope (s) and intercept (i) allow the calculation of the monolayer capacity and the BET constant:

$$n_m = \frac{1}{s+i} \quad ; \quad c = \frac{s}{i} + 1$$

The region of linearity was initially expected to cover the relative pressure range from 0.05 - 0.35 (Brunauer et al,1938). In practice however the linear range has often been found to be significantly less than this and also to be shifted to lower relative pressures. The major criticisms of the BET model are that surface heterogeneity and lateral adsorbate - adsorbate interactions are not taken into account. For certain isotherm types application of the BET method leads to an erroneous value of the specific surface area (see Section 2.3.5.1). Despite these criticisms, for certain types of isotherm the method does yield sensible values of the specific surface area and the method does enjoy widespread use.

2.3.5 Classification of Isotherms

2.3.5.1 Type I

The Type I adsorption isotherm (Figure 2.2) is characterised by a steep initial uptake of adsorptive followed by a more gentle rise to a plateau extending to high relative pressures. This isotherm is characteristic of adsorption in micropores. Application of the BET equation to the Type I isotherm yields an unrealistically high estimate of the specific surface area.

To account for such findings it has been proposed (Dubinin and Zaverina,1949) that adsorption in micropores takes place by a process of volume filling rather than by surface coverage. The most convincing evidence in support of this view relates to the "Gurvitsch-rule" (Gurvitsch,1915) whereby the volumes occupied by a variety of

adsorbates, calculated as liquid volume, have been found to agree to within a few per cent for a given solid.

The enhanced adsorption in very narrow pores is thought to be due to overlapping force fields arising from the close proximity of the pore walls. The **apparent** BET surface areas may still be used as a fingerprint parameter for the analysis of Type I isotherms, as it has been shown (Freeman and McLeod,1983) that a linear relationship exists for a wide range of microporous carbons between this quantity and the total pore volume.

2.3.5.2 Type II, IV

A Type II isotherm (see Figure 2.2) is typically obtained for a non-porous solid. The uptake of the adsorptive results in the coverage of the external surface of the adsorbent. This type of isotherm lends itself fairly readily to BET analysis providing the knee of the isotherm is fairly well defined.

Type IV isotherms follow the path of the Type II isotherm at relative pressures less than 0.4 however at higher relative pressures the adsorption is enhanced relative to that for a non-porous sample. On measuring the desorption isotherm a hysteresis loop is often defined. This type of behaviour is generally associated with mesoporous solids. The IUPAC (Sing et al,1985) classification of hysteresis loops is reproduced below:

FIGURE 2.4

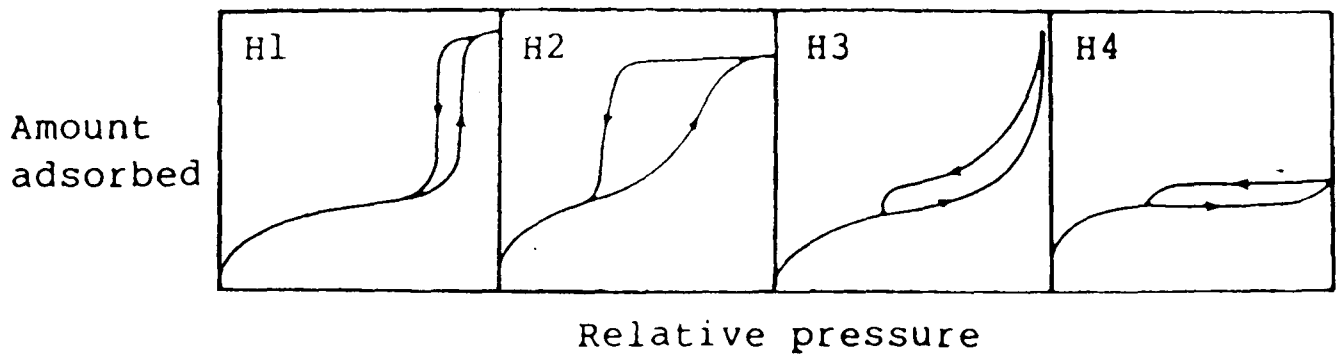

The characteristic shape of the Type IV isotherm is associated with the phenomenon of capillary condensation of the adsorbate. It has been established (Zsigmondy,1911) that capillary condensation arises because the equilibrium vapour pressure (p) over a concave meniscus must be less than the saturation vapour pressure (p^o) at the same temperature. The condensation of a vapour in the pores of a solid is then possible even though the relative pressure is less than unity. Capillary condensation is described quantitatively by the Kelvin equation :

$$\ln (p/p^o) = -2\gamma V_L/(RTr_m)$$

where γ, V_L and r_m are respectively the surface tension, molar volume of liquid adsorptive and radius of curvature of the meniscus.

A number of procedures for the computation of mesopore size distribution have been based on the Kelvin equation. The total pore volume of a mesoporous solid may be calculated from the amount adsorbed at $p/p^o = 0.95$. Obviously if the hysteresis loop is type H3 (see Figure 2.4) it is impossible to estimate this value, while for Types H1 and H2 this value can be fairly accurately determined. The amount adsorbed, usually plotted in units of cm^3 of adsorptive (STP), needs to be converted to a liquid volume by use of the liquid density at the appropriate temperature.

The alumina isotherms presented in Chapter 5 exhibit Type IV behaviour.

2.3.5.3 Type III, V

Type III and V isotherms (see Figure 2.2) are obtained when the interaction between the adsorbate and adsorbent is very weak. The Type III isotherm is characteristic of a weak interaction with a

non-porous solid while the Type V behaviour occurs for a microporous or mesoporous solid. The adsorption of water vapour on an activated carbon cloth (Chapter 6) produces Type V behaviour.

The BET procedure for evaluation of the monolayer capacity is not valid for Type III and Type V isotherms as the isotherm does not have a distinct "knee". Analysis of these types of isotherm is normally performed by comparison with standard isotherms.

CHAPTER 3 : EXPERIMENTAL

3.1 Preparation of Materials

3.1.1 Sol/Gel Alumina

Alumina was prepared using the method of Yoldas as described generally in Section 2.1. The **specific** details of preparation were as follows. Deionized, distilled water (440cm^3) was heated on a stirrer hot plate, in a conical flask (1000cm^3,B24 tapered socket), to a temperature of 75-80^{o}C. The contents of the conical flask were stirred by means of a 5 cm PTFE coated stirrer bar. Aluminium sec-butoxide (ASB,60g,Aldrich,tech.) was then added with vigorous stirring. The temperature of the resulting dispersion was maintained at 80^{o}C for a period of 20-30 minutes, after which hydrolysis of the ASB was complete. Concentrated nitric acid (1.53g) was then added. The volume of each reagent corresponded to a water:ASB:acid mole ratio of 100:1:0.07. After 5 minutes the stirrer bar was removed and the conical flask was stoppered (B24 male) with the aid of the appropriate PTFE sleeve. The stopper was secured with the aid of hooks and springs and the sealed conical flask was then transferred to an oven and maintained at 95^{o}C for 1 week. At the end of this period a clear boehmite sol (AlO(OH), 3-4%w/v) was obtained. In this form the sol was quite stable, no apparent aging occurring even though some sols were more than one year old.

To prepare a gel aliquots of a boehmite sol were transferred to a petri-dish (typically 5 cm diameter) and evaporation was commenced on a stirrer hot plate. A small stirrer bar (1.2cm) was used to help preserve thermal equilibrium throughout the sol during evaporation, so that the gelling volume could be minimised. This stirrer bar was removed just prior to the onset of gelation. At the gel point (typically corresponding to ca.25-30%w/v AlO(OH)) the petri dish was transferred to a vacuum desiccator. The drying of the gel (1 week) was

accompanied by considerable shrinkage and cracking. Nevertheless, pieces of dried gel with an area of approximately $10cm^2$ (thickness ca. 0.1cm) were obtained. Pieces of the dried gel were then heated (500^oC) to yield the final alumina. The heating environment and schedules were varied, the specific details of which are reported in Chapter 5.

3.1.2 Mesoporous Carbon Cloth

Both cloths used (designated A and B) were examples of mesoporous carbon cloth prepared from phosphate impregnated (solutions of 3%w/v $NaH_2PO_4.2H_2O$) viscose rayon. The rayon was also impregnated with 3%w/v solutions of ammonium, zinc and aluminium chlorides prior to carbonisation.

Cloth A was prepared at the Chemical Defence Establishment (CDE, Porton Down) in a continuous furnace process (Bailey et al,1973) under flowing CO_2. Cloth B was prepared batch-wise at Brunel University (with the help of Dr. J. Freeman) in a vertical tube furnace of 15cm diameter. In the latter case a furnace heating rate of 10^oC/minute to 850^oC was used with a CO_2 flow rate of 30 litres/minute throughout carbonisation and activation. An activation period of 90 minutes at 850^oC was required to produce a 70% activated cloth.

3.1.3 Sol/Gel Alumina/Carbon Composites

An aliquot of the boehmite sol (ca. $100cm^3$) was transferred to a high walled petri-dish (8cm diameter). The sol was evaporated down to the appropriate concentration on a hot plate with the aid of a small stirrer bar (1.2cm). To obtain the maximum level of boehmite loading the sol was evaporated down almost to the gel point prior to immersion of the carbon cloth. Lower loading levels were obtained by interrupting the evaporation at an earlier stage.

A piece of carbon cloth was cut to 5cm x 5cm and vacuum desiccated prior to weighing. The cloth was then immersed in the boehmite sol for 1 minute, removed and drained before transferral to a filter paper (or glass plate) for drying. Initially drying was carried out at room temperature in a vacuum desiccator (ca. 3 days). Drying was performed at 55^{o}C (oven) when it was discovered (by SEM) that the boehmite distribution was unaffected by this treatment, to hasten composite production. After drying and vacuum desiccation the final composite weight was determined. The dried composite was then heated under vacuum to produce the final alumina/carbon composite.

The concentration of the boehmite sol used for impregnation was determined by removal of a 1.00cm^{3} aliquot just prior to immersion of the cloth. This aliquot was evaporated to dryness on a pre-weighed watch glass (5cm diameter) at 55^{o}C (ie. under identical drying conditions to that used for the composites). The final weight was measured after vacuum desiccation and the boehmite concentration calculated.

3.2 Characterisation of Materials

3.2.1 Nitrogen Isotherms

A Carlo Erba 1800 series Sorptomatic was used for the determination of all nitrogen isotherms. This instrument is semi-automatic and utilises a volumetric dosing system. A diagram of the vacuum and gas-dosing circuits is reproduced in Figure 3.1. Samples were initially weighed into a sample burette (Figure 3.2). Outgassing of samples was carried out on a separate vacuum line, incorporating rotary and diffusion pumps, for a period in excess of 16 hours to a residual pressure of $<10^{-4}$ Torr. The outgassing temperature used was 110^{o}C for alumina and alumina/carbon composites and 250^{o}C for carbon

cloths (unless otherwise specified). After outgassing, the sample burette was sealed and reweighed to determine the weight loss of the sample. The weight loss due to removal of air was taken into account in calculating the outgassed sample weight. The sample burette was then transferred to the Sorptomatic for the determination of the N_2 isotherm. Oxygen-free nitrogen (>99.99%) was used as the adsorptive, the isotherms being measured at liquid nitrogen temperature (77K). Adsorption and desorption branches of the isotherm were measured. Dead-space calibrations were made by admitting a series of doses of nitrogen to an outgassed, empty sample burette. A calibration plot was drawn using the resulting equilibrium pressures. A correction for the sample volume was made using the instruments volume compensator and by assuming a sample density of $2.0 g/cm^3$.

3.2.2 Water Isotherms

The sorption of water was measured gravimetrically using a spring balance of the M^{C}Bain-Bakr (1926) type with a fused quartz spring. The apparatus (Figure 3.3) had been designed and constructed after that of Baker (1974), and consisted essentially of the following:

a) A diffusion pump (D) backed by a double stage rotary pump (R) capable of pumping the high vacuum ($<10^{-4}$ Torr) line through a liquid nitrogen trap.

b) A fused quartz spring (Q) with a sensitivity of 19.53 cm/g suspended in a balance case (B).

c) A silica sample bucket (S) suspended from the base of the spring with the aid of a thin silica rod (P).

d) A removable silica tube (H) that was used to seal the base of the vacuum line and allow sample changeover between isotherms.

e) A water jacket to maintain the temperature of the sample and spring at 298.2+/-0.1K via the passage of thermostatted water.

f) A water reservoir.

g) A cathetometer (C) that enabled the vertical extension of the spring to be measured (precision $1x10^{-5}$m) relative to a fixed point (FP) on the balance case.

h) A pressure transducer (PT)(Bell and Howell type 4-353) which was a strain gauge type giving a reported precision of <0.5% full scale deflection in both increasing and decreasing pressure cycles (Curtis,1964). The transducer was coupled to a digital voltmeter (d.v.m.) where the output was monitored in millivolts (mv). The response of the transducer/d.v.m. combination was linear and reversible over the pressure range used. The calibration factor was 1.19mmHg/mv.

Greaseless stopcocks (G.Springham and Co.Ltd.) were used throughout the apparatus. The water reservoir was filled with conductivity water which was subjected to repeated freeze-thaw cycles before use. The spring was calibrated in air by hanging weights (Cahn Instruments Co. Ltd. calibration weights) to cover an extension range greater than that in normal use. The spring was found to behave linearly and elastically over this range. A buoyancy correction was applied only to the initial position of the sample bucket prior to the admission of water vapour. Otherwise buoyancy corrections were found to be negligible and were therefore not taken into account.

For a typical isotherm a weight of sample (ca. 0.2g) was added to the sample bucket. The sample was then outgassed at 110^{o}C overnight to a residual pressure of $<1x10^{-4}$ Torr. The height of the sample bucket was measured prior to the introduction of water vapour so as the outgassed sample weight could be calculated. The sample chamber was

then isolated and water vapour was introduced. After each introduction and subsequent equilibration (>6 hours) the position of the bucket was determined (cathetometer,C) and the residual pressure noted (pressure transducer,PT). The sample and spring temperatures were regularly checked throughout isotherm determination. A series of adsorption "doses" (typically >12) was made up to relative pressures of 0.85. The rotary pump was then employed to remove water vapour allowing the measurement of the desorption branch of the isotherm. The uptake of water was determined in units of mg/g of sample (outgassed weight) and plotted against relative pressure (taking account of the saturated vapour pressure of water at the sample temperature) to yield the water sorption isotherm.

3.2.3 Scanning Electron Microscopy (SEM)

All SEM and electron microprobe analyses were carried out at the Experimental Techniques Centre (ETC) at Brunel University. A Cambridge Stereoscan S250 was used.

3.2.4 Gas Chromatography

Equipment and Gases

The gas chromatograph (GC) used was a Carlo Erba 6300 Vega (II) coupled to a Carlo Erba thermal conductivity detector (HWD430). The detector output was fed to an integrator (Pye Unicam DP88) and a chart recorder (Servoscribe RE541). The chromatograph was fitted with Packed Column Injectors. The detector base body temperature and filament temperature were set to 100°C and 200°C, respectively, for all analyses. The carrier gas used was ultra high purity (UHP) helium (>99.999%, Air Products) and the adsorptive employed was gaseous CO_2 (>99.99%, Air Products) which was injected directly onto the column using a range

of Hamilton gas tight syringes. The syringes were fitted with Chaney adaptors to aid the reproducibility of the injected volumes. The column flow rates were measured with the aid of a soap bubble flow-meter.

Column Design

The column consisted essentially of a length (5.0cm) of stainless steel (S/S) tubing (O.D. 1/4", I.D. 0.183"). At one end of the tube the outside edge was removed to leave a sharp circular edge (see insert, Figure 3.4) similar to that of a cork borer.

In this way layers of alumina/carbon composite (or unimpregnated carbon cloth) could be cut to the exact internal diameter of the tube. As successive layers were cut the "column" retreated up the tube. Columns of up to 50 layers of material were made in this way. The tube was weighed before and after packing to determine the weight of packing material incorporated. The tube was then inserted in a 1/4"-1/8" reducing union (Swagelok). A 1/4" S/S sinter was placed at the base of the tube to prevent movement of composite layers through the union during subsequent handling. The base of the tube was then made gas-tight with the aid of appropriate ferrules. Finally a piece of glass wool was pushed down the open end of the tube with the aid of a glass rod to form a wad above the column and to maintain the column under a slight compression during subsequent analysis. This unit was then added to the GC in the manner depicted in Figure 3.4. The open weave of the carbon cloth was such that the pressure drop across the column was extremely small. As a result the reference column only included a 1/4" S/S sinter, and there was no difficulty in maintaining identical, and constant, carrier flow through the two columns.

The specific operating conditions (flow rate, temperature) are described in Chapter 8.

FIGURE 3.1 - Vacuum and Gas-Dosing Circuits for Sorptomatic

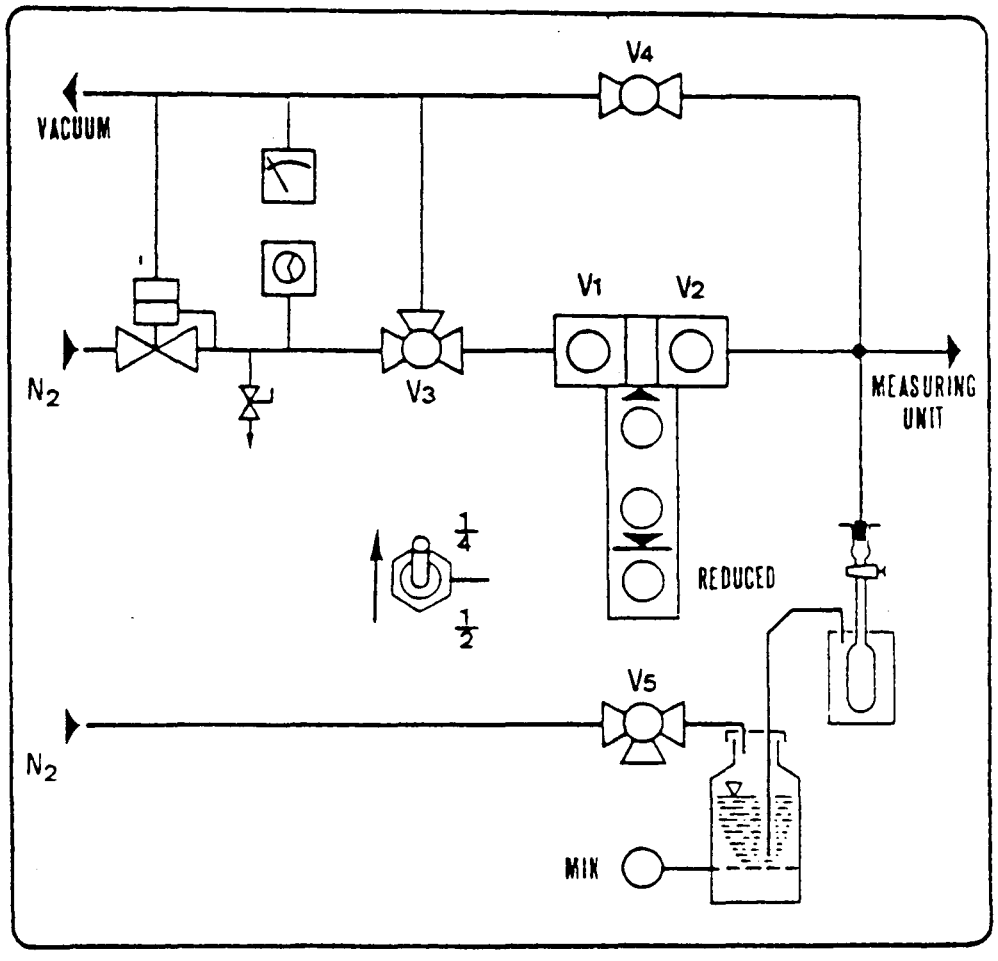

FIGURE 3.2 - Sample Burette for Sorptomatic

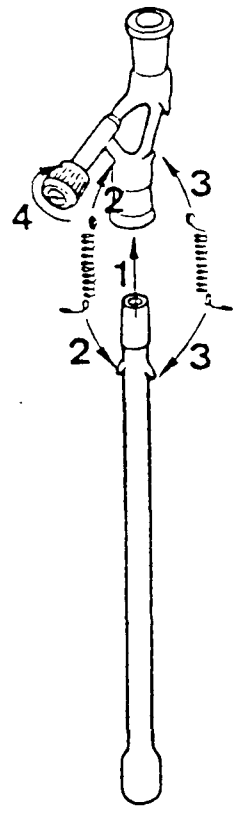

FIGURE 3.3 - Apparatus for Determination of Water Isotherms

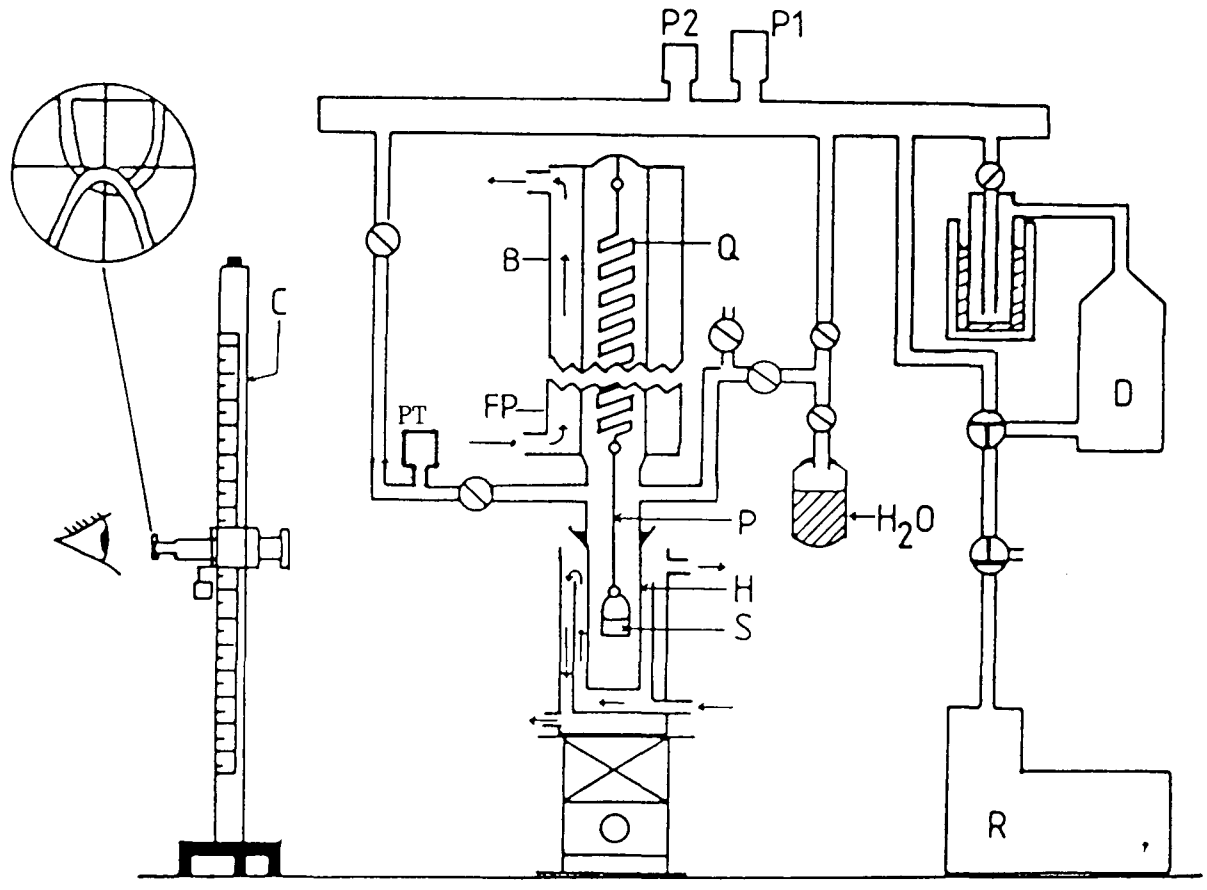

B	BALANCE CASE
C	CATHETOMETER
D	DIFFUSION PUMP
FP	FIXED POINT
H	HANG-DOWN TUBE
P	SILICA ROD
P1	PIRANI GAUGE
P2	PENNING GAUGE
PT	PRESSURE TRANSDUCER
Q	QUARTZ SPRING
R	ROTARY PUMP

FIGURE 3.4 - Construction of GC Column

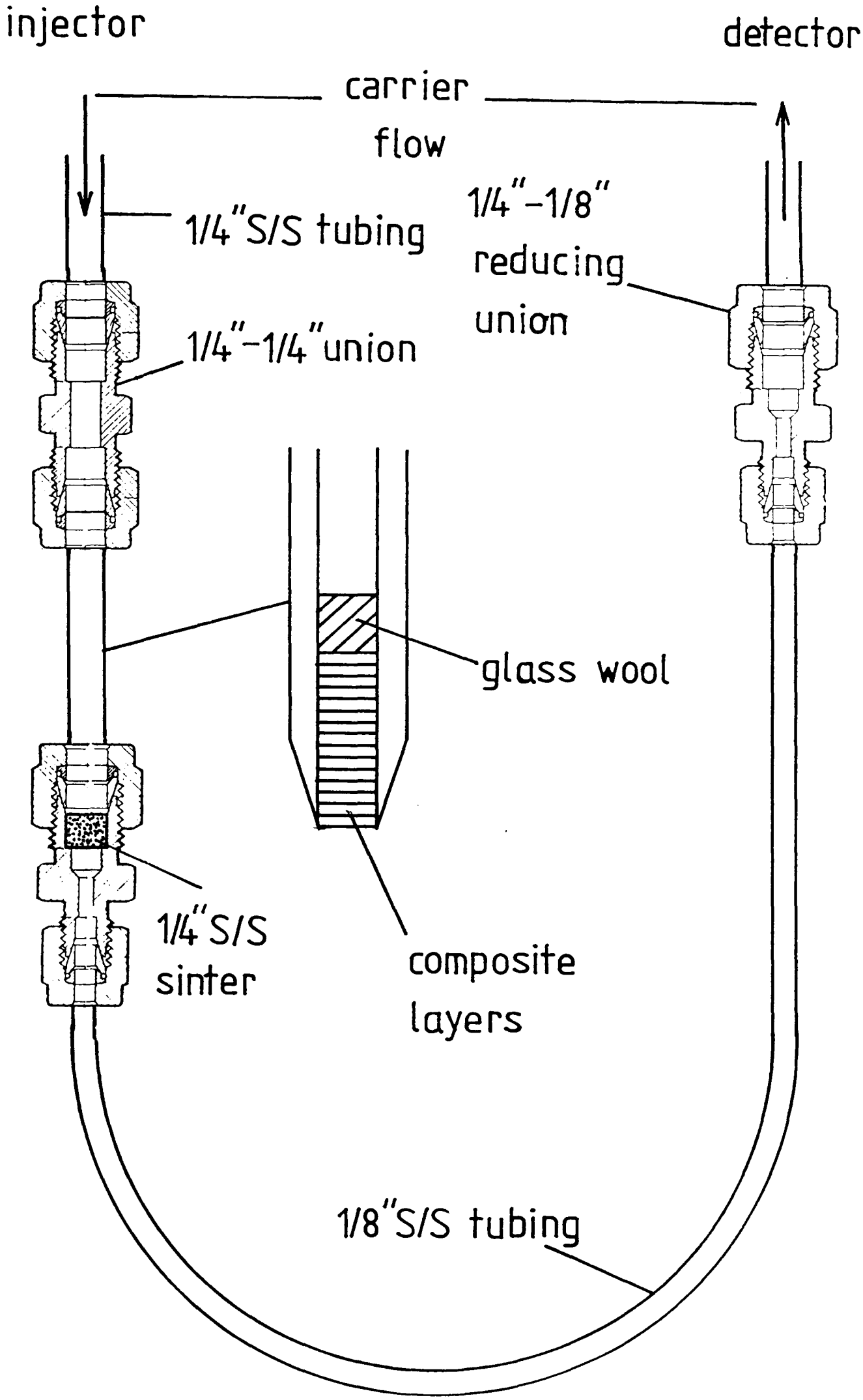

CHAPTER 4 : PRELIMINARY WORK

4.1 Introduction

Several methods of depositing alumina on activated carbon cloth were investigated in this research project. One method, involving preparation of sol/gel alumina/carbon composites occupies the bulk of this thesis. This route was found to be the most successful way of incorporating alumina within the carbon cloth. Other methods of depositing alumina that were investigated are reported briefly in this chapter. Carbon cloth A was used as the substrate for all work reported here.

4.2 Solution Deposition of Alumina

4.2.1 Single Stage Deposition

McLeod (1979) has described a method for coating particulate titanium dioxide (TiO_2) with a layer of amorphous alumina. The method basically involved raising the pH of a suspension of TiO_2 in an aluminium salt solution so as to hydrolyse and precipitate alumina on the surface of the TiO_2. An analogous procedure was employed initially in the present work, with a piece of carbon cloth being substituted for the TiO_2 support used by McLeod. Aluminium salts (either chloride, nitrate or sulphate) were added to a volume of stirred, distilled water containing a piece of carbon cloth. The initial solution pH was approximately 3. The pH of the solution (monitored continuously) was then raised slowly so as to deposit alumina on the carbon cloth. The "cloudiness" of the solution during hydrolysis indicated that exclusive precipitation of hydrated alumina on the carbon cloth was not taking place. In order to quantify this behaviour the supernatant was analysed for aluminium by Atomic Absorption (AA), after appropriate digestion. It was found that the amount of Al taken up by the carbon cloth was always less than 1% (by weight of carbon cloth), independent of the

initial concentration of the aluminium salt. In other words only a small fraction of the aluminium species present in solution could be made to precipitate on the carbon cloth. This result was not found to be affected by the temperature of hydrolysis in the range 20-50°C.

4.2.2 Double Stage Deposition

In this method pieces of carbon cloth were first impregnated with an aluminium salt and dried prior to being subjected to a separate hydrolysis stage to facilitate the transition to the final hydrated alumina. This procedure ensured that the aluminium salt was in intimate contact with the carbon cloth prior to the hydrolysis stage.

Typically, a piece of cloth of geometric area $6cm^2$ was immersed in a solution of $Al(NO_3)_3.9H_2O$ (3% w/v, 5 cm^3) in a small petri-dish. After immersion for 1 minute it was removed, drained and transferred to a glass plate for drying (55°C). The impregnation solution was assayed by AA for Al so as the uptake of Al by the carbon cloth could be determined. The volume of solution occluded by the carbon cloth was also determined gravimetrically, assuming the density of the solution to be 1.00 g/cm^3. The dried carbon cloth impregnated with the aluminium salt was then immersed in distilled water in order to hydrolyse the aluminium. The specific details of a typical impregnation run are reproduced in Table 4.1.

A loading level of 1.5 wt.% Al (per g of carbon cloth) resulted. Upon immersion in water 25% of the aluminium was found to leach out of the carbon cloth. The pH of the hydrolysis solution (in the range 3-9) was not found to affect the binding of aluminium to the carbon cloth. The aluminium loading level was found to be enhanced when the concentration of the aluminium salt solution was increased. However in this case the binding of Al was found to be proportionately lower so

that the final loading of Al was not effectively increased.

Carbon cloth was also impregnated in a similar manner with solutions of organoaluminium compounds. Aluminium isopropoxide (AIP) in isopropanol (IP) and aluminium sec-butoxide (ASB) in sec-butanol (SB) were used for this purpose. Typical impregnation data for these impregnants are reproduced in Tables 4.1 and 4.2. AIP was not found to be soluble in IP, a dispersion of AIP being produced. Some workers (Harris and Sing, 1958) have been able to dissolve AIP in IP however more recently Teichner et al (1976) have highlighted the solubility problem. As a result the ASB/SB system was found to provide a more homogeneous impregnation medium. From Tables 4.1 and 4.2 it can be seen that the loading level of Al on the carbon cloth was higher for the organoaluminium impregnants than for the aluminium salt. However the Al leach at natural pH was significantly higher in the case of the organoaluminium impregnants. Indeed almost total removal of Al was observed after AIP impregnation while in the case of ASB the Al leach was 45%.

4.3 Vapour Deposition of Alumina

4.3.1 Conventional Chemical Vapour Deposition

The chemical vapour deposition (CVD) of metals and metal oxides, via organometallic precursors, has been widely utilised as a coating method (Griffiths,1985). Aboaf (1967) has described a method and apparatus for the production of amorphous aluminium oxide films on germanium, silicon and gold substrates. The method centres on aluminium isopropoxide (AIP) which has the useful properties of melting at 118^{o}C, having a reasonable vapour pressure slightly above this temperature, and decomposing to form alumina above 270^{o}C. The applicability of such a deposition process to a porous carbon substrate (such as carbon cloth)

has not been reported in the literature. In the present project apparatus similar to that of Aboaf (1967) was constructed (Figure 4.1). Essentially the method involves passing a carrier gas (nitrogen) through an AIP melt (maintained at 130^{o}C) at a fixed flow rate. Entrained vapour is carried along a pyrex tube through the hot zone of a resistance furnace (T>270^{o}C), where the substrate to be coated is located. Pyrolysis and subsequent deposition of alumina on the substrate require careful control of furnace temperature, flow rate and the geometry and positioning of the substrate holder. The deposition parameters of flow rate and furnace temperature (300-500^{o}C) were varied in order to induce the deposition of alumina on the carbon cloth. The pieces of mesoporous carbon cloth were weighed before and after a vapour deposition run to determine whether a change of weight (indicative of alumina deposition) had taken place. Electron spectroscopy for chemical analysis (ESCA) was also used to detect the presence of aluminium. ESCA analysis of samples of carbon cloth subjected to CVD indicated significant enhancement of the Al peaks (particularly after CVD at 300 and 400^{o}C). However gravimetric analysis did not indicate any significant weight gain after CVD that could be diagnostic of large scale alumina deposition. It was generally observed that the walls of the furnace tube adjacent to the carbon cloth became preferentially coated with alumina during a vapour deposition run.

4.3.2 Condensation

The aim of this method was to load the carbon cloth with AIP prior to a separate stage designed to facilitate the transition of AIP to the final alumina. To this end a nitrogen carrier was used to transport AIP (maintained at 130^{o}C) into a sample bulb containing the carbon cloth. The temperature of the sample bulb (and hence of the

carbon cloth) could be set to various values in order to enhance the uptake of AIP. Temperatures of 150°C, 25°C, -8°C (salt/ice) and -77°C (CO_2/acetone) were used. The change in weight of the cloth due to physisorption of AIP increased dramatically as the temperature was reduced below room temperature. Changes in weight in excess of 50% were observed after 30 minutes exposure to AIP at -8 or -77°C. In this form the deposit of AIP was quite volatile and composites were observed to change weight quite rapidly at room temperature. AIP can be converted to alumina quite readily by either hydrolysis or pyrolysis. Pieces of carbon cloth containing condensed AIP were then hydrolysed (by aqueous and vapour immersion) or subjected to flash pyrolysis (490°C, nitrogen) in order to facilitate the deposition of alumina within the pore system. However all three methods succeeded only in removing the AIP from the cloth rather than causing the deposition of alumina.

4.4 Discussion

The deposition of alumina cannot be accomplished by direct material transfer, at practical temperatures, simply because of the physical properties of the alumina phase. In other words :

alumina + substrate --X-> alumina coated substrate

Instead, to deposit alumina an "alumina precursor" such as an aluminium salt solution or an organoaluminium compound (either in solution or as a vapour) is often employed. These "precursors" may be easily transformed into alumina by hydrolysis or thermal decomposition. To coat a substrate with alumina we require that the substrate is "wetted" by such an alumina precursor and secondly that this precursor remains on the substrate during the transition to the final alumina. The various methods for depositing alumina on carbon cloth that have been described in this chapter are now discussed in the context of these requirements.

The single stage deposition from solution was not found to be successful because of the propensity of the alumina phase to precipitate in solution rather than on the carbon cloth. Given that the technique (McLeod,1979) was successfully employed to coat TiO_2 one may attribute this result to the nature of the carbon phase used in the present work. When aluminium salts are dissolved in water the free metal ion, Al^{3+}, first hydrates by co-ordinating six water molecules in octahedral orientation (Fiat and Connick, 1968) and then reacts forming various hydrolytic species. Hydrolysis proceeds as the solution pH is increased. There is some disagreement in the literature over whether the hydrolysis of aluminium should be described in terms of monomeric (Raupach,1966) or polymeric species (Sillen,1959). The hydrolysis may also involve colloidal species (Matijevic, 1966). Nevertheless the deposition of the hydrolysed or colloidal aluminium species will be governed by the thermodynamics of the adsorbed species/substrate interaction. In this respect the charge of the substrate (whether positive or negative), as well as that of the species to be adsorbed must play a critical role in the initiation of the coating process. In the case of carbon cloth one may conclude that the deposition of hydrolysed aluminium species on the carbon surface was not favoured, probably as a result of such electrostatic considerations. Recently the electroadsorption of alumina particles on fibrous carbon and graphite electrodes has been reported (Cohen et al, 1987). Significant adsorption of alumina particles was only obtained when the potential of the carbon electrodes was adjusted away from the open cicuit, or natural, potential. Although in that work the scale of the deposit and substrate was significantly different from that being investigated in the present work, it does indicate that significant adsorption of "alumina" on carbon may only be possible as a result of external

manipulation of the electrostatics of the system.

The use of a double stage solution deposition method ensured that a controlled amount of the "alumina precursor" was present on the carbon cloth prior to the hydrolysis stage. However the loading level of aluminium (and consequently alumina) was limited by the solubility of the alumina precursor (making up the impregnation solution) and by the low weight fraction of Al (<15%) present in such compounds. The potential alumina loading level was further reduced because of the solubility of the precursor in water during the hydrolysis stage. As a result the highest alumina loading level achieved after double stage solution deposition was barely 1% (by weight of carbon cloth). The porosity and surface area of mesoporous carbon cloth are such that significantly greater loading levels than 1% would be required to substantially modify its adsorptive properties.

Conventional chemical vapour deposition was also not found to be a successful technique for the deposition of alumina on carbon cloth. As in the case of solution deposition the lack of affinity between the carbon and the alumina phases was the obvious cause of such a failure. Aboaf (1967) has demonstrated that the technique can be successfully employed for the coating of germanium, silica and gold substrates. In the present work the preferential coating of the silica furnace wall was observed in preference to deposition on the carbon cloth. The texture of the carbon cloth may have contributed to this result in that CVD is normally applied to flat surfaces. The nature of CVD is such that the pores of carbon cloth would not be expected to be accessible to alumina deposition. The condensation deposition method was expected to overcome the obvious failing of conventional CVD, its inability to coat porous materials, because it relied more on physisorption of AIP molecules. Physisorption, being thermodynamically favoured in pores of molecular

dimensions, would in theory result in the presence of alumina within the pore structure of the carbon cloth after conversion of AIP. In practice though, despite large scale physisorption of AIP at low temperatures, the molecule was not found to remain within the carbon cloth under the conditions required for its transition to alumina. Hydrolysis presumably resulted in solubilisation of AIP in the aqueous phase, and heat treatment in desorption of AIP, prior to the decomposition and deposition of alumina.

In summary then, the deposition methods described in this chapter either failed because no "wetting" of the carbon cloth by an "alumina precursor" occurred or because of the lack of stability of the alumina precursor on the carbon cloth under the conditions required to produce the final alumina. The prime cause of such results lay basically in the apparent lack of affinity between the carbon cloth and the alumina phases in each case. The deposition methods themselves could not be held responsible for this failing as they have been successfully employed in the coating of other, non-carbon, substrates.

TABLE 4.1 - IMPREGNATION AND HYDROLYSIS OF CARBON CLOTH A WITH ALUMINIUM NITRATE AND ALUMINIUM ISOPROPOXIDE (AIP)

	aluminium nitrate 3%w/v	AIP/IP 4%w/v
weight of cloth(g): initial	0.0531	0.0540
final	0.0609	0.0620
change in weight(g)	0.0078	0.0080
occluded volume(cm^3/g)	6.04	7.18
Al uptake(mg) as determined by:		
AAS	0.79	--
volume of solution occluded	0.65	2.02
change in wt.(assuming salt or AIP precipitated)	0.99	*1.22
wt.% Al on cloth	1.49 (AAS)	2.26 (using*)
Al leach at natural pH(%)	25.2	93.9

TABLE 4.2 - IMPREGNATION AND HYDROLYSIS OF CARBON CLOTH A WITH ALUMINIUM SEC-BUTOXIDE (ASB)

weight of cloth(g): initial	0.2972
final	0.3790
change in weight(g)	0.0818
occlusion volume(cm^3/g)	7.75
Al uptake(g):	
from volume of solution occluded	0.0108
from change in wt.	*0.0090
weight fraction of Al on cloth(%)(using*)	3.03
Al leach at natural pH(%)	45.0

FIGURE 4.1 - Schematic Diagram of Apparatus for Chemical Vapour Deposition (CVD) of Alumina

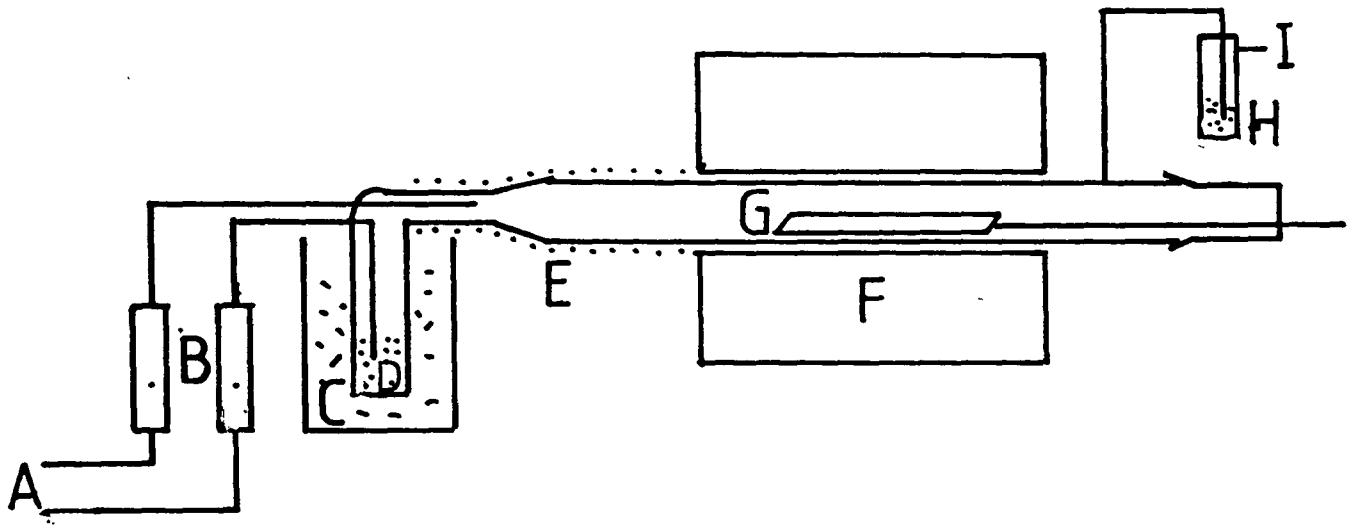

A	N_2
B	FLOWMETERS
C	HEATING MANTLE
D	ALUMINIUM ISOPROPOXIDE
E	HEATING TAPE
F	TUBE FURNACE
G	SUBSTRATE HOLDER
H	OIL BUBBLER
I	EXHAUST

CHAPTER 5 : RESULTS AND DISCUSSION I - SOL/GEL ALUMINA

5.1 Introduction

In this chapter the results pertaining to the preparation of the sol/gel alumina are described. In Chapter 6 the results relating to the preparation and characterisation of the mesoporous cloth are presented. Finally in Chapter 7 the composite material is discussed and the N_2 and H_2O isotherm data are compared with those for the individual components discussed in Chapters 5 and 6.

As has already been discussed (Section 2.1.4) the preparation of alumina from the dried boehmite gel requires heat treatment at temperatures approaching 500^{o}C. This heat treatment stage has been investigated in some detail. As the composite material includes a carbon cloth which is thermally unstable when heated in an oxidising environment the final heat treatment of the composite must be performed in an inert environment. Conventional heating of the boehmite gel is based on simple calcination (Leenaars et al,1984). The requirements of the carbon cloth were therefore responsible for an investigation of the heating environment. Heating in flowing N_2 and under vacuum were investigated along with that in air in order to determine whether a change of heating environment affected the porosity of the resulting alumina.

5.2 Nitrogen Isotherms

5.2.1 Dried Boehmite Gel

It can be seen from Figure 5.1 where the N_2 isotherms for the dried boehmite gel (sample no.1) are plotted that the sample was quite porous prior to heat treatment. Furthermore the drying of the sample (no.2,outgassed 110^{o}C) resulted in a significant decrease in the BET surface area (Table 5.2) from 383 to 301 m^2/g. The isotherms of the dried gel and of the final alumina can be seen to be Type IV in

behaviour (Section 2.3.5), the samples being significantly mesoporous. The BET plots for both the dried gels and aluminas were found to be linear over the relative pressure range 0.1-0.3. Typical BET plots are reproduced in Appendix A.

5.2.2 Heat Treatment of Gel in Nitrogen and Air

The heating conditions for all samples are reproduced in Table 5.1.

The dried gel was initially heated to 500^{o}C in N_2 (sample no.3) and flowing air (sample no.4)(1 litre/minute) at a heating rate of 10^{o}C/minute. The samples were maintained at this temperature for 17 hours. To save duplication the following notation will be used for heating schedules : Heating Rate-->Maximum Temp.(Dwell Time). The heating schedule above then was : 10-->500(17). The samples were then transferred to a burette and outgassed at 110^{o}C before determinations of the respective N_2 isotherms. As can be seen from Figure 5.2 and the relevant data in Table 5.2 very little difference between these heating environments was observed.

The heat treatment in flowing air was then conducted at a slower heating rate (1-->500,(17)) and for a shorter dwell time at the maximum temperature (1-->500,(1))(see Figure 5.3 and Table 5.2 for the relevant isotherms and associated data). No significant difference in the isotherms was observed for the three samples apart from a slight decrease in porosity for the sample subjected to extended slow heat treatment (no.5). It was therefore concluded that for these heating environments (flowing air or N_2) the heating rate and length of time at 500^{o}C do not significantly affect the transition of the dried gel.

The dried gel was also heated in **still** air (not in a flowing environment), with the sample holder open to the atmosphere. The N_2

isotherms for this alumina are compared (Figure 5.4) with that for the sample heated in flowing air under similar conditions (no.5). Significant differences in the isotherms were observed in this case. As a result the heating of the dried gel in still air was investigated further. The effect of a slow heating schedule (sample no.9) compared with a quicker one (sample no.8) on the resultant N_2 isotherm behaviour is compared in Figure 5.5. For heating in still air we do see (unlike that for flowing air) an effect of heating schedule.

5.2.3 Heat Treatment Under Vacuum

The boehmite gel was also heated under vacuum. The N_2 isotherm of the resultant alumina (sample no.11) is compared in Figure 5.6 with that for the sample heated under N_2 under otherwise similiar conditions. The heating schedule for vacuum heat treatment was 10-->500(1) while that for sample no.3 was 10-->500(17). However it has already been shown that for the flowing environment the dwell time does not affect the resultant alumina (with respect to N_2 isotherm, anyway) so a valid comparison can be made. The isotherm data do not indicate any significant difference between the two inert environments in the BET region although a slight difference is evident at higher relative pressures, the porosity decreasing from 64 to 60% (Table 5.2). The effect of heating schedule on vacuum heat treatment was also investigated (sample nos.10 and 11, Figure 5.7) and found not to affect the resultant alumina. Finally the effect of temperature (sample no.12,10-->400(3)) on vacuum heat treatment was investigated (Figure 5.8). At this lower temperature the dehydration was not completed in 1 hour as determined by the high residual pressure. Such an observation was not surprising in the light of Yoldas' thermogravimetric analysis (See Figure 2.1). The heating temperature was found to affect the

isotherm of the resultant alumina in the BET region, with A_{BET} increasing from 381 to 424m^2/g.

5.3 Analysis of Nitrogen Isotherms

5.3.1 Assessment of Pore Size Distribution

For convenience the pore size distribution analysis has been based upon a cylindrical pore model. It is recognised that a pore size distribution based on a slit-shaped pore model would better represent the structure of the alumina (see Section 5.4). However no actual significance is to be placed on the absolute values of pore size for a given alumina. Rather the plots are used simply to investigate any qualitative trends in pore size distribution for the alumina samples. Such trends would not be expected to be dependent upon the choice of model for the Pore Size Distribution (PSD).

The pore size corresponding to the maximum value of dv/dr has been extracted and reproduced in Table 5.3, for a selection of the alumina samples. This "modal" pore size can be calculated from either the adsorption or desorption branches of the isotherm. In general it can be seen (Table 5.3) that the pore radius corresponding to dv/dr_{max}(adsorption) is greater than that corresponding to dv/dr_{max}(desorption). This situation, and indeed the phenomenon of hysteresis itself, arise because for a given pore size condensation of adsorbate (and hence adsorption) occurs at a different relative pressure than does evaporation (desorption). The maximum values of each parameter were only extracted when the PSD plot passed through a definite maximum value of dv/dr. Some adsorption PSD plots did not satisfy this criterion, and for the purpose of further discussion the desorption values of dv/dr_{max} were favoured. As was observed for the values of A_{BET} (Table 5.2) extracted earlier the pore radius

corresponding to dv/dr_{max} was found to be split into just two groups depending on whether the heating environment was still air or one of the other environments. Representative PSD plots are reproduced in Figure 5.9. There was very little overlap in pore size distribution between alumina samples heated in still air and those heated in the other environments. For heating in still air the pore radius corresponding to dv/dr_{max} was found to be in the range 2.70-3.05nm. Heating in N_2, vacuum or flowing air gave a corresponding pore radius of 1.90-2.03nm. Interestingly a similar pore size analysis for the dried boehmite gel (sample no.2) gave a pore radius value of 2.07nm.

5.3.2 Assessment of Porosity

Inspection of the N_2 isotherms for the alumina samples indicate that at relative pressures greater than 0.90 all hysteresis loops are closed and that the nitrogen uptake has plateaued. The nitrogen uptake at this plateau could then be calculated with a good degree of certainty. The nitrogen uptake read from the isotherm abscissa is measured in units of cm^3 of adsorptive at STP. This volume may be converted to a liquid volume by taking a value of $0.808g/cm^3$ for the density of liquid N_2 at 77K. The pore volume and porosities of the samples were then calculated (Table 5.2). The following values for the true densities of the solids were used :- $3.0g/cm^3$ for boehmite and $3.7g/cm^3$ for Al_2O_3 (Wilson and Stacey,1981). The porosity of the gel dried at RT was 54%, with thorough drying at 110°C resulting in a decrease in porosity to 51%. Subsequent heat treatment resulted in a major increase in porosity to 59-64%. No obvious connection between heating environment and the porosity of the resulting alumina was observed.

5.3.3 The Assessment of Microporosity

The α_s method of Sing (Gregg and Sing,1982) was applied to the N_2 isotherms in order to determine whether any microporosity was responsible for the uptake of N_2. The application of the α_s technique requires adsorption data for a suitable non-porous reference material. Ideally the reference material used is chemically similar to the porous material that is to be assessed. In the present work the α_s-plots were obtained with reference to non-porous alumina (Payne,1970), silica (TK800,Carrott,1980) and carbon (Carrott et al,1987). No significant difference was observed between any of the resulting α_s-plots for a given alumina sample. Such a result is indeed quite common when N_2 is the adsorptive and the sample is not significantly microporous (Carrott et al,1987). The non-porous silica was adapted as the standard reference material as its adsorption data were the most extensive. Representative α_s-plots are reproduced in Figure 5.10 for samples of alumina heated under vacuum, N_2 and in still air.

The quantitative assessment of microporosity relies on the determination of the intercept of the lower linear region of the α_s-plot with the vertical axis. All alumina α_s-plots had a similar intercept therefore indicating that a similar degree of microporosity was present for all samples. The low pressure adsorption data were not sufficiently extensive to allow accurate calculation of this intercept, however it corresponded to 10-15 cm^3 N_2 (STP). By introducing the density of liquid nitrogen the actual pore volume was calculated to be approximately $0.02cm^3/g$. This volume may be compared with the total pore volume which was in excess of $0.40cm^3$ (see Table 5.2). Therefore it was concluded that the aluminas were very slightly microporous, and furthermore that no particular heating environment appeared to favour the production of microporosity. The form of the α_s-plot, in

particular the upswing at α_s values less than 1, suggests that secondary microporosity (possibly associated with reversible capillary condensation) is present rather than primary microporosity (Sing,1970).

5.4 Discussion

The N_2 isotherm data obtained for the alumina samples fell into two distinct groups. If the heating environment was vacuum, N_2, or air (flowing) the porosity of the resultant alumina was not markedly affected by heating schedules. However for still air heat treatment the N_2 isotherm behaviour was found to be distinctively different after heating and much more dependent on the heating schedule. The former group was characterised by A_{BET} 346-392 and closure of the hysteresis loop at p/p^o = 0.42 while the latter group had A_{BET} 206-254 and the hysteresis loop closed at relative pressures >0.5 (indeed for some samples at p/p^o>0.6 (no.9,Figure 5.4). It was surprising that such a marked difference was observed for the alumina samples when the only difference in heating conditions was the transition from, say, flowing air to still air.

The isotherm of the alumina heated in still air rises very steeply in the p/p^o range 0.6-0.8. In this region the hysteresis loop and adsorption branch rise almost vertically. In contrast the N_2 isotherms for the samples not heated in still air rise more gradually to the adsorption maximum. Such a distinction between the two types of isotherm is qualitatively indicative of the filling of relatively larger pores in the case of the still air heated alumina. The results relating to the assessment of pore size distribution support these qualitative observations with the modal pore size of the still air heated alumina being almost 1 nm (or 50%) greater than that for the alumina samples heated in other environments.

Electron microscopic studies by Leenaars et al (1984) and Yoldas (1975,a) have shown that the boehmite produced via the sol/gel route consists of very thin (<5nm) plate shaped crystallites. Leenaars et al (1984) have discussed the mechanism of formation of alumina from the boehmite precursor. The gel initially consists of an array of stacked plates (see Figure 5.11), with the plate thickness and separation between the plates (effectively pores) being very similar. Because of the small size of the crystallites the release of H_2O is accompanied by the shrinkage of the individual plates and no new pores are formed. The specific surface area and the pore size of the final alumina is then determined by how the size, shape and stacking of the boehmite crystallites are affected by this shrinkage. On the basis of the results reported here, one can only conclude that the heating environment intimately affects the shrinkage and subsequent packing of the plates making up the final alumina. Heating in still air presumably allows a gentle relaxation of the stacking during the release of the H_2O. Furthermore the observed dependence of the alumina isotherm resulting from still air heat treatment on the length of time at T_{max} (Figure 5.5) adds further weight to the argument for a gradual transition of the plate structure.

By contrast vacuum, flowing N_2 and flowing air must all be quite "active" heating environments, in that the modal pore size was substantially less than for still air heat treatment. A quick collapse of the plate structure obviously does not result in an increase in the modal pore size during the boehmite-alumina transition. The close agreement between the modal pore size for the dried gel and the "actively" heated alumina samples support this result. The rapid removal of H_2O and the accompanying rearrangement of the plates leads to a less uniform stacking of plates in the final alumina.

As has been mentioned earlier the principal aim of the investigation into the heat treatment of the boehmite gel was as a prelude to the subsequent heating of the alumina/carbon composites. Because of the thermal instability of the carbon phase in oxidising environments heating of the composite materials had to be carried out in an inert environment (N_2 or vacuum). Considerable attention was focussed on the heating of boehmite in air only because of the interesting information it provided on the mechanics of boehmite-alumina transition. This information may be of relevance in work concerned with the impregnation of calcinable supports with sol/gel alumina. In this case the composite could be heated under conditions most conducive to the regular packing of the alumina plates (ie. still air) rather than conditions conducive only to the survival of the support material.

The effective distribution of alumina about mesoporous carbon cloth was the overriding issue in this project. To this end, for the work that is reported in subsequent chapters the heating conditions were set at 10-->500(1) under vacuum. These conditions were chosen for convenience in that they minimized handling time, were conducted in an environment where the heating rate and dwell time (see Figure 5.7) have not been shown to affect the resultant alumina, and most importantly preserved the integrity of the carbon cloth. It should be noted that vacuum heat treatment results in the production of alumina with a relatively small modal pore size (Table 5.3, Figure 5.9).

5.5 Water Isotherms

As has been observed earlier the N_2 isotherms for the alumina samples fell into two distinct groups depending on the heating environment. Water isotherms on many of the samples in Table 5.1 were obtained. For the sake of clarity only two will be presented here, one

from each group (see Figure 5.12). Sample no.10 was an example of the narrow pore alumina and the heating conditions were similiar to those employed later for the alumina/carbon composites. The other isotherm is included here because it belongs to the other group of aluminas (still air heat treatment) with the wider pores. It can be observed that the narrow-pore alumina took up much more water, particularly at lower relative pressures. The alumina/carbon composites (Chapter 7) incorporate this more H_2O active alumina.

The water isotherms of the alumina samples have a distinct "knee" at low relative pressures, and may be classified as Type IV (see Section 2.3.5). It should be noted that the hysteresis loop did not close at low relative pressures. The exposure to water has presumably resulted in chemisorption of water by the alumina surface. The failure of prolonged pumping, after isotherm measurement, to remove this water supported this hypothesis. Indeed this type of behaviour has been reported (Gregg and Sing,1982,p.274) for water sorption on a number of metal oxides including alumina.

TABLE 5.1 - HEATING CONDITIONS FOR BOEHMITE GELS

Sample No.	Heating Environment	Heating Rate(^{o}C/min.)/ Temperature(^{o}C)	Dwell Time(hours)
1	Vacuum	-/RT	16
2	Vacuum	-/110	16
3	N_2,1L/min.	10/500	17
4	Air,1L/min.	10/500	17
5	Air,1L/min.	1/500	17
6	Air,1L/min.	1/500	1
7	Still Air	2/500	15
8	Still Air	2/500	6
9	Still Air	1/500	24
10	Vacuum	1/500	24
11	Vacuum	10/500	1
12	Vacuum	10/400	3

TABLE 5.2 – BET AREA[@], PORE VOLUME AND POROSITY OF ALUMINA SAMPLES

Sample No.	A_{BET} (m^2/g)	Pore Volume (cm^3/g)	Porosity (%)
1	383	0.390	53.9
2	301	0.345	50.9
3	391	0.474	63.7
4	358	0.457	62.8
5	346	0.400	59.7
6	367	0.442	62.0
7	241	0.464	63.2
8	254	0.444	62.2
9	206	0.452	62.6
10	362	0.391	59.1
11	381	0.404	59.9
12	424	0.396	59.5

[@]All samples outgassed at 110°C under vacuum prior to determination of nitrogen isotherm except for sample no. 1 which was outgassed at RT.

TABLE 5.3 - MODAL PORE SIZE FROM PORE SIZE DISTRIBUTION ANALYSIS FOR VARIOUS ALUMINA SAMPLES

Sample	Modal Pore Size (nm)	
	Adsorption	Desorption
Dried Boehmite Gel(110°C)	2.13	2.07
Vacuum Heated Alumina	-	1.90
" " "	-	1.91
Flowing N_2 Heated Alumina	2.11	1.99
Flowing Air Heated Alumina	-	2.03
Still Air Heated Alumina	3.22	2.83
" " " "	3.50	3.05

FIGURE 5.1 - Nitrogen Isotherms for Dried Boehmite Gel Outgassed at RT(X) and 110°C(□)

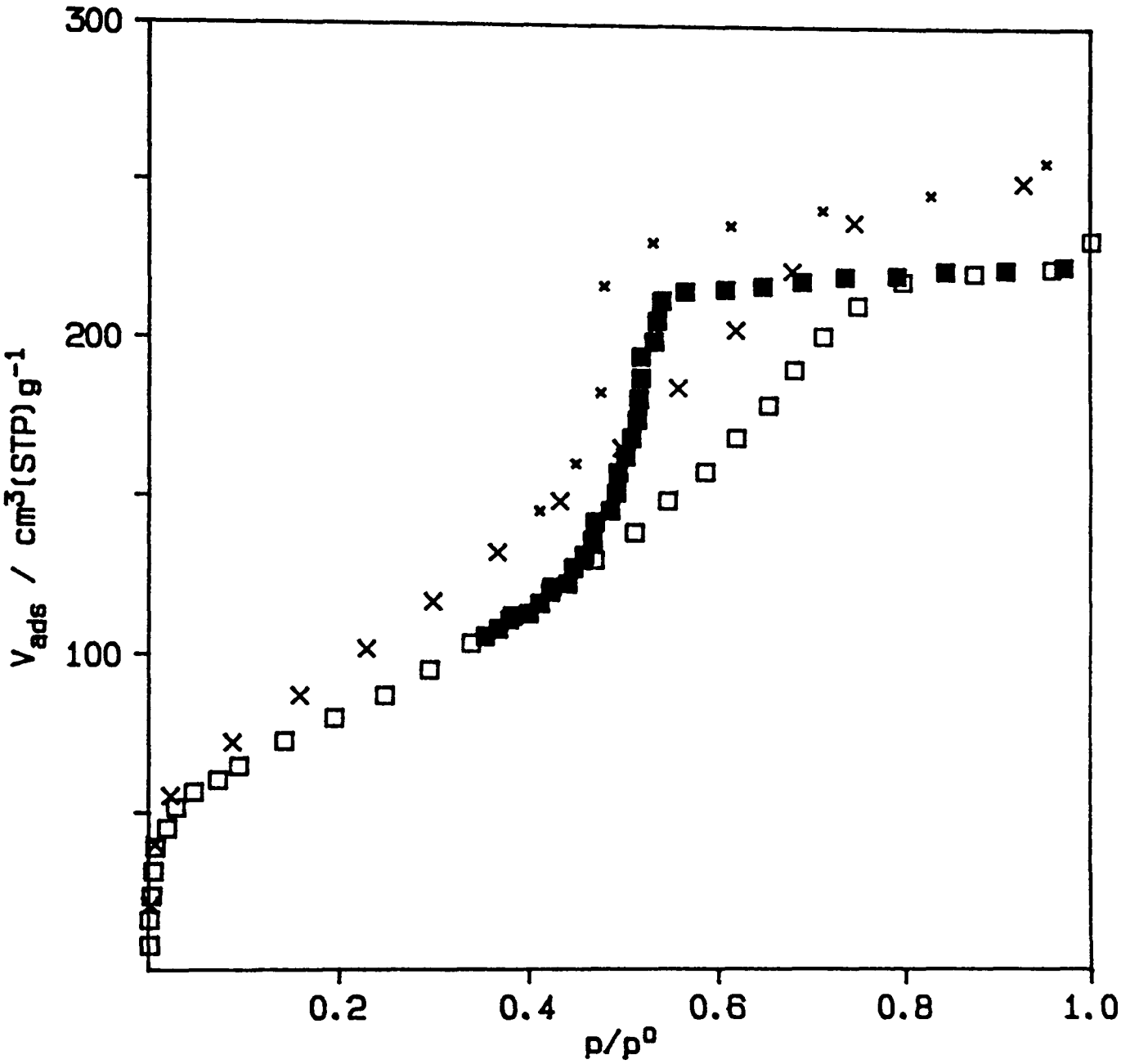

FIGURE 5.2 - Nitrogen Isotherms for Alumina Heated in Flowing Nitrogen(□) and Flowing Air(X)

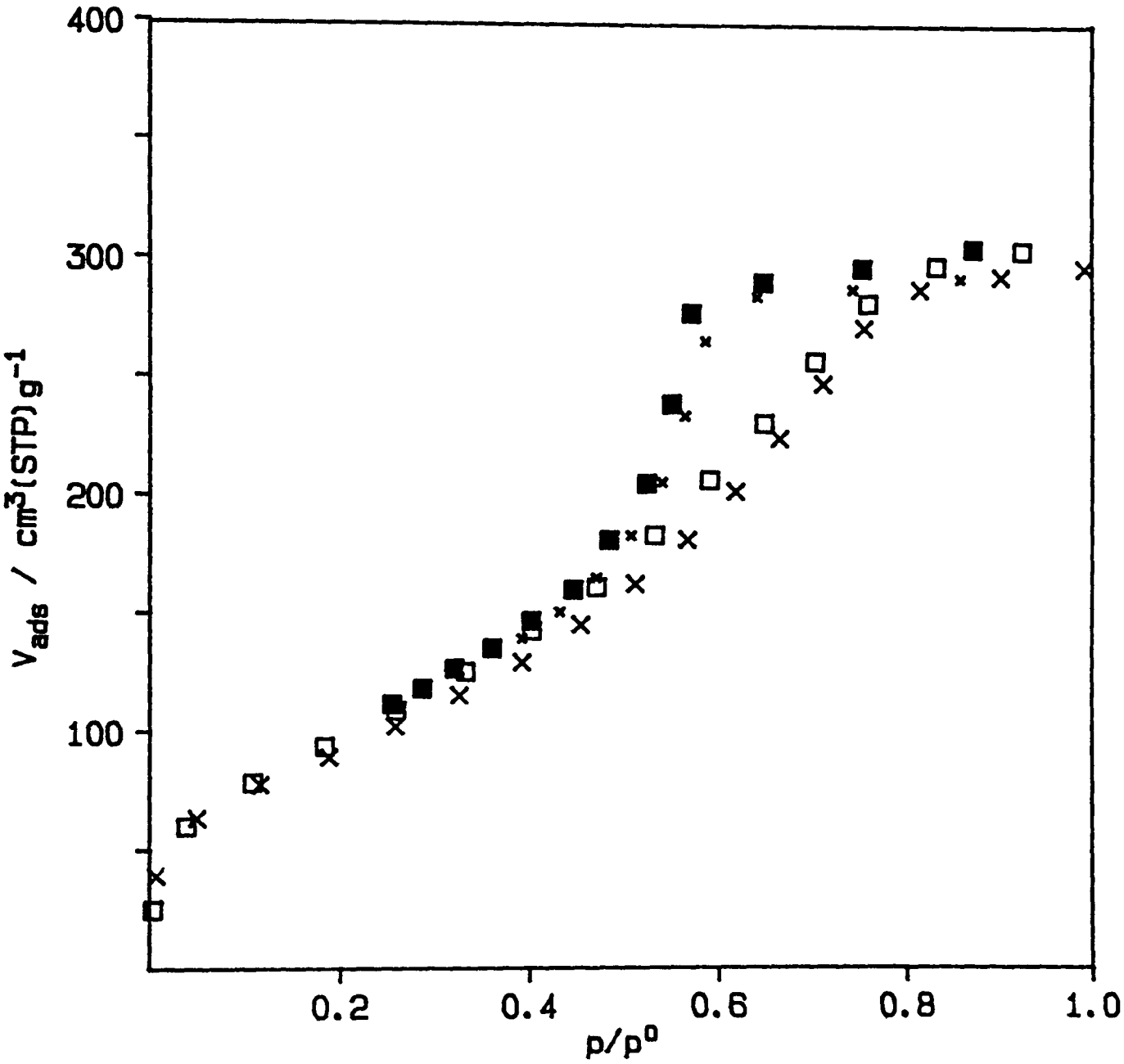

FIGURE 5.3 - Effect of Heating Rate and Length of Heat Treatment on Nitrogen Isotherms for Alumina Heated in Flowing Air

(X) 10-->500(17)

(Δ) 1-->500(17)

(□) 1-->500(1)

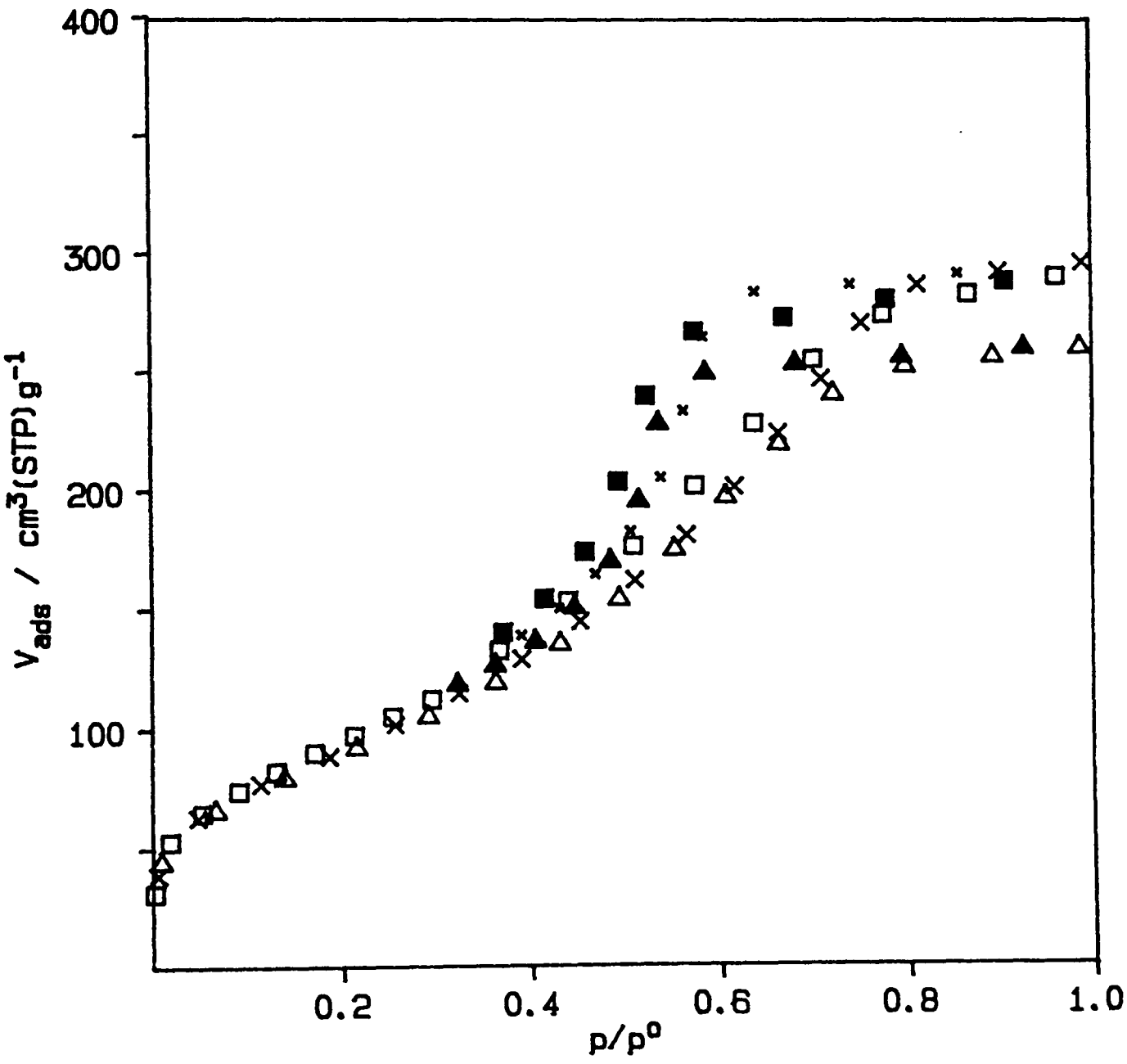

FIGURE 5.4 - Nitrogen Isotherms for Alumina Heated in Still Air(×) and Flowing Air(Δ)

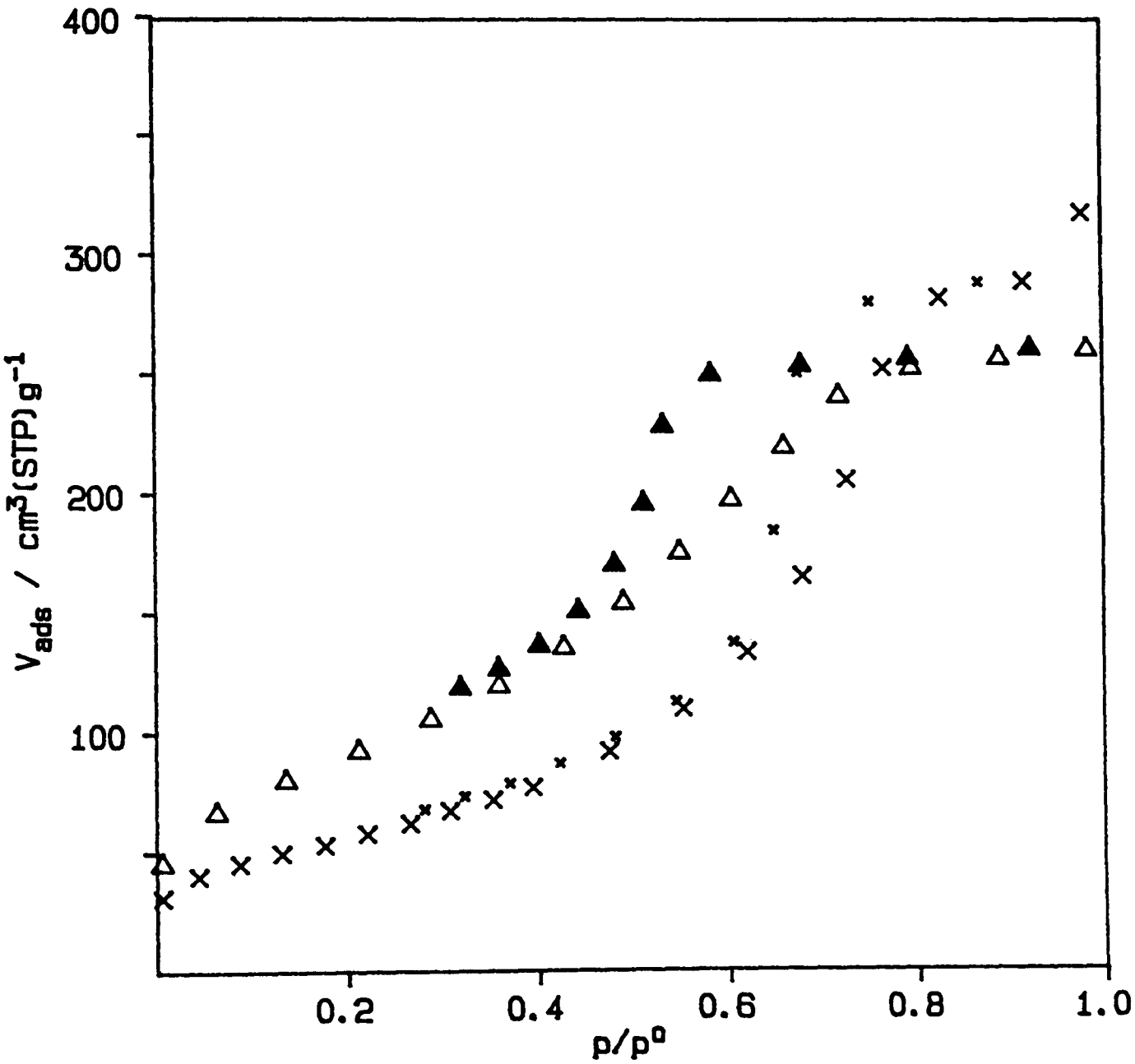

FIGURE 5.5 - Effect of Heating Rate and Length of Heat Treatment on Nitrogen Isotherms for Alumina Heated in Still Air

(□) 2-->500(6)

(×) 1-->500(24)

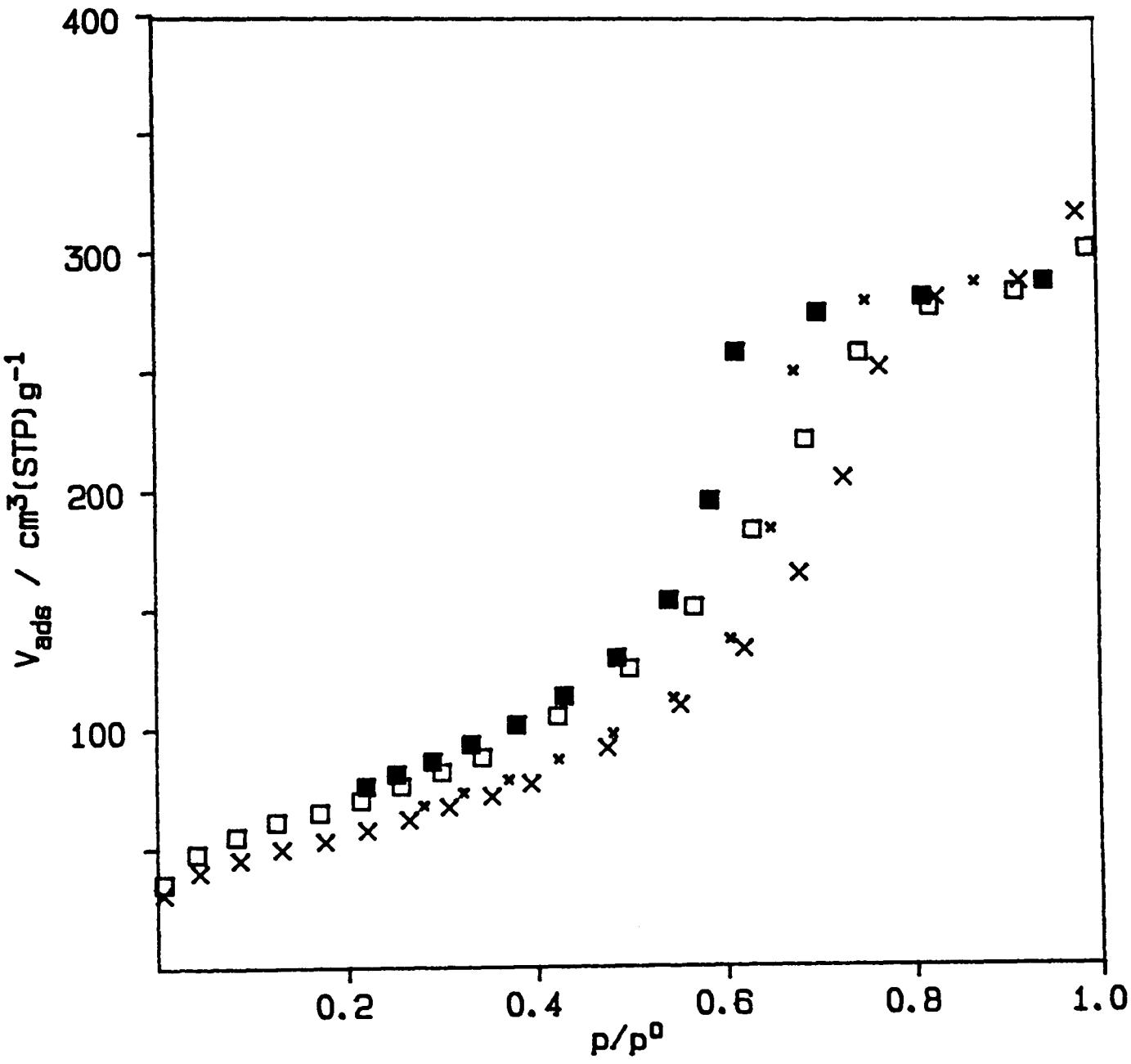

FIGURE 5.6 - Comparison of Nitrogen Isotherms for Alumina Heated under Vacuum(✕) and Flowing Nitrogen(□).

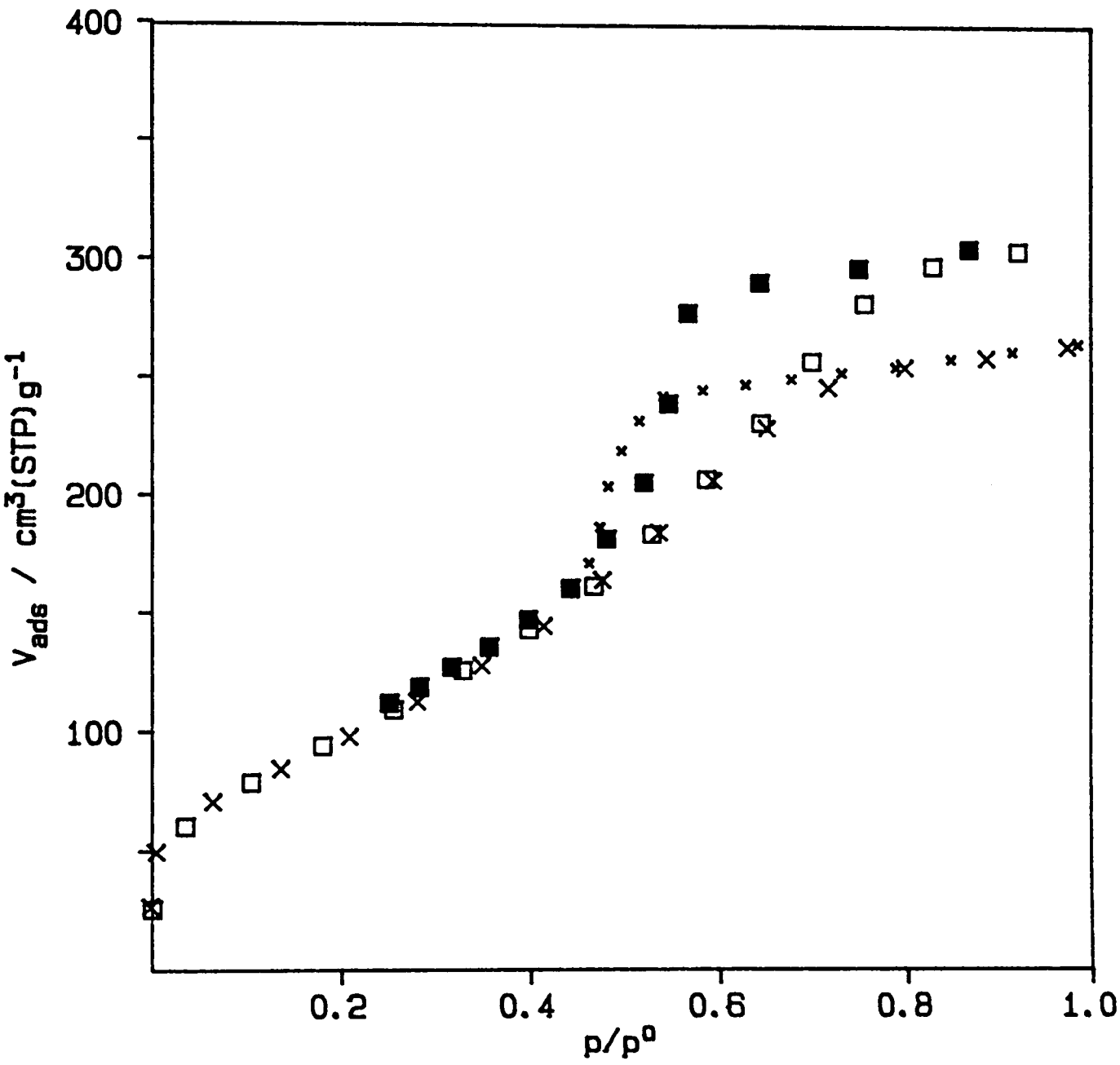

FIGURE 5.7 - Effect of Heating Rate and Length of Heat Treatment on Nitrogen Isotherms for Alumina Heated under Vacuum

(✕) 10-->500(1)

(□) 1-->500(24)

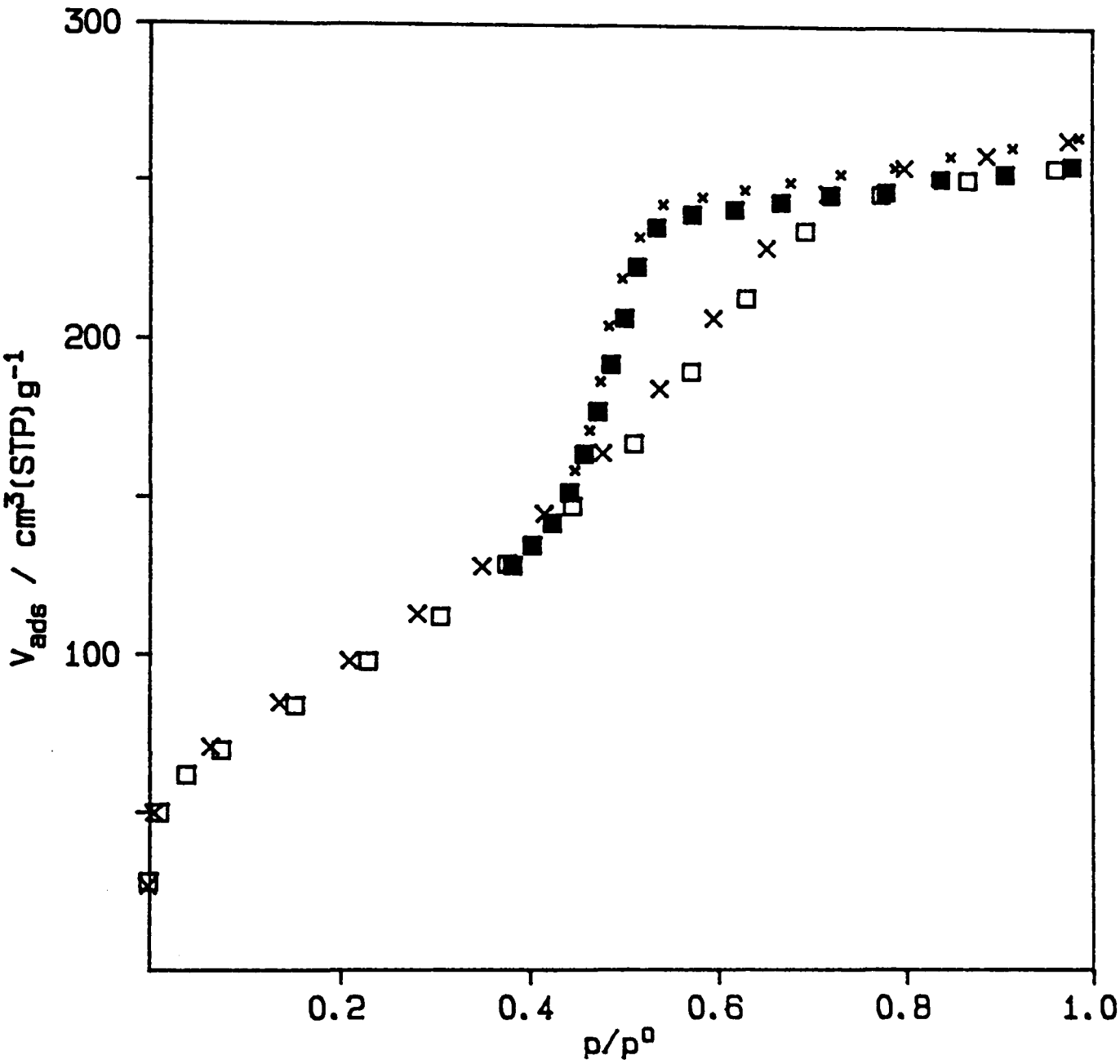

FIGURE 5.8 - Effect of Temperature on Nitrogen Isotherms for Alumina Heated under Vacuum

(□) 400°C

(×) 500°C

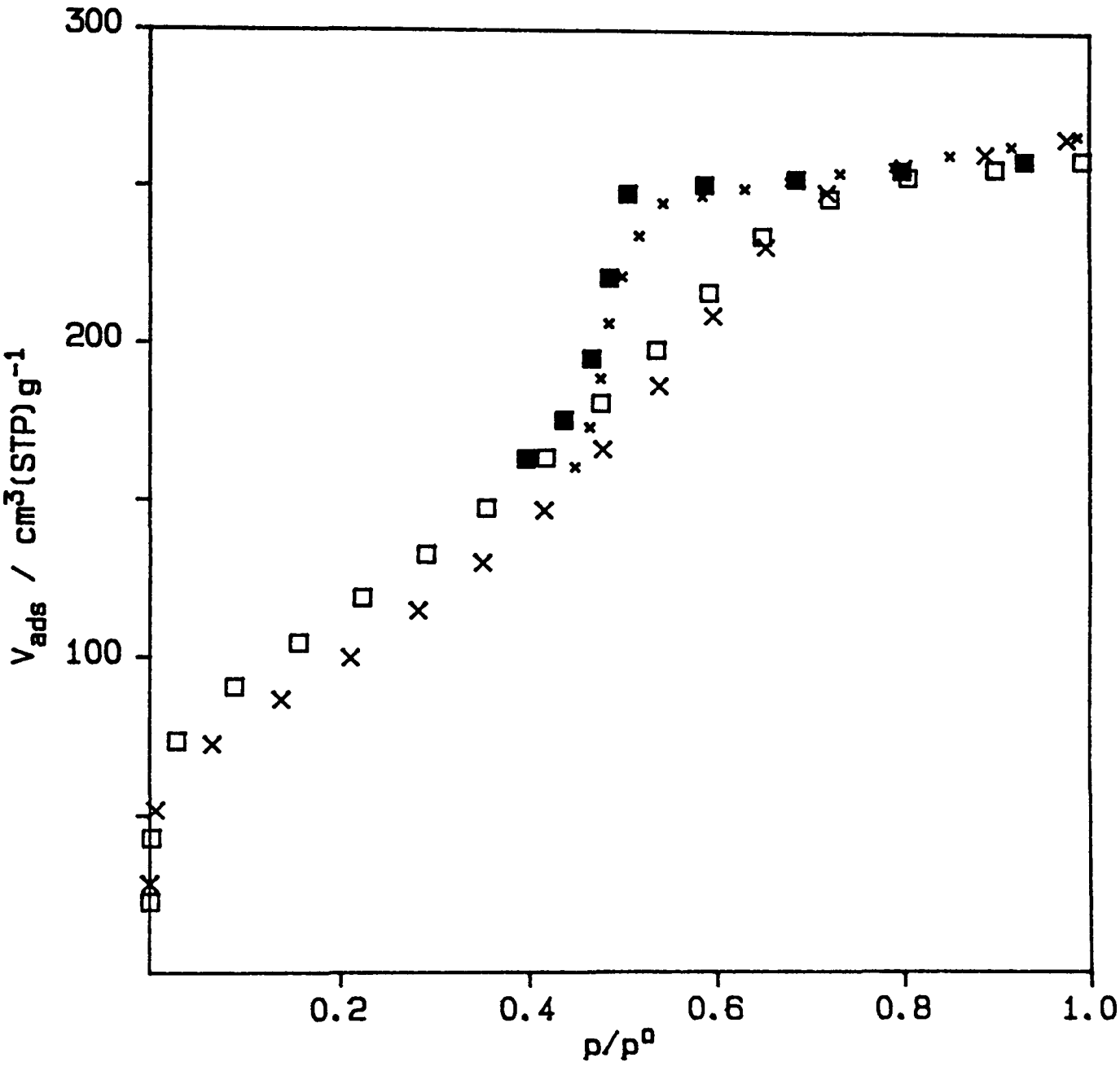

FIGURE 5.9 - Desorption P.S.D. Plots for Still Air and Vacuum Heated Alumina

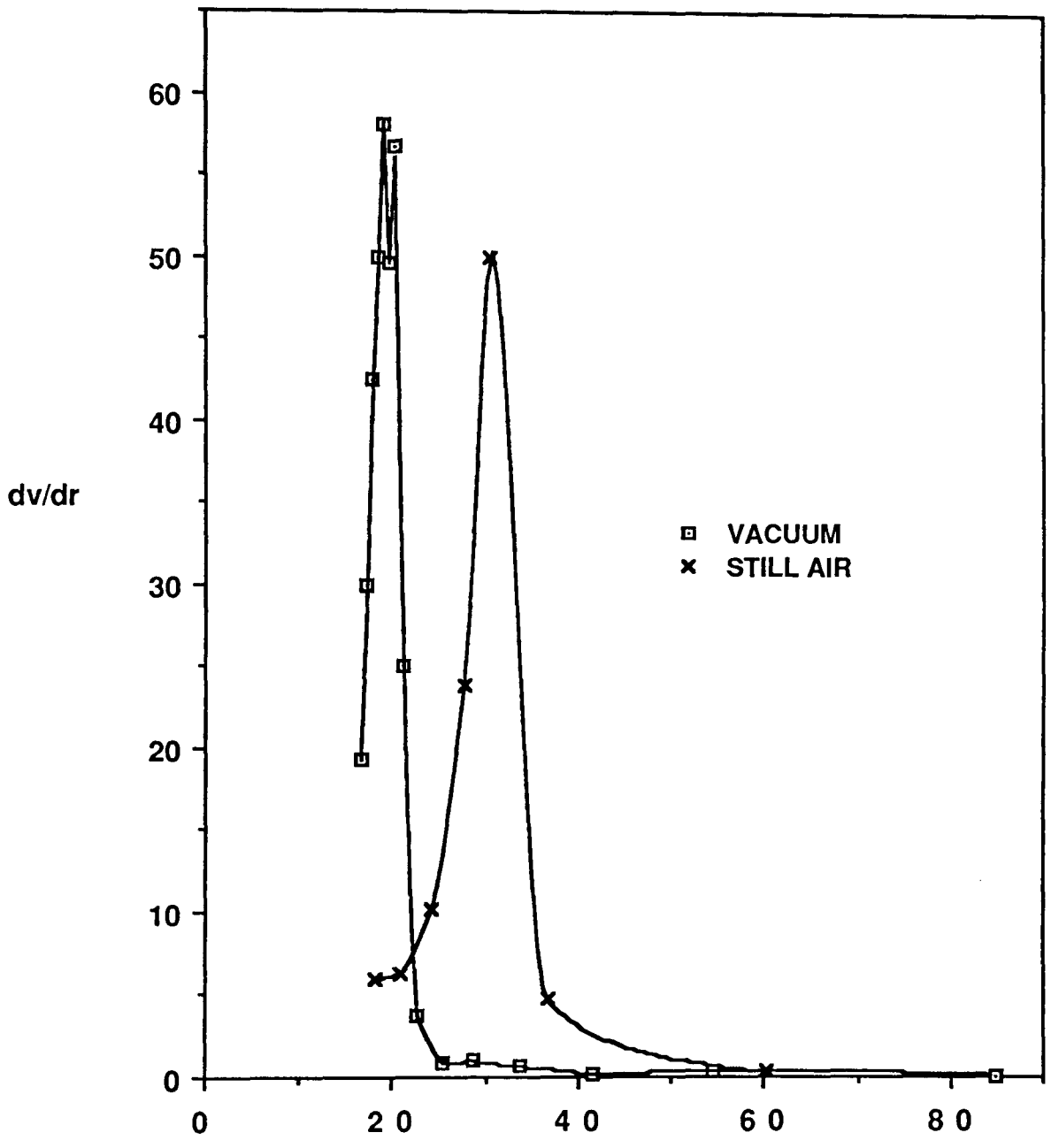

FIGURE 5.10 - Alpha-s Plots for Alumina Samples

(Δ) Vacuum

(✱) Flowing Nitrogen

(□) Still Air

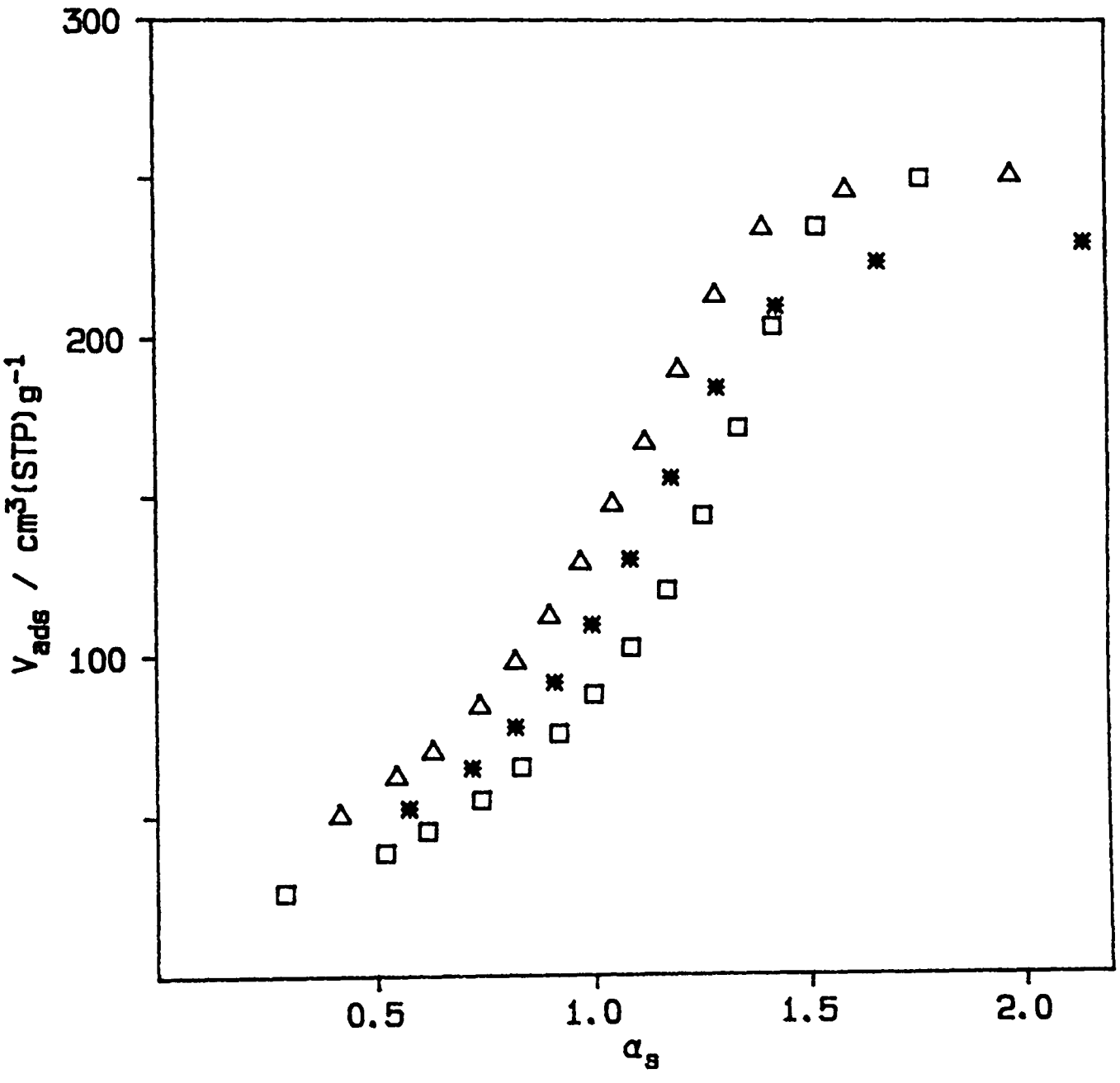

FIGURE 5.11 - Idealised Model of Plate Structure of Boehmite Gel (courtesy Leenaars et al, 1986)

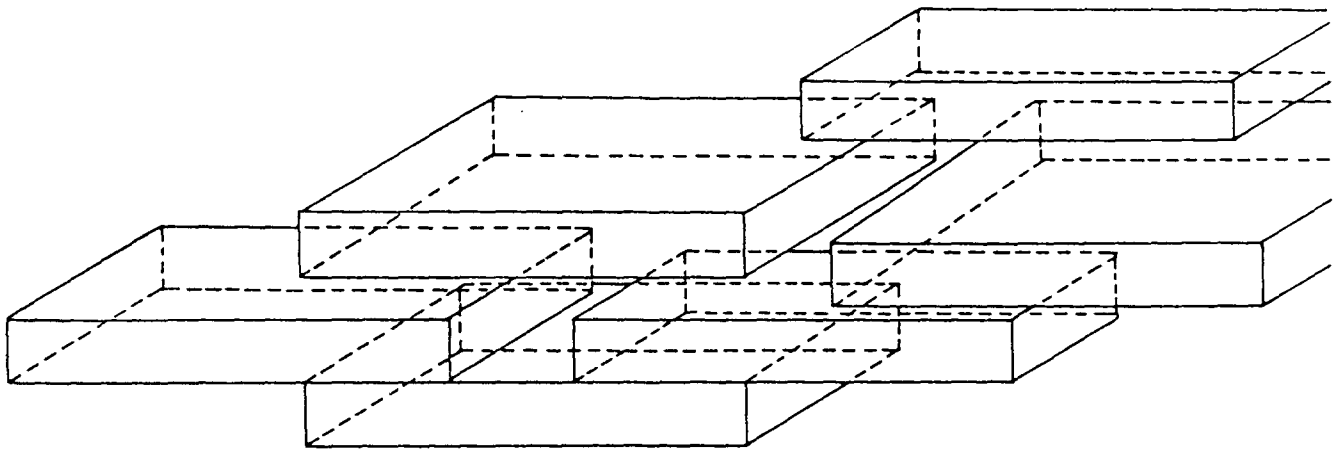

FIGURE 5.12 - Water Isotherms for Vacuum (◇) and Still Air (+) Heated Alumina

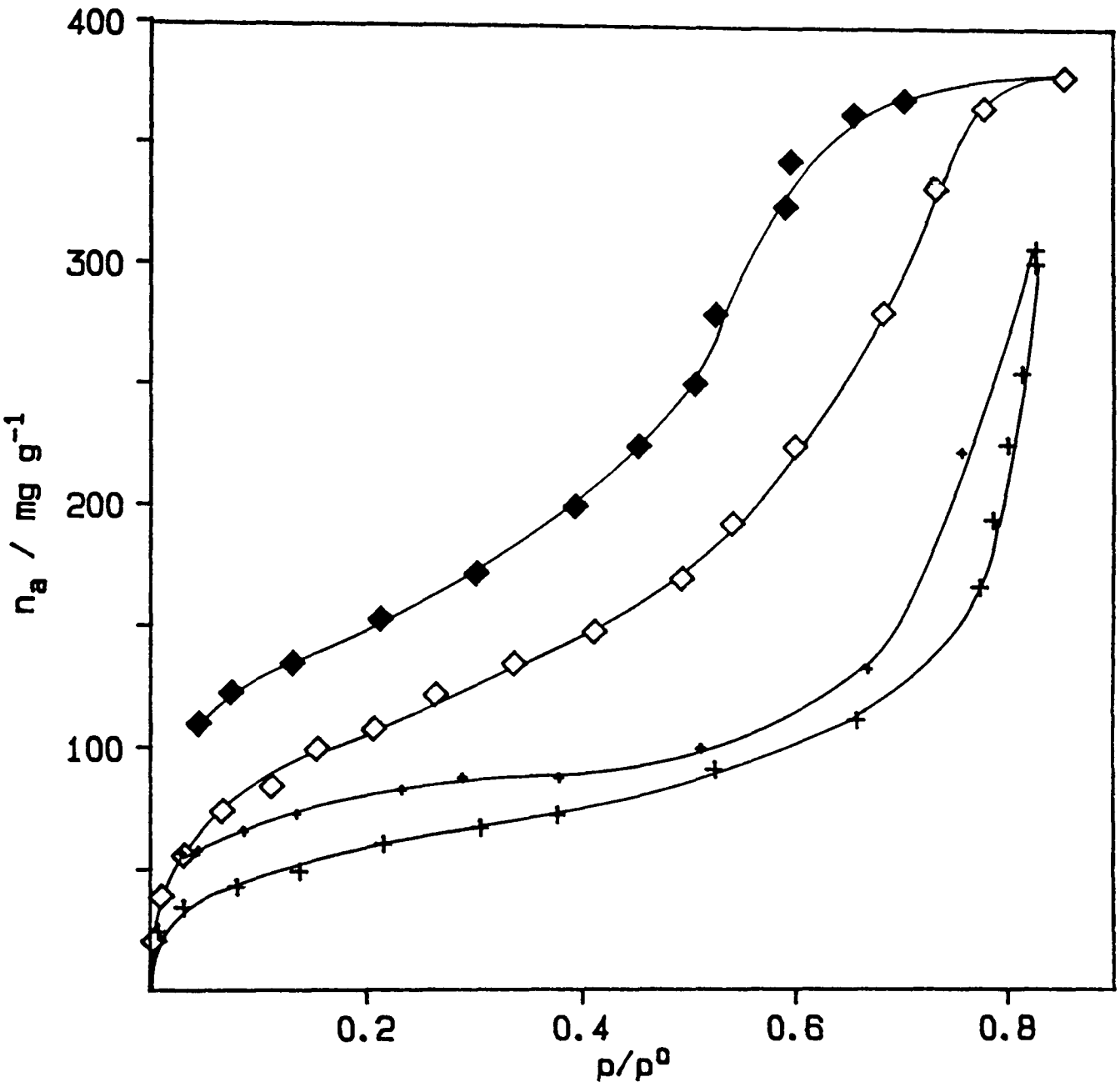

CHAPTER 6 : RESULTS AND DISCUSSION II - CARBON CLOTH

6.1 Introduction

The carbon materials used in this work were both examples of mesoporous carbon cloth. The term mesoporous carbon is used advisedly in that the carbon cloth was not exclusively mesoporous, but contained both micropores and mesopores. Both cloths were produced from a precursor of regenerated viscose rayon (see Section 3.1.2) with carbon cloth A being woven and carbon cloth B of knitted contruction.

6.2 Nitrogen Isotherms

Nitrogen isotherms were determined for both carbon cloths after outgassing at 250^{o}C (Figure 6.1). BET plots for the two carbon cloths were found to be linear over the relative pressure range 0.02-0.20 (BET plots are reproduced in Appendix B). The **apparent** BET area and the total pore volume were extracted from these isotherms (Table 6.1). Carbon cloth B had a significantly higher pore volume than carbon cloth A. The isotherms were of mixed Type I/IV (Section 2.3.5) behaviour which was expected because of the presence of both microporous **and** mesoporous networks.

Given the size of the alumina plates (>2.5nm) that were to be distributed about the carbon cloths, it was obvious that a significant fraction of the carbon cloth pore volume was not "alumina-accessible". No penetration of the micropores, for instance, is possible. However the potential "alumina-accessible" volume should still be quite considerable, particularly so for carbon cloth B where the isotherm (adsorption branch) is quite steep at relative pressures in excess of 0.4. The estimation of the alumina accessible pore volume obviously depends on a knowledge of the size of the boehmite plates and also on the geometry of the pores of the support. The dimensions of the boehmite plates have been estimated by Leenaars et al (1984) to be 2.5

nm thick with a cross-sectional dimension of 25 nm (see Figure 5.11). One must then determine which (or both) of these dimensions is critical in terms of the geometry of the receptor pores of the carbon cloth. If one cannot make this determination then any estimation of the alumina accessible volume must be necessarily approximate. The mean dimension (Leenaars et al,1984) of the alumina plates of 5.7nm was used for this purpose. From the nitrogen isotherm data it can be determined that pores of this diameter are filled at relative pressures greater than 0.65 (Gregg and Sing,1982,p.135). The pore volume corresponding to relative pressures greater than 0.65 was calculated from the isotherms of the two carbon cloths (Table 6.1) so as to serve as an indicator of the "alumina-accessible volume". This volume was significantly greater for carbon cloth B than it was for carbon cloth A.

Boehmite/carbon composites were heated to 500^{o}C under vacuum to produce the final alumina/carbon composite. To assess the effect of such heat treatment on the carbon cloth, a piece of carbon cloth A was heated under vacuum at 500^{o}C for 15hrs. The subsequently determined N_2 isotherm is compared with that of the sample subjected to normal outgassing (at 250^{o}C) in Figure 6.2. No marked change in the isotherm was observed. The microporous/mesoporous portions of the isotherm are unchanged with only a marginal difference at extremely high p/p^{o}. It was therefore concluded that heating under vacuum would not affect the carbon cloths.

6.3 Water Isotherms

Water isotherms for the two carbon cloths are reproduced in Figure 6.3. The carbon cloths were outgassed at 110^{o}C prior to the exposure to H_2O (see Section 3.2.2). These water isotherms are fairly typical of those determined for a carbon material of this

type (Roberts,a). The hydrophobicity of the carbon results in a very low uptake of water at low relative pressures ($p/p^{o}<0.3$). As the relative pressure is increased above 0.4 the uptake of water is more marked. It should be noted that despite the general classification of many carbons as "hydrophobic" the uptake of H_2O at high relative pressures can be in excess of 40% (by weight of sample).

The water isotherms were Type V in behaviour, which was expected because of the weak nature of the adsorbent/adsorbate interaction in this system. Water sorption on activated carbon is generally thought to take place by a process of pore volume filling rather than by surface coverage (Roberts,b). Therefore a water monolayer is not formed. The adsorption of a water molecule on a particularly active site (perhaps provided by an impurity centre) is then capable of nucleating other water molecules, leading to the large scale uptake of water marked by the steep upturn in the water isotherm.

Close inspection of the isotherms at low relative pressures indicate the presence of a gentle "knee". It must be remembered that the production of activated carbon cloth generally relies on the impregnation of the precursor with a number of metal halides. Despite a significant degree of volatilisation of these impregnants during carbonisation and activation, residues of the metals (presumably in oxide form) do remain (discussed further in Section 8.4). These residues may have been responsible for the slight uptake of water at low relative pressure. Interestingly the hysteresis loop did not close at low relative pressures and it is difficult to understand how the carbon cloth alone could be responsible for this behaviour, adding further weight to the argument that impurities were responsible for the small water uptake at low relative pressures.

TABLE 6.1 - APPARENT BET AREA AND PORE VOLUME FOR CARBON CLOTH A AND B

Cloth	Apparent BET Area (m^2/g)	Total Pore Volume[@] (cm^3/g)	Pore Volume[@] >p/p^o 0.65 (cm^3/g)
A	1035.4	0.83	0.20
B	1421.5	1.43	0.42

[@]using density of liquid nitrogen at 77K

FIGURE 6.1 - Nitrogen Isotherms for Carbon Cloth A(□) and B(Δ)

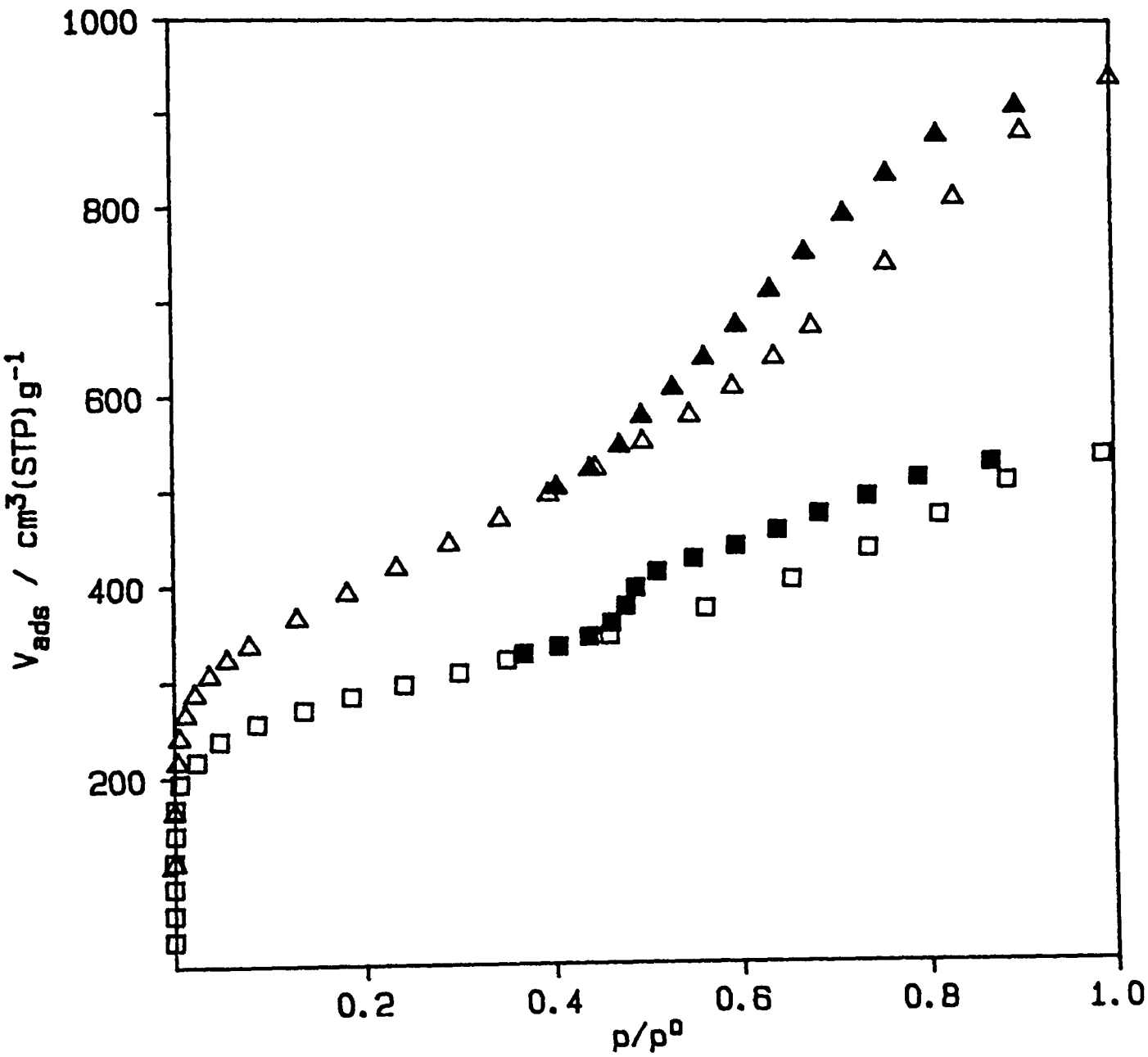

FIGURE 6.2 - Nitrogen Isotherms Showing Effect of Heating Carbon Cloth A to 500°C Under Vacuum

(□) 250°C

(×) 500°C

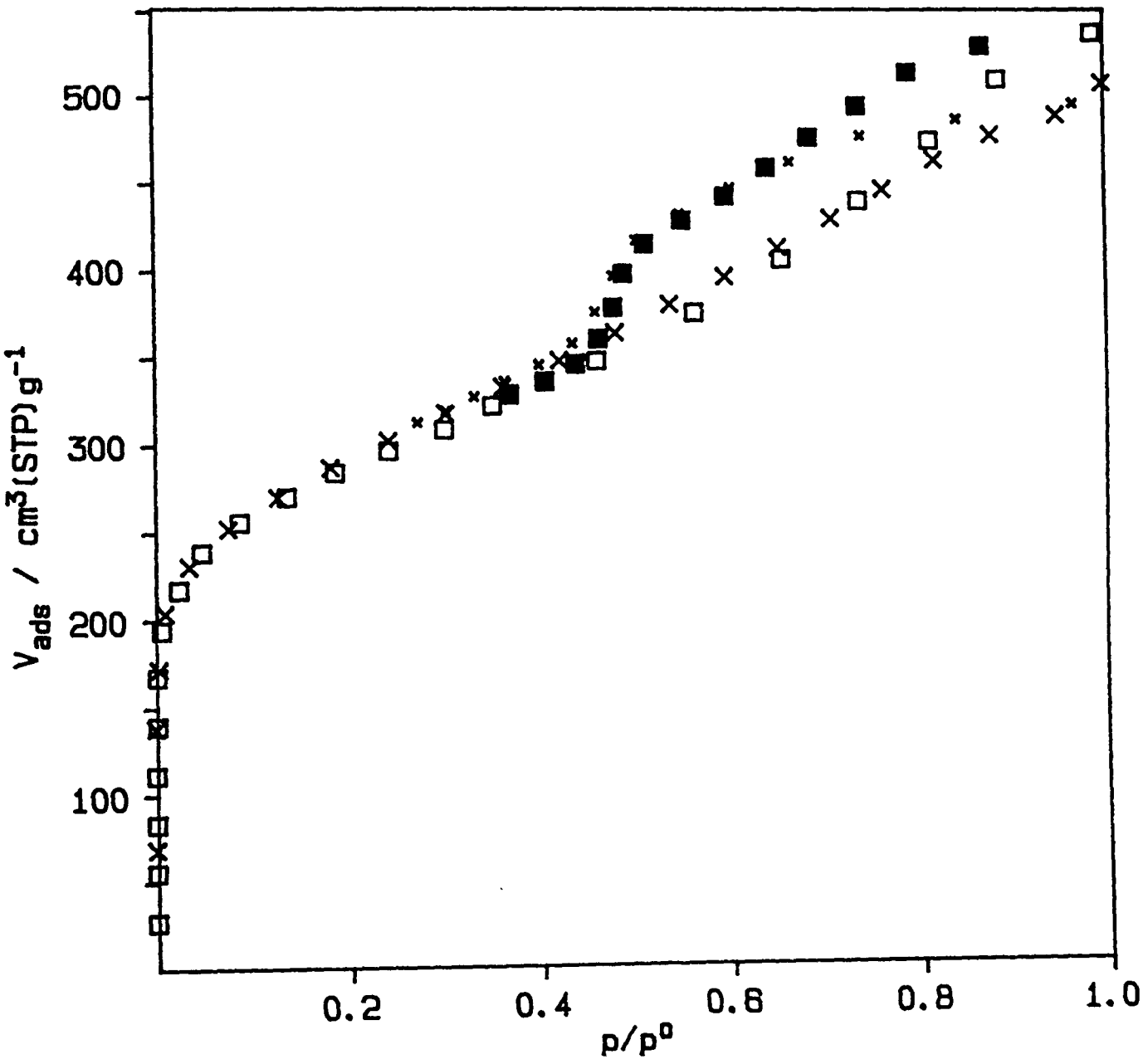

FIGURE 6.3 - Water Isotherms for Carbon Cloth A(□) (adsorption only) and Carbon Cloth B(Δ)

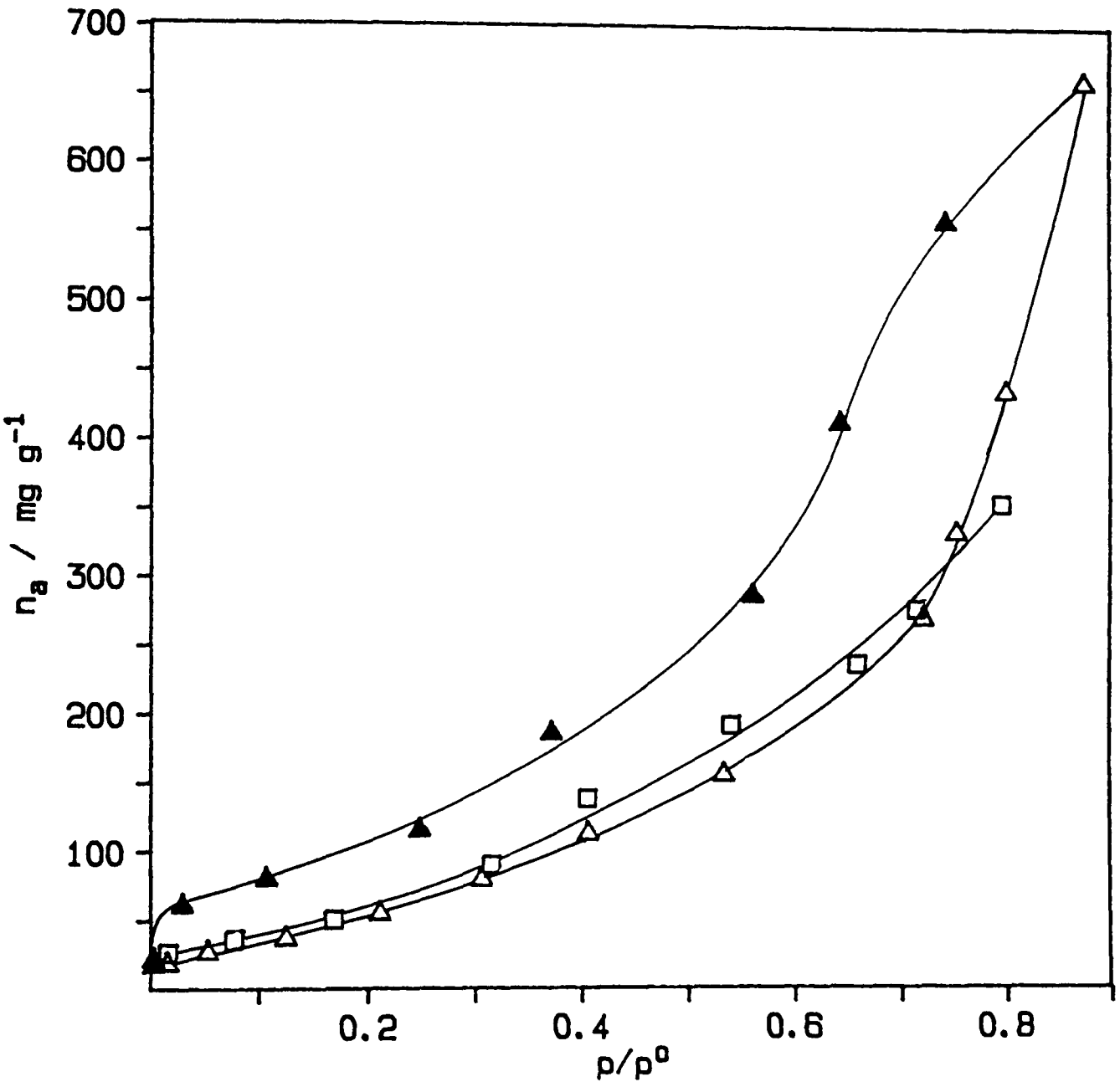

CHAPTER 7 : RESULTS AND DISCUSSION III - ALUMINA/CARBON COMPOSITES

7.1 Introduction

Mesoporous carbon cloth was impregnated by immersion in a concentrated sol of boehmite as described in Section 3.1.3. The amount of colloidal boehmite occluded could be varied by altering the concentration of the sol. A freshly prepared sol contained 3-4% w/v boehmite and evaporation on a hot plate was used to concentrate this sol. An upper practical limit to the concentration of boehmite was set by the gel point of the sol (ca. 30% w/v boehmite). In practice however sols were not concentrated to >25% w/v as the viscosity of the sol increases dramatically as the gel point is neared, making impregnation of the carbon cloth difficult. As the carbon cloths were capable of occluding 7-8 cm^3 of liquid/g a single immersion in a sol of 20% w/v would yield a loading level of approximately 150 wt.% boehmite upon drying.

7.2 Heat Treatment of Boehmite/Carbon Cloth A Composite

A sample of the composite, incorporating Carbon Cloth A, was heated to 500°C (vacuum) to dehydrate the boehmite phase. Another sample was just heated to 110°C (vacuum) so a comparision between composites containing dried boehmite and alumina could be made. These samples were subjected to analysis by Scanning Electron Microscopy (SEM) (see Figure 7.1 and 7.2). The distribution of both alumina and boehmite about the carbon cloth was found to be very poor. Microprobe analysis on clean fibres gave a very low aluminium count confirming that virtually all alumina was present in agglomerates. The heat treatment stage could not be held responsible for the poor distribution of the alumina phase, as even the sample not heated to 500°C showed significant agglomeration of boehmite on the outside of the fibre bundles. Attempts to deposit alumina on activated carbon

cloth (via chemical vapour deposition and other methods, Chapter 4) had not succeeded because of the lack of affinity between the alumina phase and the carbon cloth. The deposition of boehmite via the sol/gel route appeared to reinforce this compatibility problem.

7.2.1 Enhancing the Distribution of Alumina about the Carbon Cloth

In order to enhance the distribution of the alumina phase about the carbon cloth several methods of increasing the activity of the carbon cloth with respect to alumina were investigated. These methods all took the form of a pre-treatment stage.

7.2.1.1 Chemical Activation

Several workers (Ivanova et al,1982) have reported that chemical activation of carbon is capable of enhancing its chemical reactivity. Reagents such as nitric acid have often been used in this respect. It has been reported (Ermolenko et al,1980) that chemical activation of carbon by aluminium nitrate melts (at 140^{o}C) can be used to produce fibrous carbon ion-exchangers (FCI). This medium has advantages over nitric acid in that it can be used at higher temperatures thus making the chemical activation process more efficient by reducing the overall time required for activation.

In order to enhance the distribution of alumina about the carbon cloth chemical activation (after Ermolenko et al,1984) was investigated with the aim of using it as a pre-treatment stage.

A piece of carbonised (but not activated) viscose rayon (woven) was immersed in an $Al(NO_3)_3$ melt at 140^{o}C for 1 hour. A carbonised-only material (non-porous) was used initially so as the effect of chemical activation could best be assessed. The use of a highly porous carbon

may have obscured any pore development due to the chemical activation stage. After removal of the carbon from the melt it was subjected to the following washing sequence:

(i) hot distilled H_2O (4x)

(ii) dilute HCl (ca. 2M) (4x)

(iii) cold distilled H_2O (6x)

before being dried at 55°C. The loss in weight due to activation was found to be approximately 10%, although on subsequent outgassing (in preparation for N_2 isotherm analysis) the weight loss was much greater than that normally observed for even a highly porous carbon. Therefore one may conclude that residues from the $Al(NO_3)_3$ melt must have been retained by the cloth despite the rigorous washing procedure employed, and that outgassing at 250°C was more successful in removing these residues. N_2 isotherm analysis did not indicate the development of any porosity despite the significant weight loss. This carbon, both before and after chemical activation, was subjected to SEM analysis. Images are reproduced in Figure 7.3 and 7.4. The SEM analysis, in particular, and supported by the large weight loss, demonstrated that the effect of chemical activation was to smooth out the individual fibres of the support rather than to develop porosity.

Activated carbon cloth was also subjected to chemical activation prior to impregnation with a concentrated boehmite sol. Conventional activation of the carbon cloth results in a considerable weight loss (typically 60-80%) in producing a mesoporous material. As a result the mechanical strength of mesoporous carbon cloth is significantly less than that of a carbonised piece of the precursor. The corrosive nature of the aluminium nitrate melt considerably reduced this mechanical strength further so that after the carbon cloth was removed from the $Al(NO_3)_3$ melt it was susceptible to fracture and tearing during

subsequent handling. Carbon cloth B was found to be less prone to such mechanical breakdown than was carbon cloth A, as the former was based upon a knitted precursor while the latter's precursor was simply woven. Despite this qualification, the distribution of boehmite on chemically pre-treated carbon cloth was found to the markedly enhanced. SEM analysis indicated that no large agglomerates of boehmite were present on the outside of the fibre bundles that make up the cloth. This improved distribution (or at least lack of agglomeration) may have been due to either improved affinity between the carbon and alumina phases or perhaps just to the smoothness of the cloth fibres after chemical activation, or perhaps to a combination of both effects.

7.2.1.2 Phosphate Impregnation of the Carbon Cloth

Metal-phospate interactions are chemically quite common. It is recognised that the affinity between the two species is not universal but dependent upon the form of the metal and phospate species prior to reaction. However the possible use of phosphate as an anchor to the colloidal boehmite was thought worthy of investigation. Pieces of carbon cloth A were dipped in solutions of 10% (w/v) $NaH_2PO_4.2H_2O$ and dried at 55^{o}C prior to immersion in the boehmite sol in the conventional manner (and redrying at 55^{o}C). The composite material and a blank cloth (impregnated with phosphate but not with boehmite) were then subjected to SEM analysis. Images of the boehmite/phospate/carbon A system are reproduced in Figures 7.5 and 7.6. SEM/microprobe analysis of the blank cloth (phosphate only) indicated that no obvious agglomeration of phosphate had taken place, rather the phosphate was well distributed. Observation of the boehmite impregnated phosphate/carbon cloth A, however, showed the presence of large deposits. The images were "digimapped" in order to qualitatively

identify the elemental nature of these large deposits. This analysis indicated that the deposits were not composed solely of Al (from the boehmite sol) but rather were an Al/P amalgam. Indeed whether the image was of the fibre bundles or of individual fibres (at higher resolution) the digimaps indicated that very little independent Al (red areas) was present. Rather the Al and P were present in co-agglomerates and there was a good deal more independent P than Al. Such observations were not altogether unexpected in the light of other observations noted during the impregnation of carbon A/phosphate with boehmite. The boehmite sol was observed to commence gelling when the phosphate impregnated carbon cloth was immersed in it. Given that the sol was close to its gel point anyway this was not surprising, in that sols may be routinely "gelled" by the addition of electrolyte (the electrolyte serves to decrease the inter-particle repulsion, initiating the formation of the gel structure). Obviously the immersion of the phosphate impregnated carbon in the boehmite sol had caused some re-dissolution of the phosphate. Gelation of the boehmite sol was triggered and re-precipitation of a boehmite/phosphate amalgam occurred. One could further conclude that total re-dissolution of the phosphate did not occur as significant amounts of free phosphate (as P) were detected by digimapping of the final composite.

Despite the obvious affinity between the boehmite and phosphate phases the pre-impregnation of the carbon cloth with phosphate did not improve the distribution of boehmite about the cloth. As a result this technique was not pursued further.

7.2.1.3 Prewetting the Cloth

Carbon cloth is quite hydrophobic in nature in contrast to the alumina phase, the surface of which being highly polar is significantly

more water-avid. This distinction is reinforced by the water isotherms of the two materials (see Section 5.5 and 6.3). In the present work the alumina phase was being presented to the carbon cloth in an aqueous medium. One may speculate that the hydrophobic nature of the cloth may be responsible for the agglomeration of the deposited boehmite. That is, the dispersion of the deposit may be limited by the dispersion of its supporting medium during the initial impregnation/wetting stage. In order to test this hypothesis, and to improve the distribution of the boehmite sol about the carbon cloth a "pre-wetting" stage was incorporated into the composite preparation sequence. The cloths were immersed in distilled water and stirred to remove air bubbles so as to thoroughly wet the cloth prior to immersion in the boehmite sol. No drying of the "pre-wetted" cloth was performed, the cloth simply being gravity-drained (for approximately 5 seconds) before immediate immersion in the boehmite sol. SEM analysis indicated a major improvement in the distribution of boehmite (Figure 7.7). Large boehmite agglomerates were absent from the outside of fibre bundles (c.f. Figures 7.1 and 7.2) and individual fibres of the carbon cloth were observed to be evenly coated. These coatings were observed (by SEM) in thicknesses down to 0.2 micron. As a further aid to dispersion ultra-sonication (the impregnation container being placed in an ultra-sonic bath) was used during the pre-wetting and boehmite impregnation stages.

7.2.2 Discussion

In summary then, both chemical activation (via aluminium nitrate melts) and the use of pre-wetting/ultrasonication were found to improve the initially poor distribution of the boehmite sol about the carbon cloth. Phosphate pre-impregnation was not found to be advantageous in this respect. Of the two successful methods chemical activation was

found to be quite deleterious to the mechanical strength of the carbon cloth, making subsequent handling difficult. The procedure was also quite time consuming and expensive to perform routinely. Pre-wetting/ ultrasonication on the other hand was found to be an extremely simple method of enhancing boehmite distribution, and one that could be very readily incorporated into the composite preparation process. As a result of this convenience this technique was used exclusively for composite preparation.

Unfortunately the question of mesopore penetration by the boehmite plates could not be answered by SEM because of a resolution problem. Therefore no conclusion could be drawn at this stage as to whether the improved distribution of alumina in the microscopic range (>0.1 micron) had been translated to the mesopore range (2-50nm). The improved distribution of the boehmite plates about the carbon cloth may be thought of conveniently as a two stage process:

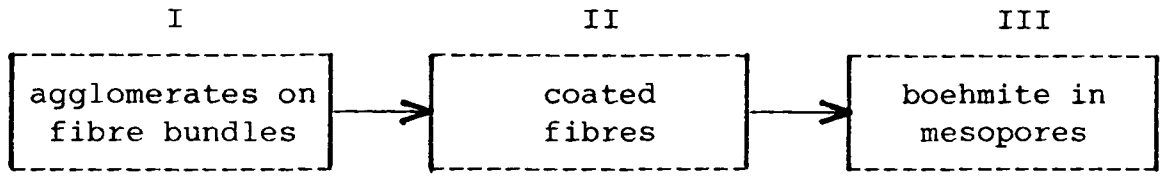

The use of chemical activation or pre-wetting has resulted in a definite movement from I to II, as shown by SEM. The lack of SEM penetration into regime "III" prevents determination of any further progress at this stage. Other characterisation techniques are described in the remaining parts of this, and the following chapter, in an attempt to assess any such progress.

7.3 The Preparation of Composite A and Composite B

In Chapters 5 and 6 the individual adsorption behaviour of the alumina and carbon phases have been presented and discussed. The

adsorption behaviour (with respect to N_2 and H_2O) of two Al_2O_3/C composites is now presented and interpreted with reference to the isotherms of the individual components. To allow proper comparison, only data pertaining to the preparation of individual components under similar conditions to those used in composite preparation was employed.

Composites A and B were prepared by the impregnation of carbon cloths A and B, respectively, with concentrated boehmite sols utilizing pre-wetting and ultrasonication to attain good distribution of boehmite particles about the mesoporous cloth. The wet composite was then dried at 55°C prior to heating under vacuum at 500°C for 1 hour (heating rate 10°C/minute). The specific impregnation details are reproduced in Table 7.1. Carbon cloth B was capable of occluding a larger volume of solution than carbon cloth A, thus the boehmite loading level of the cloth B based composite was higher than that based on cloth A. Despite the high loading level of boehmite the macroscopic appearance of the composites was not significantly altered from that of the cloths, the black colour of the cloth and its texture still dominating. The optical properties of the dried gel may have been partly responsible for this result, in that both the dried gel and the final alumina (after heat treatment) were translucent, although the good distribution of the boehmite inevitably helped in this regard. The most obvious change in the macroscopic properties of the carbon cloth as a result of boehmite deposition was to its flexibility, which was significantly reduced. At particularly high loading levels the structure of the gel begins to dominate that of the carbon cloth, to the extent that the shrinkage of the gel during drying may in extreme cases result in fracture of the cloth.

7.3.1 Calculation of Weight Fraction Alumina and Carbon

For the analysis that follows, the weight fractions of Al_2O_3 and C in the composites must be determined. The calculation of these weight fractions is quite straightforward. The weight of alumina cannot obviously be calculated directly from the change in weight of the carbon cloth after boehmite impregnation. The following factors must be taken into account :

a) The carbon cloth is impregnated with boehmite while subsequent heat treatment yields alumina. The loss of water causes the weight of alumina to be less than the weight of boehmite. The theoretical weight loss accompanying the transition from boehmite to alumina is 15%. The experimental weight loss (using the sol/gel route) is however greater than this at 18%. Yoldas (1973) has attributed this difference to

(i) the presence of a small amount of the trihydroxide

(ii) excess water initially

(iii) slightly incomplete hydrolysis.

Given that the sample was dried for 24 hours at 110^{o}C prior to calcination the second cause would be thought to be unlikely. The 18% weight loss has been confirmed in the present work for a sample of the dried boehmite gel heated initially under vacuum at 110^{o}C (for 16 hours) and then at 500^{o}C for the same period. The water activity of these boehmite gels (both before and after heat treatment) is such that accurate gravimetric analysis can be extremely difficult under ambient conditions. An accurate analysis would require that the sample be rigorously outgassed at temperatures in excess of 110^{o}C, conditions that are not conducive to rapid composite production and processing. Instead in this work another procedure was adopted, whereby both the boehmite gel and composites were dried at 55^{o}C prior to vacuum desiccation and

immediate weighing. Under these conditions the dried gel was found to undergo a fairly constant weight loss of 27% after heat treatment. This weight loss can be apportioned between the loss of internal H_2O and the amount of water retained by the incompletely dried gel. This change in weight was found (by repeated determinations) to be in the range 27+/-1%. Using this value the weight of alumina in the final composite could be readily calculated from the weight of boehmite occluded during impregnation.

b)The carbon cloth was also observed to change weight during composite production. The origins of this weight loss were two-fold:

(i) Mesoporous carbon cloth is generally activated to a higher degree than microporous carbon cloth. As a result the cloth tends to be prone to slight powdering. The pre-wetting and impregnation stages served to remove this powder from the cloth. To assess the magnitude of this weight loss pieces of carbon cloth were dipped in water (in an identical procedure to that employed during impregnation) and dried ($55^{o}C$,vacuum desiccated). The weight loss was determined to be 7+/-1% independent of the cloth employed.

(ii) Heating of the composite also caused a further slight weight loss to the carbon cloth. The heat treatment of unimpregnated carbon cloth (blanks) indicated that this weight loss was 10+/-1% (again independent of the cloth employed).

No other sources of weight loss were observed during the composite production process. The weight fractions of alumina and carbon in the two composites were then calculated. The relevant data are reproduced in Table 7.2. This procedure was employed consistently to calculate the weight of alumina and carbon for all composites reported in present work.

7.4 Nitrogen Isotherms for Composites A and B

The nitrogen isotherms for Composites A and B are reproduced in Figures 7.8 and 7.9. The isotherms for the individual components (from Chapters 5 and 6) are included for comparision. Carbon cloth A was heated under vacuum to 500°C as was the alumina (sample no.11). Carbon cloth B was heated only to the normal outgassing temperature (250°C) (it has already been shown (see Figure 5.2) that the N_2 isotherm was not significantly affected by the higher outgassing temperature).

In both cases it was observed that the uptake of N_2 by the composite material was less than that of the carbon cloth, as would be expected because the uptake of N_2/g of alumina is less than that of the cloth. Because of this effect, to plot the isotherms as a function of the outgassed sample weight was not particularly diagnostic when it came to determining whether the deposition of the mesoporous alumina on mesoporous carbon had affected the overall N_2 uptake compared with what one would expect from the individual isotherms. It can be seen that in Figure 7.8 and 7.9 the volume of N_2 adsorbed per g of pure material and per g of composite has been plotted. Although such a method is traditionally employed it was not all that helpful in the present context where the distribution of alumina was to be investigated.

7.4.1 Comparison Between Measured and Calculated Adsorption of Nitrogen

The isotherm data for the individual components were replotted as N_2 uptake per g of composite allowing comparison of the measured and "calculated" isotherms. This latter isotherm was obtained by mixing the isotherms for the individual components in the same ratio as the components were present in the composite. For Composite A (62%C, 38%Al_2O_3), the N_2 uptake for 0.62g of carbon cloth A and 0.38g of

alumina were calculated. The isotherms were then summed (see Appendix C) and replotted against the measured isotherm (Figure 7.10). The same procedure was used for Composite B for which the nitrogen uptake of 0.47g of carbon cloth B and 0.53g of alumina was calculated. The resulting "calculated" isotherm is compared with the measured isotherm in Figure 7.11. The comparison was only made for the adsorption branches of the respective isotherms.

The calculated isotherm is what one would obtain if the combination of the two phases did not affect the porosity of either phase (ie. similar to the situation where the two phases were completely separate but still present in the same gas burette during isotherm analysis). This can be thought of as the extreme case of non-distribution of the alumina phase about the carbon cloth. Indeed the SEM analysis has already shown that we have intimate distribution of alumina about the fibres of the carbon cloth on the sub-micron scale. Because the N_2 isotherms yield useful information on pores <20nm (Gregg and Sing,1982,p.135) this technique was being used as a probe for alumina distribution in the mesopore range.

As we can see from Figure 7.10 and 7.11, the correlation between the calculated and measured isotherms was very good at low relative pressures. That the correlation was so good at low p/p^o was a vindication of the technique used and of the validity of the assumptions employed in the construction of the calculated isotherm. Obviously the Al_2O_3/C balance in the composite has been fairly accurately calculated. It was not at all surprising that there was a lack of deviation between the measured and calculated isotherms at low relative pressures ($p/p^o<0.4$). Given the size of the alumina plates (minimum dimension 2.5nm) micropore penetration was obviously impossible. The deviation between the two isotherms commences at $p/p^o = 0.75$. This p/p^o

corresponds to pores of 8nm diameter (using a cylindrical pore model, Gregg and Sing,1982,p.135). However if this deviation were due to entry and subsequent blockage of the mesopores of the carbon cloth one would expect the measured N_2 uptake to be less than the calculated uptake in this relative pressure region. The converse is true - the presence of alumina about the carbon cloth has increased the N_2 uptake at high p/p^o. Despite bulk alumina being approximately 60% porous (see Table 5.2) simple penetration of carbon mesopores by boehmite plates would result in a decrease in the overall N_2 uptake at higher p/p^o. Therefore such an explanation is not valid and some other phenomenon must be responsible for the observed deviation at high p/p^o.

Let us begin our discussion by observing that the deviation between the calculated and measured isotherms was due to the filling of larger mesopores (corresponding to high relative pressure). Given the nature of our composite (2-component) the source of this mesoporosity should be fairly limited. Let us first consider the alumina phase.

Inspection of Figure 7.8 indicates that the nitrogen uptake of the alumina has reached a plateau at a relative pressure of 0.70. Therefore the pores of the alumina phase could not be responsible for the observed porosity at $p/p^o>0.75$. However this result corresponds to a well-ordered array of alumina plates. It is perhaps feasible that this regular plate structure may have been interrupted by the presence of the carbon cloth causing the generation of larger spaces (and therefore larger pores) between the alumina plates. Let us therefore consider the deposition of alumina on a fibre of the carbon cloth, such as that observed by SEM (Figure 7.7). A schematic representation of this situation is reproduced in Figure 7.12. The average fibre diameter is approximately 2 microns whereas the typical plate dimensions are 2.5 x 25nm. The size of the plates have been exaggerated in Figure 7.12

in order to demonstrate how a curved surface could cause the opening of the plate structure. In fact the relative dimensions of the plate and fibre are such that no significant opening of the plate structure could occur. To all intents and purposes the cylindrical fibre could be modelled as a flat surface as far as the deposition of alumina plates was concerned. Therefore we may conclude from this analysis that if the extra pore volume of the composite was due to the opening of the plate structure of the alumina, then deposition on the fibres of carbon cloth was not responsible. Instead, by extension of the analysis performed above we can see that only deposition of alumina plates on elements of the carbon cloth of similar size to the plates themselves could result in a signigicant interruption of the plate structure and therefore to the observed enhancement in pore volume. To summarise then, if the alumina phase was responsible for the enhanced pore volume of the composite then interaction between the alumina and the carbon cloth at a nm level (rather than a micron level) is implied.

Leenaars et al (1986) impregnated porous ceramic supports with a boehmite sol. They reported that, "...the sol is sucked into the support as a result of the capillary forces exerted by the pores of the support. When the pores of the support are small enough, the boehmite particles enter at a slower velocity than the water and the concentration of boehmite at the entrance of the pores increases." A similar mechanism is presumably operating in the present work, resulting in globular deposits of boehmite (and finally alumina) particles about the pore entrances of the carbon cloth. In this way the measured nitrogen isotherms, in particular the enhancement in nitrogen uptake at high p/p^{o} and the lack of pore blockage of the carbon cloth by the deposited alumina, would be satisfactorily explained.

Let us now consider the carbon cloth. The nitrogen isotherms of

the carbon cloths (Figures 7.8 and 7.9) indicate that the pore volume increases steadily at relative pressures in excess of 0.7. Therefore, unlike the alumina phase, the carbon cloth does include some pores that are filled by nitrogen in the relative pressure range of interest. The presence of alumina about the carbon cloth results then in more pores of this size range being formed. A possible explanation of this enhanced pore volume then, is that the boehmite plates have served to wedge open the larger mesopores of the carbon cloth, thereby increasing their pore volume further. However such an explanation would involve a significant degree of carbon cloth pore blockage therefore making a net gain in pore volume more difficult to rationalise.

7.4.2 Nitrogen Adsorption /g of Carbon Cloth.

In order to assess the overall effect on the uptake of N_2 by the carbon cloth (before and after impregnation with alumina) the volume adsorbed needs to be expressed in terms of some unit that is a dependent upon the cloth alone. That is, a parameter independent of the weight of alumina occluded. One such parameter is (to plot uptake) per unit geometric area of carbon cloth as this is a convenient macroscopic quantity that can readily be determined. The nitrogen uptake could be converted to units of volume adsorbed/100cm^2 of carbon cloth (this unit is convenient as 100cm^2 of carbon cloth weighs ca. 1g). More conventionally however, the nitrogen uptake may be expressed in units of volume adsorbed/g of carbon cloth and this procedure has been adopted in the current work. The isotherms for Composite A and Composite B, expressed in this manner, are reproduced in Figure 7.13 and 7.14. The isotherms of carbon cloth A and carbon cloth B are included for comparison. It can be clearly seen that the uptake of N_2/g of carbon cloth is significantly greater for the composite material than for the

un-impregnated cloth. Again the enhanced composite uptake at p/p^o >0.8 relative to that of the carbon cloth should be noted. For a given piece of cloth the inclusion of alumina has not caused a reduction in the pore volume. Rather the pore volume of the composite is significantly greater than that of the carbon cloth primarily due to the non-blockage of the carbon mesopores (despite the significant weight of alumina occluded), and is further enhanced by the porosity of the deposited alumina itself. The alumina has been accommodated in a finely divided form without interfering significantly with the pores of the carbon cloth. The microporous nature of the cloth has been retained simply because of the inability (due to steric considerations) of the boehmite plates to penetrate in this size regime. The mesoporous nature of the cloth has also been retained, possibly for the same reasons. The uptake of N_2 by the composite material at high relative pressures is greatly enhanced compared to that of carbon cloth, probably due to the disruption of the porous network of the alumina phase as discussed earlier.

7.5 Water Isotherms for Composites A and B

The water isotherms for the two composite materials are now presented in an analogous fashion to that just described for the N_2 isotherms. In Figure 7.15 and 7.16 the water isotherms for composite A and B are reproduced. The water isotherms of the respective carbon cloths and alumina (prepared under the similar conditions as the composite) are included for comparison. In contrast to the nitrogen isotherms, the uptake of water by alumina is greater than that by the carbon cloth, except at extremely high relative pressures.

7.5.1 Comparison Between Measured and Calculated Adsorption of Water

Using the known weight fraction of the alumina and carbon phases (Table 7.2) the "reduced" isotherms (adsorption only) were determined (for Composite A these corresponded to the uptake of H_2O by 0.62g of carbon and 0.38g of alumina). The summation of these two reduced isotherms, to yield the "calculated" isotherm is reproduced in Figure 7.17, where the measured H_2O isotherm is included for comparison. An identical procedure was applied to Composite B (for 0.47g of carbon and 0.53g of alumina), and the resulting comparison between the measured and calculated isotherms is reproduced in Figure 7.18.

As for the N_2 isotherms presented earlier the correlation between the calculated and measured isotherms at low relative pressures was remarkably good. If anything the measured H_2O uptake was marginally less than that calculated at low relative pressures (0.1-0.4), while at high relative pressures (>0.7) the measured uptake was again observed to be greater than the calculated uptake. This latter deviation was not quite so marked as for the N_2 isotherms.

Due to its highly polar nature, the interaction of H_2O with a porous material is much more complicated than that of N_2. With a N_2 isotherm there is a clear connection between the relative pressure and the dimensions of the pore being penetrated. With water sorption however, the correlation is by no means clear cut and specific interactions may tend to override the ever present (but not as strong) interactions normally associated with physisorption. The analysis of water isotherms for individual components is still the subject of much discussion, particularly for the carbon phase (Roberts,1988). The analysis of such an isotherm for a composite material is obviously even more complicated, with the presence of such a water active substance as

alumina adding a further complication (see Section 5.5). Suffice to say that the observed uptake was very similar to that predicted on the basis of the individual H_2O uptakes for the two components.

7.5.2 Water Adsorption /g of Carbon Cloth.

Finally the uptake of H_2O (adsorption only) was determined per g of carbon cloth (Figure 7.19 and 7.20) for each composite. The uptake of H_2O by the composite was significantly enhanced compared with the un-impregnated carbon. The enhancement was greater than that observed for N_2 because the water uptake of the alumina was greater than that of the cloth. For a given weight of carbon cloth the presence of alumina has resulted in approximately a two-fold increase in the H_2O uptake throughout the relative pressure range. The presence of alumina has significantly enhanced the uptake of H_2O at low relative pressures where the hydrophobicity of the carbon cloth normally results in a very low uptake.

7.6 Comparison of Boehmite Uptake Between Microporous and Mesoporous Carbon Cloth

SEM analysis of composites (Section 7.2.1.3) indicated that the boehmite phase was well distributed about the carbon cloth on the micron scale. The characterisation of the composite materials by N_2 adsorption indicated that the alumina was not blocking the accessible mesopores, but rather the mesoporous volume of the composite material was enhanced by the presence of alumina.

In order to obtain further information on the interaction between the alumina phase and the mesopores of the carbon cloth a quantitative investigation of the uptake of alumina by a microporous carbon cloth was initiated for comparative purposes. It should be remembered that due to

the size of the boehmite plates, no penetration of micropores would be possible on steric grounds (micropores <2nm diameter). A microporous carbon cloth (low burn off, 3/3/3 mix) was chosen which had a minimal mesopore volume. The N_2 isotherm of this microporous carbon (reproduced in Figure 7.21) was highly rectangular.

7.6.1 Impregnation with Concentrated Boehmite Sol

The highly mesoporous carbon cloth B was used for comparison. The cloths were impregnated in the usual manner with the aid of pre-wetting and ultrasonication. The relevant impregnation data for the two cloths is reproduced in Table 7.3. From this data we indeed see that the mesoporous cloth occludes a greater weight of boehmite/g of cloth than does the microporous carbon. However this comparison also shows that the microporous carbon cloth does not by any means reject the boehmite sol because of a lack of appropriately sized mesopores.

7.6.2 Impregnation with Dilute Boehmite Sol

The impregnation experiment was repeated at a much lower concentration of boehmite (ca. 100 ppm). The microporous and mesoporous cloths were impregnated with this dilute boehmite sol in the normal manner. The concentration of boehmite was determined by AA for aluminium, as a gravimetric analysis was not sufficiently accurate at this concentration level. The concentration difference before and after impregnation of the carbon cloth allowed the uptake of boehmite by the respective cloths to be calculated. The relevant data are reproduced in Table 7.4.

This data again confirms the results of the previous impregnation experiment (high [boehmite]), in that on a weight basis the mesoporous cloth is capable of removing more boehmite during impregnation than the

microporous cloth.

7.6.3 Discussion

The results reported above reinforce those arising from the nitrogen isotherms for the alumina/carbon composites. If the mesopores of the carbon cloth were required to accommodate the deposited boehmite then one would have expected a much more drastic difference in boehmite uptake between the microporous and mesoporous carbon cloth. The predominant deposition of boehmite at pore entrances is therefore confirmed. The slight difference in uptake of boehmite between the two cloths is probably due to the more significant clustering of boehmite plates allowed at the wider pore entrances of the mesoporous cloth.

An interesting feature of the low concentration impregnation experiment was the specific interaction between boehmite and the carbon cloth in this concentration regime. The impregnation of carbon cloth (both microporous and mesoporous) with a whole range of impregnants (including aluminium and phosphate salts, see for example Tables 4.1 and 4.2)) has been shown (Hayes,b) to be non-specific in the percentage concentration regime. That is, for impregnation concentrations in the range 1-25% (w/v) the uptake of the salt is governed simply by the volume of solution occluded by the carbon cloth during the impregnation stage. For example the impregnation of a cloth that occludes 5 cm^3/g of a 1% w/v impregnation solution will result in a 5%w/v loading of the salt upon drying. The initial high [boehmite] impregnation experiment (Table 7.3) followed this relationship. The data at the base of Table 7.4 indicate that at much lower concentrations of impregnant (ca. 0.01% w/v in this case) the uptake of impregnant is much higher than one would expect from the volume of solution occluded. Indeed the measured uptake is 7-8 times greater than expected. This

observation is not specific to colloidal boehmite impregnation as a similar enhanced uptake has been observed for Pt sols (Hayes,c). One may perhaps think of the uptake of an impregnant by the carbon cloth in terms of two independent processes. At low impregnant concentrations we may model the uptake by an "sorption" process. Here a specific interaction between the carbon cloth and the impregnant prevails. However at higher concentrations uptake of impregnant occurs via occlusion and subsequent precipitation during drying of the carbon cloth. At these high concentrations the magnitude of the uptake relying on solution occlusion is such that any underlying specific uptake of the impregnant will be swamped. Only at sufficiently low concentrations does the sorption of impregnant prevail. Interestingly it is much more likely that deposition relying on sorption will result in better distribution of the impregnant about the cloth than will deposition relying on occlusion (and subsequent precipitation). The latter technique tends to coat the fibre bundles of the carbon cloth leading to agglomeration, as indeed was the case in the present investigation before pre-wetting/ultrasonication was employed to aid boehmite distribution about the cloth.

TABLE 7.1 - IMPREGNATION DATA FOR COMPOSITE A AND COMPOSITE B

	Composite A	Composite B
Initial Weight[@] of Carbon Cloth (g)	0.2537	0.1728
Final Weight[@] of Boehmite Impregnated Carbon Cloth (g)	0.4135	0.3856
Dimensions of Cloth (cm)	5.0x5.1	4.9x5.5
[Boehmite sol] (%w/v)	20.0	16.9

[@]samples vacuum desiccated prior to weighing.

TABLE 7.2 - WEIGHT FRACTIONS ALUMINA AND CARBON FOR COMPOSITE A AND COMPOSITE B

	Composite A	Composite B
Weight of Carbon Cloth (g):		
Initially	0.2537	0.1728
After Impregnation	0.2359	0.1607
After Heating to 500^{o}C/vacuum	0.2123	0.1446
Weight of Boehmite (g)	0.1776	0.2249
Weight of Alumina After Heating (g)	0.1296	0.1642
Weight % Carbon	62	47
Weight % Alumina	38	53

TABLE 7.3 - COMPARISON OF BOEHMITE UPTAKE FROM CONCENTRATED SOL BETWEEN MICROPOROUS AND MESOPOROUS CARBON CLOTH

Carbon Cloth	Microporous	Mesoporous
Geometric Area of Cloth (cm^2)	25.5	23.3
[Boehmite sol] (%w/v)	20.15	18.44
Initial Weight[@] of Cloth (g)	0.3266	0.1477
Final Weight[@] of Boehmite Impregnated Cloth (g)	0.6280	0.3424
Weight of Boehmite Occluded (g)	0.3014	0.1947
Loading of Boehmite (wt.%)	92.3	131.8

[@]samples vacuum desiccated prior to weighing

TABLE 7.4 - COMPARISON OF BOEHMITE UPTAKE FROM DILUTE SOL BETWEEN MICROPOROUS AND MESOPOROUS CARBON CLOTH

Carbon Cloth	Microporous	Mesoporous
Geometric Area of Cloth (cm^2)	25.9	24.5
Initial [Boehmite sol] (mg/L)	122.5	122.5
Final [Boehmite sol] (mg/L)	55.6	61.1
Initial Weight of Cloth (g)	0.3212	0.1780
Weight of Boehmite Occluded (mg)	1.73	1.37
Loading of Boehmite (wt.%)	0.54	0.77
Volume of Boehmite sol (cm^3)	25.89	22.31
Volume of sol Occluded by Cloth (cm^3)	1.70	1.60
Expected Weight of Boehmite Occluded (g)	0.21	0.20

FIGURE 7.1 - Boehmite/Carbon Cloth A Composite Heated to 500°C(vacuum)

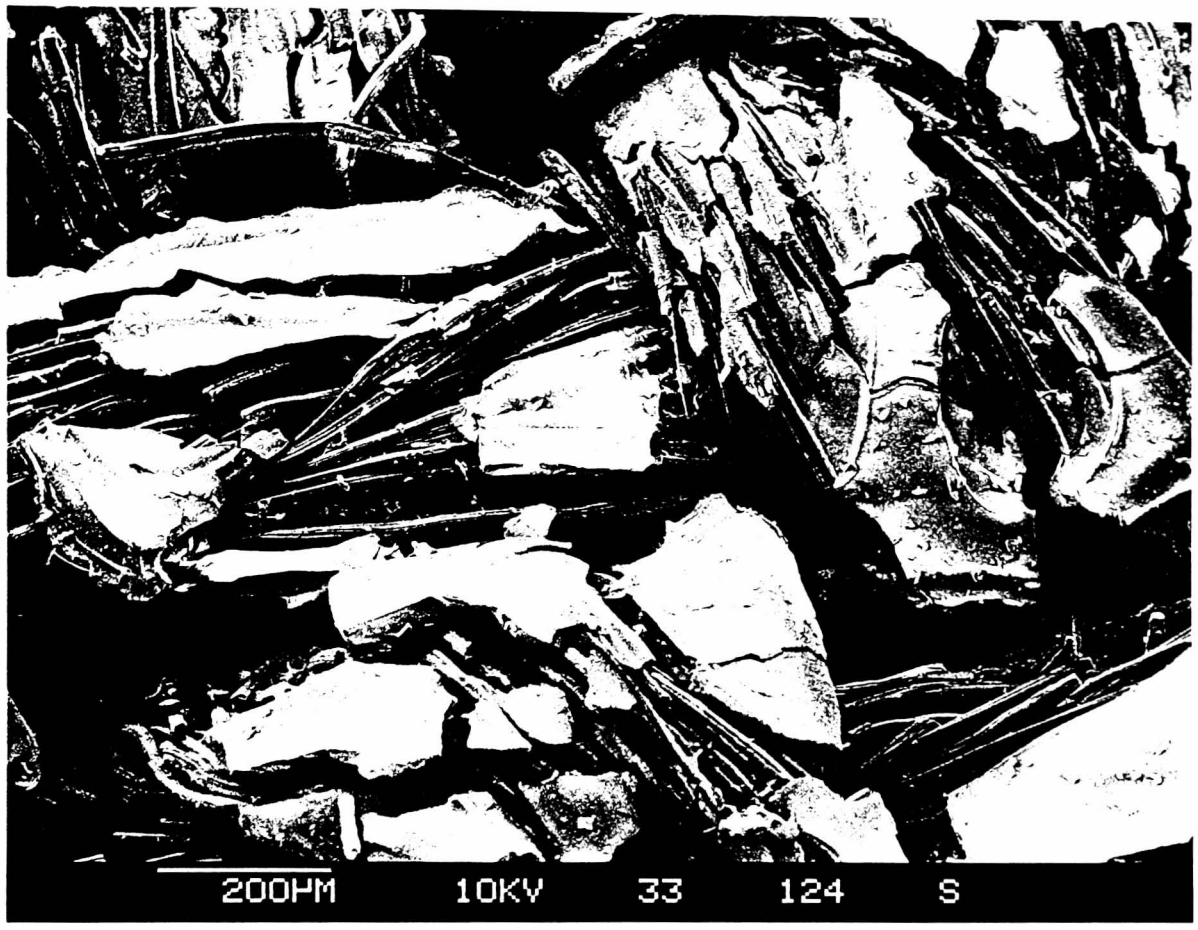

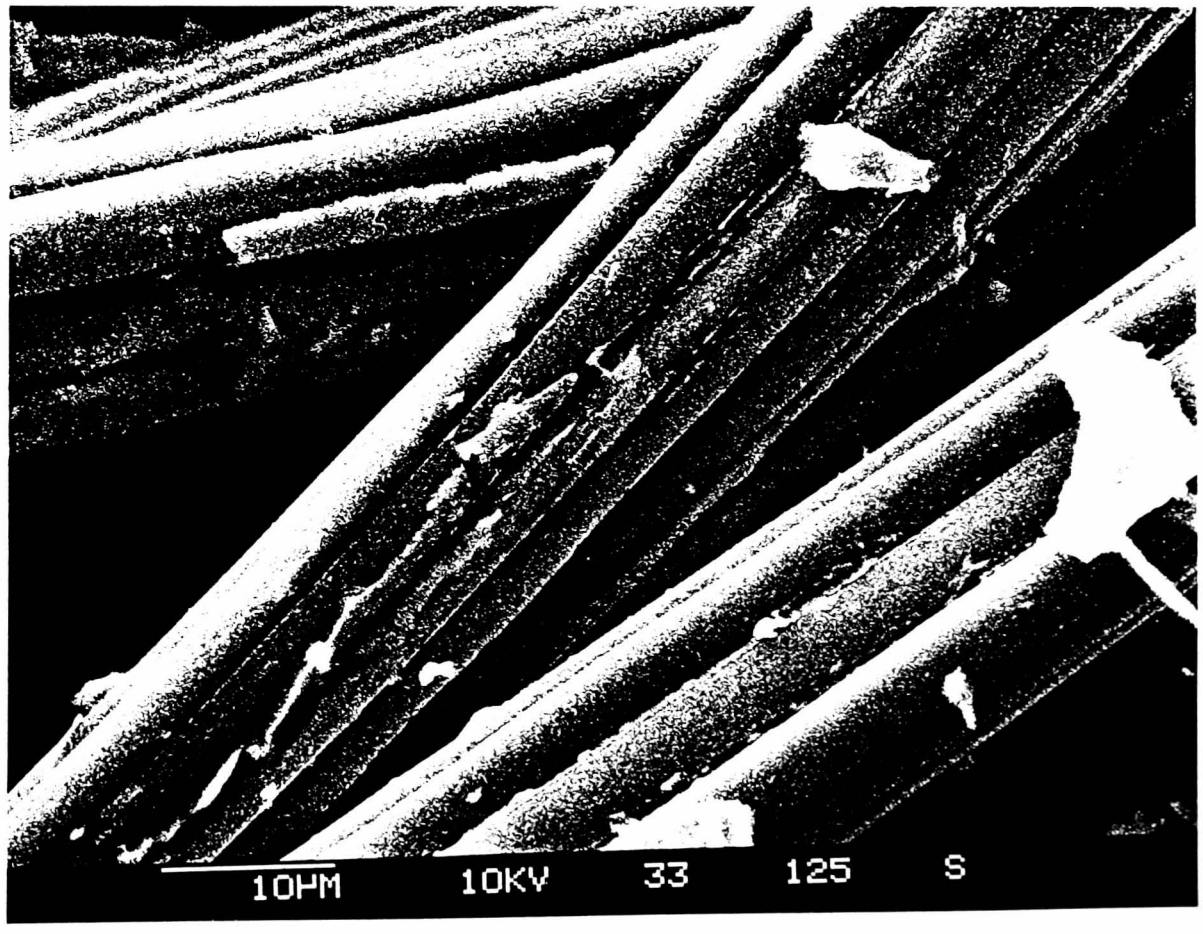

FIGURE 7.2 - Boehmite/Carbon Cloth A Composite Heated to 110°C(vacuum)

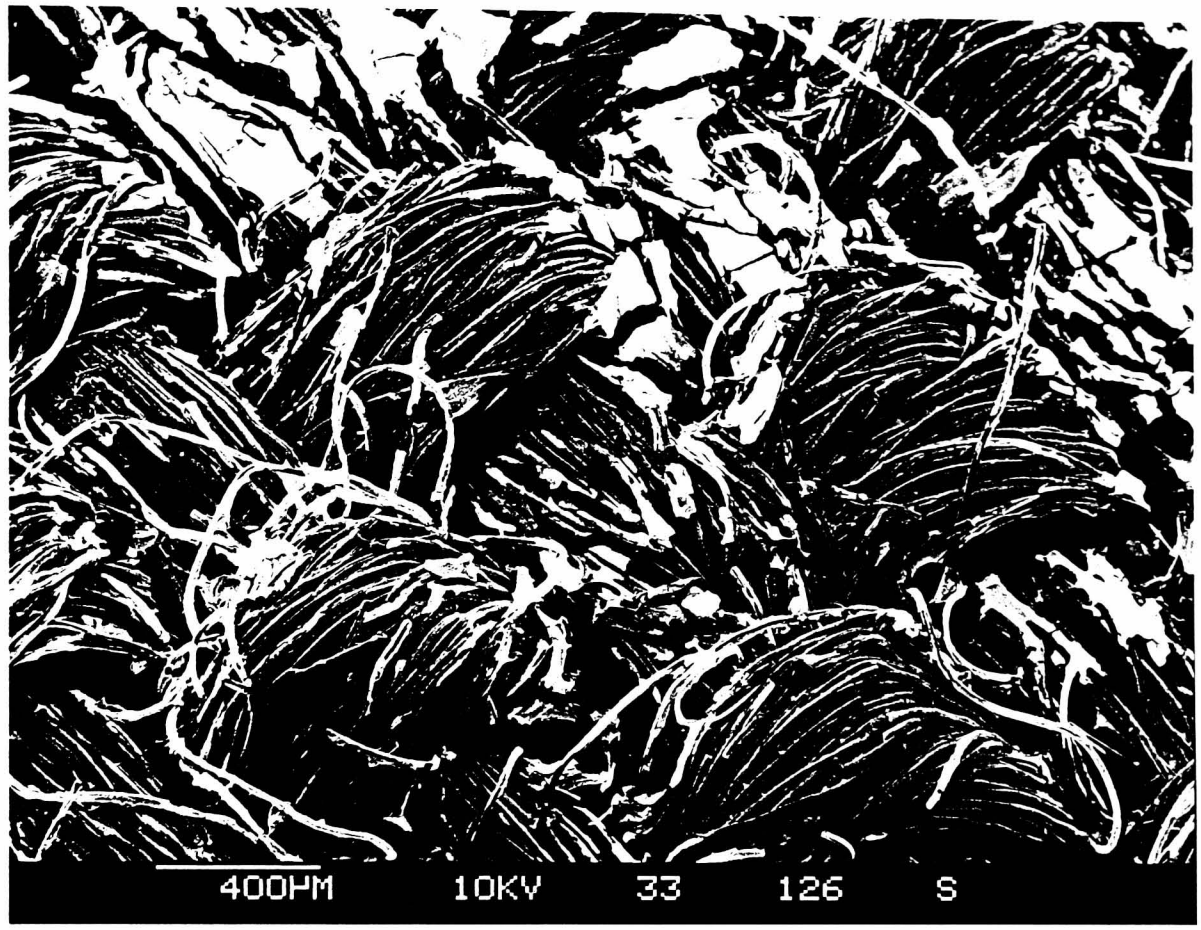

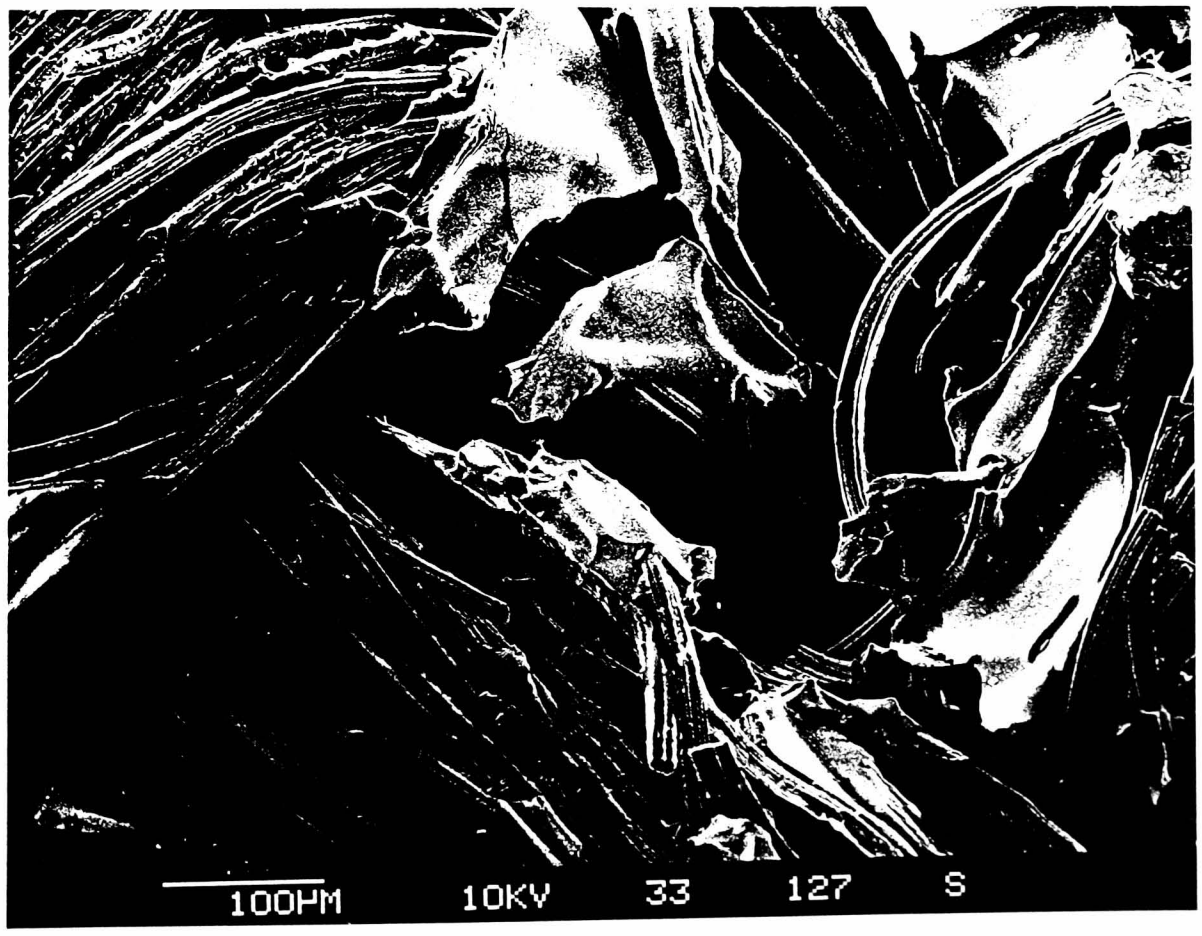

FIGURE 7.3 - Carbonised Fibre of Carbon Cloth A

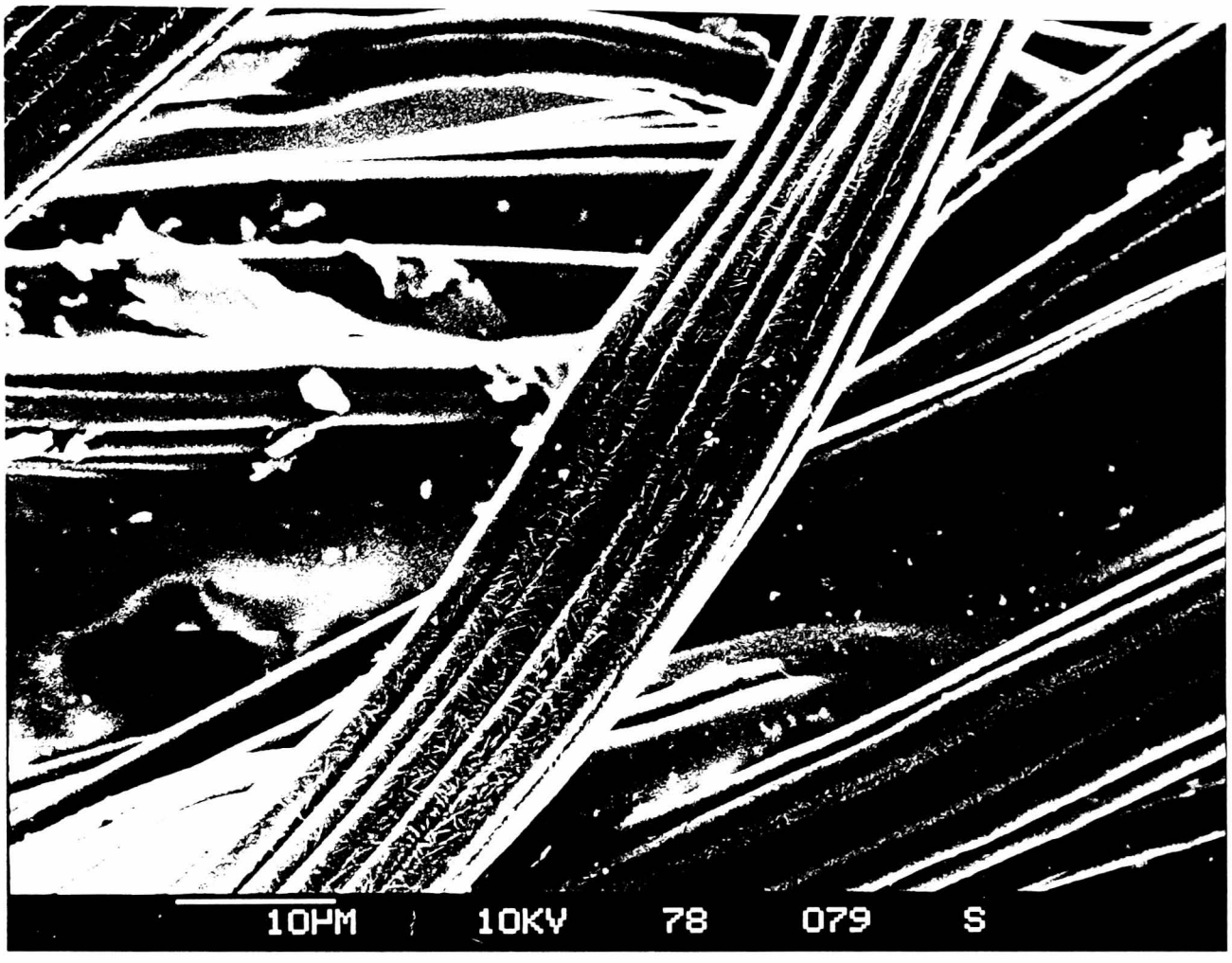

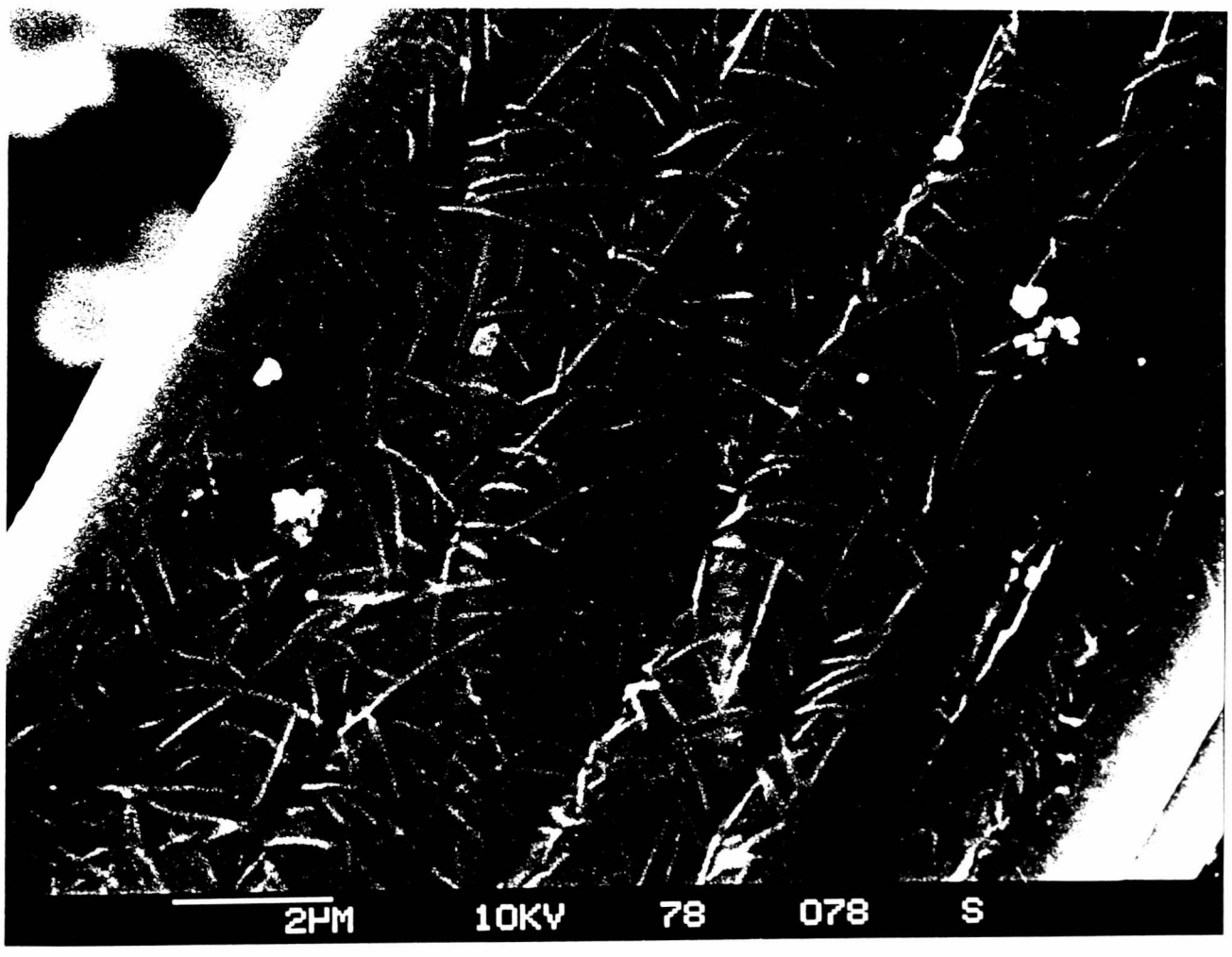

FIGURE 7.4 - Carbonised Fibre of Carbon Cloth A after Treatment with Aluminium Nitrate Melt

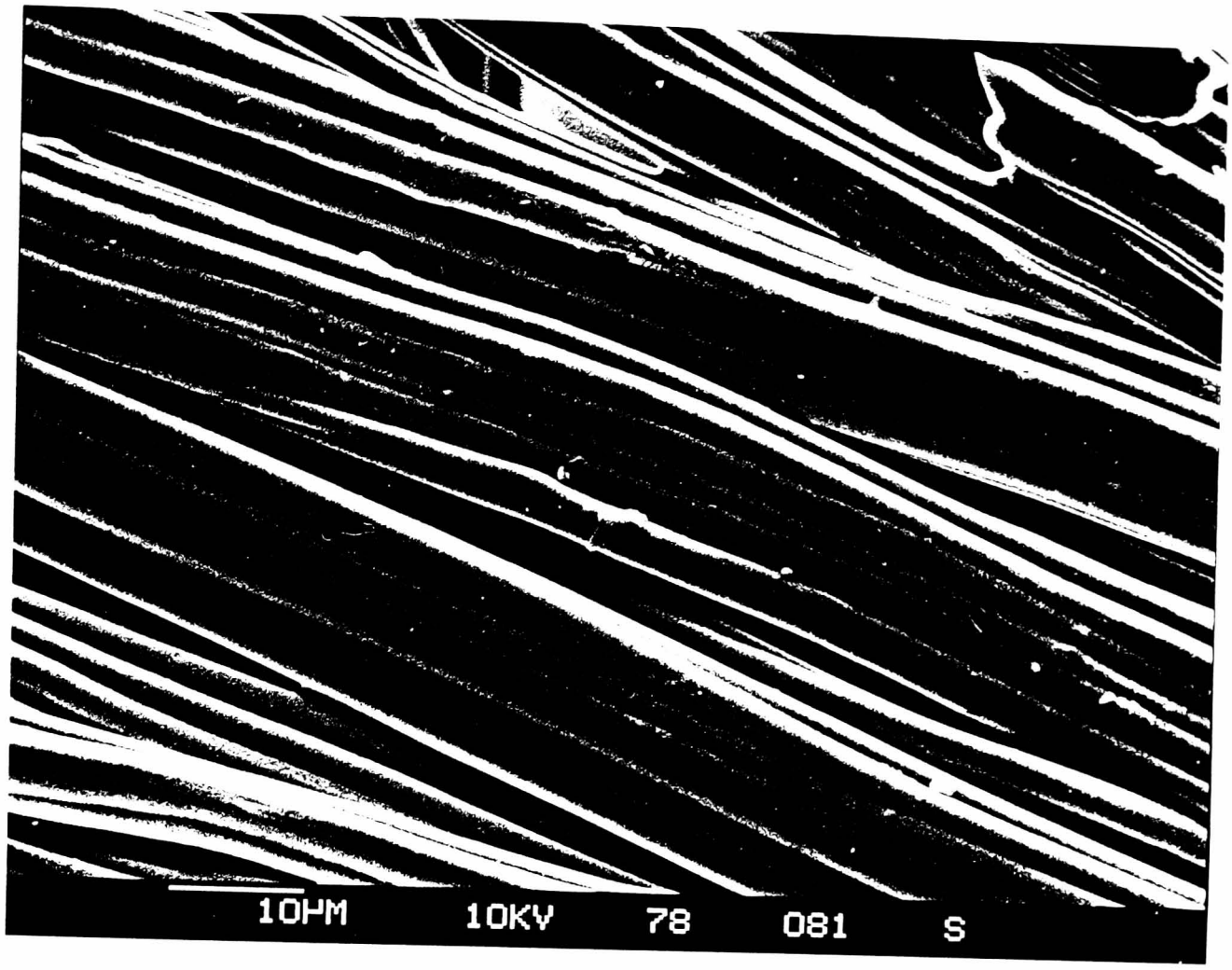

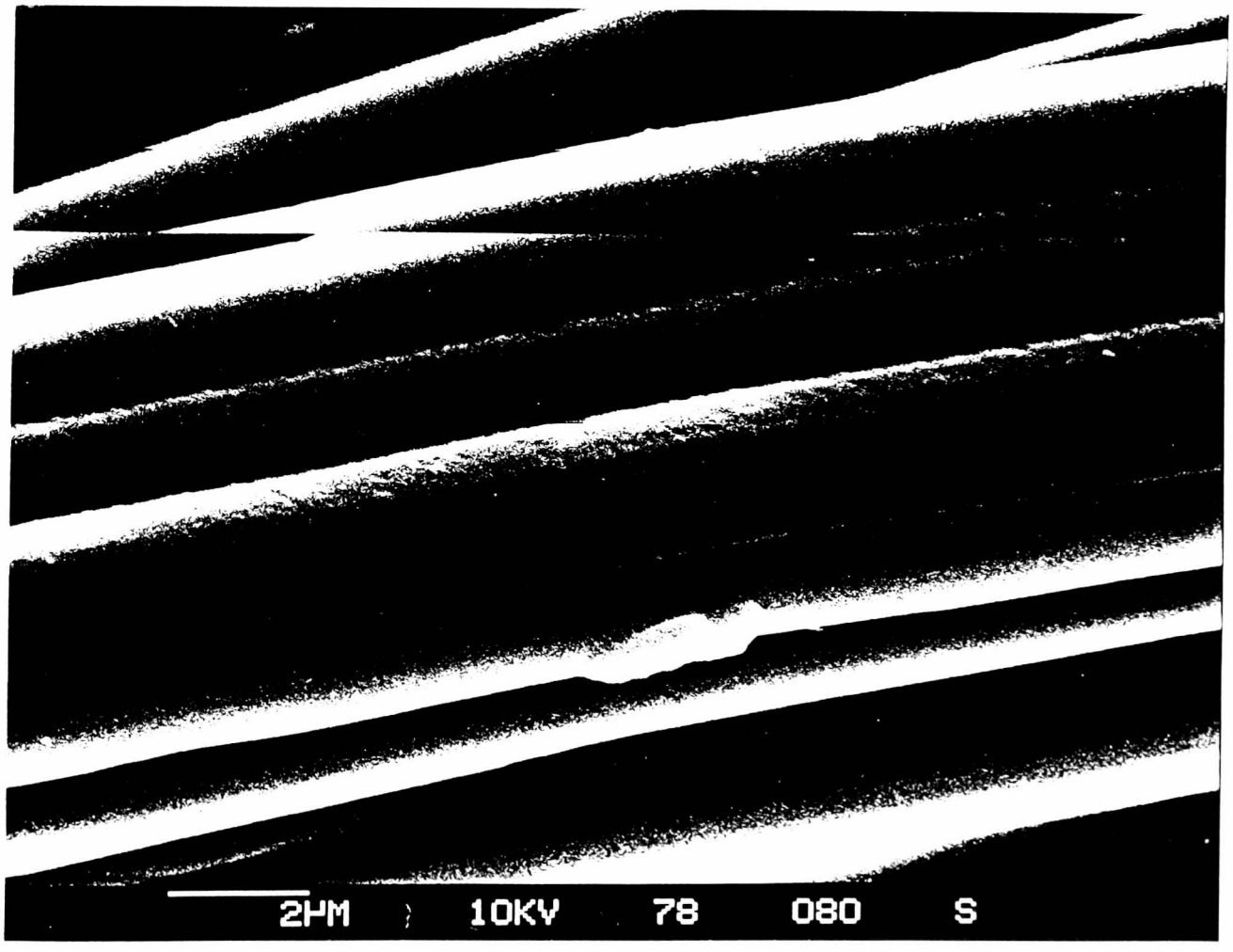

FIGURE 7.5 - Wide-Scan Image and Digimap of Boehmite Deposition on Phosphate Impregnated Carbon Cloth A

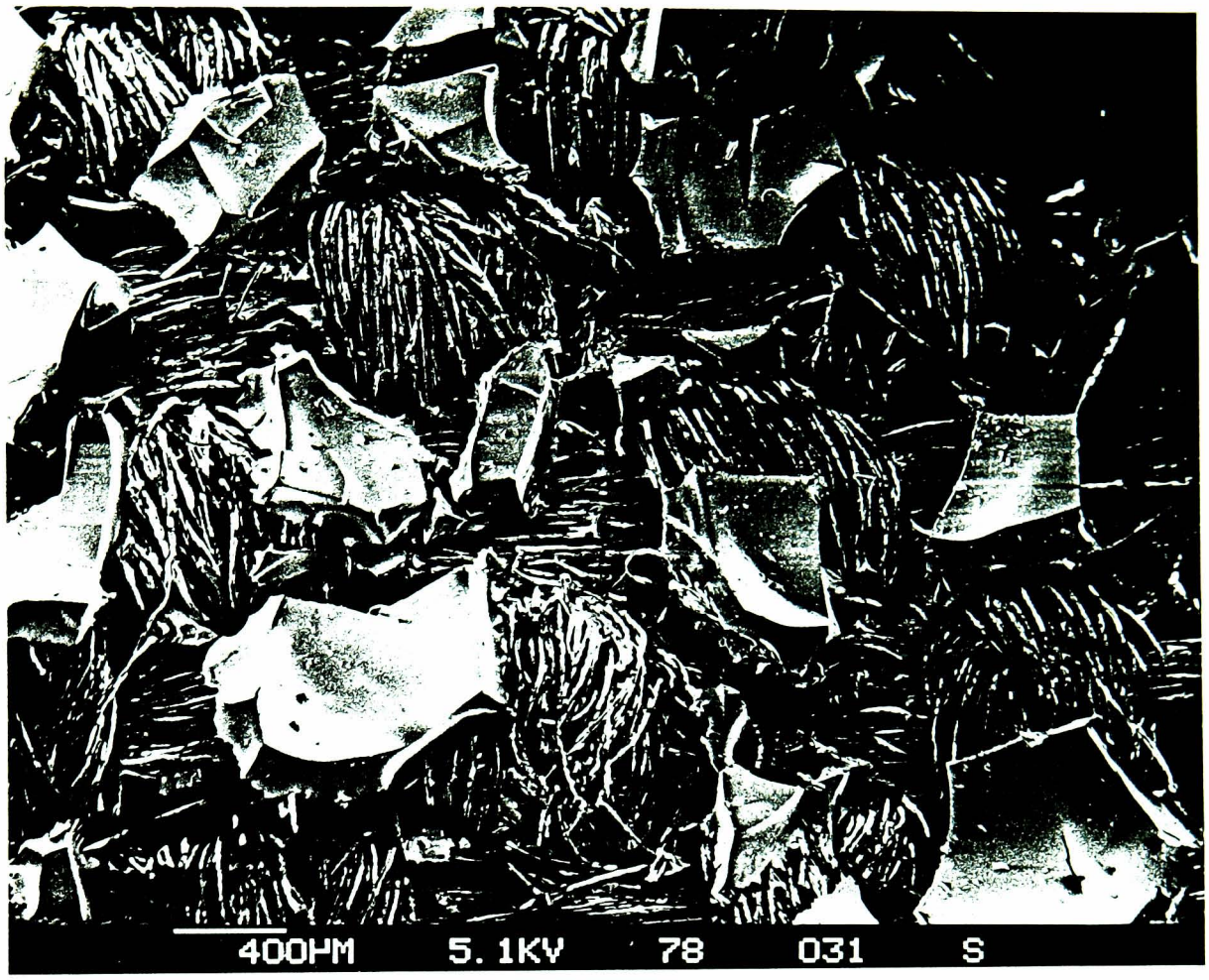

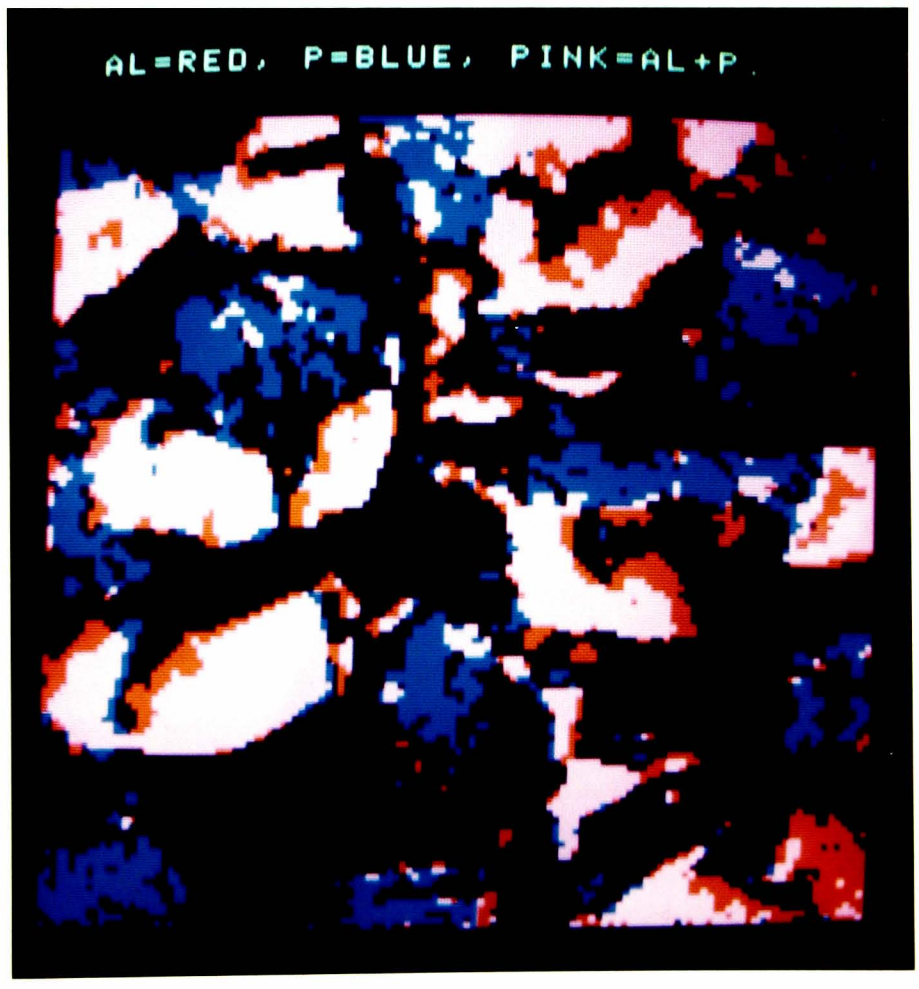

FIGURE 7.6 - Higher Resolution Image and Digimap of Boehmite Deposition on Phosphate Impregnated Carbon Cloth A

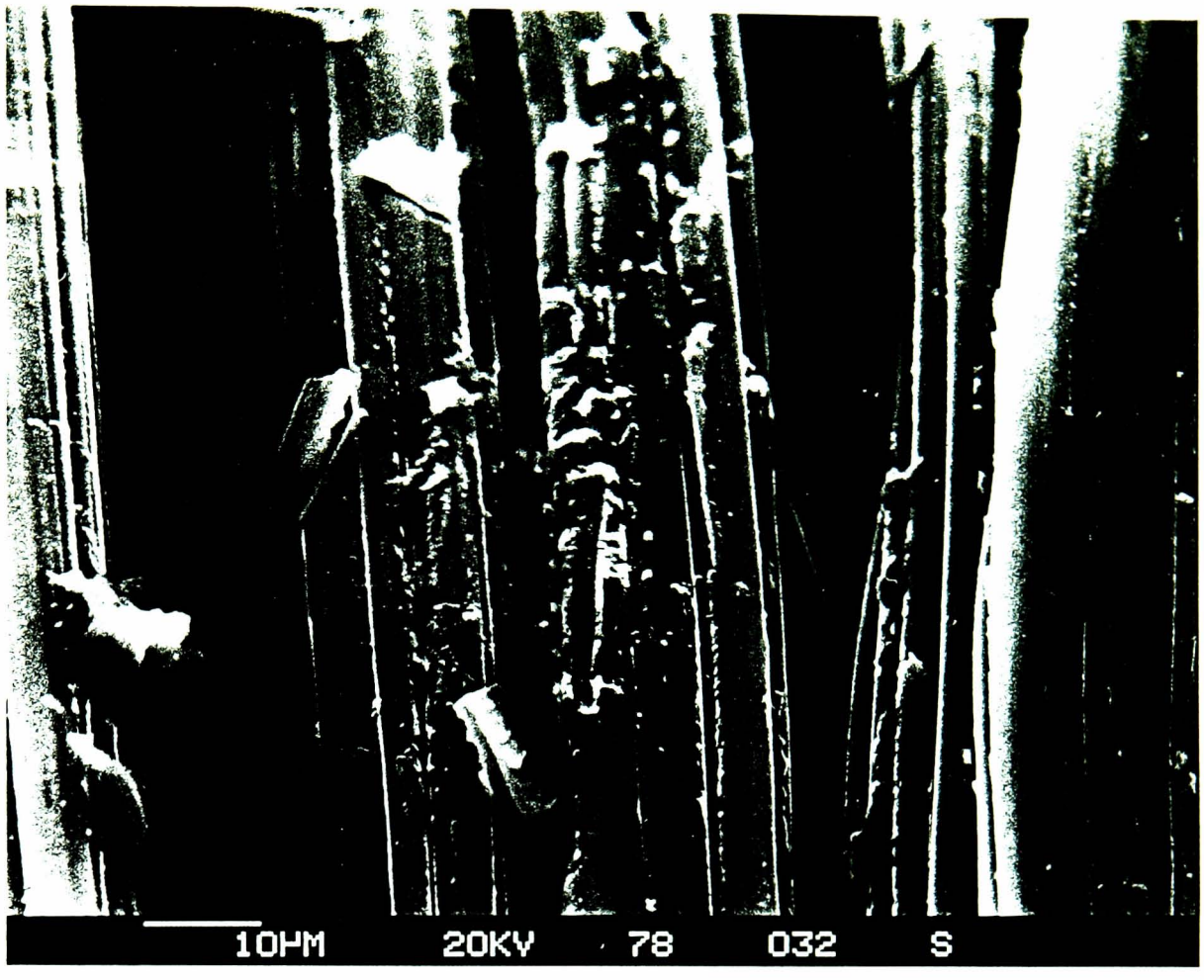

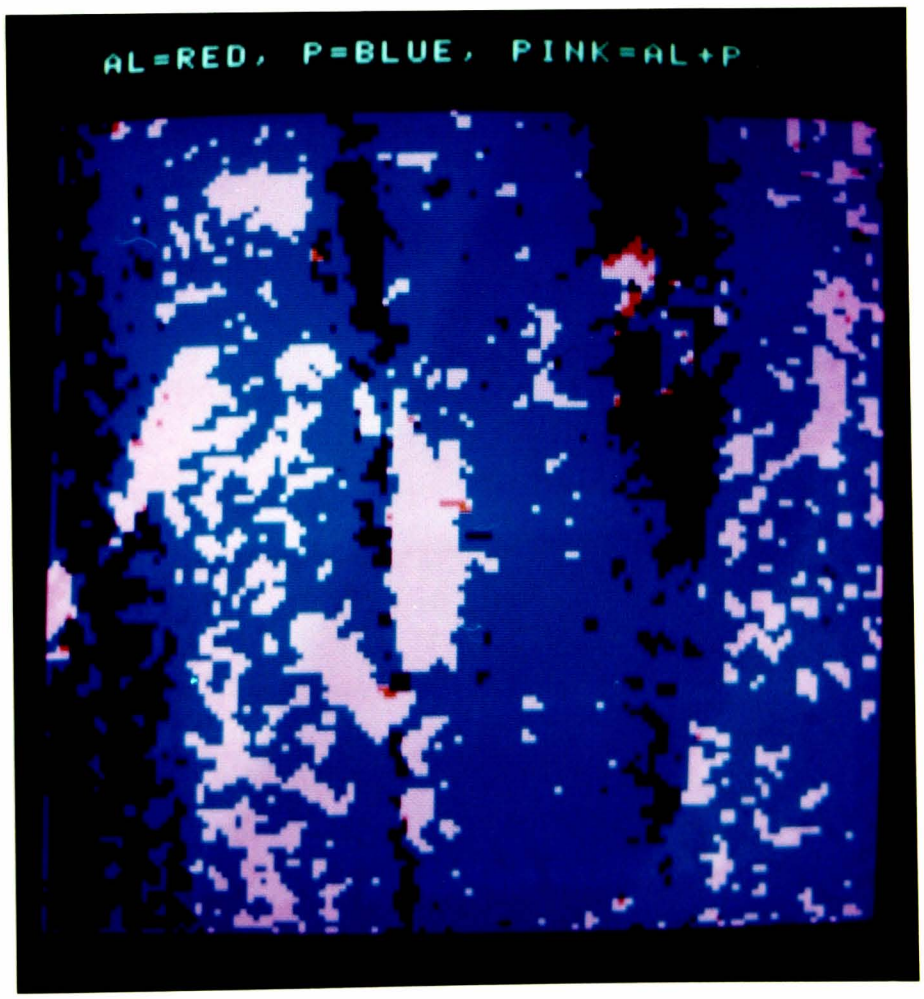

FIGURE 7.7 - Boehmite Deposition on Pre-Wetted Carbon Cloth A

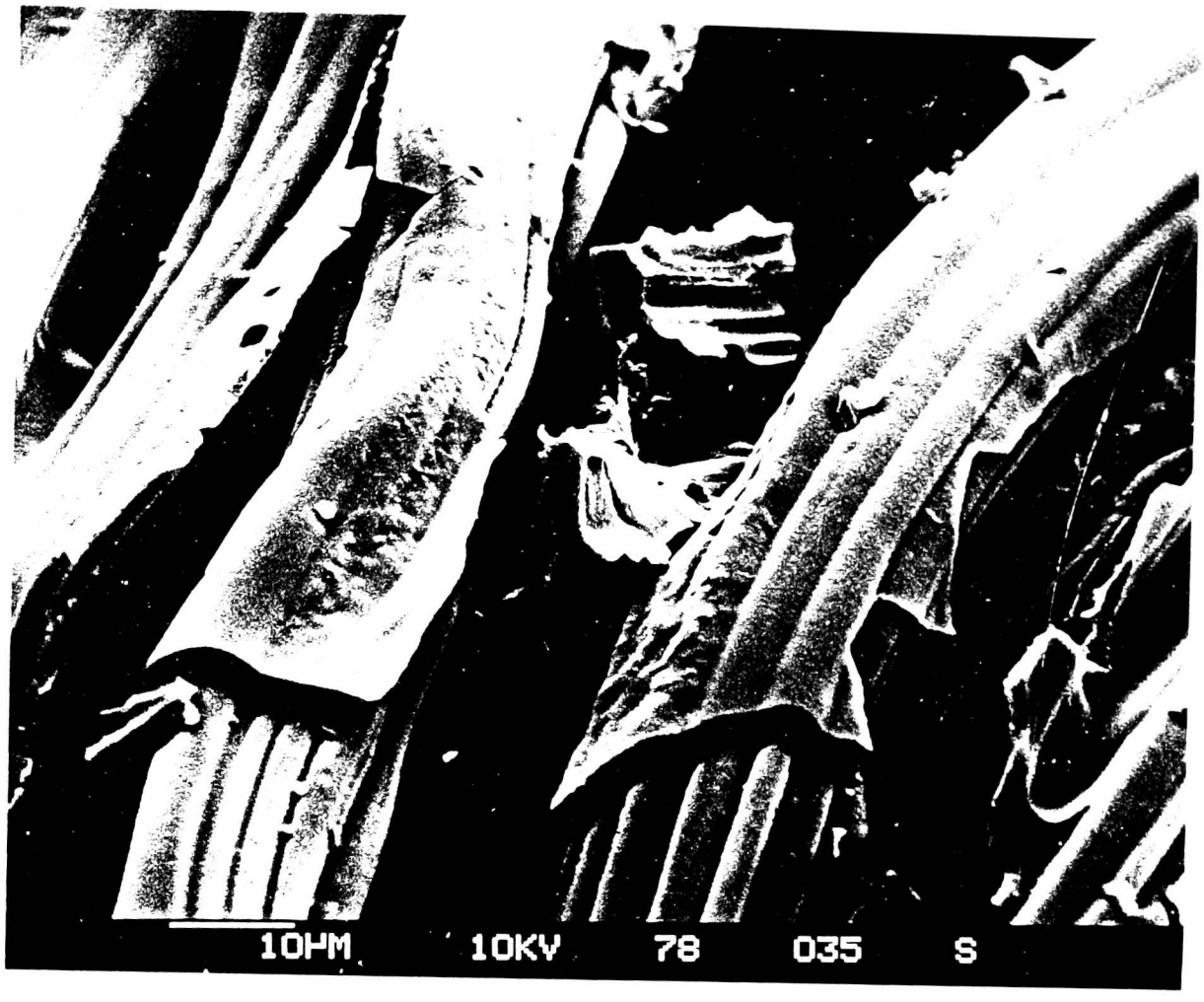

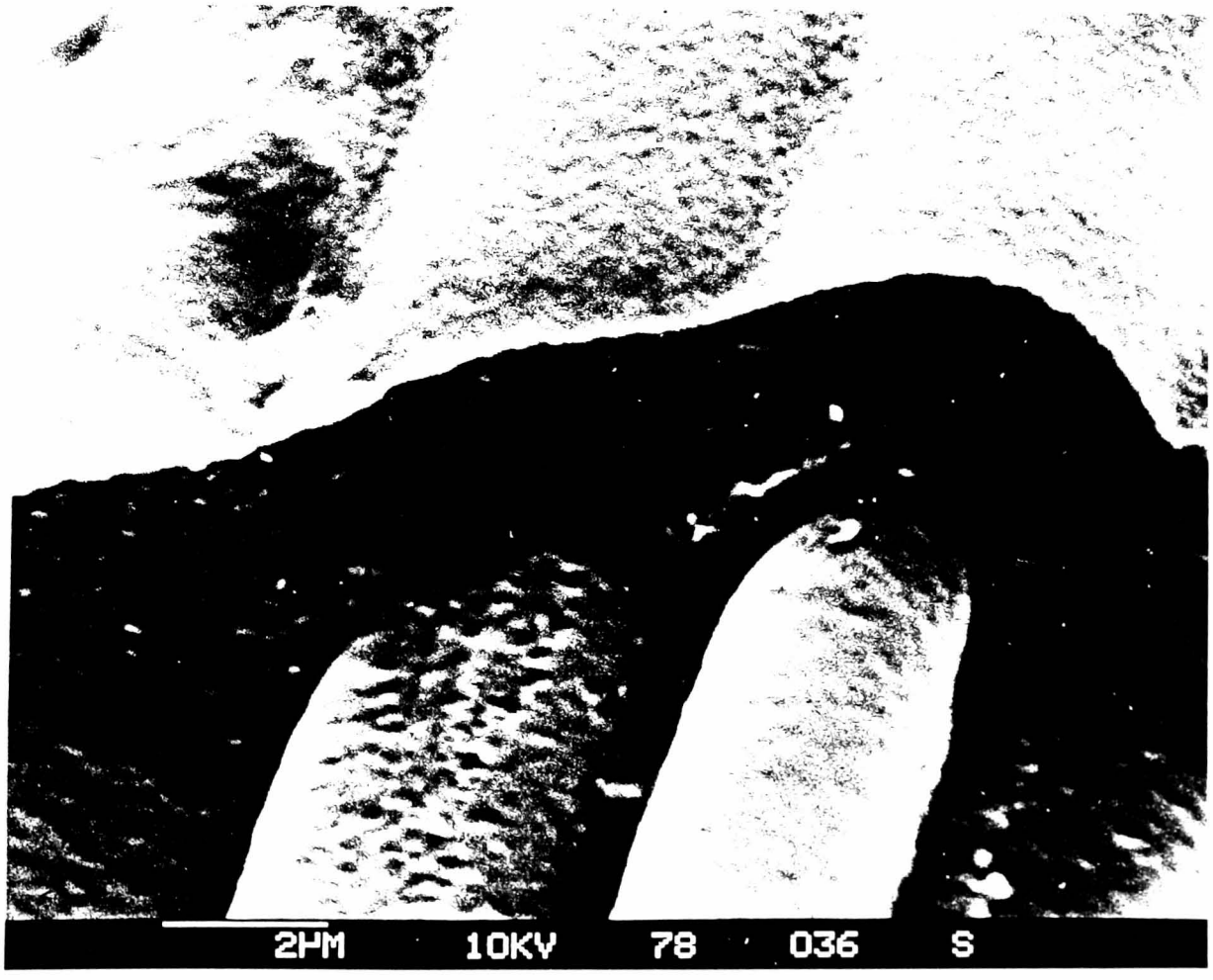

FIGURE 7.8 - Nitrogen Isotherm for Composite A
(Isotherms for Carbon Cloth A and Alumina
included for comparison)

(×) Composite A

(Δ) Carbon Cloth A

(+) Alumina

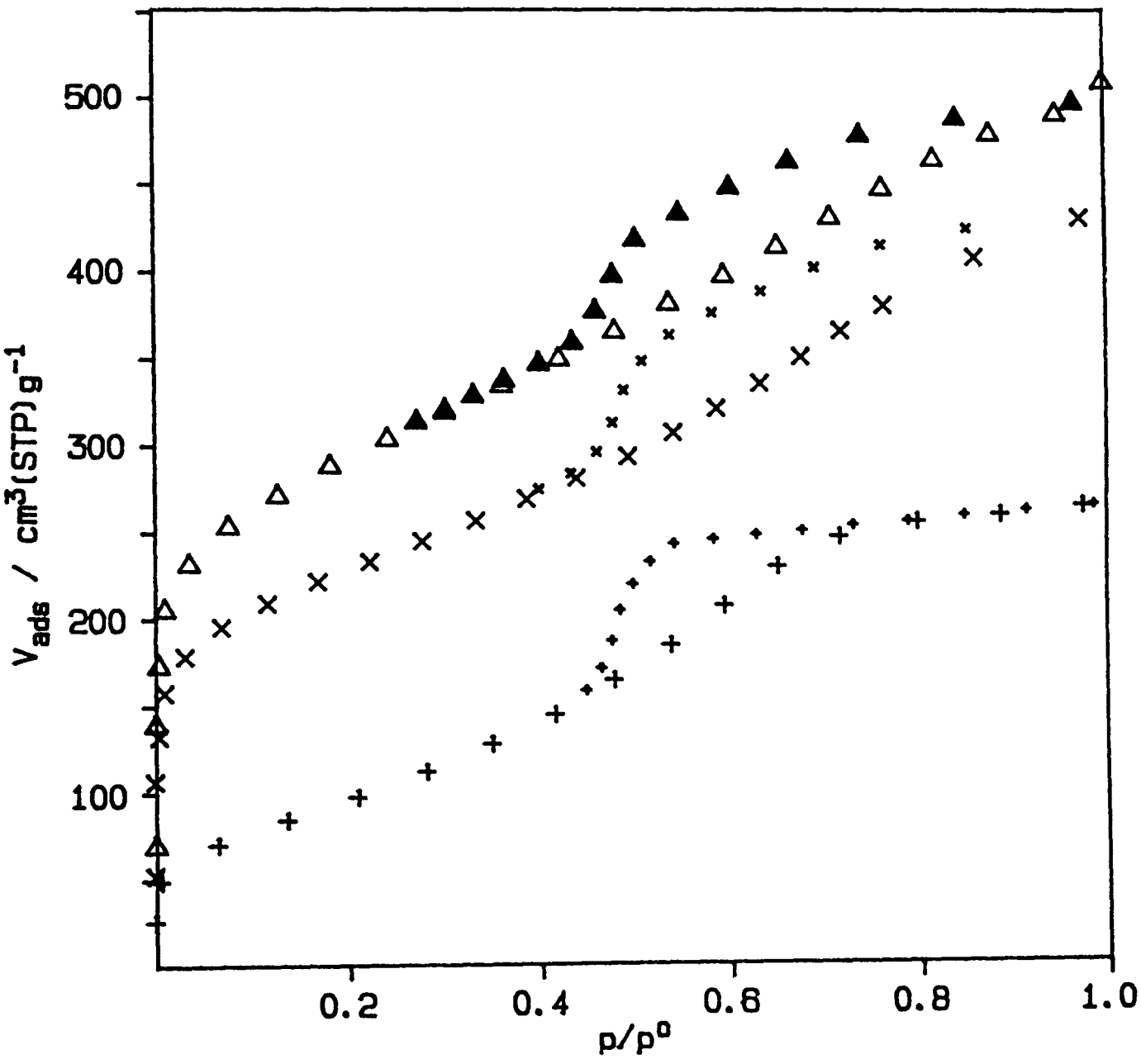

FIGURE 7.9 - Nitrogen Isotherms for Composite B
(Isotherms for Carbon Cloth B and Alumina included for comparison)

(×) Composite B

(Δ) Carbon Cloth B

(+) Alumina

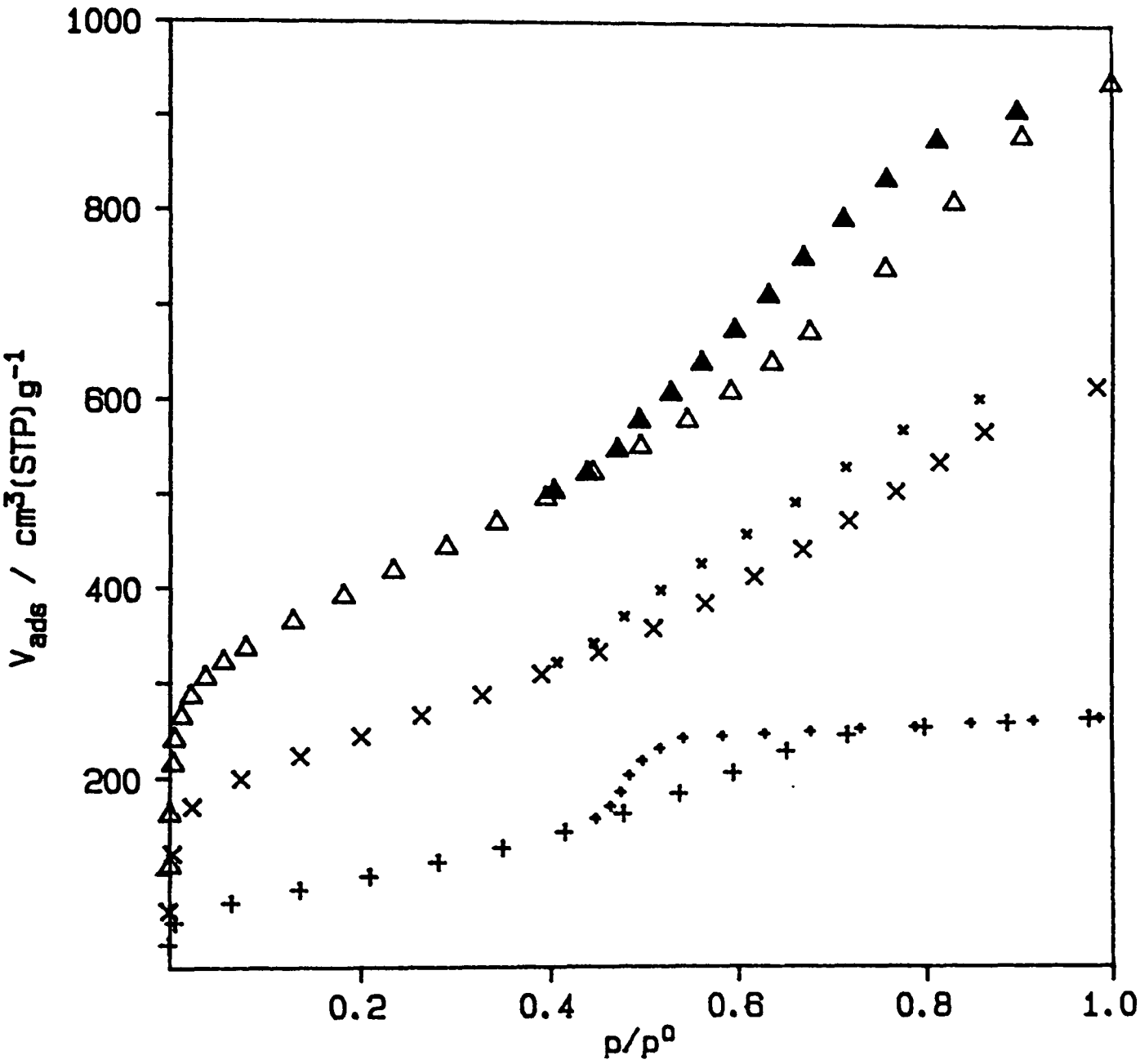

FIGURE 7.10 - Comparison Between Calculated(□) and Measured(×) Adsorption of Nitrogen for Composite A

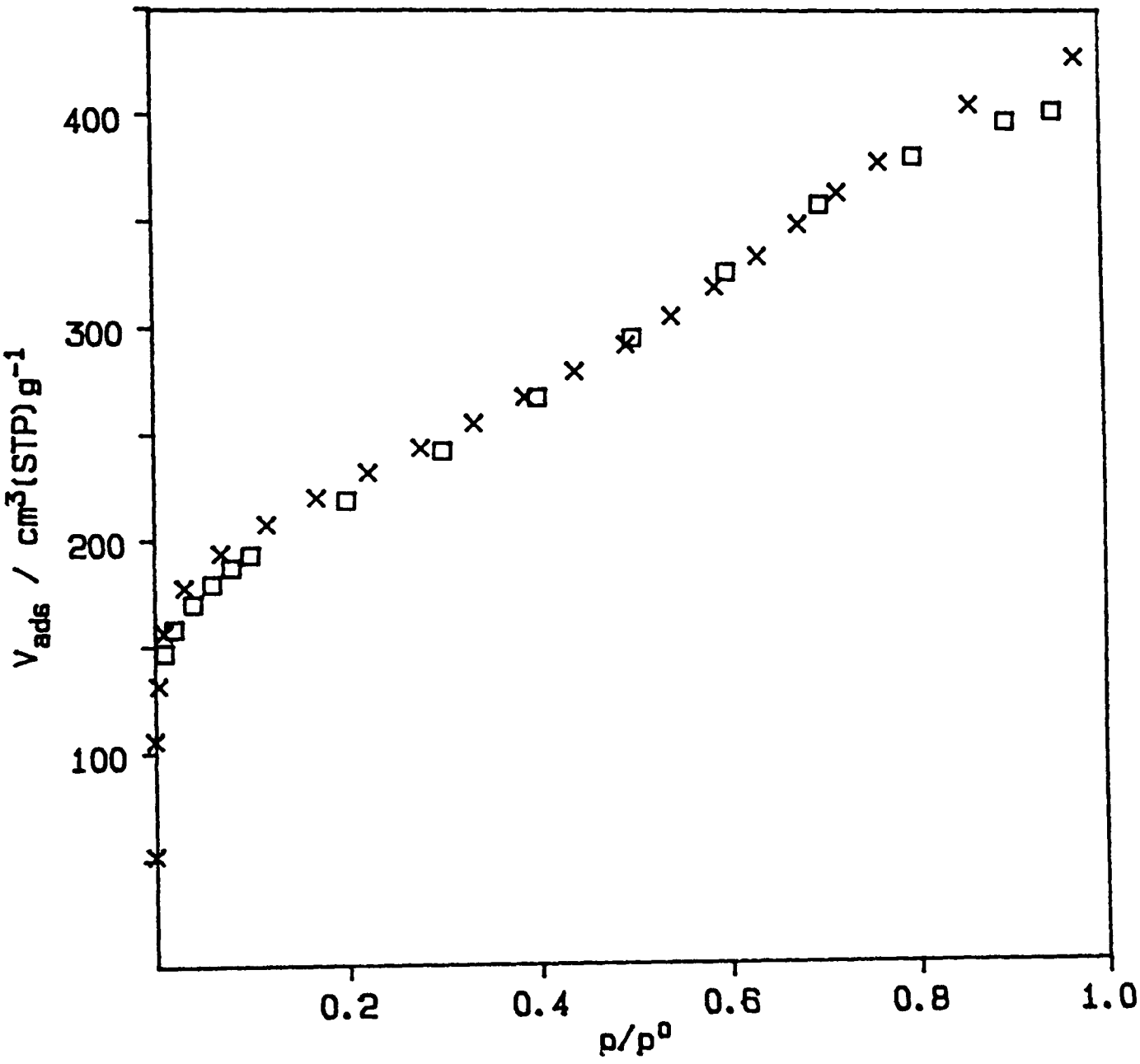

FIGURE 7.11 - Comparison Between Calculated(□) and Measured(×) Adsorption of Nitrogen for Composite B

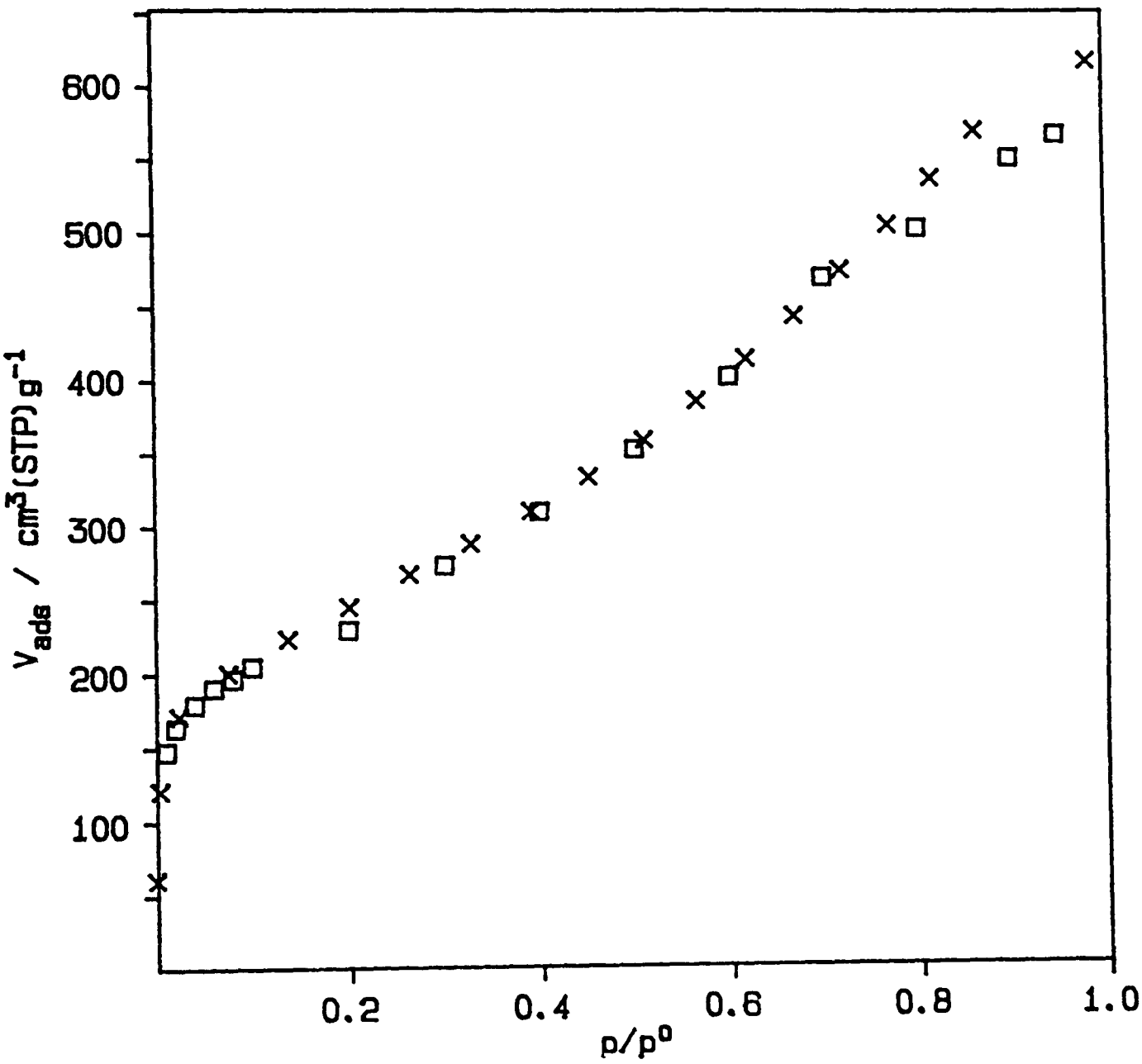

FIGURE 7.12 - Conceptual Model of Alumina Coating of a Fibre of Carbon Cloth

Minimum plate separation identical in both cases.

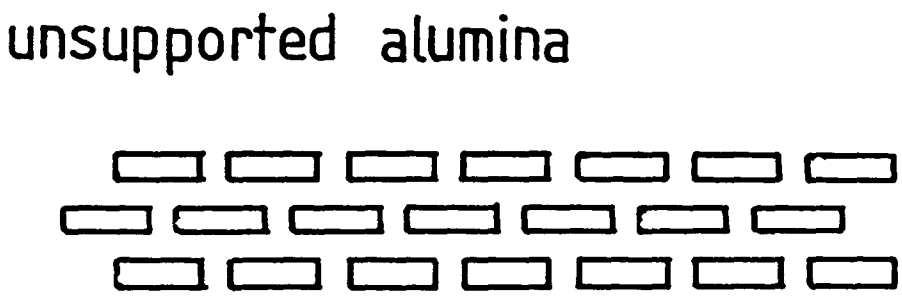

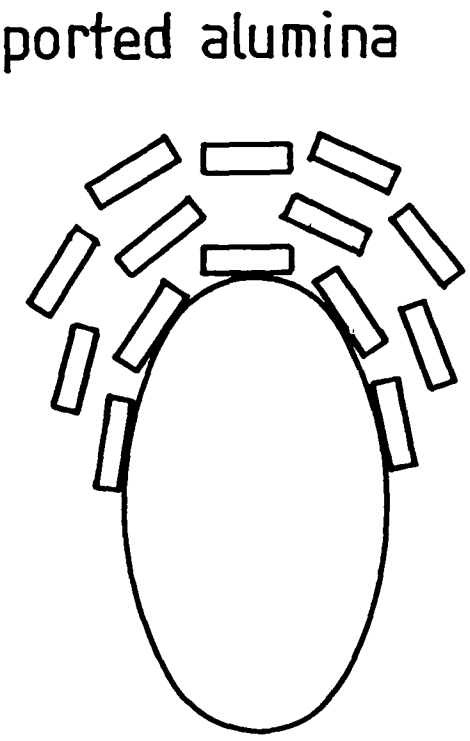

FIGURE 7.13 - Nitrogen Isotherm for Composite A /g of Carbon Cloth
(Isotherm for Carbon Cloth A included for comparison)

(✕) Composite A

(Δ) Carbon Cloth A

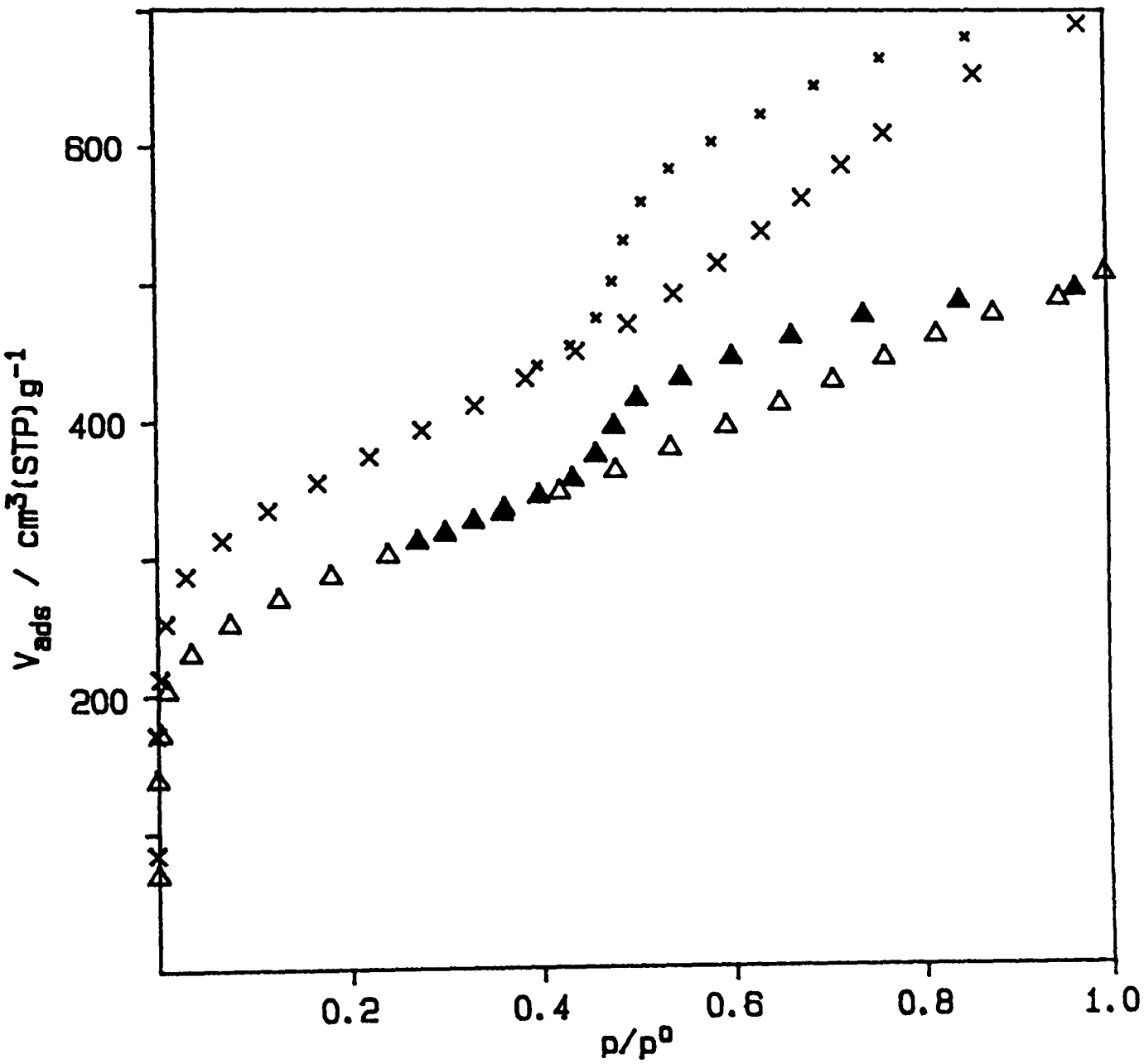

FIGURE 7.14 - Nitrogen Isotherm for Composite B /g of Carbon Cloth (Isotherm for Carbon Cloth B included for comparison)

(×) Composite B

(Δ) Carbon Cloth B

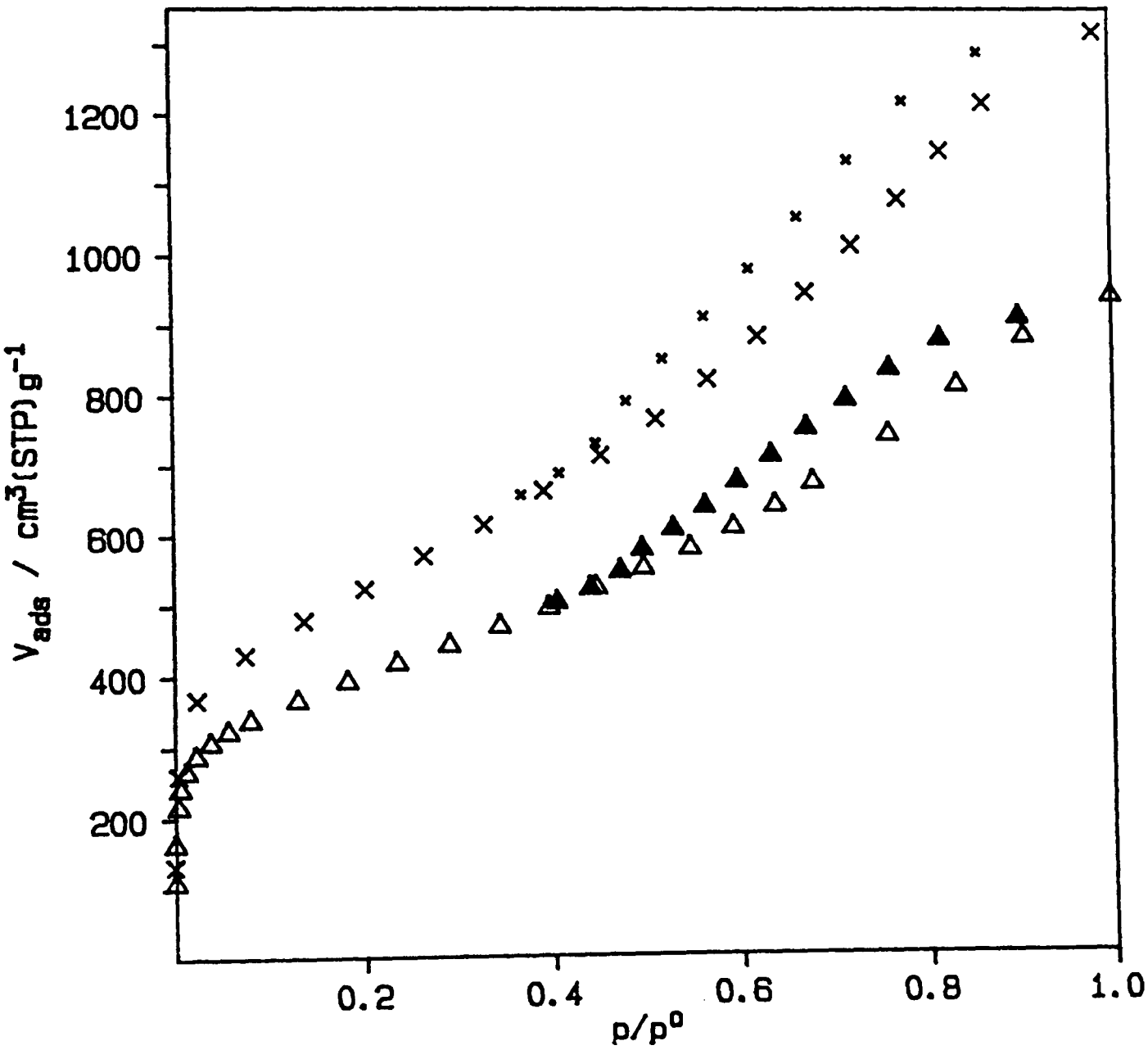

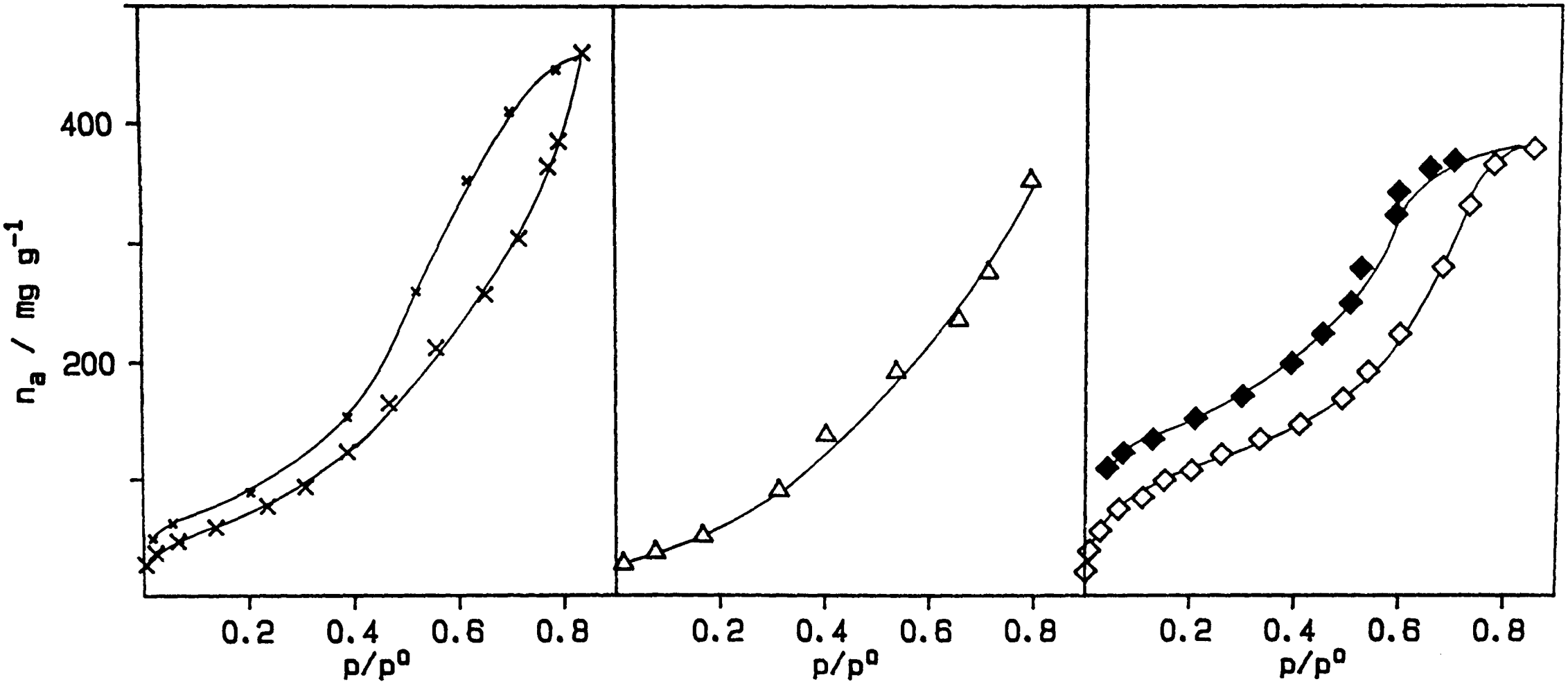

FIGURE 7.15 - Water Isotherm for Composite A
(Isotherms for Carbon Cloth A and Alumina
included for comparison)

(×) Composite A

(Δ) Carbon Cloth A (adsorption only)

(◇) Alumina

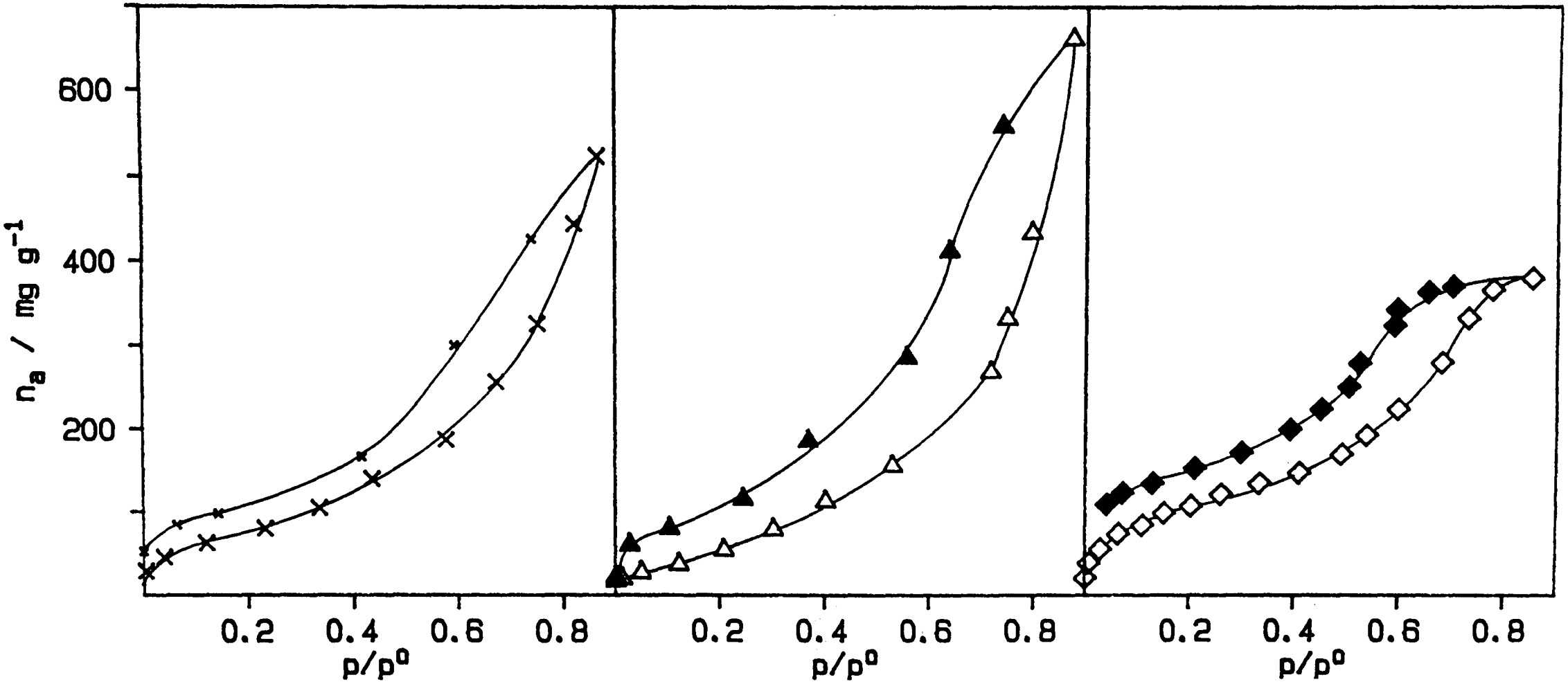

FIGURE 7.16 - Water Isotherm for Composite B
(Isotherms for Carbon Cloth B and Alumina included for comparison)

(×) Composite B

(Δ) Carbon Cloth B

(◇) Alumina

FIGURE 7.17 - Comparison Between Calculated(□) and Measured(×) Sorption of Water for Composite A

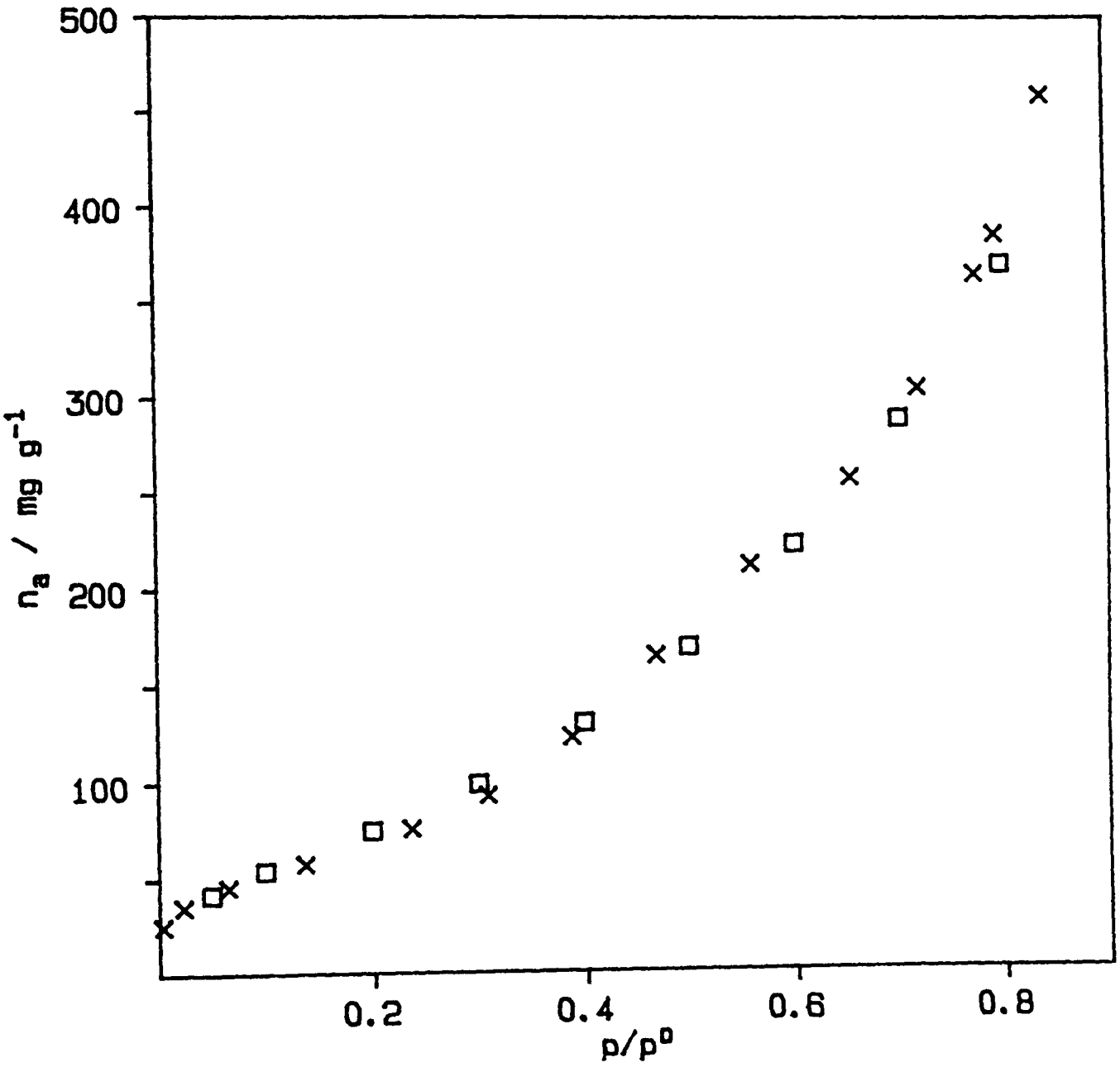

FIGURE 7.18 - Comparison Between Calculated(□) and Measured(×) Sorption of Water for Composite B

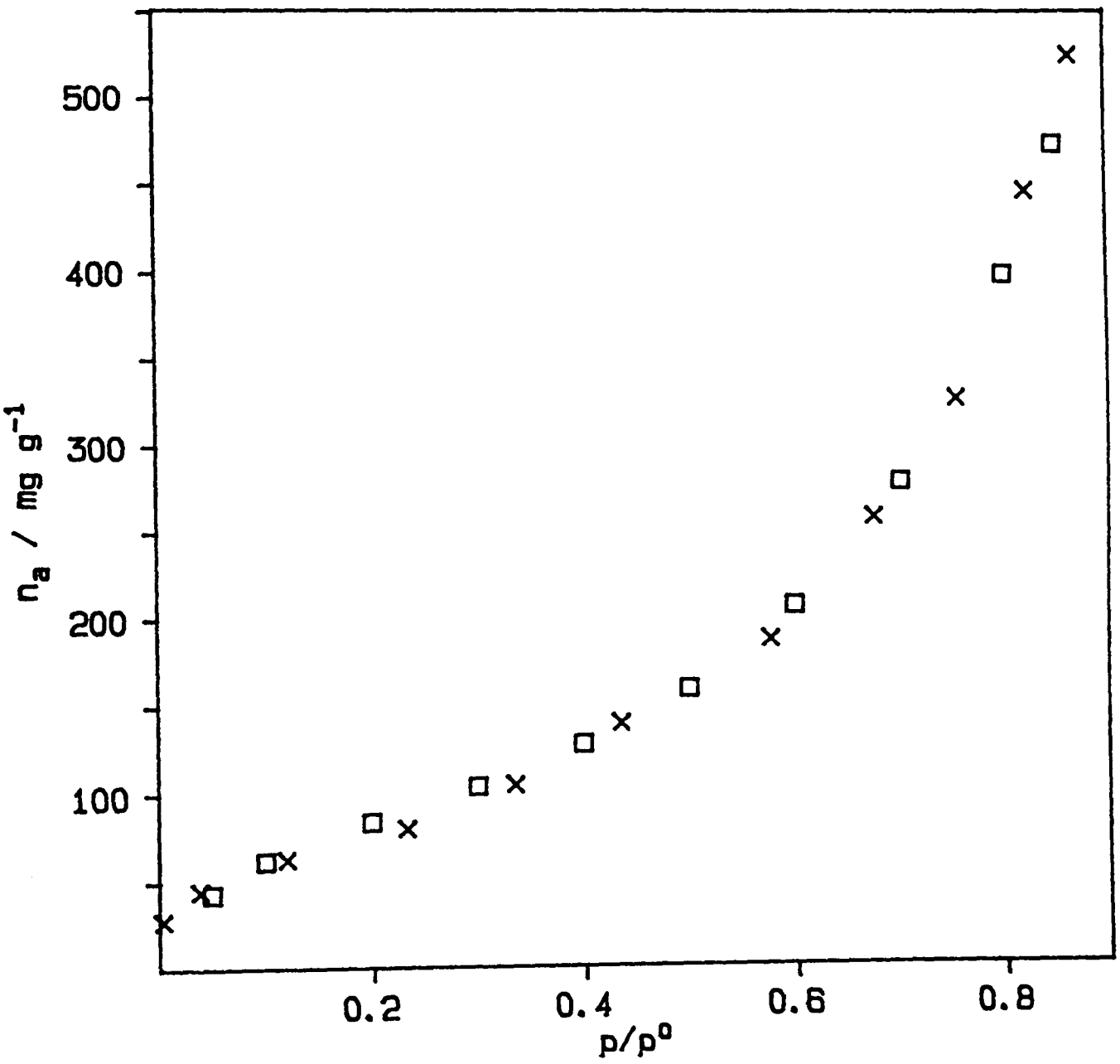

FIGURE 7.19 - Water Isotherm (adsorption only) for Composite A /g of Carbon Cloth
(Isotherm for Carbon Cloth A included for comparison)

(×) Composite A

(Δ) Carbon Cloth A

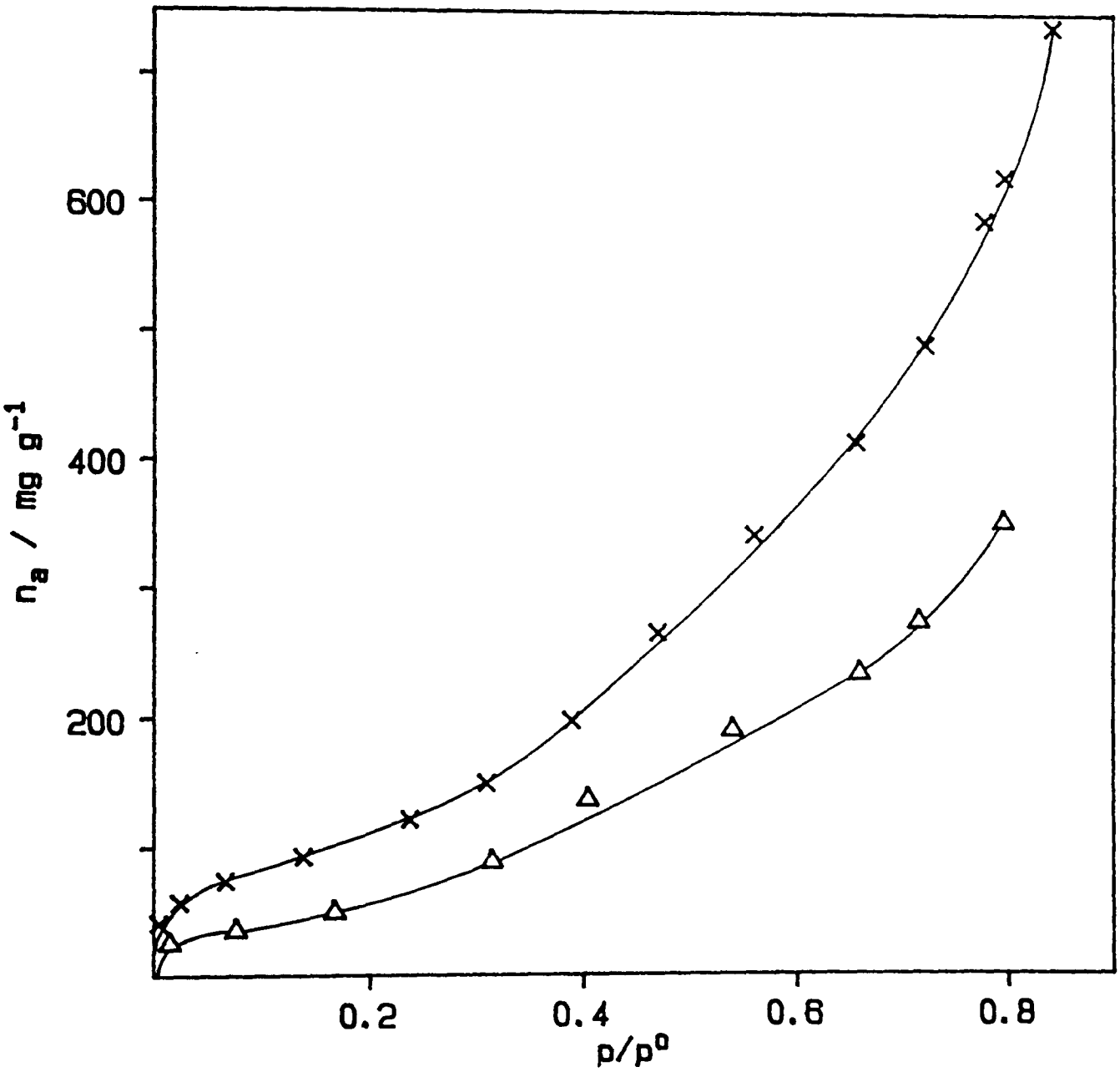

FIGURE 7.20 - Water Isotherm for Composite B /g of Carbon Cloth
(Isotherm for Carbon Cloth B included for comparison)

(×) Composite B

(Δ) Carbon Cloth B

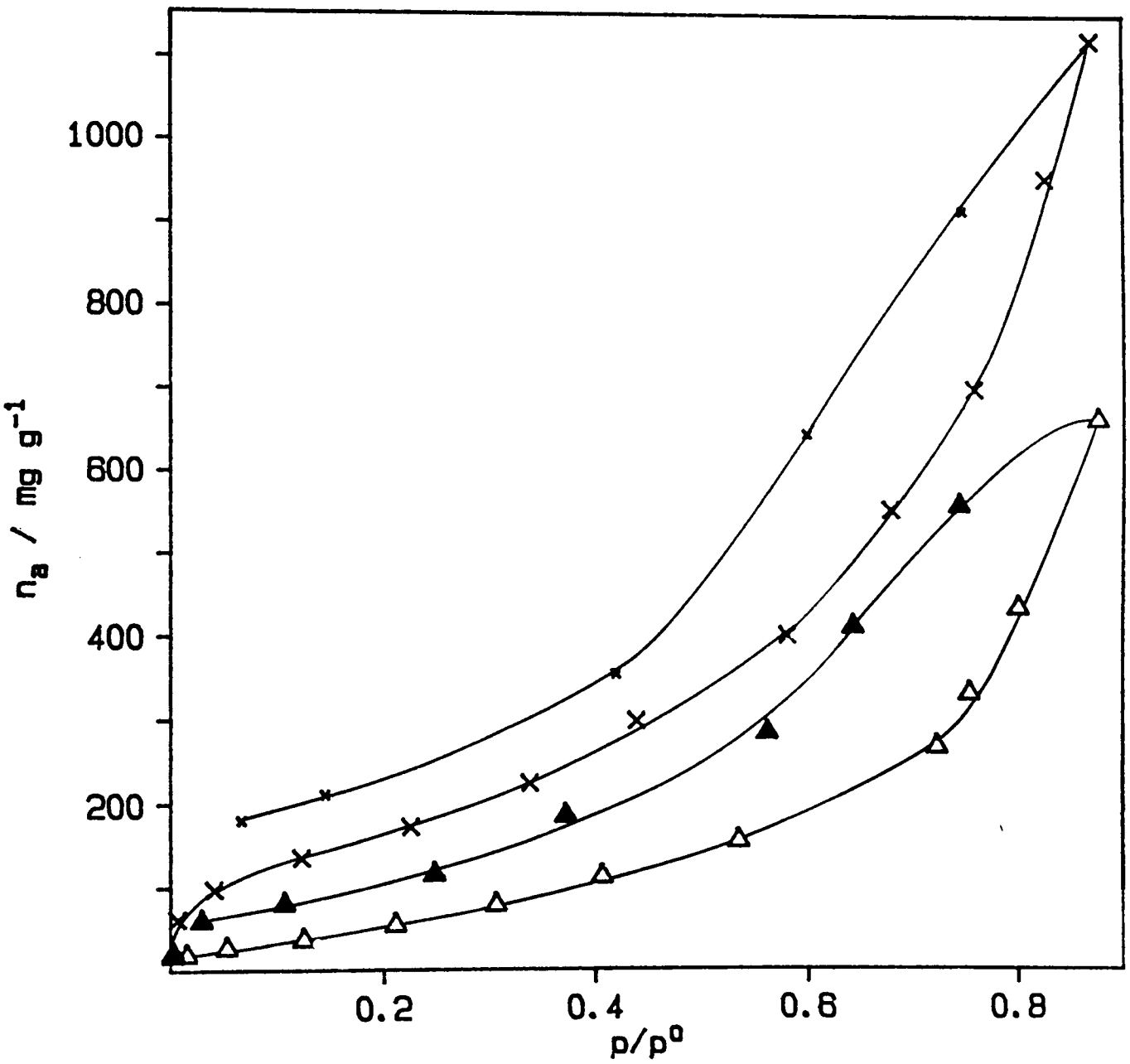

FIGURE 7.21 - Nitrogen Isotherm for Microporous Carbon Cloth

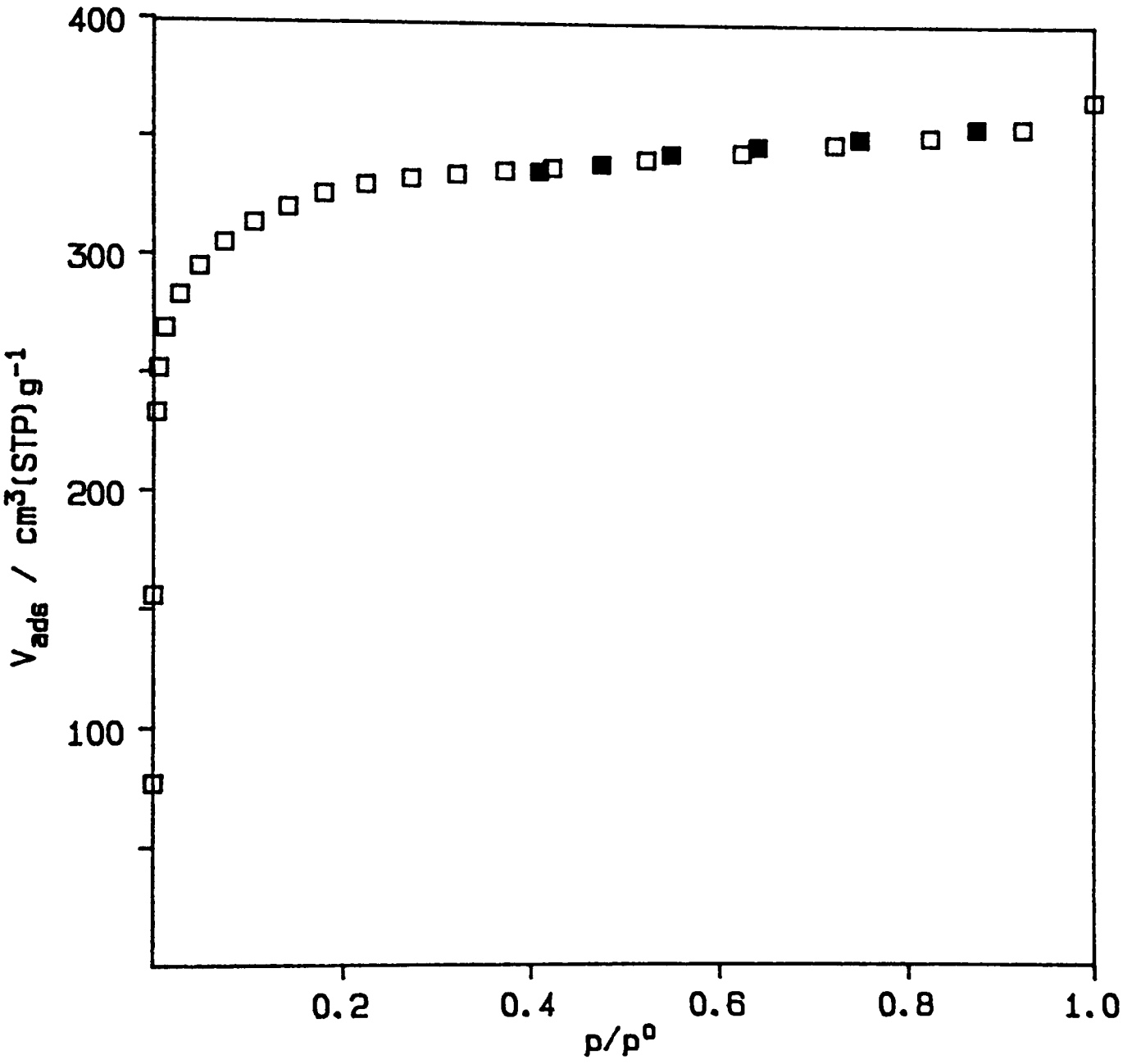

CHAPTER 8 : RESULTS AND DISCUSSION IV - THE CO_2 ACTIVITY OF ALUMINA/CARBON COMPOSITES.

8.1 Introduction

The inclusion of alumina within the carbon cloth, particularly on the scale attained (in excess of 50 wt.% of the total composite weight), has presumably changed the nature of the cloth. The fact that the two phases are so dissimilar should result in changes in the chemistry of the composite compared with the carbon cloth. The presence of alumina has already been shown to significantly enhance the interaction of the composite with water (Section 6.5) and one may conclude that the incorporation of the more polar alumina phase has presumably enhanced the polarity of the composite relative to the virgin carbon cloth.

Carbon cloth has been shown to be quite active in hydrocarbon separations (Carrott and Sing,1986). In this application microporous carbons have been shown to be effective and the separation relies on differences in polarisability between adsorptives. Long chain hydrocarbons being more highly polarisable are more tightly held by such carbons than are those with shorter alkyl groups. The low polarity of the surface though does not help the separation of a polar/non-polar combination of molecules of similar size and polarisability. Propane and propene for example, cannot be effectively separated by carbon cloth.

There is considerable interest (Werner,1986) at the present time in CO_2 removal from gas streams. The interaction between the alumina/carbon composites and this acid gas is now described.

8.2 The Interaction Between CO_2 and the Alumina/Carbon Composite

A gas chromatographic technique was used to study the interaction between CO_2 and the composite materials. This approach was favoured because

a) the composite was prepared in a form that was readily amenable to the production of a GC column, albeit a non-conventional column,

and b) the GC provided a controlled environment in which these alumina/carbon columns could be investigated.

Initial work centred on a column made up of a 51.7 wt.% alumina/carbon composite (30 layers - 0.0590g). All composites used in the GC work were prepared using carbon cloth B and boehmite sols in the standard manner (as described in Sections 3.1.3 and 7.2.2) prior to vacuum heat treatment at 500°C. The column construction is described in detail in Section 3.2.4. Basically it consisted of a number of layers of composite (typically ca. 30) closely packed in a 1/4" O.D. S/S tube. The pressure drop across such a short column was minimal. Unless otherwise specified the column temperature was held at 40.0°C during CO_2 injections and the carrier flow rate was set at 13.0cm^3/min.

Under these conditions the column was initially injected with an aliquot of 10 microlitres of pure CO_2 (collected at RT, ambient pressure). The resulting chromatogram consisted of 2 peaks (as shown in Figure 8.1). The first sharp peak was identified as an air hold-up peak in that its retention time was identical to that for a pure air injection. Furthermore, zero volume injections yielded an air peak of almost identical peak height and retention time. It was therefore concluded that this air was entering the injector in addition to the injected volume of CO_2 as the septum was perforated.

The second peak was due to the elution of injected CO_2. Its retention time was typically twice as long as that of the air hold-up peak. The retention time of the CO_2 peak was found to decrease with successive CO_2 injections, usually becoming reproducible after 3 or 4 injections. In order to investigate the cause of this non-reproduc-

ibility the column was heated to successively higher temperatures (in the range 100-450°C), prior to CO_2 injection. A ballistic temperature program was used with a maximum heating rate of 50°C/minute being employed. The dwell time at the maximum temperature was 5.0 minutes. After each temperature ramp the column was returned to 40.0°C and CO_2 injections were repeated. It was noted that upon heating to temperatures in excess of 200°C, a large peak was eluted. The temperature corresponding to maximum elution was found to be approximately 350°C. Thus when the column was ramped to only 250 or 300°C this peak was not fully eluted. The chromatograms at 40°C changed after each succcessive ramp in that the CO_2 retention time for the first injection was found to increase dramatically (See Table 8.1). Finally after heating to 400 and 450°C no CO_2 elution was observed, even over a period of 3 hours. However successive CO_2 injections did result in CO_2 elution. In an attempt to drive the CO_2 off the column after the first injection the flow rate was increased to 60 cm^3/min. However even at this elevated flow rate the initial volume of CO_2 could not be driven of a freshly heated (to 400,450°C) column.

This phenomenon of complete CO_2 retention by "fresh" columns of the alumina/carbon composite is now discussed and put on a quantitative basis. The term "fresh column" is used to describe a column that has been heated to a temperature sufficient to remove CO_2 and that has not subsequently been exposed to CO_2. The basic approach involved heating the columns to 400°C at a elevated heating rate (50°C/min.)(350°C may have sufficed but would have required a longer dwell time, and 450°C was not found to alter the subsequent column behaviour c.f. 400°C). Therefore 400°C was chosen for convenience in that a rapid ramp and short dwell to this temperature were sufficient to clean the column. After cooling to the desired column temperature (usually 40.0°C) a

series of CO_2 injections were made and the degree of CO_2 elution determined. If CO_2 was to be eluted from a given column it was observed in preliminary experiments to closely follow the air hold up peak, that is appear in the first five minutes after injection. Therefore as a general rule, if no CO_2 was eluted for 10 minutes after injection it was assumed that total retention of the injected volume had taken place.

8.2.1 The Analysis of Chromatograms

A series of chromatograms for the "fresh" 51.7 wt.% Al_2O_3 column were determined for injection volumes of 10, 20 and 50 microlitres. The chromatograms for the 10 microlitre series are reproduced in Figure 8.2. Complete CO_2 retention was observed for an initial injection volume of 10 microlitres. The subsequent 10 microlitre injection (or even the initial 20 microlitre injection) resulted in a small amount of CO_2 being eluted. The initial injection of 50 microlitres of CO_2 resulted in immediate, although not total elution of CO_2. For each series of injections there was obviously a critical volume of CO_2 which could be totally retained by the column. For the 51.7 wt.% alumina column at this particular temperature and flow rate ($40^{o}C, 13cm^3/min.$ respectively) this critical volume was between 10 and 20 microlitres. Subsequent injections of CO_2 after this critical volume had been taken up by the column resulted in partial elution of CO_2. In other words, a fraction of the CO_2 was still being retained while the remainder was eluted. Further injections resulted in the eluted CO_2 peak area rising to a constant value. For the purpose of the analysis which follows it was assumed that this elution plateau corresponded to 100% elution of the injected volume. The volume of CO_2 eluted after each injection was then calculated by comparison with the peak area (or height) corresponding to 100% elution. The resulting data are collected in

Table 8.2.

As can be seen from Figure 8.2 the CO_2 peak tails significantly, particularly for low injection volumes. The measurement of peak area was not correctly performed by the integrator. Instead peaks were photocopied, cut out by hand and weighed to determine their area. This process was very time consuming and an alternative method, involving measurement of the maximum height of the CO_2 peak, was also investigated. A comparison of the two methods (peak area versus peak height) is made in Figures 8.3 and 8.4 where the relevant "breakthrough" curves have been plotted (using the data in Table 8.2). In order to facilitate the calculation of the CO_2 volume corresponding to complete retention and the total CO_2 volume retained, the breakthrough data was plotted with the "fractional volume of CO_2 eluted" on the vertical axis and the "cumulative volume of CO_2 injected" on the horizontal axis. By comparison of the peak area (or height) of the eluted CO_2 peak with that corresponding to complete elution (plateau region) the volume of CO_2 eluted was calculated for a given injection volume.

The correlation between peak height and peak area (Figure 8.3 and 8.4) can be seen to be quite acceptable. As a result peak heights were used routinely in the remaining work because of their ease of measurement. The CO_2 peak height can be measured at least as accurately as the peak area using the method of cutting out peaks. It is recognised that a true correlation between peak height and elution volume is strictly only found for regular Gaussian elution peaks that are not significantly skewed or tailing (Conder and Young,1979,p.122). The reason for the good correlation between the breakthrough curves based on peak height and peak area probably lay in the construction of the breakthrough curve itself. The volume of CO_2 eluted after any injection was calculated by comparing the peak area (or peak height)

with the peak area (or peak height) corresponding to complete elution. No great reliance was therefore placed on calculating the absolute value of the volume of CO_2 eluted, rather the fractional volume was used. Therefore a peak area was only being compared with the peak area corresponding to complete elution, and like-wise for the peak heights. The use of a constant injected volume throughout a given injecton series and the resulting similarities in eluted CO_2 peak shapes was then the reason for the good correlation between peak height and area in the present context.

8.3 The CO_2 Capacity of a 51.7 Wt.% Alumina Composite

As can be seen from Figure 8.3 the calculation of the breakthrough volume requires the intercept on the horizontal axis to be interpolated. (For reasons of clarity the volume of CO_2 that can be completely retained by a column was termed the "breakthrough" volume, as distinct from the "total volume of CO_2 retained". The actual mode of extraction of the values for the "breakthrough volume" and the "total volume of CO_2 retained" from the breakthrough curves is described in Appendix D).

A "fresh" 51.7 wt.% alumina composite was subjected to a series of 5 microlitre injections (after an initial 10 microlitre injection). The breakthrough curve is reproduced in Figure 8.5. The breakthrough data are tabled in Appendix D. From this data a breakthrough volume of 14.1 microlitres was calculated - from the intercept with the horizontal axis. The **total** volume of CO_2 retained by the column was 18.1 microlitres.

8.4 The Retention of CO_2 by Unimpregnated Carbon Cloth

The interaction between CO_2 and an alumina/carbon composite has been described in the previous section. In order to come to understand this interaction, and the effect of the individual components, the behaviour of a piece of virgin carbon cloth B (ie. one not impregnated in the usual manner with alumina) was investigated. A column of 50 layers of carbon cloth B (0.0622g) was prepared and heated to 400°C in the usual manner prior to a series of CO_2 injections (He flow rate 13.0cm^3/min). A 0.5 microlitre and a 1.0 microlitre series of injections were made. The relevant data are plotted in the usual manner in Figure 8.6. It can be readily seen that the carbon cloth alone was responsible for some CO_2 retention. Admittedly this retention was a degree of magnitude less than that for the composite material. Using the breakthrough curve corresponding to the 0.5 microlitre series of injections the breakthrough volume was calculated to be 1.65 microlitres while the total volume of CO_2 retained by the column was marginally greater at 1.67 microlitres. The corresponding values for the 1.0 microlitre series of injections were 1.57 and 1.78 microlitres. The difference between the value of the breakthrough volume for the two series' can be explained by a better estimate of the intercept for the 0.5 microlitre series (3 points in the range 1-2 microlitres instead of 2). The difference in the total volume of CO_2 retained was not so easily rationalised. It is difficult to see how this CO_2 capacity could depend on the injection volume. However the difference between the values is only of the order of 6% which could quite reasonably be explained by experimental error. Furthermore the way in which the breakthrough curves are plotted suggests a large difference in the total volume of CO_2 retained when in fact the magnitude of this difference is small. The vertical scale in Figure 8.6 compresses the curve for the

1.0 microlitre series by a factor of two compared with the 0.5 microlitre series. This effect can be better explained by inspection of Figure 8.7 where the breakthrough data have been replotted with the actual volume of CO_2 eluted on the ordinate (rather than the fractional volume). The difference between the two curves is then not as marked and indeed no intersection of the curves actually takes place. In general the values of the breakthrough volume and total volume of CO_2 retained were extracted from the breakthrough curve with the most data points. The choice of the injecton series with the smallest injecton volume obviously satisfied this criterion.

The CO_2 uptake by the carbon cloth in the absence of alumina was surprising. In order to investigate this result further a piece of carbon cloth B was washed in distilled water, dried at 55^{o}C and heated to 500^{o}C under vacuum. This procedure duplicated the process conditions used in the preparation of composite materials. This material was subsequently made up into a GC column (50 layers - 0.0610g). A series of 0.5 microlitre CO_2 injections were made to a fresh column - the results of which are plotted in Figure 8.8 (the data for the "uncleaned" carbon cloth are included for comparison). The cleaning of the cloth has obviously led to a marked decrease in the CO_2 actvity. The injection of the minimum volume of CO_2 (0.5 microlitre) onto the clean column resulted in immediate elution of CO_2. There was still some slight retention of CO_2 by the clean column (ca. 0.3 microlitre) and this was most likely due to incomplete cleaning of the carbon cloth.

In the production of carbon cloths the viscose rayon precursor is impregnated with various salts (Al, Zn and NH_4 chlorides, NaH_2PO_4, etc) in order to control the carbonisation yield and porosity of the material during carbonisation and activation. A large proportion of these salts are volatilized during the heating process however measurable quantities

of the metals, in particular Al and Zn remain in the final product. The CO_2 uptake of the uncleaned carbon cloth was probably due to such residues. The marked decrease in CO_2 activity after simply washing the cloth in distilled water and heating under vacuum supports this view, and futhermore shows that the bulk of these residues can be easily removed from the carbon cloth.

The composite materials prepared in this work incorporated washing and heating stages routinely in their preparation. As a result it can reasonably be concluded that the CO_2 activity of the composite materials was due to addition of alumina (via the sol/gel route) to the carbon cloth rather than to the presence of carbonisation and activation residues.

8.5 Effect of Temperature

The retention of CO_2 by the 51.7 wt.% alumina composite was also investigated at $28^{o}C$ and at $100^{o}C$, at a carrier flow rate of $13.0cm^3$/minute. The relevant data are reproduced graphically in Figure 8.9 along with the data corresponding to a column temperature of $40^{o}C$. The phenomenon of complete retention of CO_2 by the composite column was observed even at $100^{o}C$. However both the breakthrough volume and total volume of CO_2 retained decreased as the temperature was increased (Table 8.3).

The flow rate for the $100^{o}C$ injection series was measured with the column temperature at $40.0^{o}C$, whereas flow rates for the 28.0 and $40.0^{o}C$ injection series' were measured with the column at the correct temperature. As a result the actual flow rate for the $100^{o}C$ injection series was not $13.0cm^3$/minute. The actual flow rate (F) can be easily calculated by taking account of the absolute values of the temperature (T/K)(Conder and Young,1979,p.28).

$$F_1 = T_1F_2/T_2$$

The actual flow rate for the 100°C injection series was therefore 15.5cm^3/minute. The effect of flow rate on CO_2 retention is discussed in detail in the next section for a wide range of flow rates. Suffice for the present to say that the observed reduction in CO_2 activity observed at 100°C could not be explained by an increase in flow rate of only 20%. The CO_2 activity at a flow rate of 13.0cm^3/minute (100°C) would be only marginally greater than that observed.

CO_2 retention was observed qualitatively at temperatures as high as 200°C. However the rate of elution of both the air hold-up and CO_2 peaks made the quantitative analysis of such data extremely difficult. The maximum temperature for CO_2 retention is probably better estimated from the elution temperature of the CO_2 peak during column regeneration. The minimum temperature marking the commencement of significant CO_2 elution for ballistic heating was approximately 300°C. Therefore CO_2 retention by a fresh composite column is possible even up to this elevated temperature. The volume of such a high temperature retention would be expected to be limited in the light of the results in Table 8.3, where the volume of CO_2 retained at 100°C has been reduced to approximately 60% of that at 40°C.

8.6 Effect of Flow Rate

The carrier flow rate through the 51.7 wt.% alumina column was varied in the range 6-60cm^3/minute in order to determine whether the observed CO_2 retention was sensitive to this parameter. The temperature of a fresh column was maintained at 40.0°C prior to each series of injections. The relevant data are reproduced in Figure 8.10 for flow rates of 5.9, 13.0, 29.5 and 58.7cm^3/minute. From these breakthrough curves the breakthrough volume and the total volume of CO_2 retained were

extracted and are collected in Table 8.4. The volume of CO_2 retained by the composite column decreased as the flow rate increased. However a 10-fold increase in flow rate resulted in only a 20% decrease in the total volume of CO_2 retained. At higher flow rates there was a sharper rise in the breakthrough curve from the complete retention region.

8.7 Effect of Bed Depth

A composite of 58.4 wt.% alumina on carbon cloth B was used in the investigation of bed depth on CO_2 retention.

Initially a column of just 5 layers (0.0116g) of this composite was prepared and investigated (the design of the columns allowed the subsequent addition of more layers, and columns with a total of 10, 20 and 30 layers were studied). At a carrier flow rate of 13.0cm^3/minute and temperature of 40.0^oC a series of 1.0 microlitre and of 2.0 microlitre injections were made to the fresh 5-layer column. Although some CO_2 was retained (see Figure 8.11) the capacity of such a short column was less than the minimum injection volume (1.0 microlitre). A proper analysis of the data requires at least one point on the horizontal axis (ie. corresponding to complete CO_2 retention) in that only then can a lower limit to the breakthrough volume be set. In order to satisfy this criterion the flow rate was decreased to 5cm^3/minute and a series of 1.0 microlitre injections repeated, so as to better define the breakthrough curve for this bed depth. The relevant data are also reproduced in Figure 8.11. At this lower flow rate we were indeed able to obtain an injection volume for which the column was capable of complete retention. This result confirms that the carrier flow rate and therefore the "presentation rate" of CO_2 to a column is an important parameter (see Section 8.6). Obviously for a CO_2 injection volume that closely matches the CO_2 capacity of a given column there is a delicate

balance between total retention and partial elution of CO_2, which can be easily affected.

Columns of 10 layers (0.0227g), 20 layers (0.0447g) and 30 layers (0.0660g) of the 58.4 wt.% alumina composite were also studied. These columns contained sufficient CO_2-active material so that the usual flow rate of 13.0cm^3/minute could be used. The relevant data are reproduced graphically in Figure 8.12. From the breakthrough curves the breakthrough volumes were extracted in the usual way (Table 8.5). These values were then plotted as a function of column packing weight in Figure 8.13. The adsorbent capacity of the column increased with bed depth as would be expected. The increase was approximately linear with respect to column packing weight with the CO_2-capacity of the longest column being slightly greater than what one would expect, assuming linearity. In practical terms therefore, if more of the composite material can be incorporated in a column then a greater volume of CO_2 can be adsorbed per unit weight of packing. From Figure 8.12 it can be seen that the critical bed depth (cbd) for CO_2 breakthrough (at flow rate 13.0cm^3/min) corresponded to between 5 and 10 layers of composite. A column of 10 layers of composite had a depth of only 5mm, therefore this cbd corresponds to an extremely short column. The cbd could be reduced even further by decreasing the carrier flow rate to 5cm^3/minute where the cbd was less than 5 layers (Figure 8.11).

8.8 The Effect of Alumina Loading Level

Thus far several parameters affecting the behavior of an alumina/carbon composite with respect to CO_2 have been investigated in an empirical fashion. However the specific cause of the CO_2 interaction has not been isolated. For a 2 component system, such as the one under study, several possibilities existed:

either a) one or other of the components was individually directly responsible for the behaviour,

or b) the combination of the two phases resulted in a response that neither component was individually capable of.

More specifically, the possibility of the carbon cloth being responsible for the CO_2 interaction has already been dismissed (Section 8.4). The ceramic nature of the alumina phase did not allow the preparation of a pure alumina column to study its CO_2 behaviour in the absence of the support material.

Therefore it could only be concluded at this stage that **either** the alumina phase was solely responsible for the CO_2 behaviour of the composite **or** that the distribution of the alumina phase about the cloth had modified the carbon cloth so that it was rendered more CO_2 active (say by making the carbon cloth more polar). To distinguish between these two hypotheses the CO_2 behaviour of composite materials of varying weight fractions of alumina were investigated.

8.8.1 Low Loading Levels

One would expect that if a change in polarity, say, of the carbon cloth was responsible for the observed CO_2 activity then a subtle effect such as this may occur at low alumina loadings. To this end a composite containing very little alumina (0.70 wt.%) was prepared in the normal manner. This material was a legacy of the alumina sorption experiment described earlier (Section 7.6.2). The concentration of the boehmite sol used to impregnate the carbon cloth (ca. 100ppm) was in the concentration regime where specific uptake of the boehmite sol was observed (ie. the loading level was much greater than would be expected on the basis of the volume of sol occluded by the cloth.) If a subtle modification of the carbon cloth was responsible for the observed CO_2

activity then this type of material (low loading level alumina) would be a prime candidate.

A column of 50 layers (0.0602g) of this composite was prepared and a fresh column was injected with series' of 0.5 and 1.0 microlitre aliquots of CO_2. The breakthrough data are reproduced in Figure 8.14. The breakthrough curve for the column of "cleaned" carbon cloth B (unimpregnated) is included for comparison. The 0.70 wt.% composite was not capable of retaining the minimum injected volume of CO_2 (0.5 microlitres). Indeed, this composite was found to be less CO_2 - active than clean carbon cloth B. The total volume of CO_2 retained by the 0.70 wt.% composite was 0.11 microlitres compared with 0.33 microlitres for the unimpregnated cloth. This surprising observation probably reflected more on the cleanliness of carbon cloth B than in any ability of a small amount of alumina to actually depress the CO_2 activity. It should be remembered that the blank result was obtained by dipping the cloth in distilled water prior to heating under vacuum to 500°C. The preparation of composites incorporated a further stage of immersion/ultrasonication when the carbon cloth was actually brought into contact with the boehmite sol. This extra stage may have been responsible for the partial removal of any remaining residues that would be required to explain the minor difference in CO_2 activity between the 0.70 wt.% alumina composite and the unimpregnated cloth. Also the uncertainties in the measured chromatographic parameters in this low CO_2 volume regime were enhanced by both volumetric difficulties and the lack of sensitivity of the detector to such low quantities of CO_2.

In conclusion then, a low loading level of alumina was not sufficient to cause any enhancement of the CO_2 activity of the composite relative to the unimpregnated carbon cloth.

8.8.2 High Loading Levels

The lack of CO_2 activity conferred on the composite by a low loading level of alumina paved the way for a more detailed investigation of the effect of higher loading levels. Composites of 22.2 and 40.2 wt.% alumina were prepared. Columns of 30 layers of each composite (0.0353 and 0.0491 g respectively) were prepared and investigated under the usual conditions. Breakthrough curves for these two columns are reproduced graphically in Figure 8.15. The data for the 51.7 and 58.4 wt.% composites are included for comparison. These columns also consisted of 30 layers of the respective composites and all data were measured at 40.0^{o}C with a carrier flow rate of 13.0cm^{3}/minute.

For a given number of layers of composite the CO_2 activity increased as the weight fraction of alumina was increased. In order to put this relationship on a more quantitative basis the breakthrough volumes were extracted in the usual way and compared with the weight fractions of alumina and carbon for each composite (Table 8.6). The breakthrough volume was plotted against the weight of alumina (Figure 8.16). It can be seen that the breakthrough volume increased almost linearly with the weight of alumina throughout the range investigated. The total volume of CO_2 retained was also plotted against the weight of alumina (Figure 8.16). The separation between the two curves reflects the increase in the difference between the total volume of CO_2 retained and the breakthrough volume as the weight fraction of alumina is increased. Inspection of Figure 8.15 indicates that at a low weight fraction of alumina the breakthrough curve rises steeply from the total retention region to the total elution plateau, with the values of breakthrough volume and total volume of CO_2 retained being similar. At higher weight fractions of alumina there is a more gradual rise in the breakthrough curve, resulting in a larger difference between the

breakthrough volume and the total volume of CO_2 retained.

Inspection of Table 8.6 reveals that the weight of carbon cloth present in each column was constant despite the gradually increasing proportion of alumina. This result was not unexpected in that each column was based on the same number of layers of cloth.

8.9 Discussion

The observed linear dependence of CO_2 breakthrough volume on weight of alumina strongly suggests that the alumina phase was responsible for the actual "entrapment" of CO_2. If the carbon cloth (or more correctly modification of the cloth due to alumina impregnation) was responsible for the observed CO_2 activity then one would have expected the form of the "breakthrough volume/weight of alumina" plot to be different. In this case the plot would not have been expected to be linear over such an extended range of alumina weight. A loading level of 58.4 wt.% alumina should be more than sufficient to modify the polarity (say) of the cloth, if indeed such a mechanism was to be responsible for the observed CO_2 activity. The lack of CO_2 activity of the unimpregnated carbon cloth and also of the 0.70 wt.% alumina composite also strengthen the argument that the alumina phase alone was responsible for the observed CO_2 activity of high loading level composites.

The most likely conclusion is that the carbon cloth was acting simply as a support material. It helped to distribute the alumina well, thus increasing the CO_2 activity of the alumina phase, and very importantly rendered the alumina into a useful form for study in the present context. The fabrication of a pure unsupported alumina column is not at present feasible utilizing the sol-gel route. Such columns would need to be extremely thin to allow adequate permeability of the

gas stream and then the CO_2 capacity would be limited by the low weight of alumina. The presence of some type of support is therefore vital. The carbon cloth does not prevent the inclusion of a large weight fraction of alumina, although under such conditions the mechanical strength of the composite is reduced significantly. More importantly it spreads the alumina over a useful column length which is readily amenable to CO_2 extraction with good efficiency.

Cutting et al (1971) have investigated the entrapment of molecules in microporous alumina aerogels during their preparation. One of the trapped molecules they investigated was indeed CO_2. No investigation of whether CO_2 could be similarly trapped by a mesoporous alumina has been reported in the literature. One would expect that microporous entrapment may depend on steric considerations particularly as such entrapment has only been observed for small molecules. Mesoporous entrapment on the other hand could not rely on such a mechanism, given the relative dimensions of a CO_2 molecule and the alumina mesopore, and a more specific interaction between the alumina phase and the CO_2 would be required. The aluminas prepared and characterised earlier (Chapter 5) were indeed found to be slightly microporous. Leenears et al (1984) have also reported such partial microporosity for aluminas prepared similarly by the sol/gel route. The preservation of this microporosity in the preparation of composites cannot be assessed in the present work due to the dominant microporosity of the carbon cloth used.

Although the alumina phase has fairly conclusively been shown to be responsible for the observed CO_2 activity of the composite material the connection of such a phenomenon to say the predominantly mesoporous network or to the less predominant microporous one cannot definitely be made. The micropore volume of the alumina present in the 58.4 wt.%

alumina composite was 0.77 microlitre (using the micropore volume for bulk alumina of 20 microlitre/g determined earlier in Section 4.3.3). The total CO_2 capacity of this column was 25 microlitres, this latter volume being measured at ambient temperature and pressure. One would expect the density of the trapped CO_2 to exceed its density under ambient conditions. To establish whether this densification was sufficient to allow complete accommodation of CO_2 within the alumina micropores requires the knowledge of the density of the trapped CO_2. Unfortunately this value cannot be determined.

Another factor mitigating against the specific involvement of alumina micropores in the observed CO_2 activity is the lack of the CO_2 activity by the unimpregnated carbon cloth. This cloth contains a comparitively vast micropore volume (in excess of $0.2cm^3/g$) yet very little CO_2 activity was observed. Therefore micropores "per se" cannot be responsible for this effect. The nature of the CO_2 activity was thought therefore to be alumina specific rather than pore type (micropore versus mesopore) specific.

The alumina phase was simply considered to contain a certain number of CO_2 active sites. In this context, let us now reconsider the results obtained earlier with respect to temperature and flow rate. For a given composite we have a fixed weight of alumina and therefore presumably a consistent number of sites that may trap CO_2. However, the amount of CO_2 that could be trapped was found to decrease as:

a) the temperature of the column was increased (Table 8.3)

and b) the flow rate was increased (Table 8.4)

Admittedly these effects were not marked in the range of temperature and flow rate that were investigated however definite trends did exist. From inspection of Tables 8.3 and 8.4 we observe that **both** the breakthrough volume and the total volume of CO_2 retained decrease as the

temperature and flow rate through the column increase. Now the breakthrough volume and the total volume of CO_2 retained are not independent quantities. The total volume of CO_2 retained may be partitioned between the breakthrough volume and the "transition" volume of CO_2 that can be absorbed by the column (corresponding to the region of transition between total retention and total elution on the breakthrough curve). The magnitude of this "transition" volume did not follow any obvious trend with respect to temperature and flow rate. It was therefore concluded that the breakthrough volume alone was affected by the change in temperature and carrier flow rate and that the variation in the total volume of CO_2 retained only resulted from the "inheritance" of this difference in breakthrough volume.

Let us therefore focus upon the temperature and flow dependency of the breakthrough volume. The breakthrough volume, it will be remembered, is the volume of CO_2 that can be completely retained by the composite column. It was not surprising that this breakthrough volume decreased with increasing temperature and flow rate. One could imagine that kinetic factors associated with the CO_2-alumina interaction affect the ability of the alumina to completely retain the injected volume of CO_2. This situation may be better explained with reference to Figure 8.17. Consider the injection of a fixed amount of CO_2 onto a given column at both low and high flow rates. If this volume is significantly less than the CO_2 capacity of the column total retention will take place at both high and low flow rates. However when the "dose" of CO_2 is similar to the CO_2 capacity the "presentation" rate becomes more important. At a low presentation level (corresponding to low flow rate) almost all the sites could be filled and the CO_2 would be completely retained. However at a higher presentation level filling of the last few empty sites may not be completed before the removal of some of the

adsorptive by the carrier stream. Empty sites would be filled by the subsequent passage of CO_2.

This model would also predict that the total volume of CO_2 that could be retained by a given column would be independent of flow rate, despite the difference in breakthrough volume. It was surprising then, that the experimental results indicated that the total volume of CO_2 retained was dependent on flow rate and temperature. The results therefore suggested that the total number of CO_2-active sites was not invariant but flow rate and temperature dependent. Therefore although the "site" model was capable of explaining the observed trends in breakthrough volume it was not adequate for the explanation of total CO_2 capacities.

The retention of CO_2, at temperatures significantly greater than its sublimation temperature, by alumina was sufficiently marked for one to infer a specific interaction between the gas and solid. CO_2 possesses a permanent quadrupole moment (Barrer,1978,p.207) and its adsorption is known to be very sensitive to the presence of polar groups or ions on the surface of a solid (Gregg and Sing,1982,p.82). The observed strong retention was only observed, it should be remembered, when the alumina was heated to a temperature of $400^{o}C$. One may therefore speculate that under these conditions cationic Al^{3+} sites would be exposed which would interact strongly with the CO_2 quadrupole. Indeed the interaction between water, which possesses a permanent dipole moment, and alumina has been explained by the involvement of exposed Al^{3+} cations (Carruthers et al,1971; Baker et al,1971). Several workers have studied the interaction between alumina and CO_2 (Parkyns,1965; Peri,1966; Gregg and Ramsay,1969). The interaction is thought to involve chemisorption of CO_2 on the more active alumina sites.

TABLE 8.1 - EFFECT OF TEMPERATURE ON THE RETENTION TIME FOR CO_2 AT 40°C

Maximum Temperature[@] of Column (°C)	Retention Time (s)
100	57
200	69
300	87
350	110
400	no CO_2 eluted
450	no CO_2 eluted

[@]A ballistic heating program was used with heating rate 50°C/min. and dwell time at T_{max} of 5 min. before cooling to an isothermal temperature of 40.0°C for measurement of chromatograms.

TABLE 8.2 - COMPARISON OF PEAK AREA AND PEAK HEIGHT METHOD OF ANALYSIS OF CO_2 BREAKTHROUGH DATA FOR THE 51.7WT.% ALUMINA COMPOSITE

Injection Volume (microlitres)	Fractional Volume of CO_2 Eluted (%)		Cumulative Volume of CO_2 Injected (microlitres)
	Peak Area	Peak Height	
10	-	-	10
"	35.7	13.2	20
"	82.7	72.3	30
"	100.0	100.0	40
"	87.9	89.5	50
20	12.5	30.6	20
"	95.5	81.5	40
"	100.0	100.0	60
"	97.9	97.3	80
50	58.1	41.2	50
"	92.9	89.4	100
"	100.0	97.9	150
"	97.1	100.0	200

TABLE 8.3 - EFFECT OF TEMPERATURE ON CO_2 BREAKTHROUGH VOLUME FOR 51.7 WT.% ALUMINA COMPOSITE

Temperature (^oC)	Breakthrough Volume (microlitres)	Total Volume of CO_2 Retained (microlitres)
28.0	17.6	20.0
40.0	14.1	18.1
100.0	9.3	10.8

TABLE 8.4 - EFFECT OF FLOW RATE ON CO_2 BREAKTHROUGH VOLUME FOR 51.7 WT.% ALUMINA COMPOSITE

Flow Rate (cm^3/min.)	Breakthrough Volume[@] (microlitres)	Total Volume of CO_2 Retained (microlitres)
5.9	17.2	19.5
13.0	14.1	18.1
29.5	13.7	18.1
58.7	12.0	16.3

[@]Measured at 40.0^{o}C

TABLE 8.5 - EFFECT OF BED DEPTH ON CO_2 BREAKTHROUGH VOLUME FOR A 58.4 WT.% ALUMINA COMPOSITE

Bed Depth (layers)	Breakthrough Volume[@] (microlitres)	Total Volume of CO_2 Retained (microlitres)	Column Packing Weight (mg)
5	ca.0.7	1.2	11.6
10	3.5	6.8	22.7
20	9.6	12.8	44.7
30	19.1	24.9	66.0

[@]Measured at 40.0°C

TABLE 8.6 - EFFECT OF ALUMINA LOADING LEVEL ON CO_2 BREAKTHROUGH VOLUME

Alumina Loading (%)	Packing Weight (mg)	Alumina Weight (mg)	Carbon Weight (mg)	Breakthrough[@] Volume (microlitres)	Total Volume of CO_2 Retained (microlitres)
22.2	35.3	7.8	27.5	1.7	2.6
40.2	49.1	19.7	29.4	8.5	9.1
51.7	59.0	30.5	28.5	14.1	18.1
58.4	66.0	38.5	27.5	19.1	24.9

[@]Measured at 40.0°C, carrier flow rate 13.0cm^3/min.

FIGURE 8.1 - Typical Chromatogram for Alumina/Carbon Composite Column Injected with CO_2

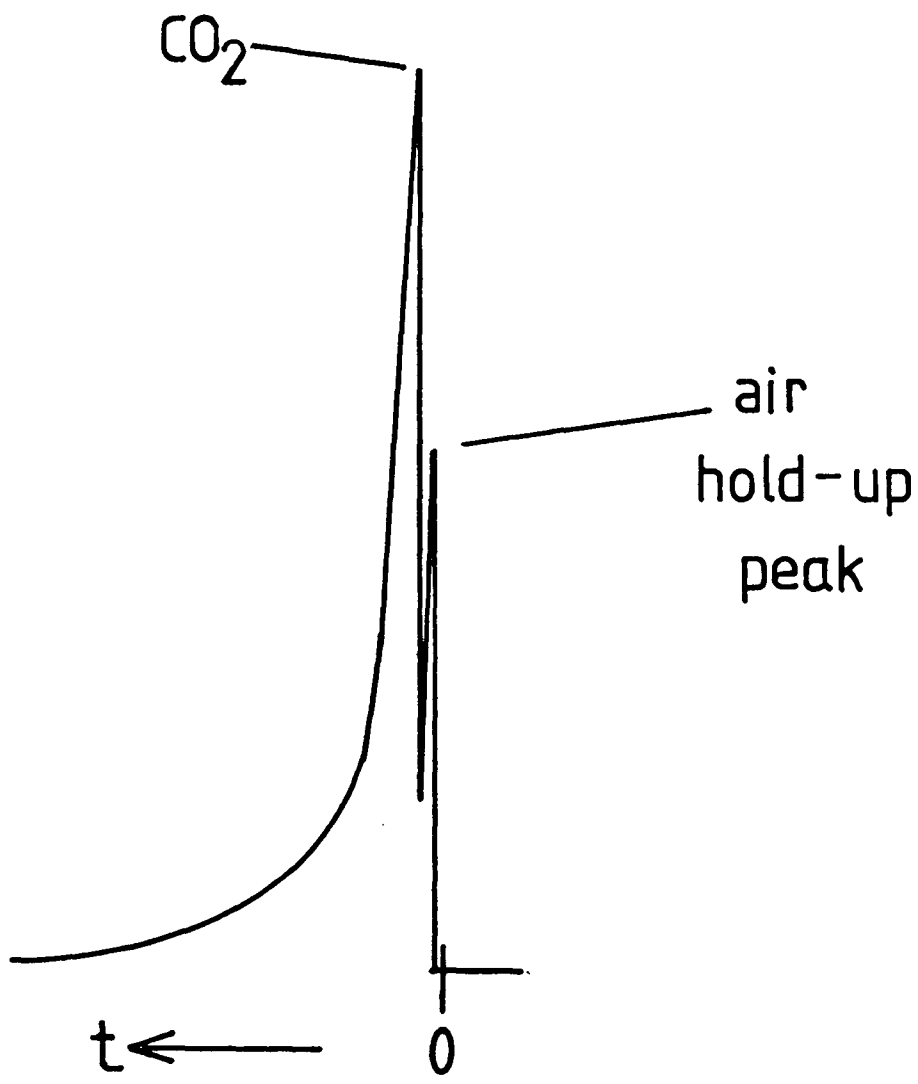

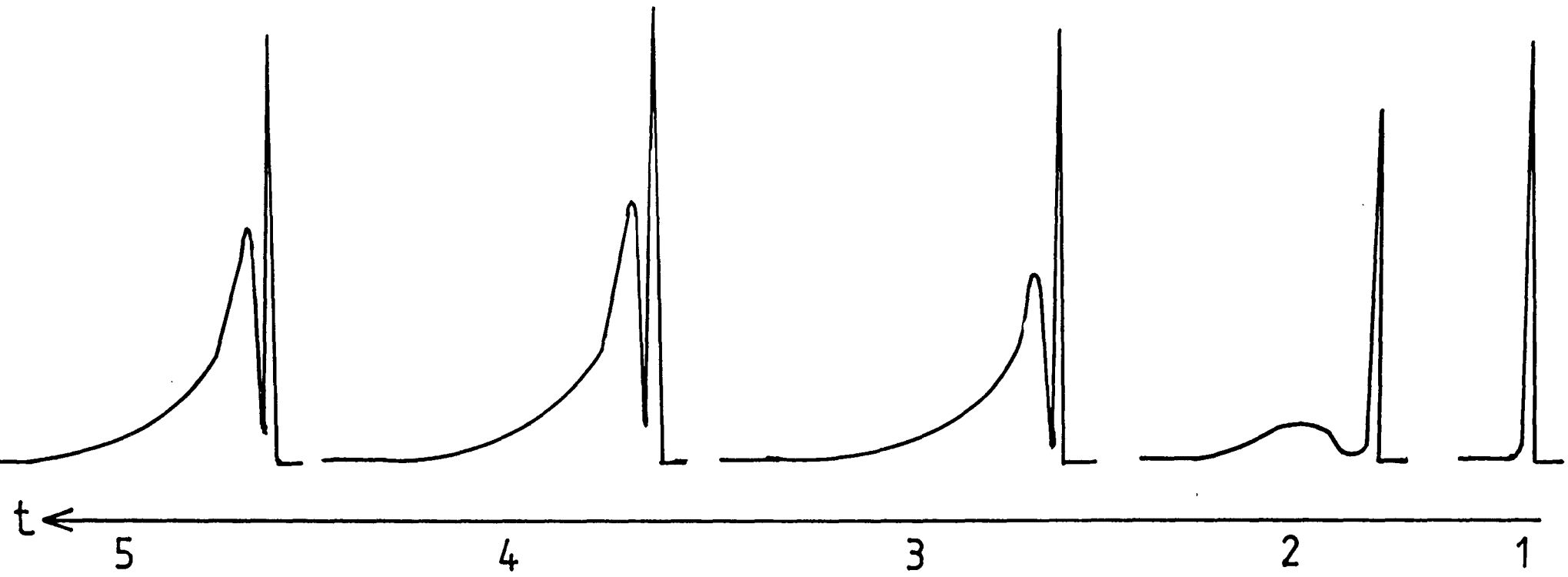

FIGURE 8.2 - Series of Chromatograms for a Fresh 51.7 Wt.% Alumina Composite Injected with 10 µl Aliquots of CO_2

FIGURE 8.3 : BREAKTHROUGH CURVE FOR 51.7 WT.% ALUMINA COMPOSITE - 10 µl INJECTIONS

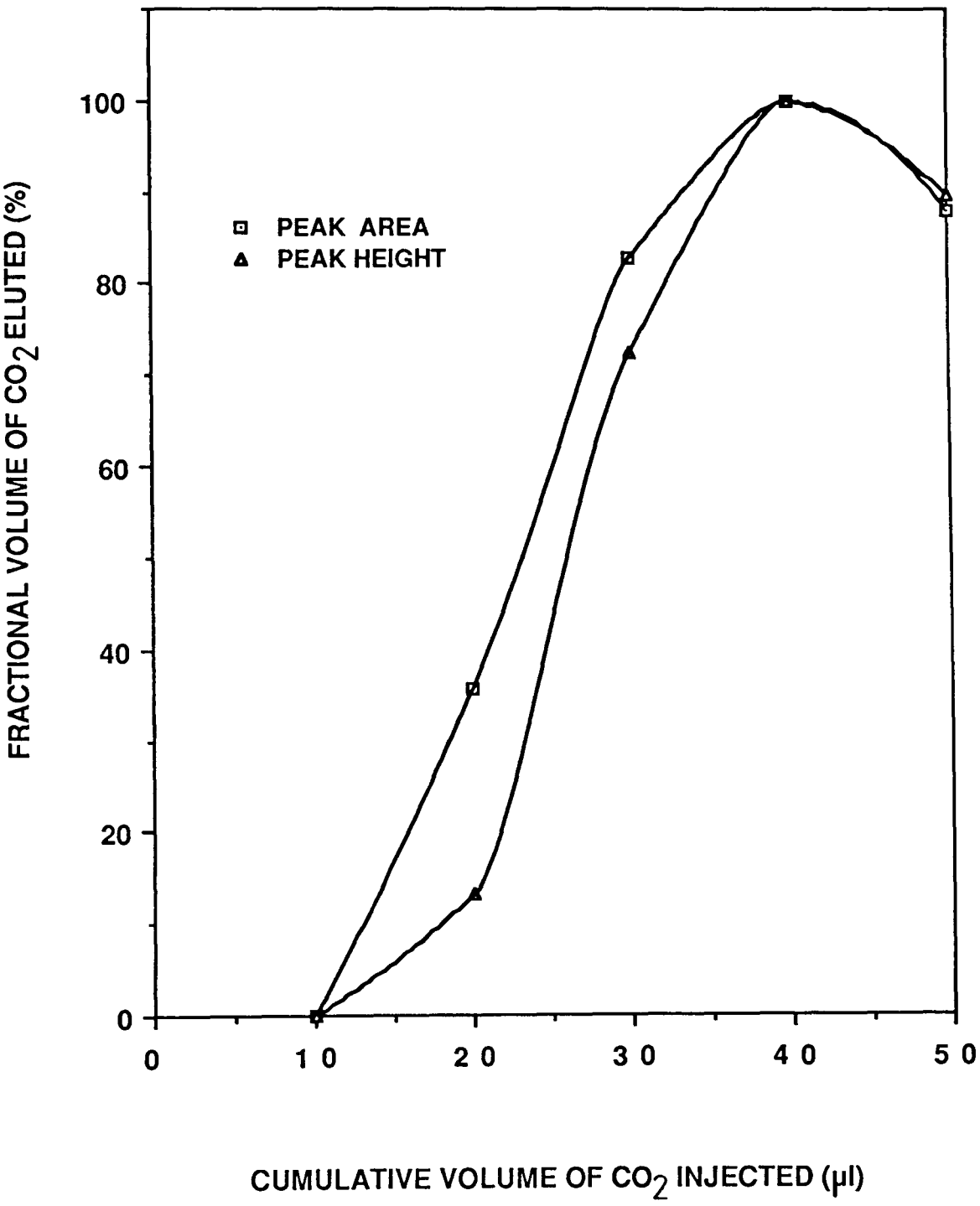

FIGURE 8.4 : BREAKTHROUGH CURVE FOR 51.7 WT.% ALUMINA COMPOSITE -20, 50 µl INJECTIONS OF CO_2

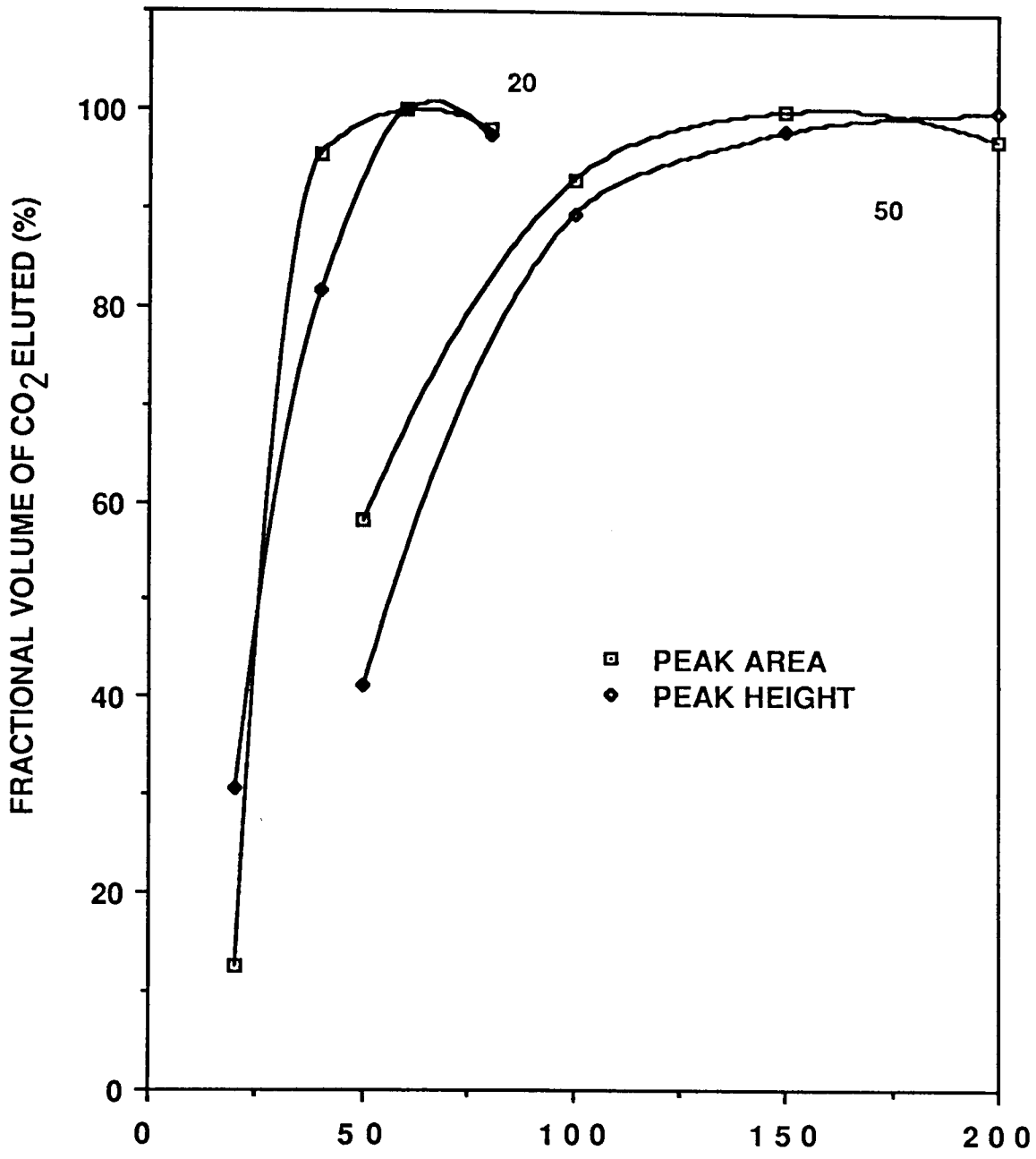

FIGURE 8.5 : BREAKTHROUGH CURVE FOR 51.7 WT.% ALUMINA COMPOSITE - 5.0 µl INJECTIONS OF CO_2

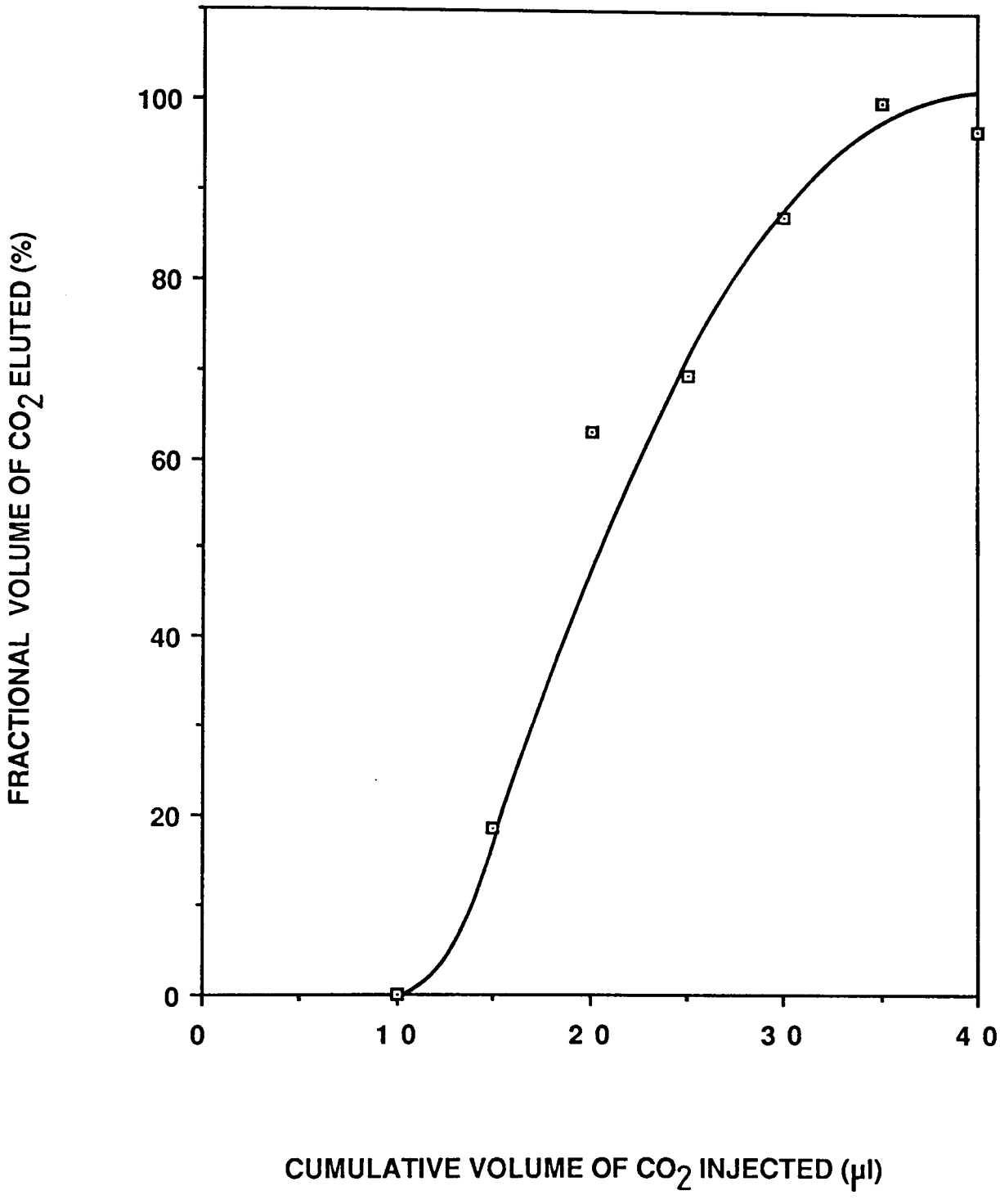

FIGURE 8.6 : BREAKTHROUGH CURVE FOR UNIMPREGNATED CARBON CLOTH B (I) - 0.5 AND 1.0 µl INJECTIONS OF CO_2

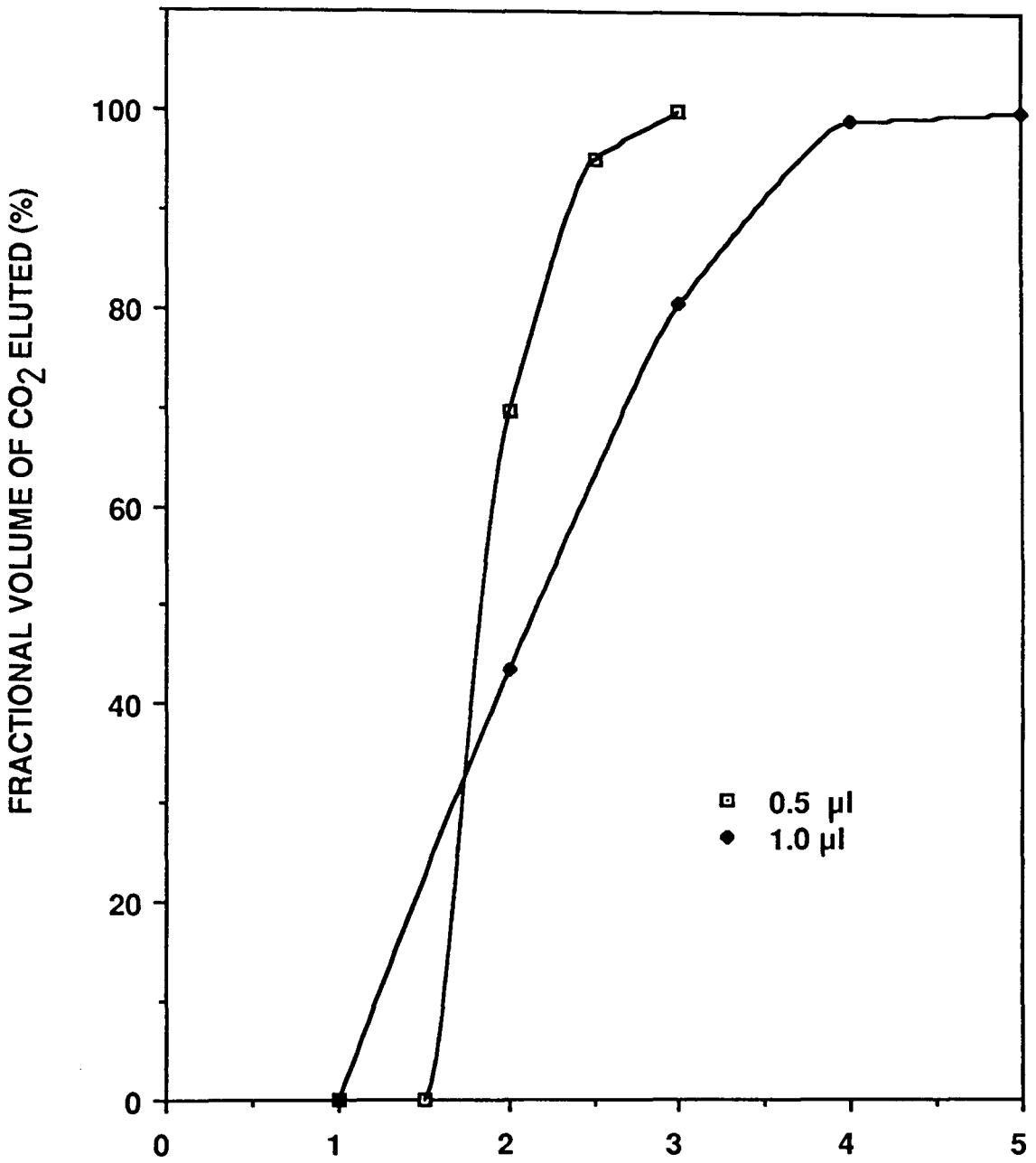

FIGURE 8.7 : BREAKTHROUGH CURVE FOR UNIMPREGNATED CARBON CLOTH B (II)

- 0.5 AND 1.0 µl INJECTIONS OF CO_2

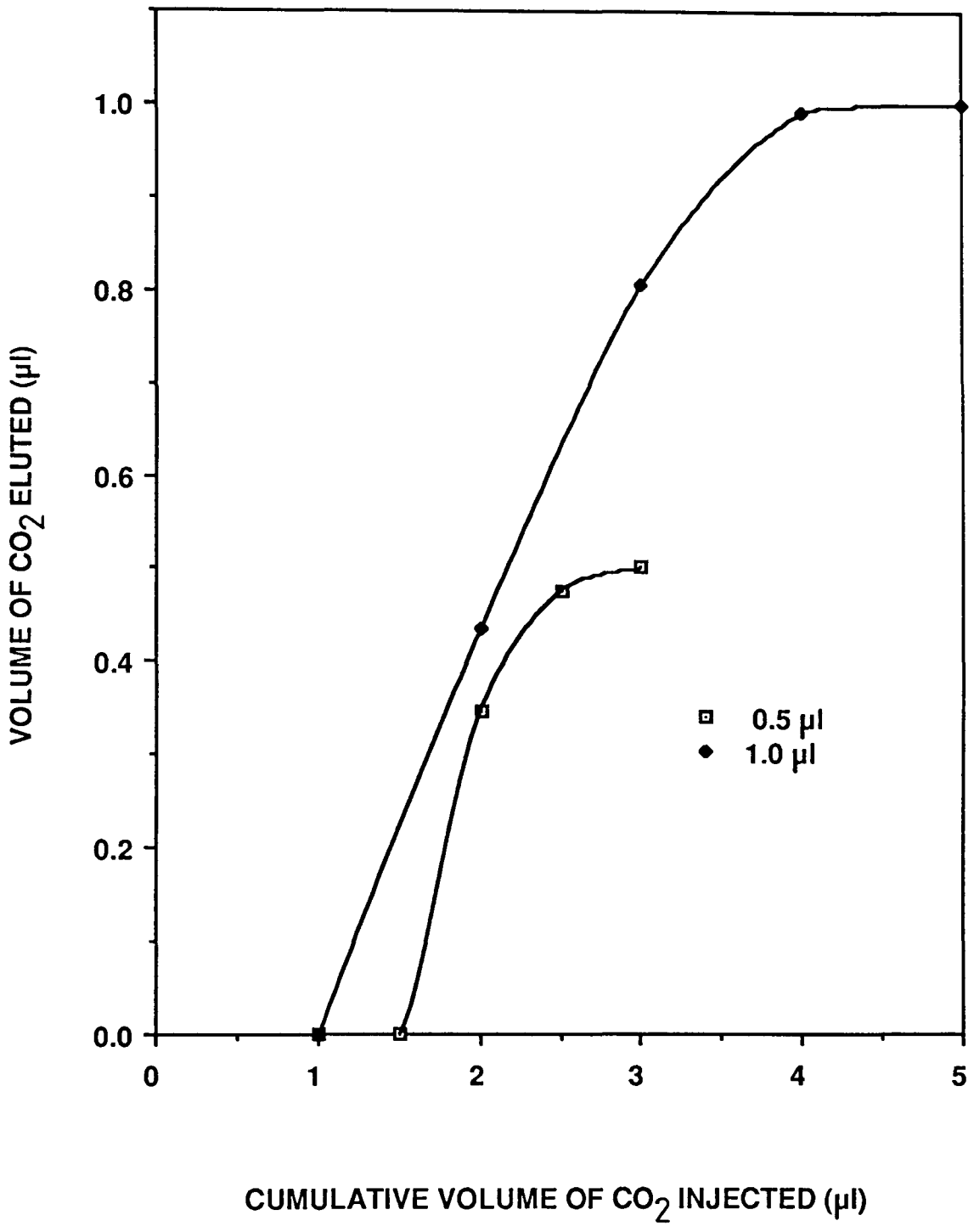

FIGURE 8.8 : BREAKTHROUGH CURVE FOR CLEANED CARBON CLOTH B

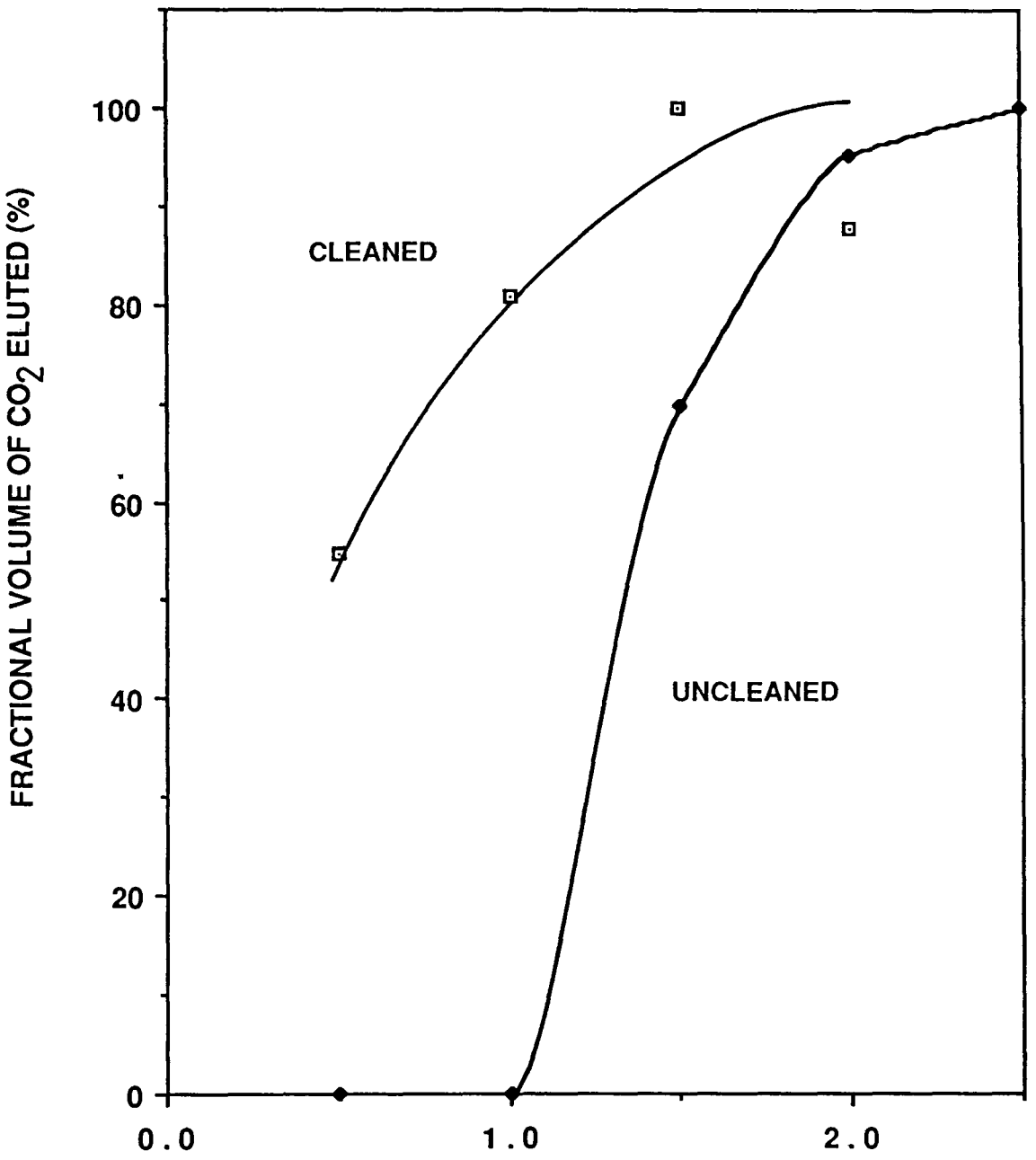

FIGURE 8.9 : EFFECT OF TEMPERATURE ON CO_2 BREAKTHROUGH CURVE

FOR 51.7 WT.% ALUMINA COMPOSITE

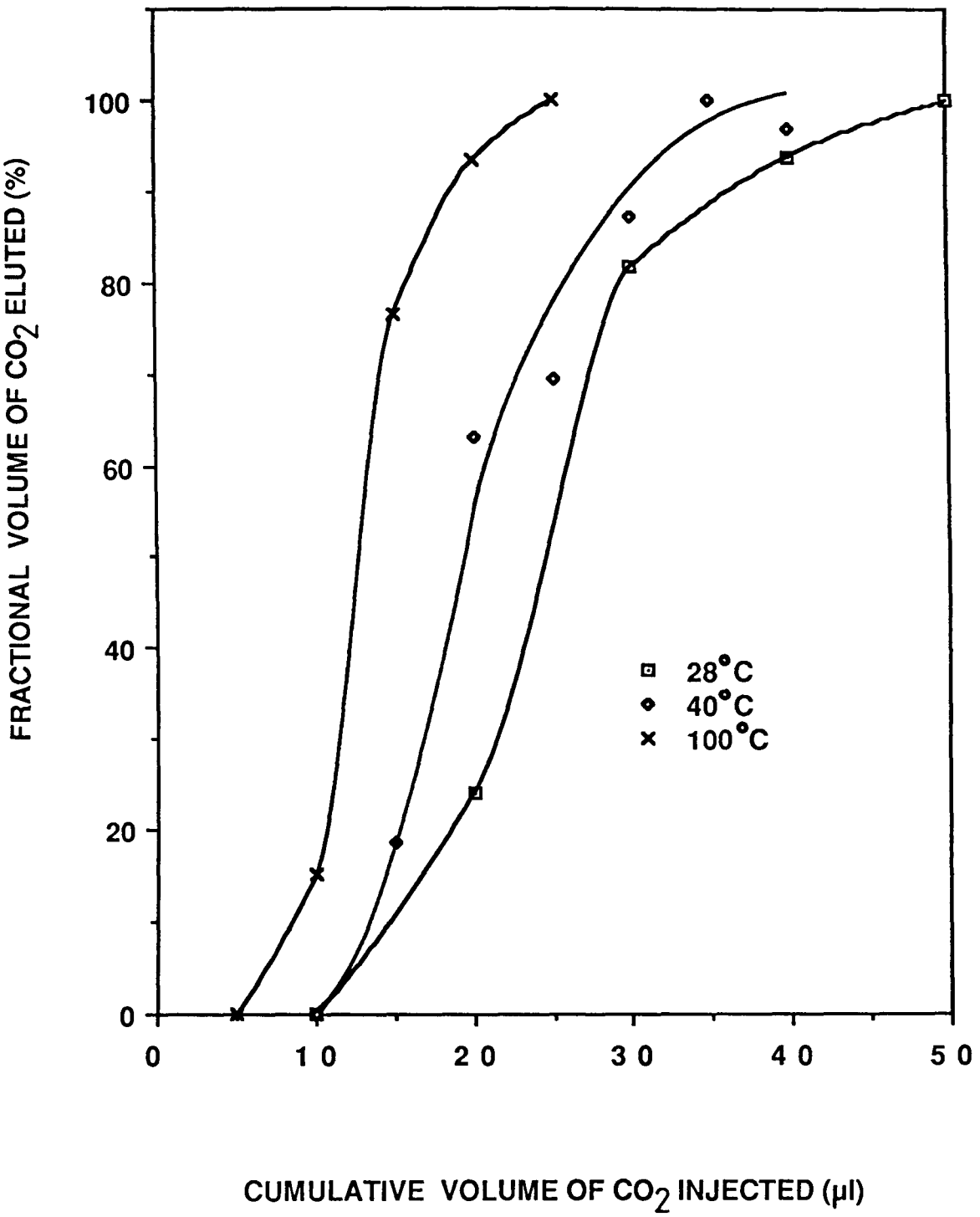

FIGURE 8.10 : EFFECT OF CARRIER FLOW RATE ON CO_2 BREAKTHROUGH CURVE FOR 51.7 WT.% ALUMINA COMPOSITE

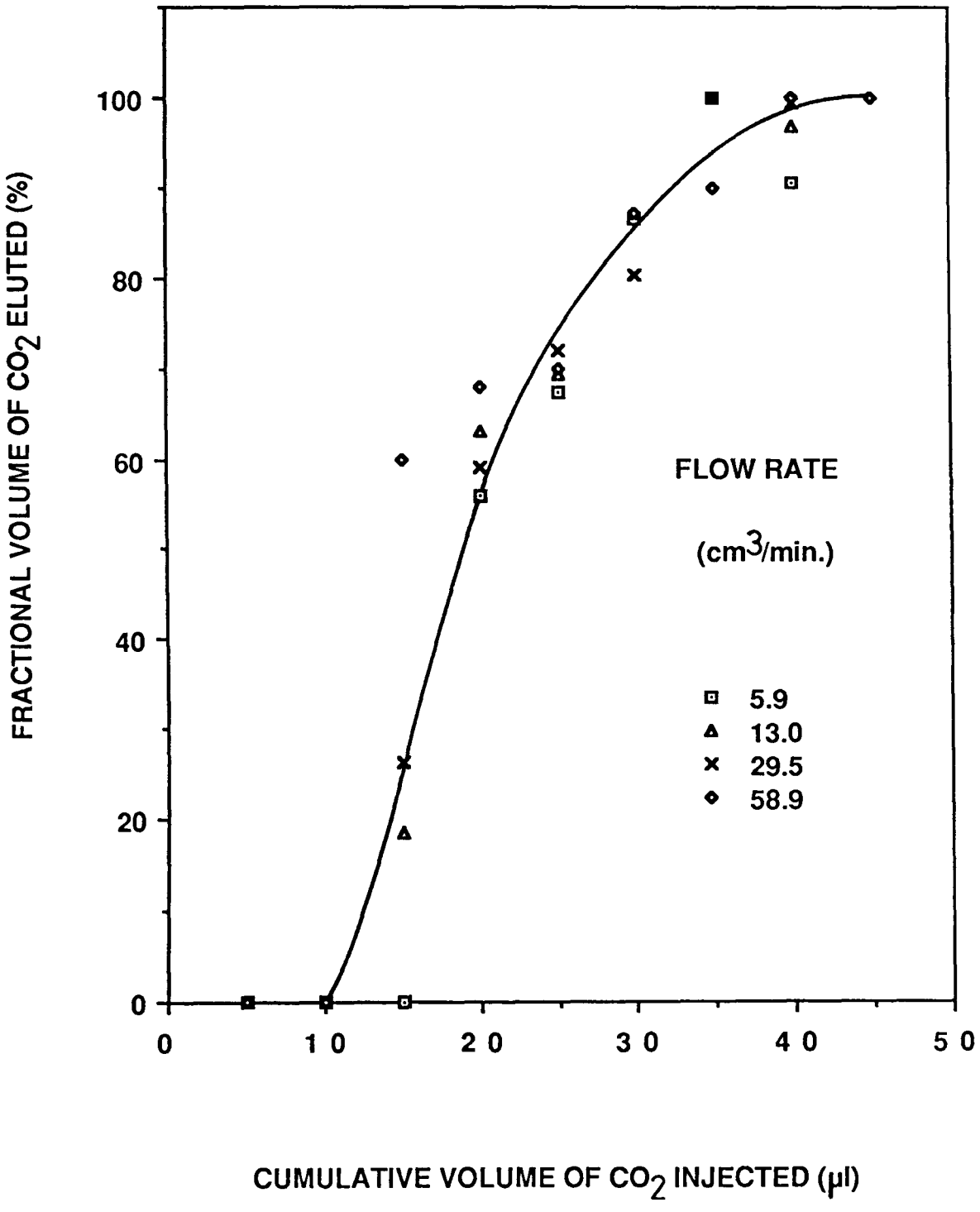

FIGURE 8.11 : CO_2 BREAKTHROUGH CURVE FOR 5 LAYERS OF 58.4 WT.% ALUMINA COMPOSITE

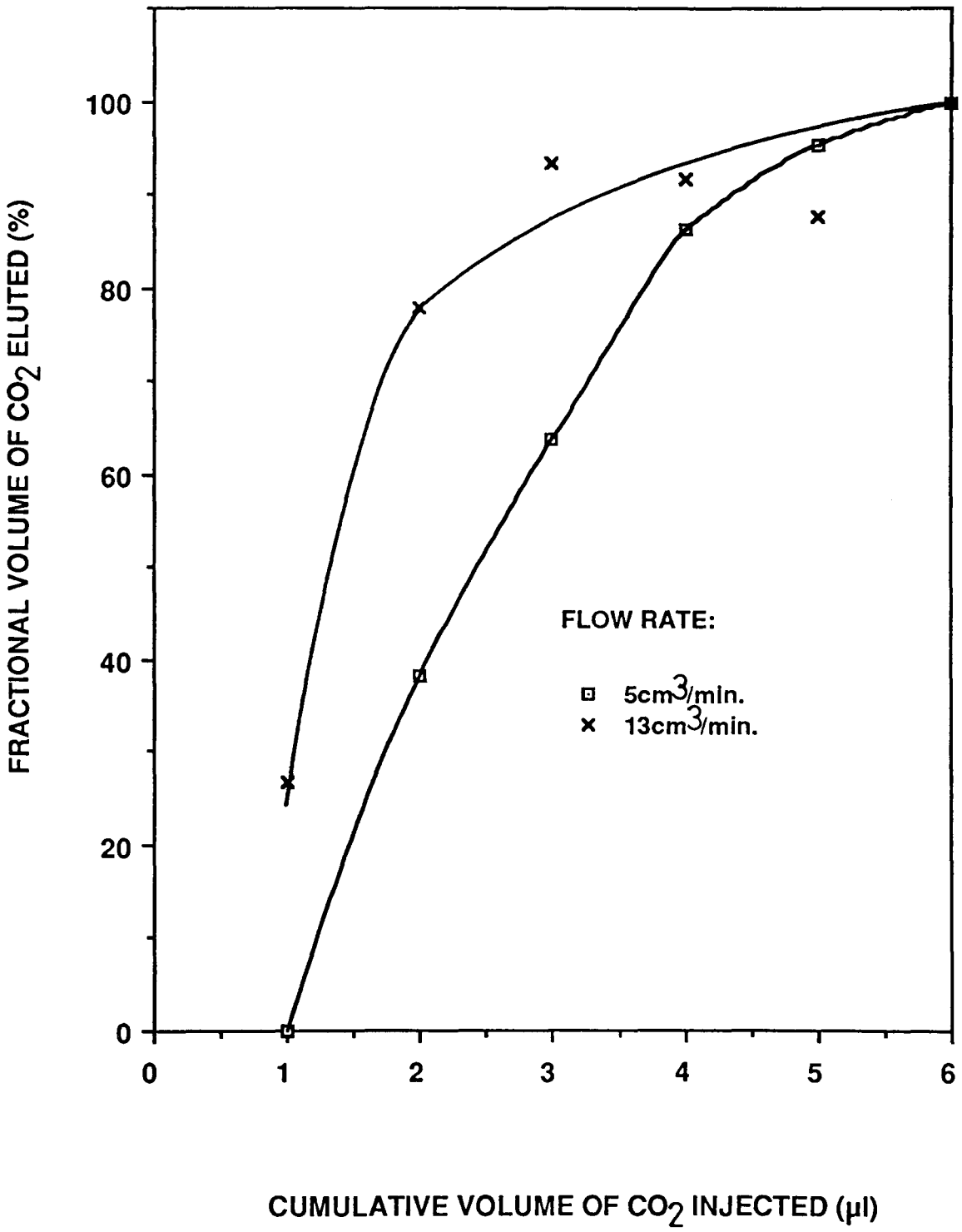

FIGURE 8.12 : EFFECT OF BED DEPTH ON CO_2 BREAKTHROUGH CURVES

FOR 58.4 WT.% ALUMINA COMPOSITE

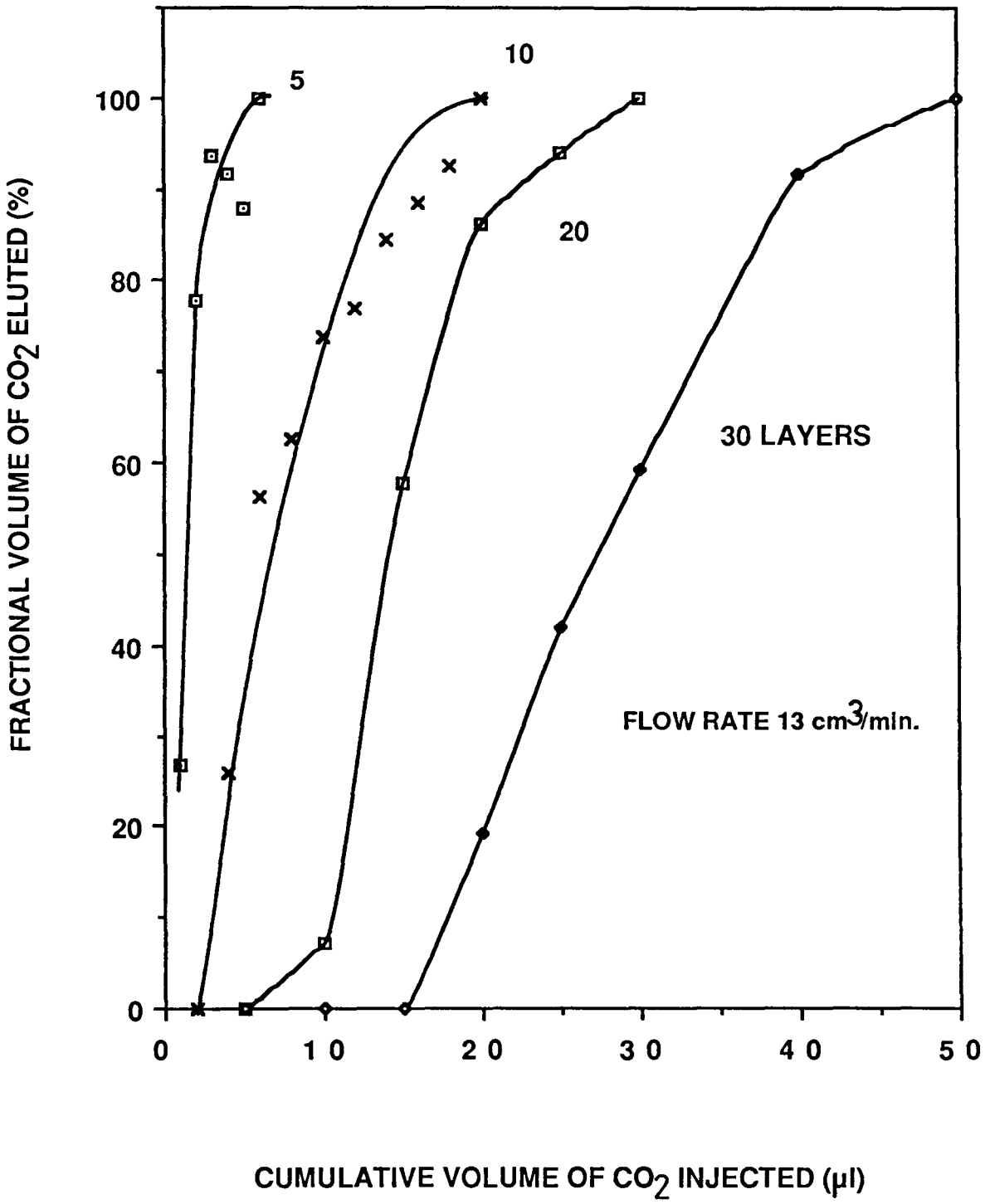

FIGURE 8.13 : VOLUME OF CO_2 RETAINED /g OF 58.4 WT.% ALUMINA COMPOSITE

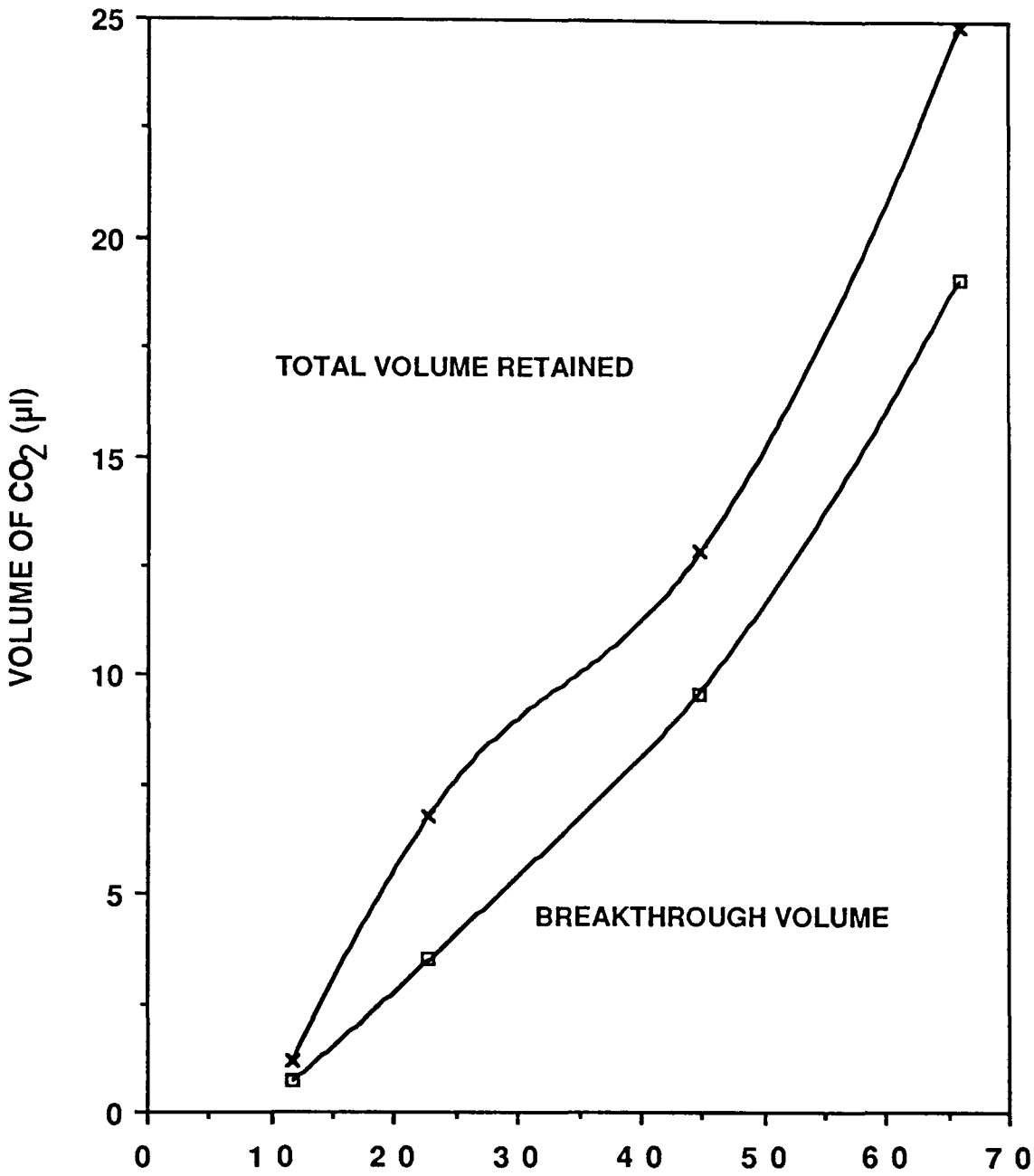

FIGURE 8.14 : CO_2 BREAKTHROUGH CURVE FOR 0.70 WT.% ALUMINA COMPOSITE

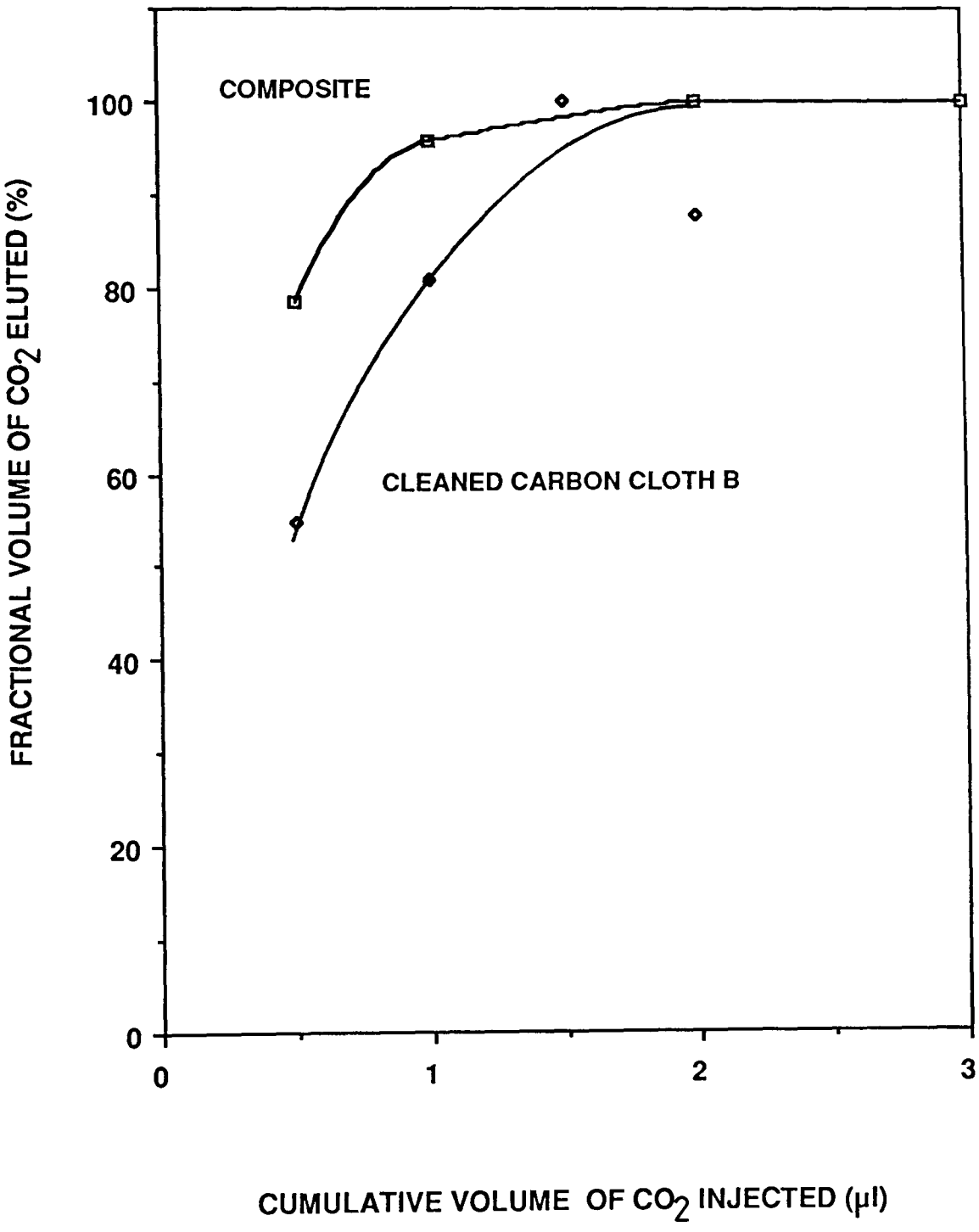

FIGURE 8.15 : EFFECT OF ALUMINA LOADING LEVEL ON CO_2 BREAKTHROUGH CURVE

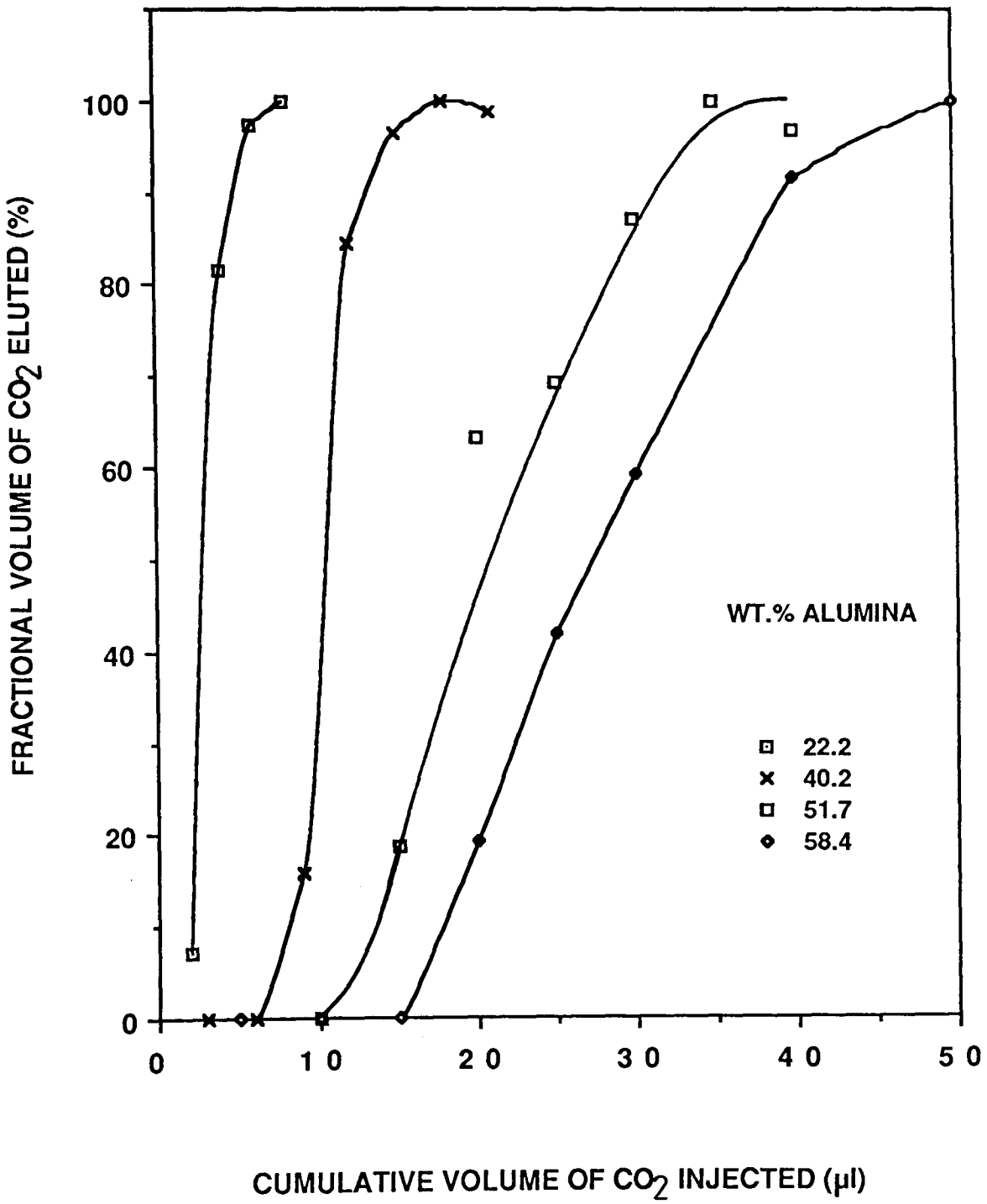

FIGURE 8.16 : VOLUME OF CO_2 RETAINED AS A FUNCTION OF WEIGHT OF ALUMINA

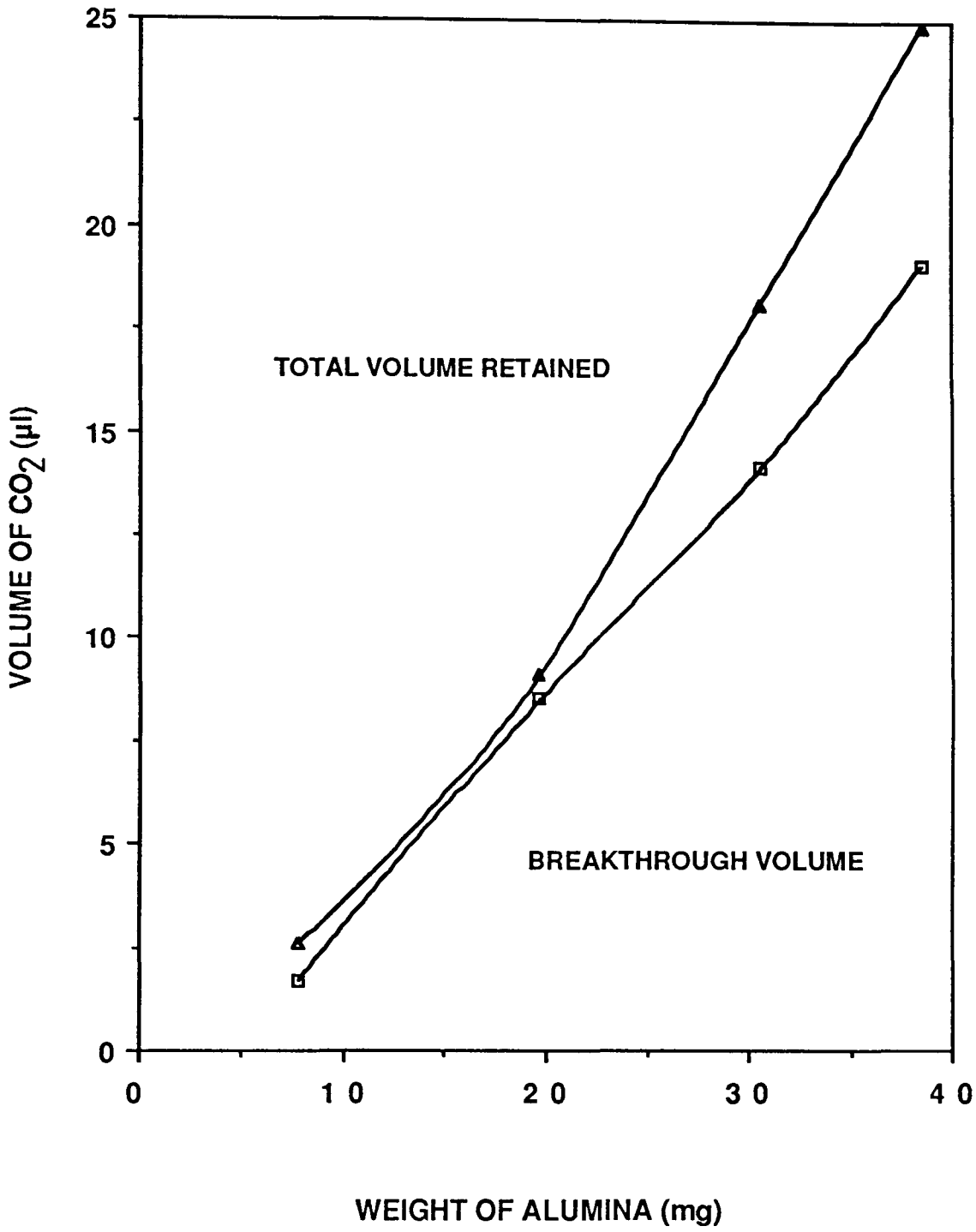

FIGURE 8.17 - Site Model for CO_2 Retention

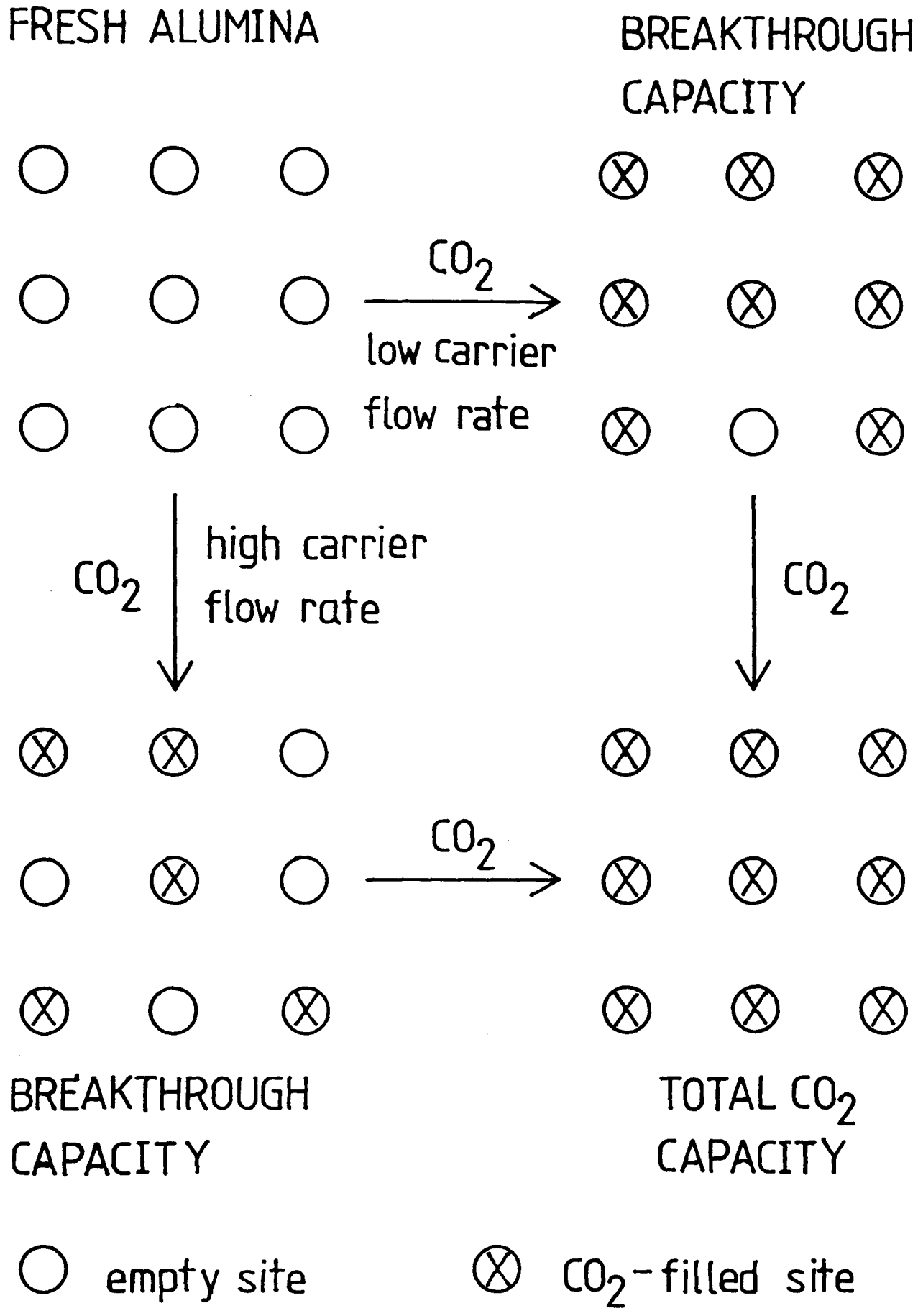

CHAPTER 9 : GENERAL DISCUSSION AND SUMMARY

The prime aim of the present work was to modify the properties of activated carbon cloth by the deposition of a second phase, thus broadening its range of application. To this end the impregnation of mesoporous carbon cloth with alumina was investigated. The **effective** deposition of a highly polar material on the significantly less polar carbon cloth would result in a significant modification of the properties of the carbon phase.

Deposition from solution and vapour deposition were not found to be satisfactory methods of depositing alumina on carbon cloth despite their successful application to the coating of other substrates. This result was thought to reflect on the basic incompatibility between the alumina and carbon phases. The use of the sol/gel derived alumina for impregnation was favoured over other methods of producing alumina for two basic reasons. Firstly the intermediate, boehmite, is quite stable under the conditions required to produce the final alumina, and secondly the boehmite sols can be readily concentrated so that high loading levels of boehmite, and subsequently alumina, on the carbon cloth can be attained with only a single impregnation stage.

Yoldas (1975,b) found that the dehydration of the boehmite gel to alumina, studied by TG and EGA, was not affected by the heating environment. In the present work the nature of the heating environment was investigated in some detail. It was found that heating in flowing nitrogen, flowing air or under vacuum resulted in the production of an alumina with a relatively invariant pore size distribution. However heating in still air gave an alumina with a distinctly different pore size distribution (see Table 5.3 and Figure 5.9). In the latter case

the modal pore size was significantly greater, and the porosity of the resultant alumina was found to be dependent on the heating rate and length of heat treatment. The dehydration of the boehmite gel is normally accompanied by a shrinkage of the component boehmite plates and a widening of the pores (Leenaars et al,1984), as for the case of the still air heated alumina. However under flowing nitrogen, flowing air or vacuum, dehydration was completed so quickly that the normal relaxation of the plate structure did not occur, and the final pore size was not different from that of the dried boehmite gel.

The boehmite/carbon composites were heated under vacuum so as to preserve the integrity of the carbon cloth during the conversion of boehmite to alumina. The alumina produced by vacuum heat treatment was found to have a much greater nitrogen BET surface area (see Table 4.2) and also to be more water-active (see Figure 4.12) than the alumina produced as a result of the more conventional still air heat treatment.

The distribution of the alumina phase about the carbon cloth was obviously an important factor in the modification of the behaviour of the carbon cloth. One would expect that significant modification of the chemistry of the cloth would be aided by a well-distributed alumina phase. The initial distribution of boehmite about the mesoporous cloth was found to be poor. However the incorporation of a pre-wetting stage prior to immersion of the carbon cloth in the boehmite sol was shown to significantly enhance the distribution of boehmite about the cloth on a microscopic scale.

One of the disadvantages of deposition of colloidal boehmite (and indeed of other colloids) on porous materials results from the size of the primary deposit. Obviously because of steric considerations "receptor" pores must be at least as large as the particles to be deposited. The colloidal boehmite used in the present work had a

minimum particle dimension of 2.5 nm. This dimension is indeed quite small (in the colloidal range) but is still sufficient to preclude the penetration of the micropores (<2nm) of the carbon cloth. The colloidal penetration of mesopores (2-50nm) by boehmite plates, however, should not be precluded on steric grounds, although in this context the maximum plate dimension (ca. 25nm, Leenaars et al,1984) would be more important. The activated carbon cloths used in the present work were chosen because of their predominantly mesoporous nature.

Because of a resolution problem the penetration of boehmite into the mesopores of the carbon cloth could not be determined directly by electron microscopy. The adsorption of nitrogen (at 77K) was used to probe the mesopore range for the presence of alumina. Isotherms for the individual components and for the alumina/carbon composites were determined. Comparison of these isotherms indicated that the mesopores of the carbon cloths had not been penetrated by the alumina plates. Instead of a blocking of carbon cloth mesopores (and consequent reduction of pore volume) an increase in pore volume was measured. It was concluded that the extra pore volume was produced by a disruption of the plate structure of the alumina by the carbon cloth. This disruption was most probably caused by the clustering of alumina about the pore entrances of the carbon cloth. Indeed Leenaars et al (1986) have used this phenomenon in the preparation of alumina membranes from boehmite sols on porous ceramic supports. Capillary action results in the supporting water rushing into pores leaving the boehmite particles clustered about the pore entrances. In the present work a microporous carbon cloth was also observed to occlude a significant weight of boehmite, therefore confirming that mesopore volume was not a necessary requirement in this regard.

It remained for the activity of the composite material with

respect to polar molecules to be assessed, as it was in this regard that the presence of the more polar alumina phase would be expected to most affect the behaviour of the carbon cloth. Water isotherms for the alumina/carbon composites were determined. Carbon cloth is reasonably hydrophobic in nature and the deposition of alumina resulted in a significant enhancement of the water activity as demonstrated by the uptake of water at low relative pressures. The uptake of water by the composite material was enhanced by a factor of two relative to that of the carbon cloth.

The activity of the composite material was also investigated with respect to CO_2. To this end the composite material was made up into a GC column. Two basic types of behaviour were exhibited by such columns. Without any "cleaning" of the composite column CO_2 was found to be "held up" relative to air. However by far the most striking behaviour was exhibited after the columns were "cleaned" by heating to temperatures in excess of 400^{o}C. After this treatment the composite was capable of completely retaining the injected volume of CO_2 with no elution taking place. In this regard the CO_2 activity of virgin carbon cloth was found to be almost negligible at <2 µl of CO_2 retained/g whereas the presence of alumina gave a corresponding value of up to 906 µl/g of carbon. This behaviour was found to be dependent on the weight of alumina deposited on the carbon cloth. The retention of CO_2 was thought to be due to the interaction between the CO_2 quadrupole moment and the electric field associated with Al^{3+} cations exposed by heating to 400^{o}C. Leenaars et al (1986) have reported that sol/gel alumina prepared as a membrane was CO_2-active, but only after the alumina phase was further modified by impregnation with other chemical entities. This extra impregnation stage may greatly enhance the CO_2 activity of their membrane, however the present work demonstrates that the alumina itself has a significant

degree of CO_2 activity in its own right.

Because of the enhanced activity of the carbon cloth with respect to H_2O and CO_2 it is concluded that the activity of the cloth with respect to polar molecules in general would be greatly improved by the presence of alumina.

CHAPTER 10 : CONCLUSIONS

1. The solution or vapour deposition of alumina on activated carbon cloth, in amounts significant enough to affect the chemistry of the carbon phase, is not readily attained.

2. A more suitable procedure involves the impregnation of the carbon cloth with boehmite sols, and subsequent vacuum heat treatment. In this way alumina/carbon composites with alumina loading levels in excess of 100 wt.% may be readily obtained.

3. The distribution of boehmite about the carbon cloth is significantly enhanced by the incorporation of a "pre-wetting" (of the carbon cloth) stage into the composite production sequence.

4. The incorporation of alumina does not result in blockage of the pores of the carbon cloth.

5. The activity of the carbon cloth with respect to polar molecules such as water, and particularly carbon dioxide is enhanced by the presence of alumina.

APPENDIX A : SOL/GEL ALUMINA ADSORPTION DATA

A1 - Nitrogen Adsorption Data

Isotherms measured at 77K. All samples were outgassed at 110°C except for sample no.1 which was outgassed at RT.

Sample no.1. Dried (RT) Boehmite Gel.

Adsorption		Desorption	
p/p^o	V_{ads} (cm^3/g)	p/p^o	V_{ads} (cm^3/g)
0.001	20.9	0.952	256.8
0.006	40.3	0.827	246.2
0.022	55.5	0.710	241.1
0.087	72.3	0.612	235.9
0.157	87.0	0.529	230.6
0.227	101.7	0.477	216.5
0.297	116.5	0.474	182.7
0.365	132.2	0.448	160.2
0.431	148.5	0.410	145.2
0.496	165.3		
0.556	184.3		
0.617	202.7		
0.677	221.6		
0.744	237.3		
0.927	250.1		
0.994	310.0		

Sample no.2. Dried (110°C) Boehmite Gel.

Adsorption		Desorption	
p/p^o	V_{ads} (cm^3/g)	p/p^o	V_{ads} (cm^3/g)
0.000	8.0	0.970	223.6
0.000	16.1	0.907	222.1
0.002	23.8	0.842	221.8
0.004	31.6	0.789	220.1
0.006	39.2	0.733	219.7
0.018	45.3	0.687	218.2
0.027	51.7	0.645	216.6
0.046	56.5	0.605	215.3
0.071	60.4	0.563	214.7
0.093	64.7	0.538	211.7
0.141	72.5	0.533	205.4
0.193	79.7	0.530	198.7
0.246	86.9	0.516	194.0
0.293	95.0	0.516	187.1
0.337	103.4	0.514	180.5
0.381	112.0	0.512	174.0
0.423	121.0	0.506	168.1
0.467	129.6	0.500	162.3
0.510	138.4	0.492	157.1
0.545	148.5	0.490	150.8
0.585	157.6	0.484	145.2
0.617	168.4	0.468	141.6
0.651	178.7	0.465	135.7
0.679	189.9	0.457	131.0
0.710	200.7	0.445	127.0
0.747	210.5	0.439	122.0
0.796	218.3	0.421	119.4
0.873	221.2	0.410	115.8
0.957	222.9	0.398	112.5
1.000	231.7	0.378	110.7
		0.366	107.7
		0.352	105.4

Sample no.3. Alumina Heated in Flowing Nitrogen (10-->500(17)).

Adsorption		Desorption	
p/p^o	$V_{ads}(cm^3/g)$	p/p^o	$V_{ads}(cm^3/g)$
0.001	25.3	0.869	304.7
0.036	60.2	0.749	296.4
0.105	78.6	0.644	290.4
0.181	93.8	0.568	277.3
0.256	109.1	0.547	238.8
0.329	125.6	0.521	205.2
0.400	142.8	0.482	181.4
0.469	161.2	0.444	160.3
0.530	183.4	0.399	147.0
0.588	206.9	0.357	135.5
0.645	231.0	0.317	127.0
0.699	257.0	0.283	118.3
0.755	281.7	0.251	111.8
0.829	297.6	0.222	106.0
0.922	304.0		
0.994	321.2		

Sample no.4. Alumina Heated in Flowing Air (10-->500(17)).

Adsorption		Desorption	
p/p^o	$V_{ads}(cm^3/g)$	p/p^o	$V_{ads}(cm^3/g)$
0.005	39.6	0.855	292.4
0.047	64.0	0.739	287.8
0.113	78.1	0.638	284.6
0.186	89.6	0.583	265.7
0.255	102.6	0.562	234.2
0.323	115.7	0.538	206.1
0.390	129.8	0.505	183.5
0.452	145.5	0.469	165.2
0.510	162.9	0.430	150.8
0.565	181.9	0.390	139.8
0.616	202.5		
0.662	224.8		
0.708	247.6		
0.751	271.5		
0.812	287.8		
0.899	293.2		
0.990	297.1		

Sample no.5. Alumina Heated in Flowing Air (1-->500(17)).

Adsorption		Desorption	
p/p^o	V_{ads} (cm^3/g)	p/p^o	V_{ads} (cm^3/g)
0.008	44.8	0.925	260.2
0.065	66.4	0.794	256.4
0.138	80.1	0.680	253.5
0.214	92.5	0.585	249.9
0.289	105.5	0.535	228.5
0.361	119.8	0.514	196.0
0.430	135.8	0.483	170.4
0.493	154.4	0.445	150.9
0.551	175.4	0.404	136.8
0.606	197.6	0.361	126.8
0.662	219.8	0.321	119.0
0.720	240.7		
0.797	252.5		
0.892	256.4		
0.986	260.2		
0.990	306.9		

Sample no.6. Alumina Heated in Flowing Air (1-->500(1)).

Adsorption		Desorption	
p/p^o	V_{ads} (cm^3/g)	p/p^o	V_{ads} (cm^3/g)
0.001	31.6	0.905	289.0
0.018	53.7	0.777	281.1
0.052	65.5	0.668	273.4
0.090	75.0	0.573	267.5
0.130	82.9	0.522	240.4
0.170	90.7	0.492	204.0
0.212	97.8	0.457	174.5
0.252	105.7	0.414	154.6
0.294	112.7	0.370	140.4
0.366	133.4	0.329	129.3
0.439	154.0	0.290	120.8
0.508	177.0	0.256	113.0
0.573	202.4		
0.636	228.6		
0.699	255.6		
0.774	274.6		
0.866	283.4		
0.961	290.6		
0.990	338.1		

Sample no.7. Alumina Heated in Still Air (2-->500(15)).

Adsorption		Desorption	
p/p^o	V_{ads} (cm^3/g)	p/p^o	V_{ads} (cm^3/g)
0.007	31.0	0.925	302.0
0.039	43.4	0.797	296.0
0.080	50.3	0.689	289.4
0.123	55.4	0.654	235.1
0.166	60.4	0.624	180.8
0.209	65.5	0.578	143.1
0.254	69.6	0.520	120.7
0.295	75.6	0.461	106.5
0.339	80.6	0.405	97.1
0.380	86.6	0.357	88.1
0.460	101.5	0.312	81.7
0.535	120.0	0.273	76.4
0.601	144.2	0.238	72.5
0.658	175.8	0.208	68.6
0.703	214.7		
0.744	257.4		
0.799	289.9		
0.889	297.4		
0.982	303.0		

Sample no.8. Alumina Heated in Still Air (2-->500(6)).

Adsorption		Desorption	
p/p^o	V_{ads} (cm^3/g)	p/p^o	V_{ads} (cm^3/g)
0.009	35.2	0.946	288.8
0.044	48.0	0.814	282.0
0.085	55.2	0.702	275.2
0.128	61.3	0.615	258.8
0.173	65.1	0.587	196.3
0.217	70.1	0.543	153.8
0.259	76.2	0.488	129.5
0.302	82.2	0.432	113.5
0.345	88.3	0.381	101.7
0.425	105.2	0.333	93.7
0.501	125.4	0.292	86.3
0.570	151.2	0.254	81.0
0.632	183.7	0.222	76.0
0.688	221.8		
0.745	258.8		
0.822	277.9		
0.914	284.6		
0.992	302.6		

Sample no.9. Alumina Heated in Still Air (1-->500(24)).

Adsorption		Desorption	
p/p^o	V_{ads} (cm^3/g)	p/p^o	V_{ads} (cm^3/g)
0.009	31.1	0.871	288.9
0.047	40.4	0.753	280.8
0.090	45.8	0.677	250.9
0.134	50.2	0.652	184.7
0.179	53.6	0.609	138.0
0.223	58.0	0.548	113.1
0.268	62.4	0.484	98.4
0.310	67.8	0.426	87.4
0.355	72.2	0.373	79.3
0.397	77.6	0.325	73.6
0.478	92.5	0.283	68.3
0.555	110.3		
0.623	134.1		
0.682	165.8		
0.729	206.5		
0.768	253.0		
0.829	282.7		
0.919	289.7		
0.982	318.5		

Sample no.10. Alumina Heated Under Vacuum (1-->500(24)).

Adsorption		Desorption	
p/p^o	V_{ads} (cm^3/g)	p/p^o	V_{ads} (cm^3/g)
0.000	27.8	0.979	255.5
0.011	49.8	0.907	252.7
0.039	61.8	0.838	250.9
0.076	69.5	0.779	246.8
0.153	83.6	0.720	245.5
0.229	97.6	0.667	243.1
0.305	111.7	0.618	240.8
0.376	128.6	0.572	239.2
0.445	147.0	0.534	235.0
0.511	166.8	0.513	222.6
0.571	189.5	0.500	206.4
0.630	212.9	0.486	191.7
0.693	234.1	0.472	176.8
0.774	246.0	0.458	163.3
0.867	250.8	0.442	151.3
0.962	254.8	0.424	141.6
0.989	295.4	0.403	134.3
		0.382	128.0
		0.361	122.6
		0.341	117.5

Sample no.11. Alumina Heated Under Vacuum (10-->500(1)).

Adsorption		Desorption	
p/p^o	$V_{ads}(cm^3/g)$	p/p^o	$V_{ads}(cm^3/g)$
0.000	26.7	0.987	264.9
0.006	49.9	0.916	261.5
0.065	70.8	0.849	258.5
0.137	84.8	0.789	254.8
0.210	98.0	0.731	252.5
0.281	112.7	0.678	249.8
0.350	128.0	0.629	247.4
0.416	144.7	0.584	245.0
0.478	164.2	0.542	242.5
0.538	184.4	0.517	232.1
0.595	206.7	0.498	219.2
0.652	229.0	0.484	204.1
0.717	246.4	0.475	186.6
0.799	254.8	0.464	171.1
0.888	259.0	0.449	158.4
0.976	263.9		
0.989	310.5		

Sample no.12. Alumina Heated Under Vacuum (10-->400(3)).

Adsorption		Desorption	
p/p^o	$V_{ads}(cm^3/g)$	p/p^o	$V_{ads}(cm^3/g)$
0.000	20.7	0.930	256.6
0.001	41.0	0.797	253.3
0.028	71.5	0.684	250.4
0.088	88.5	0.586	248.3
0.155	102.3	0.504	245.3
0.222	116.6	0.484	218.6
0.289	130.4	0.465	192.7
0.354	145.2	0.436	173.2
0.417	161.1	0.396	160.7
0.475	178.5	0.357	151.1
0.535	195.5	0.321	142.5
0.591	214.0	0.287	135.9
0.648	232.0	0.257	129.3
0.720	244.2		
0.804	251.1		
0.898	253.9		
0.992	256.7		

A2 - Nitrogen BET Plots

Nitrogen BET plots were found to be of similar form for all boehmite/alumina samples. As such, only a selection is reproduced here covering the range of heating environments.

Sample I.D.	Heating Environment
no.1,Dried Gel (RT)	-
no.2,Dried Gel (110^{o}C)	-
no.3,Alumina	N_2
no.4,Alumina	air(flowing)
no.10,Alumina	air(still)
no.11,Alumina	vacuum

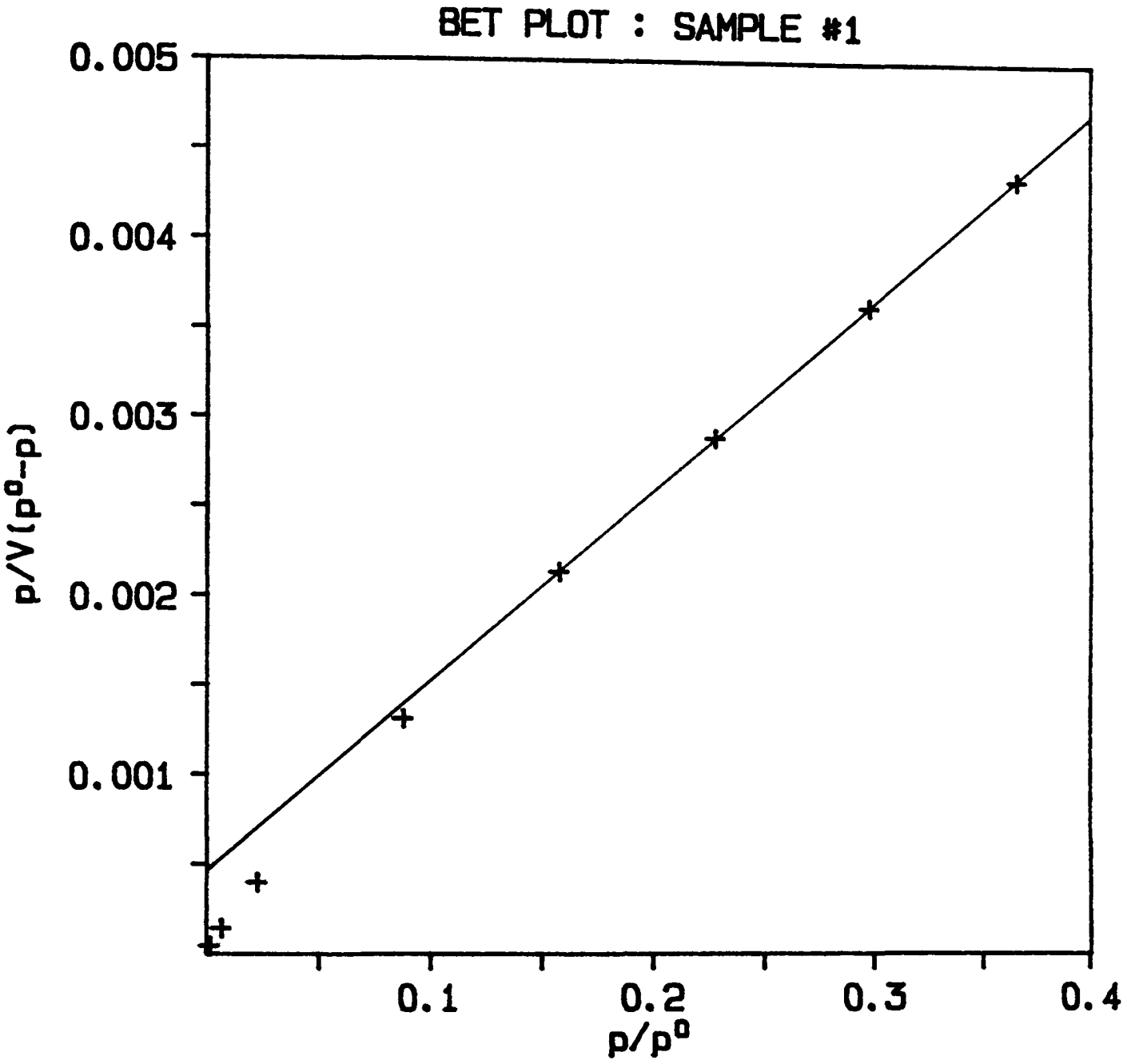
BET PLOT : SAMPLE #1
0.005
0.004
0.003
0.002
0.001
p/V(p°-p)
0.1
0.2
0.3
0.4
p/p°

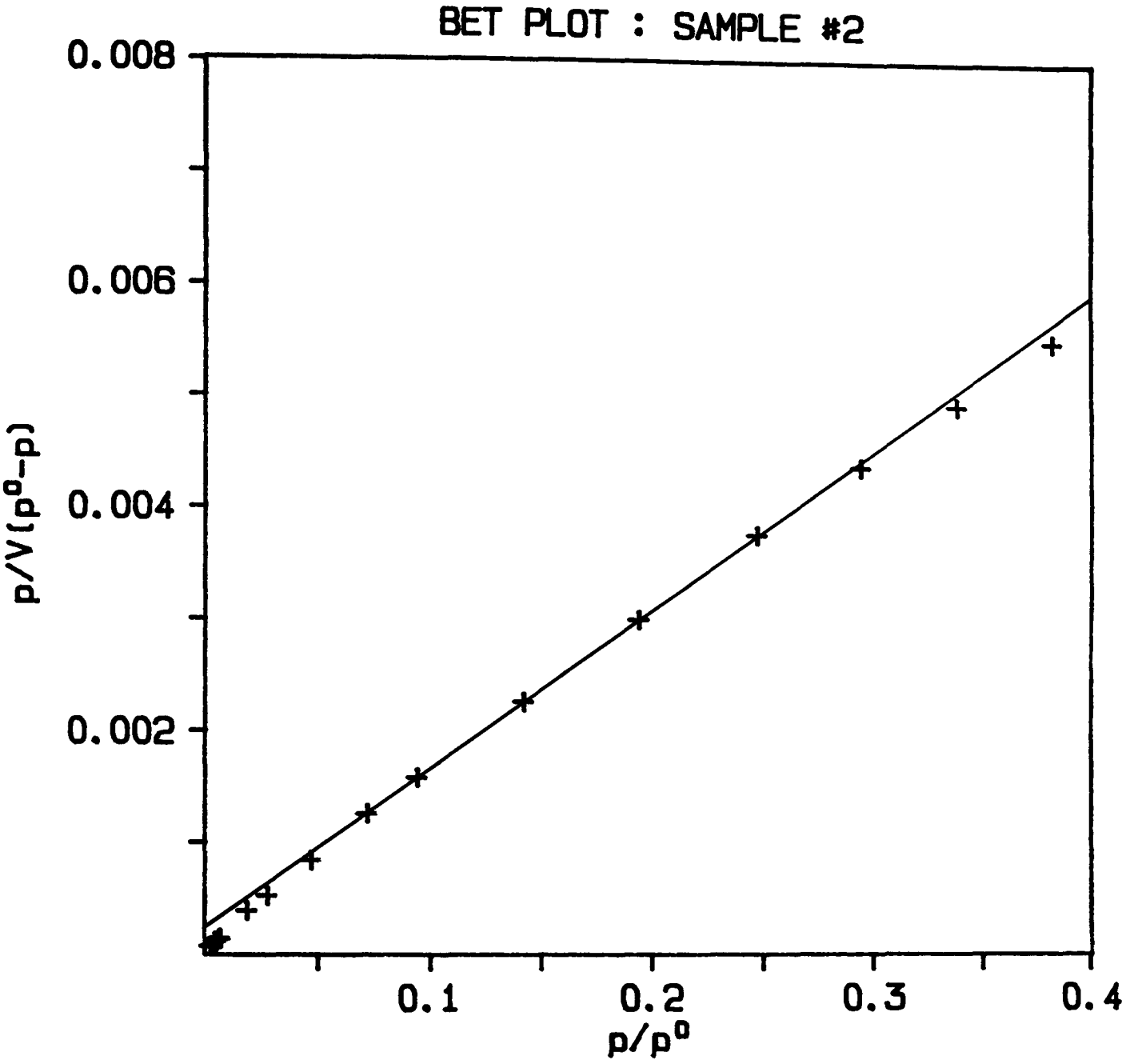
BET PLOT : SAMPLE #2
0.008
0.006
0.004
0.002
p/V(p°-p)
0.1
0.2
0.3
0.4
p/p°

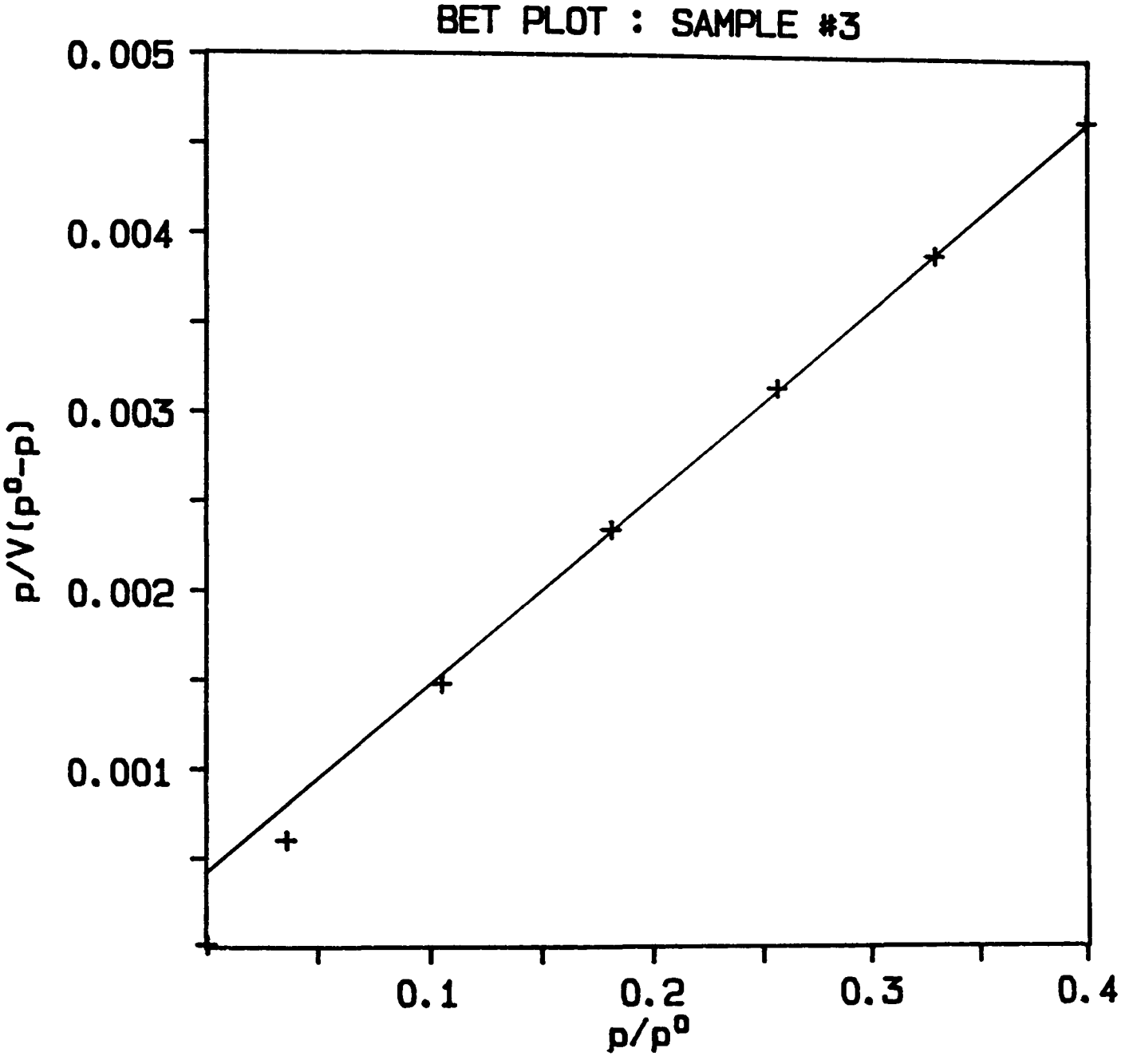
BET PLOT : SAMPLE #3
0.005
0.004
0.003
0.002
0.001
p/V(p°-p)
0.1
0.2
0.3
0.4
p/p°

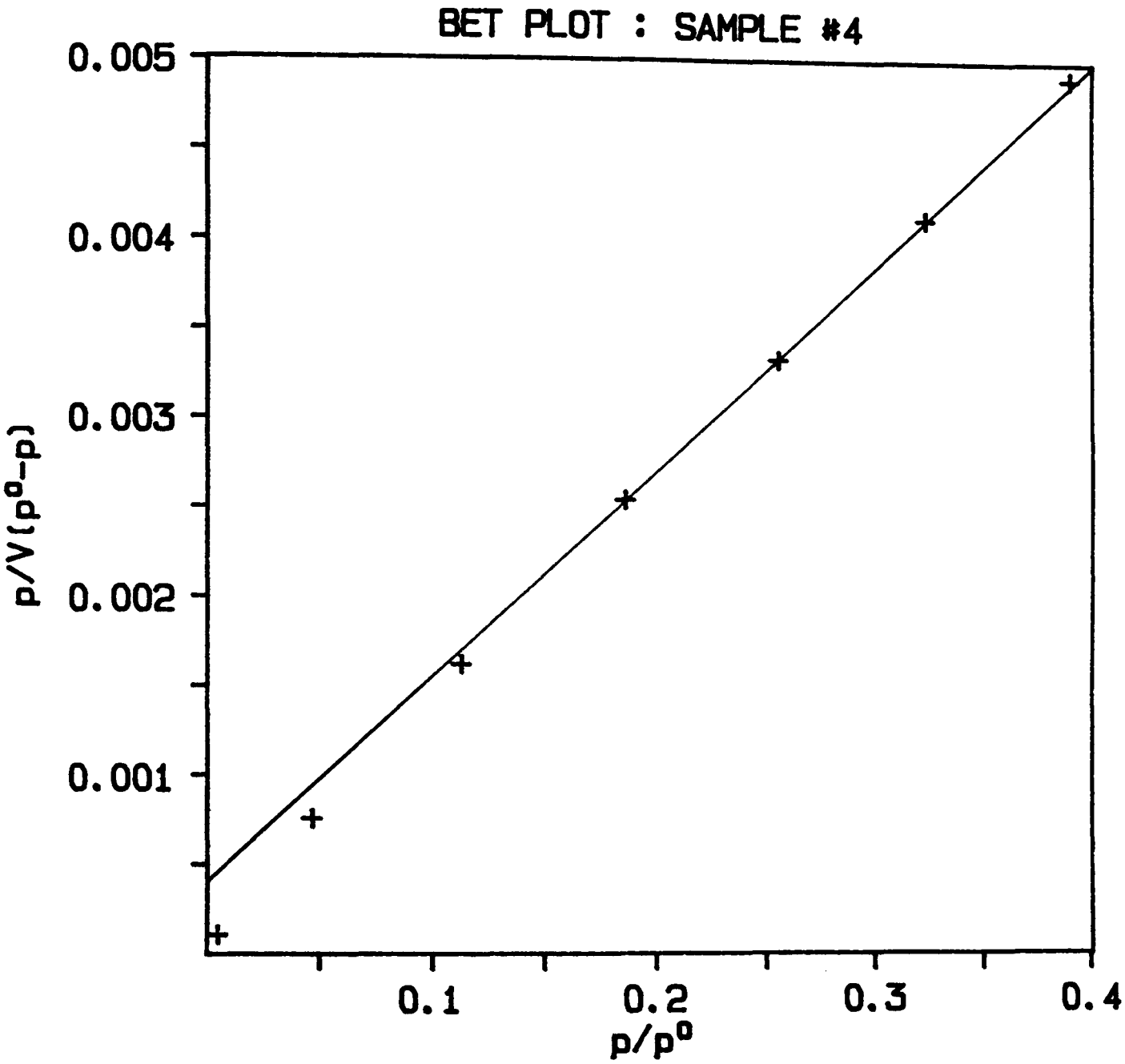
BET PLOT : SAMPLE #4
0.005
0.004
0.003
0.002
0.001
p/V(p°-p)
0.1
0.2
0.3
0.4
p/p°

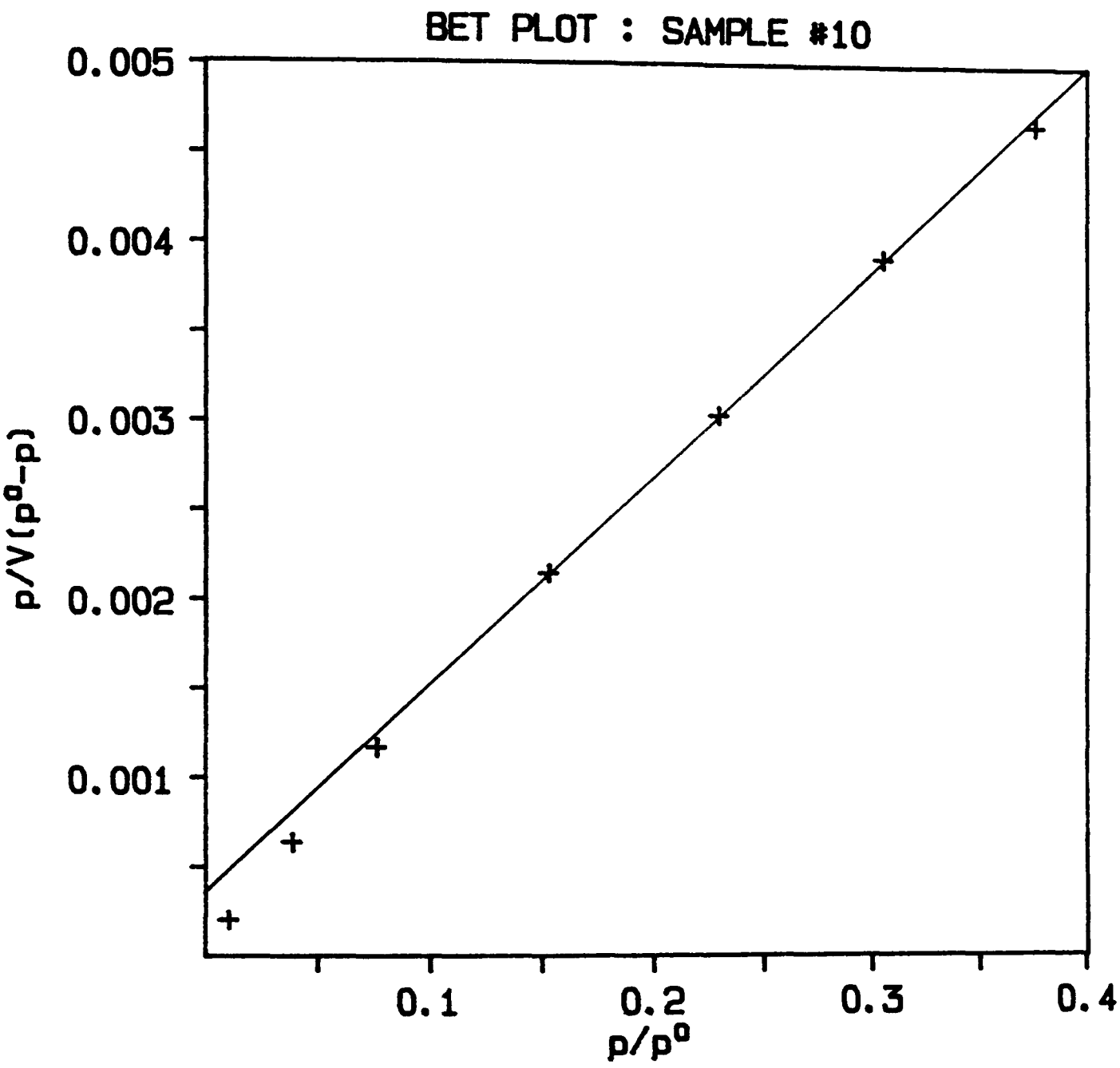
BET PLOT : SAMPLE #10
0.005
0.004
0.003
0.002
0.001
p/V(p⁰-p)
0.1
0.2
0.3
0.4
p/p⁰

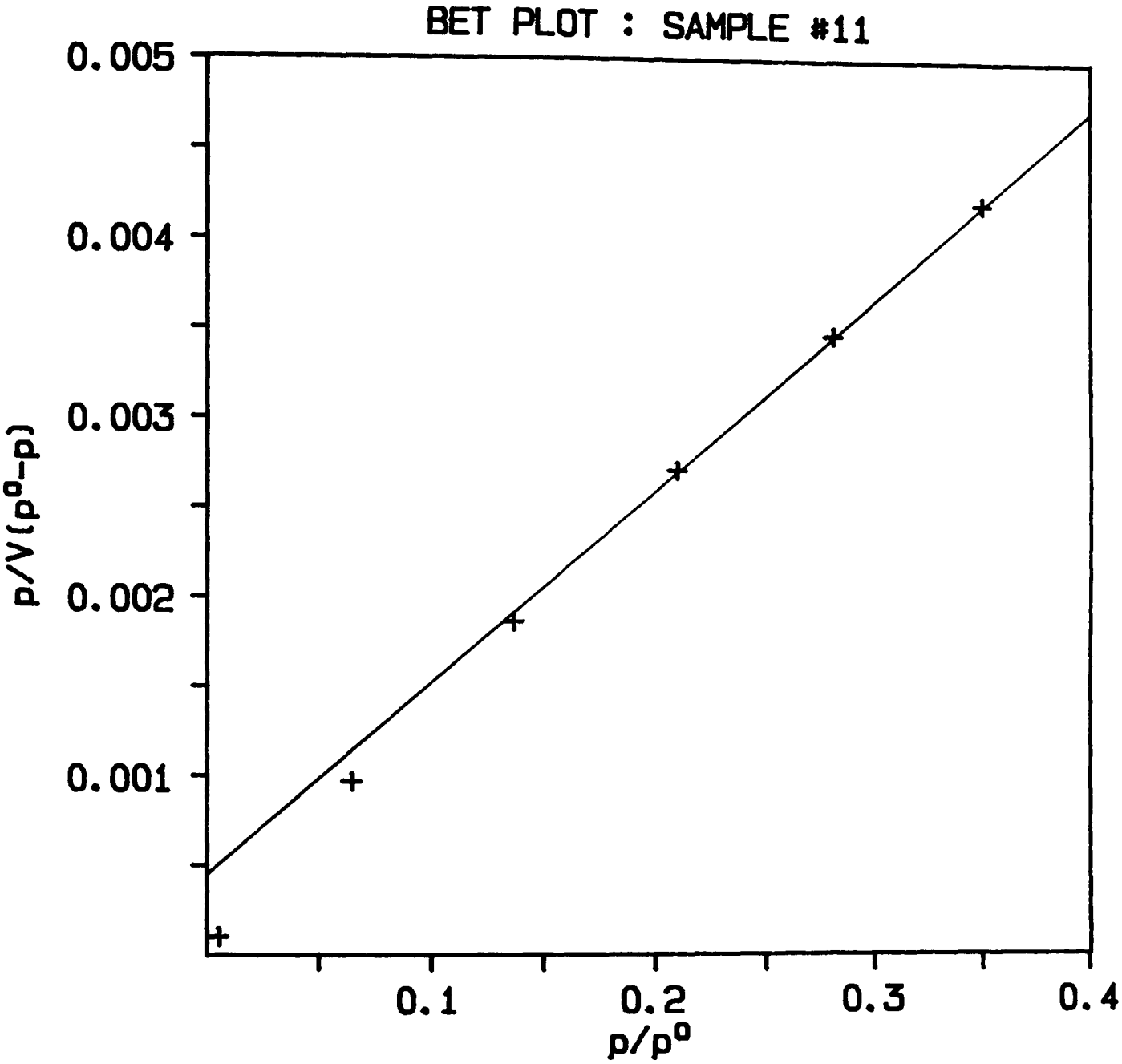
BET PLOT : SAMPLE #11
0.005
0.004
0.003
0.002
0.001
p/V(p°-p)
0.1
0.2
0.3
0.4
p/p°

A3 - Water Adsorption Data

All samples were outgassed at 110°C prior to the determination of the water isotherm at 298K.

Sample no.9. Alumina Heated in Still Air (1-->500(24)).

Adsorption		Desorption	
p/p^o	Amount Adsorbed(mg/g)	p/p^o	Amount Adsorbed(mg/g)
0.006	24.8	0.754	223
0.029	34.6	0.666	133
0.078	43.2	0.509	100
0.136	49.6	0.376	88.1
0.213	60.7	0.286	88.5
0.303	67.5	0.230	82.9
0.375	72.7	0.133	72.6
0.522	91.5	0.084	66.3
0.656	112	0.042	58.1
0.772	167	0.026	56.8
0.784	195		
0.798	226		
0.812	256		
0.825	308		
0.825	302		

Sample no.10. Alumina Heated Under Vacuum (1-->500(24)).

Adsorption		Desorption	
p/p^o	Amount Adsorbed(mg/g)	p/p^o	Amount Adsorbed(mg/g)
0.001	21.0	0.700	370
0.008	39.1	0.652	364
0.029	56.2	0.593	344
0.064	74.4	0.588	325
0.110	84.4	0.522	280
0.152	99.6	0.503	251
0.204	108	0.450	225
0.261	122	0.391	200
0.334	135	0.299	172
0.409	148	0.210	153
0.491	170	0.129	135
0.538	193	0.072	123
0.597	225	0.042	110
0.680	281	0.000	65.7
0.730	333		
0.776	367		
0.852	380		

APPENDIX B : CARBON CLOTH ADSORPTION DATA

B1 - Nitrogen Adsorption Data

All isotherms measured at 77K.

Carbon Cloth A. Outgassed at 250°C.

Adsorption		Desorption	
p/p^o	V_{ads} (cm^3/g)	p/p^o	V_{ads} (cm^3/g)
0.000	28.0	0.868	529.4
0.000	56.1	0.789	513.7
0.000	84.1	0.735	494.0
0.000	112.0	0.684	475.4
0.001	139.9	0.639	457.8
0.001	167.8	0.595	441.5
0.006	194.5	0.550	427.9
0.024	217.5	0.511	414.3
0.048	238.7	0.488	397.5
0.087	255.9	0.477	378.0
0.136	270.2	0.462	360.1
0.186	284.2	0.438	345.9
0.241	296.8	0.405	335.9
0.299	308.7	0.368	328.7
0.350	322.3		
0.460	347.6		
0.563	375.1		
0.655	405.5		
0.736	438.9		
0.812	473.9		
0.885	509.7		
0.988	537.2		

Carbon Cloth A. Outgassed at 500°C.

Adsorption		Desorption	
p/p^o	V_{ads} (cm^3/g)	p/p^o	V_{ads} (cm^3/g)
0.000	69.5	0.967	495.6
0.000	138.9	0.842	486.6
0.003	172.6	0.739	476.5
0.010	204.5	0.664	461.5
0.035	231.0	0.601	446.5
0.076	252.5	0.548	431.6
0.127	270.6	0.502	416.9
0.182	287.4	0.478	396.4
0.241	303.0	0.459	375.8
0.301	318.2	0.435	357.9
0.361	333.3	0.400	345.8
0.421	348.5	0.363	336.3
0.480	364.1	0.331	327.4
0.537	380.1	0.301	319.4
0.595	396.1	0.272	312.7
0.651	412.5		
0.707	428.9		
0.762	445.8		
0.817	462.6		
0.878	477.3		
0.949	489.1		
0.999	507.7		

Carbon Cloth B. Outgassed at 250°C.

Adsorption		Desorption	
p/p^o	V_{ads} (cm^3/g)	p/p^o	V_{ads} (cm^3/g)
0.000	109.0	0.898	908.7
0.000	163.1	0.812	877.3
0.003	215.9	0.757	835.1
0.005	241.5	0.711	792.4
0.012	265.1	0.669	751.7
0.022	286.7	0.632	711.9
0.037	305.7	0.596	674.7
0.056	322.7	0.561	640.0
0.079	337.5	0.528	607.9
0.129	365.4	0.495	578.8
0.182	392.0	0.471	547.3
0.234	418.6	0.439	522.9
0.289	443.8	0.404	503.1
0.343	469.7	0.370	486.5
0.395	496.3	0.339	470.7
0.446	523.6	0.309	457.1
0.496	551.5	0.284	443.9
0.546	579.4	0.258	433.0
0.592	609.3		
0.636	640.6		
0.676	673.2		
0.756	740.6		
0.830	810.6		
0.903	881.4		
1.000	939.3		

Microporous Carbon Cloth. Outgassed at 250°C.

Adsorption		Desorption	
p/p^o	V_{ads} (cm^3/g)	p/p^o	V_{ads} (cm^3/g)
0.000	78.5	0.873	356.7
0.000	157.0	0.748	352.1
0.003	234.5	0.640	348.4
0.005	253.0	0.548	345.0
0.012	270.1	0.474	340.4
0.027	284.3	0.408	337.3
0.048	296.3	0.351	334.6
0.074	306.3	0.303	331.8
0.105	315.0	0.263	328.8
0.141	321.7	0.228	326.1
0.179	327.5	0.202	322.3
0.223	331.5	0.177	319.7
0.271	334.0	0.159	315.4
0.320	336.1		
0.371	337.7		
0.422	338.8		
0.522	342.6		
0.623	345.9		
0.722	349.7		
0.823	352.9		
0.923	356.7		
1.000	368.4		

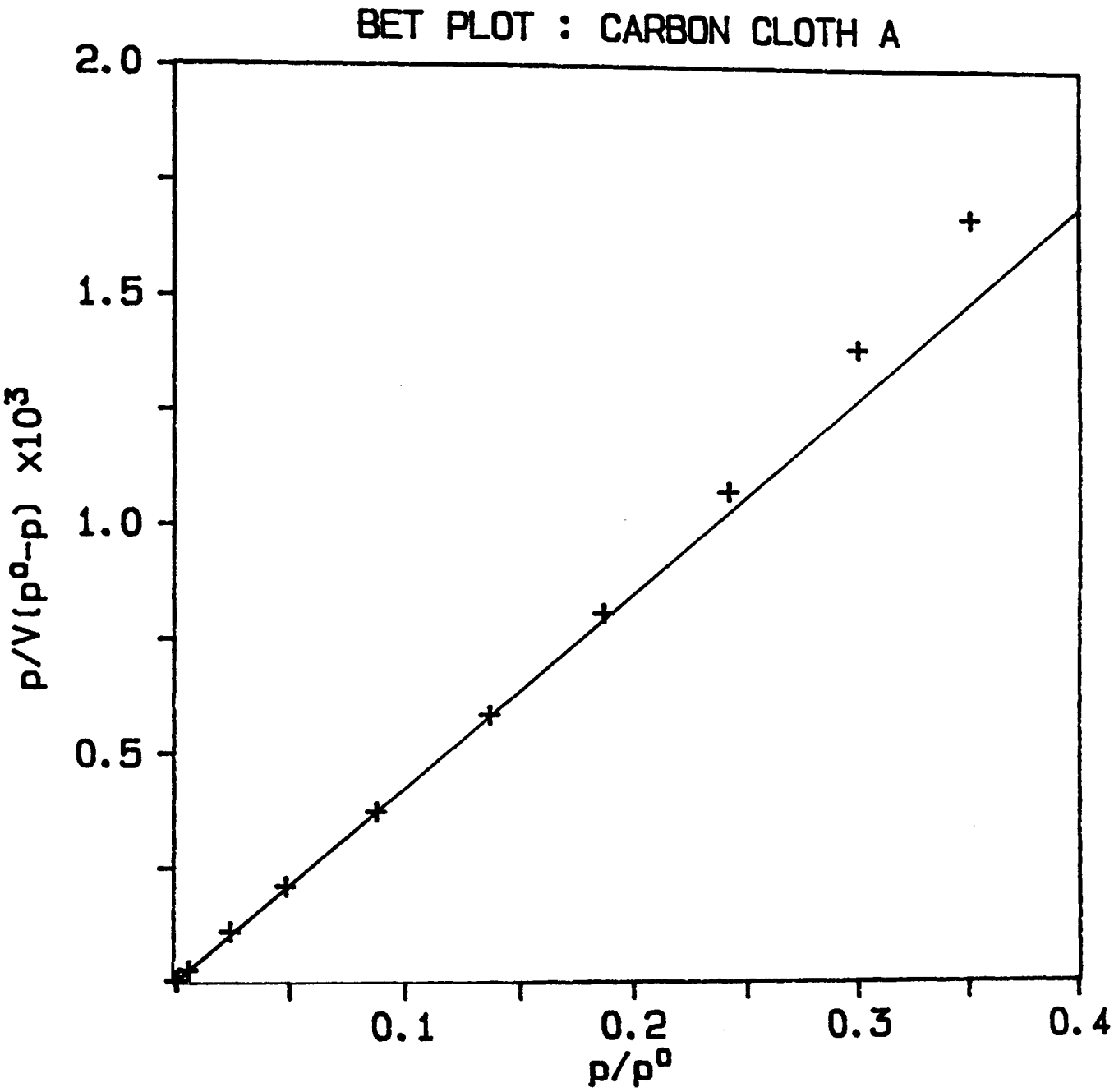
BET PLOT : CARBON CLOTH A
2.0
1.5
1.0
0.5
p/V(p⁰-p) x10³
0.1
0.2
0.3
0.4
p/p⁰

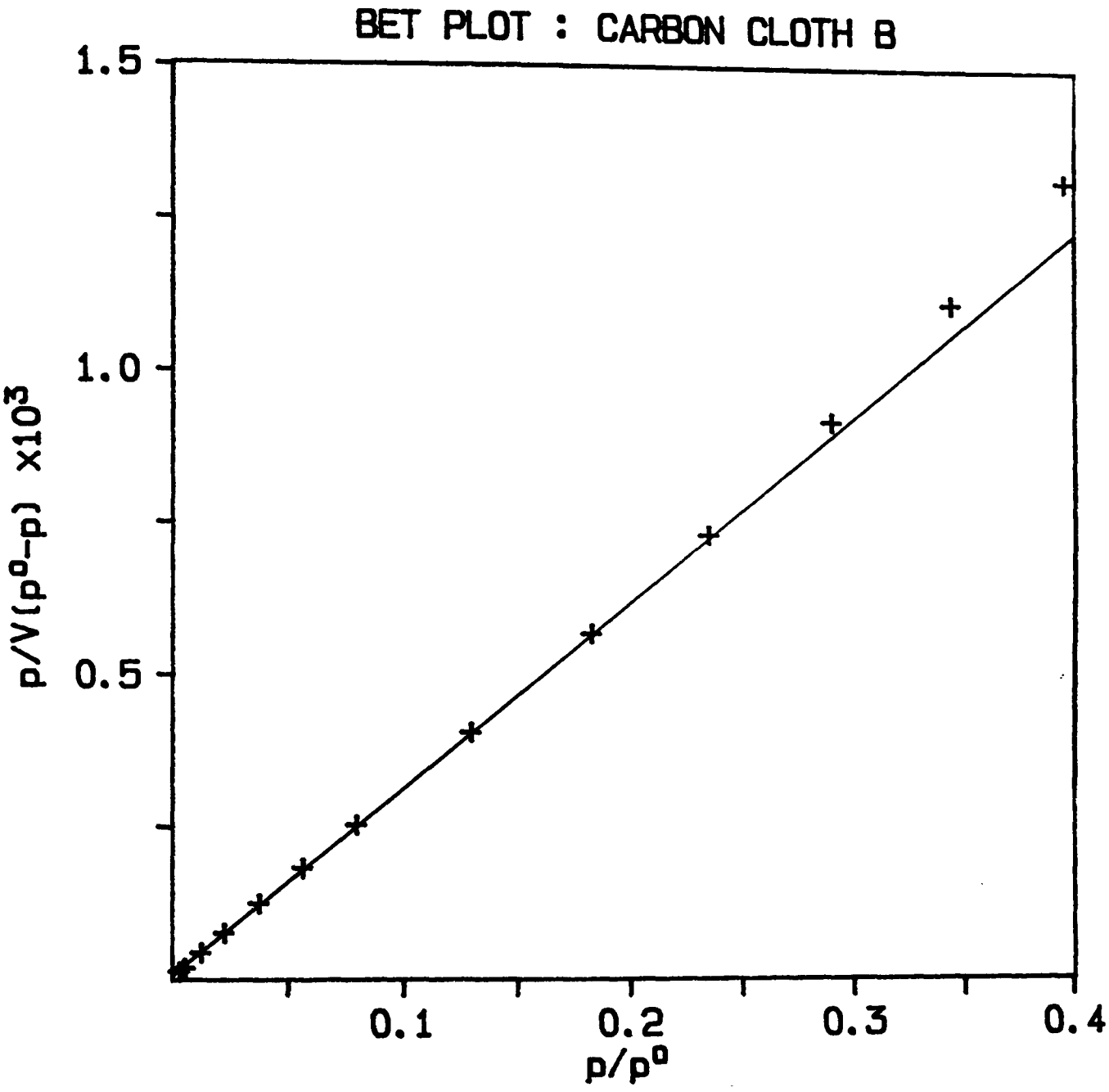
BET PLOT : CARBON CLOTH B
1.5
1.0
0.5
p/V(p⁰-p) X10³
0.1
0.2
0.3
0.4
p/p⁰

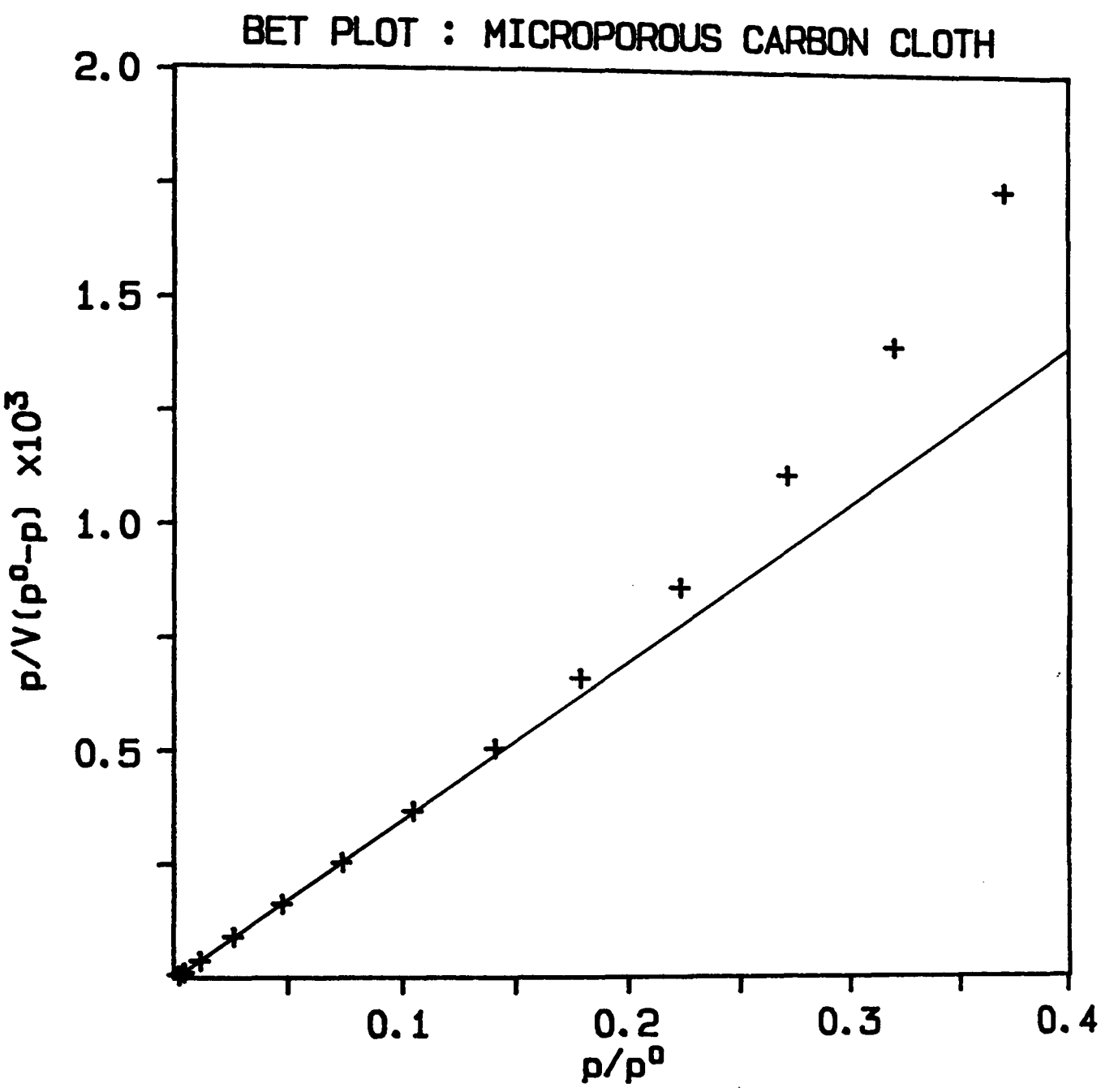
BET PLOT : MICROPOROUS CARBON CLOTH
2.0
1.5
1.0
0.5
p/V(p°-p) x10³
0.1
0.2
0.3
0.4
p/p°

B3 - Water Adsorption Data

All samples were outgassed at 110°C prior to the determination of the water isotherm at 298K.

Carbon Cloth A.

Adsorption (only)

p/p^o	Amount Adsorbed(mg/g)
0.014	27.0
0.075	37.4
0.166	51.2
0.313	90.0
0.403	138
0.538	192
0.657	236
0.713	276
0.793	353

Carbon Cloth B.

Adsorption		Desorption	
p/p^o	Amount Adsorbed(mg/g)	p/p^o	Amount Adsorbed(mg/g)
0.012	19.4	0.740	558
0.050	27.6	0.639	411
0.122	37.4	0.558	286
0.208	54.9	0.369	186
0.303	79.3	0.245	116
0.403	113	0.104	80.3
0.531	155	0.027	60.9
0.719	269	0.000	22.5
0.750	332		
0.797	434		
0.873	661		

APPENDIX C : ALUMINA / CARBON COMPOSITE ADSORPTION DATA

Nitrogen Adsorption Data

Measured Isotherms

Isotherms measured at 77K. Samples outgassed at 110°C.

Composite A.

Adsorption		Desorption	
p/p^o	V_{ads} (cm^3/g)	p/p^o	V_{ads} (cm^3/g)
0.000	53.7	0.853	423.4
0.000	107.5	0.761	413.9
0.004	133.1	0.692	401.1
0.010	158.0	0.635	387.7
0.031	179.0	0.583	375.2
0.069	195.4	0.539	362.7
0.117	209.0	0.509	347.6
0.169	221.5	0.490	330.6
0.223	233.3	0.478	312.0
0.278	245.1	0.461	295.6
0.334	256.5	0.434	283.2
0.387	268.7	0.400	274.2
0.440	280.8	0.366	266.7
0.494	293.0		
0.542	306.5		
0.588	320.4		
0.634	334.7		
0.677	349.7		
0.719	364.7		
0.764	379.3		
0.861	406.5		
0.974	429.4		

Composite B.

Adsorption		Desorption	
p/p^o	V_{ads} (cm^3/g)	p/p^o	V_{ads} (cm^3/g)
0.000	62.6	0.858	604.0
0.004	122.7	0.776	571.0
0.024	172.3	0.716	530.9
0.075	201.6	0.662	492.7
0.137	224.4	0.610	458.6
0.201	245.6	0.562	427.3
0.264	267.6	0.518	398.5
0.328	288.7	0.479	370.7
0.391	310.7	0.447	342.5
0.452	334.3	0.408	322.6
0.511	358.7	0.367	308.0
0.566	385.6	0.330	295.9
0.619	414.1	0.296	285.2
0.670	443.4	0.267	274.4
0.719	474.3		
0.769	505.2		
0.816	536.9		
0.863	569.5		
0.984	617.6		

Calculated Isotherms.

Composite A was composed of 62% carbon and 38% alumina. Composite B was composed of 47% carbon and 53% alumina. Using the adsorption data for the respective carbon cloth and the alumina(sample £11), the "reduced" N_2 uptake due to each component in the composite was calculated. ie. in the case of Composite A the N_2 uptake by 0.62g of Carbon Cloth A and 0.38g of alumina. These "reduced" isotherms are reproduced below, along with the isotherms for the two composites. The reduced isotherms were summed to yield the "calculated" isotherms. The analysis was restricted to the adsorption branch of the isotherms only.

p/p^o	$V_{ads}(cm^3/g)$	
	Composite A	Composite B
0.01	148.3	148.3
0.02	159.2	164.3
0.04	171.0	179.7
0.06	180.3	190.9
0.08	188.0	197.3
0.10	194.0	205.3
0.20	220.0	229.5
0.30	243.3	273.6
0.40	268.3	309.7
0.50	296.0	352.5
0.60	327.0	401.6
0.70	358.7	469.3
0.80	381.7	502.4
0.90	398.3	550.4
0.95	403.3	566.4

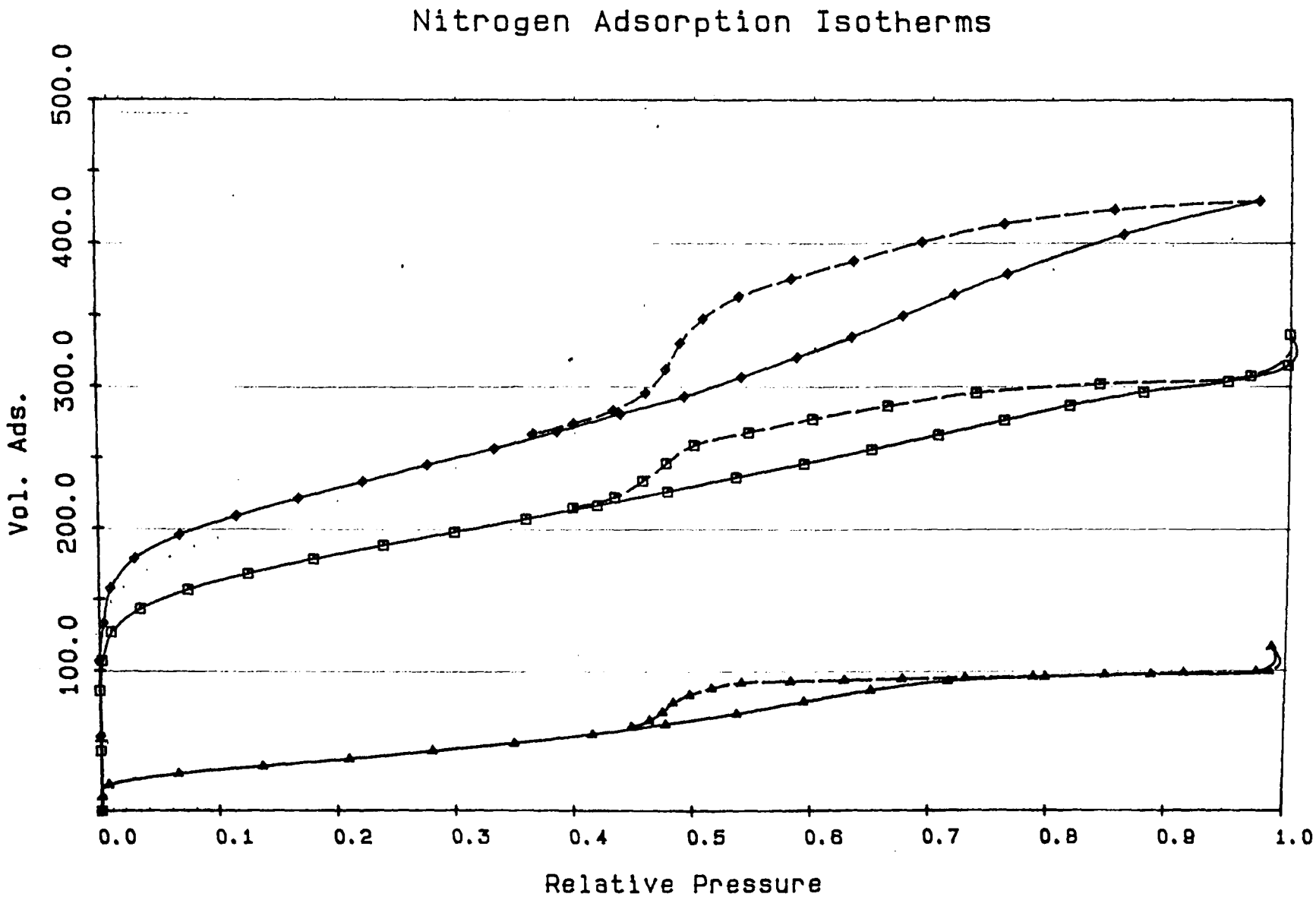

Uptake of N_2 by Carbon Cloth A (□) and Alumina (▲) /g of Composite.

(The isotherm for Composite A (◆) is included for comparison).

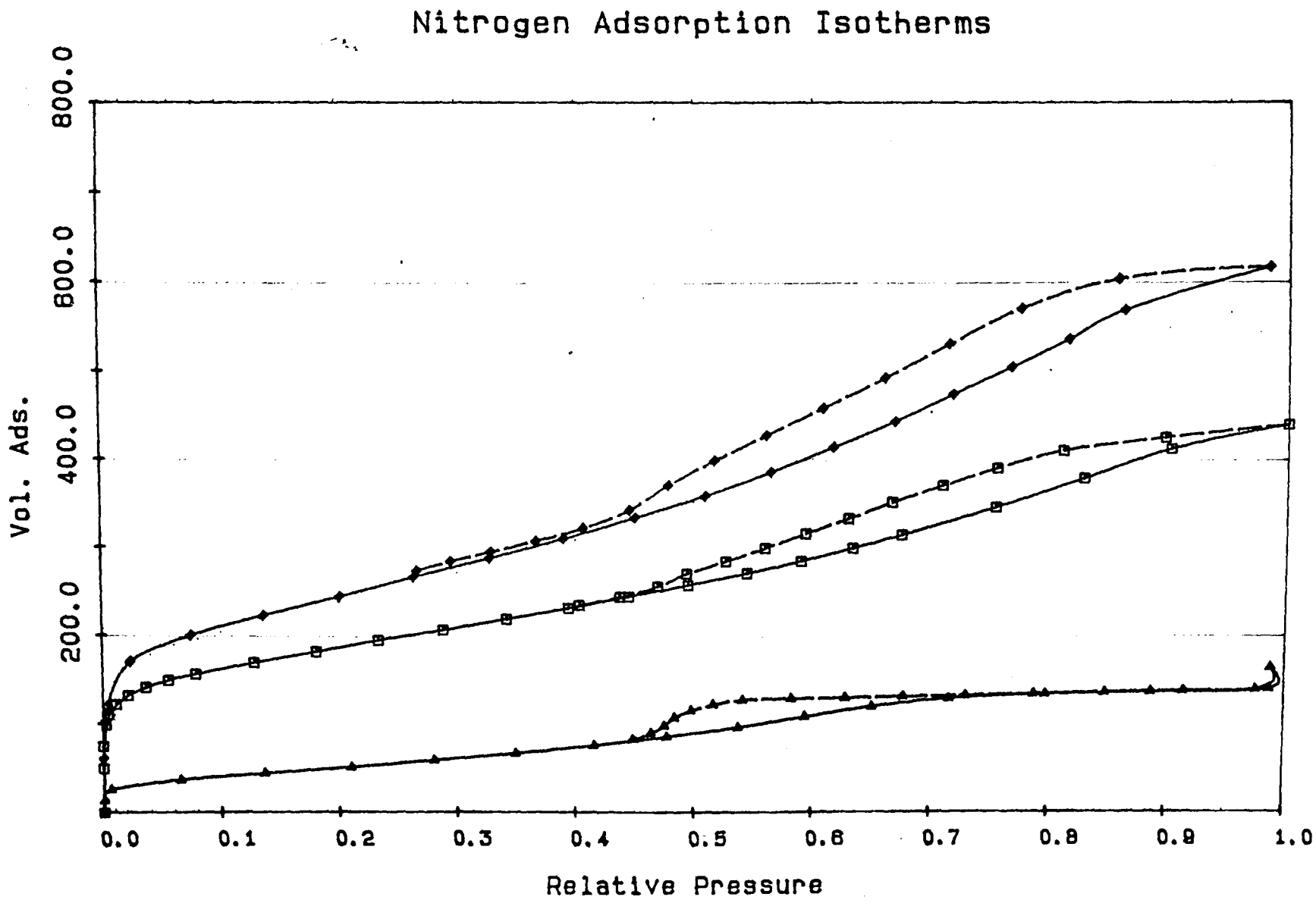

Uptake of N_2 by Carbon Cloth B (□) and Alumina (▲) /g of Composite.

(The isotherm for Composite B (◆) is included for comparison).

C2 - Water Adsorption Data

Measured Isotherms

Samples were outgassed at 110°C prior to the determination of the water isotherm at 298K.

Composite A.

Adsorption		Desorption	
p/p^o	Amount Adsorbed (mg/g)	p/p^o	Amount Adsorbed (mg/g)
0.005	27.1	0.792	445
0.024	36.9	0.703	410
0.066	47.3	0.621	353
0.138	58.6	0.522	260
0.237	76.7	0.389	154
0.309	94.2	0.205	89.0
0.389	124	0.057	62.6
0.469	166	0.018	49.3
0.559	213	0.000	23.3
0.654	258		
0.719	305		
0.775	365		
0.795	386		
0.842	460		

Composite B.

Adsorption		Desorption	
p/p^o	Amount Adsorbed (mg/g)	p/p^o	Amount Adsorbed (mg/g)
0.005	29.6	0.743	428
0.039	46.3	0.595	301
0.121	63.7	0.417	166
0.233	81.1	0.143	98.9
0.336	106	0.064	84.8
0.436	140	0.000	53.0
0.578	188		
0.675	259		
0.754	327		
0.823	446		
0.867	525		

Calculated Water Isotherms

p/p^o	Amount Adsorbed (mg/g)	
	Composite A	Composite B
0.05	42.7	44.0
0.10	55.0	62.4
0.20	75.7	84.4
0.30	100	105
0.40	131	128
0.50	170	160
0.60	223	207
0.70	289	279
0.80	370	398
0.85	-	473

Uptake of Water by Carbon Cloth A (△) and Alumina (◇) /g of Composite.

(The isotherm for Composite A (×) is included for comparison).

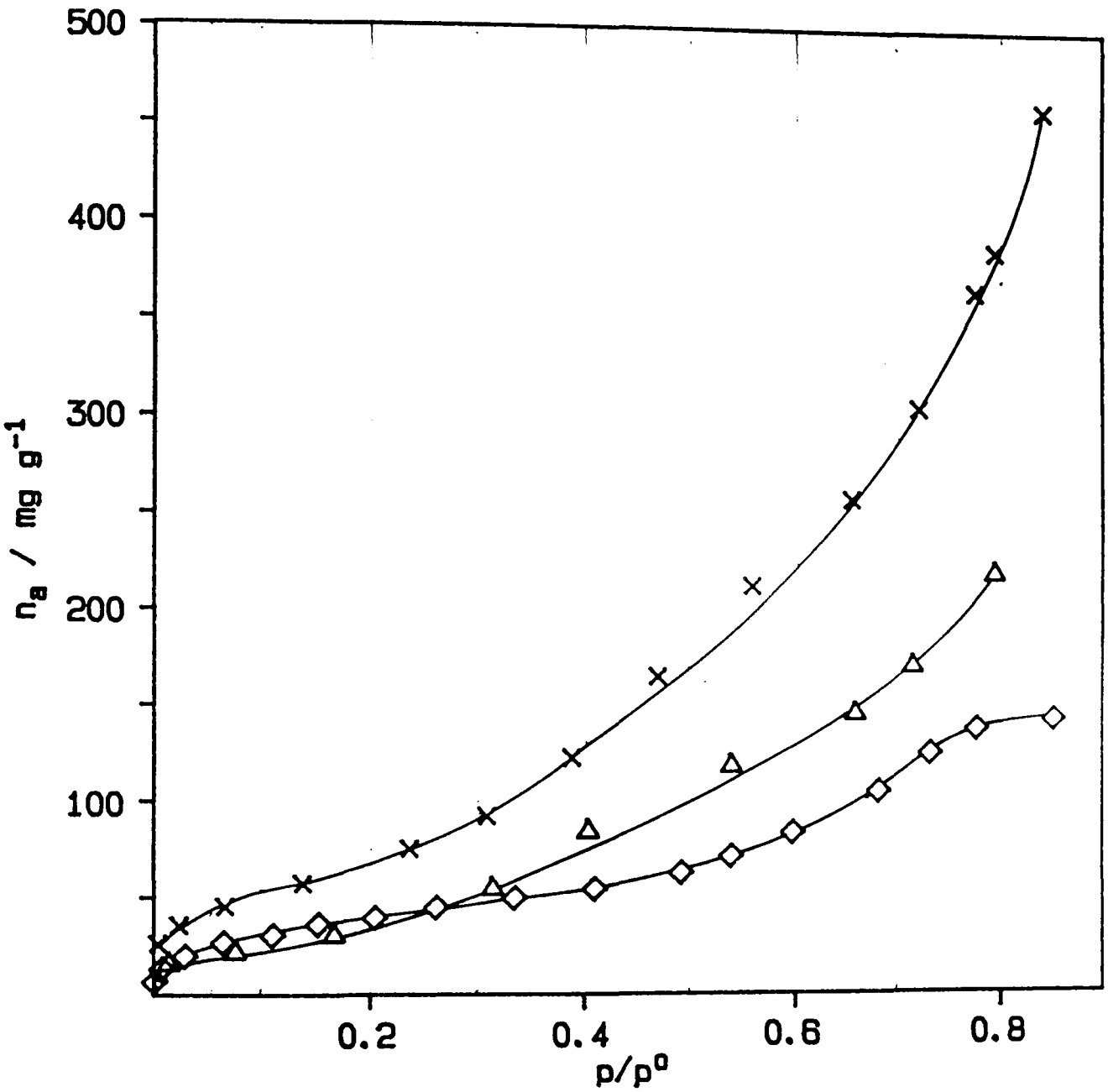

Uptake of Water by Carbon Cloth B (Δ) and Alumina (◇) /g of Composite.

(The isotherm for Composite B (×) is included for comparison).

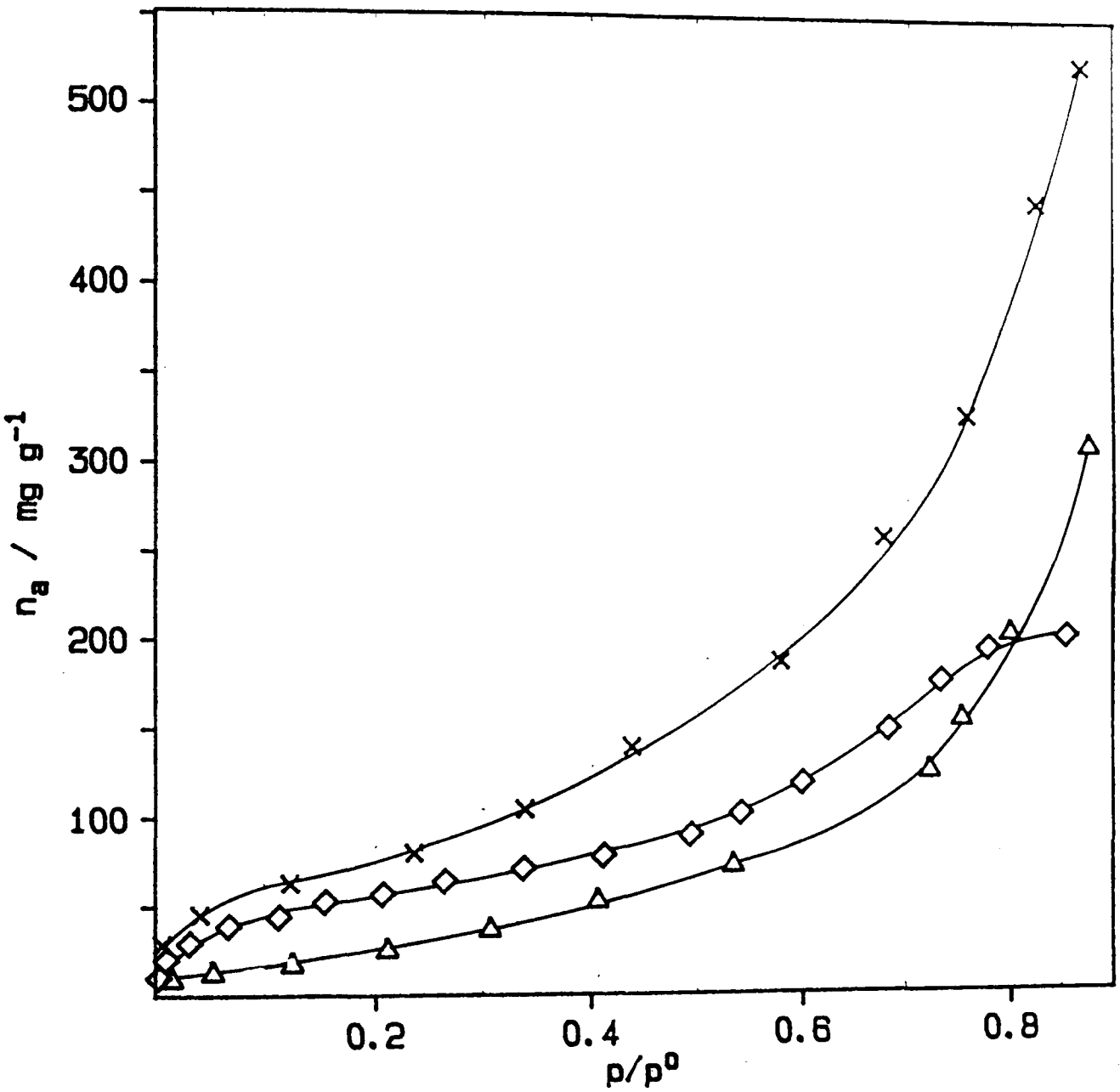

APPENDIX D : CO_2 BREAKTHROUGH DATA

D1 - CO_2 Breakthrough Data

The following notation is used in the tables of breakthrough data :

T The column temperature (^oC) at which chromatograms were measured.

F The carrier flow rate (cm^3/min.).

m The column packing weight (g).

All volumes have units of microlitres (µl).

Carbon Cloth B.

m = 0.0622, T = 40.0, F = 13.0.

Injection Volume	Volume of CO_2 Eluted		Cumulative Volume of CO_2 Injected
	Actual	Fractional (%)	
1.0	0.0	0.0	1.0
"	0.434	43.4	2.0
"	0.804	80.4	3.0
"	0.990	99.0	4.0
"	1.00	100.0	5.0
1.0	0.0	0.0	1.0
0.5	0.0	0.0	1.5
"	0.348	69.5	2.0
"	0.476	95.1	2.5
"	0.500	100.0	3.0

Cleaned Carbon Cloth B.

m = 0.0610, T = 40.0, F = 13.0.

Injection Volume	Fractional Volume of CO_2 Eluted (%)	Cumulative Volume of CO_2 Injected
0.5	54.8	0.5
"	80.8	1.0
"	100.0	1.5
"	87.7	2.0

0.70 Wt.% Alumina Composite.

m = 0.0602, T = 40.0, F = 13.0.

Injection Volume	Fractional Volume of CO_2 Eluted (%)	Cumulative Volume of CO_2 Injected
0.5	78.6	0.5
"	95.7	1.0
1.0	100.0	2.0
"	100.0	3.0

22.2 Wt.% Alumina Composite.

m = 0.0353, T = 40.0, F = 13.0.

Injection Volume	Fractional Volume of CO_2 Eluted (%)	Cumulative Volume of CO_2 Injected
2.0	7.2	2.0
"	81.7	4.0
"	97.3	6.0
"	100.0	8.0

40.2 Wt.% Alumina Composite

m = 0.0491, T = 40.0, F = 13.0.

Injection Volume	Fractional Volume of CO_2 Eluted (%)	Cumulative Volume of CO_2 Injected
3.0	0.0	3.0
"	0.0	6.0
"	15.7	9.0
"	84.3	12.0
"	96.6	15.0
"	100.0	18.0
"	98.9	21.0

51.7 Wt.% Alumina Composite

m = 0.0590.

T = 28.0, F = 13.0.

Injection Volume	Fractional Volume of CO_2 Eluted (%)	Cumulative Volume of CO_2 Injected
10.0	0.0	10.0
"	24.2	20.0
"	81.6	30.0
"	93.8	40.0
"	100.0	50.0

T = 40.0, F = 13.0.

Injection Volume	Fractional Volume of CO_2 Eluted (%)	Cumulative Volume of CO_2 Injected
10.0	0.0	10.0
5.0	18.7	15.0
"	63.1	20.0
"	69.3	25.0
"	87.1	30.0
"	100.0	35.0
"	96.8	40.0

T = 100.0, F = 15.5.

Injection Volume	Fractional Volume of CO_2 Eluted (%)	Cumulative Volume of CO_2 Injected
5.0	0.0	5.0
"	15.1	10.0
"	76.6	15.0
"	93.3	20.0
"	100.0	25.0

T = 40.0, F = 5.9.

Injection Volume	Fractional Volume of CO_2 Eluted (%)	Cumulative Volume of CO_2 Injected
5.0	0.0	5.0
"	0.0	10.0
"	0.0	15.0
"	55.8	20.0
"	67.3	25.0
"	86.4	30.0
"	100.0	35.0
"	90.5	40.0

T = 40.0, F = 29.5.

Injection Volume	Fractional Volume of CO_2 Eluted (%)	Cumulative Volume of CO_2 Injected
5.0	0.0	5.0
"	0.0	10.0
"	26.3	15.0
"	59.0	20.0
"	71.8	25.0
"	80.1	30.0
"	100.0	35.0
"	99.4	40.0

T = 40.0, F = 58.7.

Injection Volume	Fractional Volume of CO_2 Eluted (%)	Cumulative Volume of CO_2 Injected
5.0	0.0	5.0
"	0.0	10.0
"	60.0	15.0
"	68.0	20.0
"	70.0	25.0
"	87.0	30.0
"	90.0	35.0
"	100.0	40.0
"	100.0	45.0

58.4 Wt.% Alumina Composite.

5 layers, m = 0.0116.

T = 40.0, F = 5.0.

Injection Volume	Fractional Volume of CO_2 Eluted (%)	Cumulative Volume of CO_2 Injected
1.0	0.0	1.0
"	38.4	2.0
"	63.9	3.0
"	86.4	4.0
"	95.5	5.0
"	100.0	6.0

T = 40.0, F = 13.0.

Injection Volume	Fractional Volume of CO_2 Eluted (%)	Cumulative Volume of CO_2 Injected
1.0	26.7	1.0
"	77.9	2.0
"	93.5	3.0
"	91.6	4.0
"	87.8	5.0
"	100.0	6.0

10 layers, m = 0.0227, T = 40.0, F = 13.0.

Injection Volume	Fractional Volume of CO_2 Eluted (%)	Cumulative Volume of CO_2 Injected
2.0	0.0	2.0
"	25.9	4.0
"	56.2	6.0
"	62.7	8.0
"	73.9	10.0
"	76.9	12.0
"	84.3	14.0
"	88.5	16.0
"	92.5	18.0
"	100.0	20.0

20 layers, m = 0.0447, T = 40.0, F = 13.0.

Injection Volume	Fractional Volume of CO_2 Eluted (%)	Cumulative Volume of CO_2 Injected
5.0	0.0	5.0
"	7.3	10.0
"	57.6	15.0
"	86.3	20.0
"	93.9	25.0
"	100.0	30.0

30 layers, m = 0.0660, T = 40.0, F = 13.0.

Injection Volume	Fractional Volume of CO_2 Eluted (%)	Cumulative Volume of CO_2 Injected
5.0	0.0	5.0
"	0.0	10.0
"	0.0	15.0
"	19.2	20.0
"	41.9	25.0
"	59.1	30.0
10.0	91.5	40.0
"	100.0	50.0

D2 - Method of Extraction of "Breakthrough Volume" and "Total Volume of CO_2 Retained" from Breakthrough Data

The breakthrough volume corresponds to the intercept of the breakthrough curve with the "Cumulative Volume of CO_2 Injected" axis. Ideally, with sufficient points on the breakthrough curve, this intercept could be determined quite accurately by drawing a line of best fit through the points.

However the experimental data were such that the small number of points in the "transition" region did not allow a unique breakthrough curve (and subsequent intercept) to be determined. This situation arose primarily because of the steepness of the breakthrough curve in the transition region and was compounded by the experimental technique which required constant volume aliquots of CO_2 to be made so as the resulting chromatograms could be satisfactorily analysed using the "Peak Height" method.

In order to **objectively** estimate the breakthrough volume the following procedure was universally applied:

The last experimental point corresponding to complete retention and the first experimental point in the transition region were the focus of the analysis. Assume for the present discussion that these points had co-ordinates $(x_1,0)$ and (x_2,y_2) respectively. The breakthrough volume (B.V.) was then given by the equation

$$B.V. = x_2 - \frac{y_2(x_2-x_1)}{100}$$

The use of this equation was found to give sensible estimates of the breakthrough volume for a given series of breakthrough curves, however it was recognised that its universal application to breakthrough curves would not necessarily be justifiable. Its success in the present

context arose simply because the breakthrough curves being compared were of similar shape and differed primarily in the lateral position of the transition region in each case. The prime advantage of such an analysis method, however simple, was that a subjective curve fit was not required to yield the breakthrough volume.

The "total volume of CO_2 retained" was obtained simply by summation of the volume retained after each injection. In the "complete retention" region the volume retained after each injection corresponded to the injection volume, while in the "transition" region only a calculated fraction of the CO_2 volume was retained.

REFERENCES

Aboaf, J.A., J. Electrochem. Soc., **114**(9), 948 (1967).

Alford, N.McN., Birchall, J.D. and Kendall, K., Mat. Sci. Tech., **2**, 329 (1986).

Atkinson, D., McLeod, A.I., Sing, K.S.W. and Capon, A., Carbon, **20**, 339 (1982).

Avery, R.G. and Ramsay, J.D.F., in "Adsorption and Catalysis on Oxide Surfaces", Che, M. and Bond, G.C. (Eds), Studies in Surface Science and Catalysis, **21**, p.149, Elsevier, Amsterdam (1985).

Bailey, A., Maggs, F.A.P. and Williams, J.H., Brit. Pat. No. 1,310,011 (1973).

Baker, F.S., Carruthers, J.D., Day, R.E., Sing, K.S.W. and Stryker, L.J., Disc. Faraday Soc., **52**, 173 (1971).

Baker, F.S., Ph.D. Thesis, Brunel University (1974).

Barrer, R.M., J. Coll. Int. Sci., **21**, 415 (1966).

Barrer, R.M., "Zeolites and Clay Minerals as Sorbents and Molecular Sieves", Academic Press, London (1978).

Bonis, S.A., Electronic Packaging and Production, **14**(2), 46 (1974).

Brunauer, S., Emmett, P.H. and Teller, E., J.A.C.S., **60**, 309 (1938).

Brunauer, S., Deming, L.S., Deming, W.S. and Teller, E., J.A.C.S., **62**, 1723 (1940).

Capon, A. and Maggs, F.A.P., Proc. 1st. Europ. Symp. Therm. Anal., Salford, UK, 176 (1976).

Carrott, P.J.M., Ph.D. Thesis, Brunel University (1980).

Carrott, P.J.M. and Sing, K.S.W., Chem. Ind., 360 (1986).

Carrott, P.J.M., Roberts, R.A. and Sing, K.S.W., Carbon, **25**(6), 769 (1987).

Carrubba, R.V., Urbanic, J.E., Wagner, N.J. and Zanitsch, R.H., AIChE Symp. Ser., **80**, 76 (1984).

Carruthers, J.D., Payne, D.A., Sing, K.S.W. and Stryker, L.J., J. Coll. Int. Sci., **36**(2), 205 (1971).

Cheriminisoff, P.N. and Morresi, A.C., "Carbon Adsorption Handbook" (Cheriminisoff, P.N. and Ellerbusch, F., Eds.), p.1, Ann Harbor Science Publishers (1978).

Cohen, H., Soffer, A. and Oren, Y., J. Coll. Int. Sci., **120**(1), 272 (1987).

Conder, J.R. and Young, C.L., "Physicochemical Measurement by Gas Chromatography", Wiley-Interscience, Chichester, (1979).

Curtis, J.C.L., BSIRA Report No. A139 (1964).

Cutting, P.A., Parkyns, N.D. and Sing, K.S.W., J. Cat., **27**, 222 (1972).

Dubinin, M.M. and Zaverina, E.D., Zh. Fiz. Khim., **23**, 1129 (1949).

Ermolenko, I.N., Gul'ko, N.V. and Lyubliner, I.P., Byull. Izobret., **6**, 93 (1980).

Ermolenko, I.N., Gul'ko, N.V. and Lyubliner, I.P., Zh. Prik. Khim., **57**(8), 1721 (1984).

Fiat, D. and Connick, R.E., J.A.C.S., **90**, 608 (1968).

Freeman, J.J. and McLeod, A.I., Fuel, **62**, 1090 (1983).

Freeman, J.J., Ph.D. Thesis, Brunel University (1986).

Freeman, J.J. and Gimblett, G.R., Carbon, **26**(4), 501 (1988).

Gregg, S.J. and Ramsay, J.D.F., J. Phys. Chem., **73**(5), 1243 (1969).

Gregg, S.J. and Sing, K.S.W., "Adsorption Surface Area and Porosity," 2nd edn., Academic Press, London (1982).

Griffiths, R.J.M., Chem. Ind., 247 (1985).

Gruninger, M.F., Wachtman Jr., J.B. and Haber, R.A., Mat. Res. Soc. Symp. Proc., **54**, 823 (1986).

Guglielmi, M. and Maddalena, A., J. Mat. Sci. Lett., **4**, 123 (1985).

Gurvitsch, L., J. Phys. Chem. Soc. Russ., **47**, 805 (1915).

Harris, M.R. and Sing, K.S.W., J. Appl. Chem., **8**, 586 (1958).

Hayes, R.A., a, b, c, unpublished results.

Ivanova, T.G., Lazerko, G.A., Gul'ko, N.V., Ermolenko, I.N. and Lyubliner, I.P., Zh. Prik. Khim., **55**(3), 544 (1982).

Kochling, K.-H., McEnaney, B., Rozploch, F. and Fitzer, E., Carbon, **20**, 445 (1982).

Kochling, K.-H., McEnaney, B., Neumann, S. and Fitzer, E., Carbon, **21**, 517 (1983).

Kordas, G., Weeks, R.A. and Arftsen, N., J. Appl. Phys., **57**, 3812 (1985).

Kruyt, H.R., ed., "Colloid Science", Elsevier, Amsterdam (1952).

Langmuir, I., J.A.C.S., **38**, 2221 (1916).

Lannutti, J.J. and Clark, D.E., Ceram. Engng. Sci. Proc., **5**, 574 (1984).

Leenaars, A.F.M., Keizer,K. and Burggraaf, A.J., J. Mat. Sci., **19**, 1077 (1984).

Leenaars, A.F.M. and Burggraaf, A.J., a, J. Membrane Sci., **24**, 245 (1985).

Leenaars, A.F.M. and Burggraaf, A.J., b, J. Membrane Sci., **24**, 261 (1985).

Leenaars, A.F.M., Keizer, K. and Burggraaf, A.J., Chemtech, **16**(9), 560 (1986).

Lennard-Jones, J.E., Physica (Eindhoven), **4**, 941 (1937).

Lewis, W.K. and Metzner, A.B., Ind. Engng. Chem., **46**, 849 (1954).

Maggs, F.A.P., Smith, M.E. and Robins, G.A., Ext. Abs. 13th Biennial Conf. Carbon, California, p.3 (1977).

Matijevic, E., Mathai, K.G., Ottewill, R.H. and Kerker, M., J. Phys. Chem., **65**, 826 (1966).

McBain, J.W. and Bakr, A.M., J.A.C.S., **48**, 690 (1926).

McLeod, A.I., Ph.D. Thesis, Brunel University (1979).

Mukherjee, S.P. and Lowdermilk, W.H., J. Non-Cryst. Solids, **48**, 177 (1982).

Parkyns, N.D., "Third Congress on Catalysis", Vol. 2, North Holland Publishing Co., Amsterdam, p.914 (1965).

Payne, D.A., Ph.D. Thesis, Brunel University (1970).

Peri, J.B., J. Phys. Chem., **70**(10), 3168 (1966).

Ramsay, J.D.F., Daish, S.R. and Wright, C.J., Disc. Faraday Soc., **65**, 65 (1978).

Raupach, M., Aust. J. Soil Res., **1**, 36 (1963).

Roberts, R.A., a, b, personal communication.

Roberts, R.A., Ph.D. Thesis, Brunel University (1988).

Robinson, R.A. and Peck, D.A., J. Phys. Chem., **39**, 1125 (1935).

Segal, D.L., United Kingdom Atomic Energy Authority, Report No. 12018 (1985).

Sillen, L.G., Quart. Rev., **13**, 146 (1959).

Simpson, K., Brit. Pat. No. 1,570,677 (1980).

Sing, K.S.W. in "Surface Area Determination", eds. Everett, D.H. and Ottewill, R.H., Butterworths, London, p.25 (1970).

Sing, K.S.W., Everett, D.H., Haul, R.A.W., Moscou, L., Pierotti, R.A., Rouquerol, J. and Siemieniewska, T., Pure and Appl. Chem., **57**, 603 (1985).

Teichner, S.J., Nicalaon, G.A., Vicarini, M.A. and Gardes, G.E.E., Adv. Coll. Int. Sci., **5**, 245 (1976).

Werner, U., Proc. 4th BOC Priestley Conf., Leeds, 43 (1986).

Wilson, S.J., McConnell, J.D.C. and Stacey, M.H., J. Mat. Sci., **15**, 3081, (1980).

Wilson, S.J. and Stacey, M.H., J. Coll. Int. Sci., **82**, 507 (1981).

Yoldas, B.E., J. Appl. Chem. Biotech., **23**, 803 (1973)

Yoldas, B.E., a, Ceram. Bull., **54**(3), 286 (1975).

Yoldas, B.E., b, J. Mat. Sci., **10**, 1856, (1975).

Yoldas, B.E., J. Mat. Sci., **12**, 1203 (1977).

Yoldas, B.E., Partlow, D.P. and Mattox, D.M., Report ARO-13970 (1979).

Yoldas, B.E., Appl. Optics, **19**(9), 1425 (1980).

Zsigmondy, A., Z. Anorg. Chem., **71**, 356 (1911).